2013-03-07

Development of Viscosity Model for Petroleum Industry Applications

Motahhari, Hamed reza

UNIVERSITY OF CALGARY

Development of Viscosity Model for Petroleum Industry Applications

by

Hamed reza Motahhari

A THESIS

SUBMITTED TO THE FACULTY OF GRADUATE STUDIES

IN PARTIAL FULFILLMENT OF THE REQUIREMENTS FOR THE

DEGREE OF DOCTOR OF PHILOSOPHY

DEPARTMENT OF CHEMICAL AND PETROLEUM ENGINEERING

CALGARY, ALBERTA

MARCH, 2013

UNIVERSITY OF CALGARY

FACULTY OF GRADUATE STUDIES

The undersigned certify that they have read, and recommend to the Faculty of Graduate Studies for acceptance, a thesis entitled "Development of Viscosity Model for Petroleum Industry Applications" submitted by Hamed reza Motahhari in partial fulfilment of the requirements of the degree of Doctor of Philosophy.

_____

Supervisor, Dr. Harvey W. Yarranton,
Department of Chemical and Petroleum Engineering

_____

Dr. Brij Maini,
Department of Chemical and Petroleum Engineering

_____

Dr. Ian D. Gates,
Department of Chemical and Petroleum Engineering

_____

Dr. Mingzhe Dong,
Department of Chemical and Petroleum Engineering

_____

Dr. Stephen R. Larter,
Department of Geology and Geophysics

_____

External Examiner, Dr. Jefferson L. Creek,
Chevron Energy Technology Company

_____

Date

Abstract

Heavy oil and bitumen are challenging to produce and process due to their very high viscosity, but their viscosity can be reduced either by heating or dilution with a solvent. Given the key role of viscosity, an accurate viscosity model suitable for use with reservoir and process simulators is essential. While there are several viscosity models for natural gases and conventional oils, a compositional model applicable to heavy petroleum and diluents is lacking. The objective of this thesis is to develop a general compositional viscosity model that is applicable to natural gas mixtures, conventional crudes oils, heavy petroleum fluids, and their mixtures with solvents and other crudes.

The recently developed Expanded Fluid (EF) viscosity correlation was selected as a suitable compositional viscosity model for petroleum applications. The correlation relates the viscosity of the fluid to its density over a broad range of pressures and temperatures. The other inputs are pressure and the dilute gas viscosity. Each fluid is characterized for the correlation by a set of fluid-specific parameters which are tuned to fit data.

First, the applicability of the EF correlation was extended to asymmetric mixtures and liquid mixtures containing dissolved gas components. A new set of mass-fraction based mixing rules was developed to calculate the fluid-specific parameters for mixtures. The EF correlation with the new set of mixing rules predicted the viscosity of over 100 mixtures of hydrocarbon compounds and carbon dioxide with overall average absolute relative deviations (AARD) of less than 10% either with measured densities or densities estimated by Advanced Peng-Robinson equation of state (APR EoS). To improve the viscosity predictions with APR EoS-estimated densities, general correlations were developed for non-zero viscosity binary interaction parameters.

The EF correlation was extended to non-hydrocarbon compounds typically encountered in natural gas industry. It was demonstrated that the framework of the correlation is valid for these compounds, except for compounds with strong hydrogen bonding such as water. A temperature dependency was introduced into the correlation for strongly hydrogen

bonding compounds. The EF correlation fit the viscosity data of pure non-hydrocarbon compounds with AARDs below 6% and predicted the viscosity of sour and sweet natural gases and aqueous solutions of organic alcohols with overall AARDs less than 9%.

An internally consistent estimation method was also developed to calculate the fluid-specific parameters for hydrocarbons when no experimental viscosity data are available. The method correlates the fluid-specific parameters to the molecular weight and specific gravity. The method was evaluated against viscosity data of over 250 pure hydrocarbon compounds and petroleum distillations cuts. The EF correlation predictions were found to be within the same order of magnitude of the measurements with an overall AARD of 31%.

A methodology was then proposed to apply the EF viscosity correlation to crude oils characterized as mixtures of the defined components and pseudo-components. The above estimation methods are used to calculate the fluid-specific parameters for pseudo-components. Guidelines are provided for tuning of the correlation to available viscosity data, calculating the dilute gas viscosities, and improving the densities calculated with the Peng-Robinson EoS. The viscosities of over 10 dead and live crude oils and bitumen were predicted within a factor of 3 of the measured values using the measured density of the oils as the input. It was shown that single parameter tuning of the model improved the viscosity prediction to within 30% of the measured values.

Finally, the performance of the EF correlation was evaluated for diluted heavy oils and bitumens. The required density and viscosity data were collected for over 20 diluted dead and live bitumen mixtures using an in-house capillary viscometer also equipped with an in-line density-meter at temperatures and pressures up to 175 °C and 10 MPa. The predictions of the correlation were found within the same order of magnitude of the measured values with overall AARDs less than 20%. It was shown that the predictions of the correlation with generalized non-zero interaction parameters for the solvent-oil pairs were improved to overall AARDs less than 10%.

Acknowledgements

I would like to express my deepest and profound gratitude to my supervisor, Dr. Harvey Yarranton, for his continuous support, excellent guidance and encouragements throughout the course of this study. His willingness to support and inputs on modeling and experimental work and technical writing were highly precious. It was a privilege and honor for me to be a member of his research group and work under his supervision toward my Ph.D. degree.

I also would like to thank Dr. Marco Satyro who supported me with his thoughtful advices. I highly appreciate his insights on the physical properties estimations approaches and the equations of state. I could always rely on his wealth of knowledge on the scientific literature of this area of research. I also thank him and Virtual Material Group for providing me with VMGSim simulator package and the technical support.

I am particularly grateful to Florian Schoeggl, our PVT lab manager, for his constant support and assistance throughout the experimental work of my study. Technical interactions with him allowed me to develop practical knowledge on the subject of the property measurements and beyond. He was always in lab, no matter how soon I tried to start my measurements.

My gratitude also extends to Dr. Creek, Dr. Dong, Dr. Gates, Dr. Larter and Dr. Maini for serving on my Ph.D. defense examination committee. I am thankful to Dr. Shawn Taylor for proving me the opportunity of experiencing the research atmosphere in DBR Technology Center.

I am thankful to the Department of Chemical and Petroleum Engineering at the University of Calgary for giving me the opportunity to pursue my Ph.D. studies and the financial support by the graduate scholarships. I also thank the sponsors of the Industrial Research Chair in Heavy Oil Properties and Processing (HOPP), including NSERC,

Shell, Schlumberger and Petrobras, for supporting the thesis project and providing the crude oil samples.

I also thank all past and present members of Dr. Harvey Yarranton's research groups (HOPP and C-AER) for their co-operations and useful discussions. I especially thank Eliane Baydak, Fatemeh Saryazdi, Pawan Agrawal, Catalina Sanchez and Asok Tharanivasan. I also thank summer student, Yakun Li, who helped me in conducting some experiments.

Finally, I am profoundly indebted to my parents, for their constant support, dedications and continuous inspiration throughout all stages of my life. Last but not least, I express my deepest gratitude to my lovely wife, Maryam, for her understanding, moral support and encouragements during the course of my Ph.D. study. Without her patience, the completion of this thesis was not possible.

To my beautiful and lovely wife, Maryam,

and to my Parents

for their care and support

Table of Contents

List of Tables

List of Figures

List of Symbols, Abbreviations and Nomenclature

The definitions of the symbols are context-dependent.

Uppercase Symbols

A : fluid-specific coefficient [mPa.s] in Yaws (1999, 2008), Equation 2.13, or
: fluid-specific coeff. in Andrade (1934) equation, Equation 2.17, or
: fluid-specific coeff. in Vodel (1934) equation, Equation 2.18, or
: fluid-specific coeff. in Yaws (2008) and API (1997), Equation 2.19, or
: coefficient in Doolittle (1951) model, Equation 2.23

A_{ij} : adjustable constant in volume shift mixing rules of APR EoS, Equation B.16

B : fluid-specific coeff. [mPa.s/K] in Yaws (1999,2008), Equation 2.13, or
: fluid-specific coeff. in Andrade (1934) equation, Equation 2.17, or
: fluid-specific coeff. in Vodel (1934) equation, Equation 2.18, or
: fluid-specific coeff. in Yaws (2008) and API (1997), Equation 2.19

B_{ij} : interaction parameter in Mehrotra et al. (1989) mixing rule, or
: adjustable constant in volume shift mixing rules of APR EoS, Equation B.16

C : fluid-specific coeff. [mPa.s/K^2] in Yaws (1999,2008), Equation 2.13, or
: fluid-specific coeff. in Vogel (1934) equation, Equation 2.18, or
: fluid-specific coeff. in Yaws (2008) and API (1997), Equation 2.19

C_f : tuning parameter in Sǿreide (1989) correlation

D : fluid-specific coeff. [mPa.s/K^3] in Yaws (1999,2008), Equation 2.13
: fluid-specific coeff. in Yaws (2008) and API (1997), Equation 2.19

E : fluid-specific coeff. in Yaws (2008) and API (1997), Equation 2.19, or
: parameter of energy transfers in Hildebrand (1971) model, Equation 2.22

F_c : empirical correction factor in Chung et al. (1984), Equation 2.7

F^o_P : correction Factor for polarity effects in Lucas (1980) model

F^o_Q : correction Factor for quantum effects in Lucas (1980) model

I_d dipole moment [debyes]

I_d^* dimensionless dipole moment defined by Chung et al. (1984), Equation 2.8

G_{ij} : binary interaction parameter in Gruenberg Equation

K_c : adjustable viscosity parameter in Friction Theory model

K_{c2} : fitting parameter in temperature dependent parameter c_2, equation 6.1

K_z : adjustable volume translation parameter in Friction Theory model

N_A : Avogadro's number(=6.022×10^{23} mol^{-1})

P : pressure [kPa]

R : universal Gas Constant (=8.314 J/kmol.K)

R_μ : roughness factor

T : temperature [K or C]

T^* : dimensionless temperature (=kT/ε)

T_b : normal boiling point [K]

X X any of parameters c_2, c_3 or ρ_s^o of EF correlation

Z_{RA} : Rackett compressibility

Lowercase Symbols

$a_0 \ldots a_6$: constants of estimation methods for reference n-paraffins (EF Ccorrelation), Equations 7.20, 7.22 and 7.23 and Table 7.3

$a_0 \ldots a_7$: universal constants in Assael et al. (1992 a) model

b : excluded volume [cm3/mol] (=$2/3\pi NA\sigma^3$), Equation 2.55, or

: fitting parameter for in Svrcek and Mehrotra (1988) study, Equation 2.61

$b_0 \ldots b_4$: constants in departure functions (EF correlation) , Equation 7.24 table 7.3

b_1 : fluid-specific coeff. in ASTM kinematic viscosity correlation, Equation 2.21

b_2 : fluid-specific coeff. in ASTM kinematic viscosity correlation, Equation 2.22

c : fluid-specific volume translation parameter [cm3/mol], Equation 7.12

c_1 : fixed coefficient in EF correlation

(=0.65 for *version 1* and =0.4214 for *version 2*)

c_2 : fluid-specific parameter in EF correlation

$c_{2\infty}$: ultimate value of parameter c_2 at high temperatures in EF correlation

c_3 : fluid- specific parameter of pressure dependency in EF correlation [kPa^{-1}]

c_4 : parameter of pressure dependency in EF correlation, version 2 [dimensionless]

d : coefficient in Doolittle (1951) model, Equation 2.23

f_C : correlating function of difference in property C (i.e. *MW*, compressed state density, T_c, *WK*)

$f_{i,o}$: temperature reduction parameter in Corresponding States model

$g(\sigma)$: radial distribution function

$h_{i,o}$: volume reduction parameter in Corresponding States model

k : Boltzmann's constant (=1.380148×10^{-23} J/K)

n : empirical exponent in EF correlation (=0.165 for *version 1* and =0.4872 for *version 2*)

nc : number of components

u : velocity [m/s]

v_0 : Closed packed volume of the molecules [cm^3/mol], Equation 2.58

v_∞ : intrinsic molar volume [cm^3/mol], Equation 2.22

w : mass fraction

x : mole fraction, or

: x-direction

x' : effective mole fraction in Lederer (1933) mixing rule, Equation 2.29

y : distance in y direction [m]

z : mole, mass or volume fraction, Equation 2.24

Greek Symbols

α : degree of association in Lederer (1933) mixing rule, Equation 2.29, or

: rotational coupling coefficient, Equation 2.44, or

: decay rate of β_{ij} from atmospheric to high pressure [1/kPa], Equation 5.15, or

: degree of association in Lederer (1933) mixing rule, Equation 2.29

α_X : common tuning multiplier, (X: parameters c_2, c_3 or ρ_s^o of EF correlation)

β : correlating parameter between density and viscosity in EF correlation

β_{ij} : binary interaction parameter in EF correlation

β_{ij}° reference binary interaction parameter at 298.15 K in EF correlation

γ_0 : fixed volume translation parameter [cm^3/mol] , Equation 7.13

γ_1 : temperature dependency term [cm^3/mol.K], , Equation 7.13

γ'_0 : fixed volume shift parameter [cm^3/mol] , Equation B.17

γ'_1 : temperature dependency term [cm^3/mol.K], , Equation B.17

γ_{c2} : fitting parameter in temperature dependent parameter c_2, equation 6.1

ΔX : change in variable (X) in respect to the value for the reference n-paraffin

ε : characteristic energy well of the potential function [J]

ζ : volume translation in Friction Theory model

$\theta_{i,o}$: temperature shape factor in Extended Corresponding States model

κ : empirical association parameter in Chung et al. (1984), Equation 2.7, or

: viscous friction coefficient in Friction Theory model

$\hat{\kappa}$: reduced viscous friction coefficient in Friction Theory model

λ : characteristic viscosity reducing parameter in Jossi et al. (1962) model

μ : viscosity [mPa.s]

$\hat{\mu}_f$: reduced frictional viscosity

ξ : viscosity reducing parameter in [(mPa.s)-1], Equation 2.12 and 2.27

ρ : density [kg/m^3]

ρ_s^* : compressed state density [kg/m^3]

ρ_s^o : compressed state density in vacuum [kg/m^3]

σ : hard sphere diameter of the molecules [Å]

τ : shear stress [N/m^2]

φ : volume fraction

$\phi_{i,o}$: volume shape factor in Extended Corresponding States model

φ_{ij} : weighting factor in dilute gas viscosity mixing rule

ω : acentric factor

Ω_v : collision integral

υ : geometric mean of mass and mole fraction, Equation 2.63

Subscripts

a attractive

b bounding

c	critical property
C30+	C_{30+} residue
cond-oil	condensate-oil binary
corr	correlation/ correlated
EOS	equation of state
exp	experimental
min	minimum
mix	mixture
norm	normalized
o	dilute gas property
oil	oil
r	reduced /or repulsive
(ref)	reference n-paraffin(s)
s	saturated liquid
sol-oil	solvent-oil binary

Abbreviations

AAD	average absolute deviation
ABP	average boiling point
AOSTRA	Alberta Oil Sands Technology and Research Authority
API	American Petroleum Institute
APR	Advanded Peng-Robinson
ASTM	American Society of Testing and Materials
BWR	Benedict-Webb-Rubin
CS	corresponding states
CSS	cyclic steam stimulation
DEG	diethylene glycol
ECN	effective carbon number
EF	Expanded Fluid

EG	ethylene glycol
EoS	equation of state
ES-SAGD	expanding solvent SAGD
GC	gas chromatography
GOR	gas-oil Ratio
HC	hydrocarbon
LASER	liquid addition to steam for enhanced recovery
LBC	Lohrenz-Bray-Clark
LGE	Lee-Gonzalez-Eakin
MAD	maximum absolute deviation
MARD	maximum absolute relative deviation (%)
MBWR	modified Benedict-Webb-Rubin
MD	molecular dynamics
MET	modified Enskog theory
MW	molecular weight
NBP	normal boiling point
NIST	National Institute of Standards and Technology
PNA	paraffins-naphthenes-aromatics
PR	Peng-Robinson
PT	Patel-Teja
PVT	Pressure-Volume-Temperature
RMS	root mean square
SAGD	steam-assisted gravity drainage
SAP	solvent aided process
SARA	saturates-aromatics-resins-asphaltenes
SAS	steam alternating solvent
SCN	Single carbon number
SG	specific gravity
SIMDIST	simulated distillation

SRK	Soave-Redlich-Kwong
TBP	true boiling point
TEG	triethylene glycol
TRAPP	TRAnsport Properties Prediction
TRC	Thermodynamics Research Centre
VAPEX	vapor extraction process
VBI	viscosity blending index
VMG	Vitrual Material Group
WK	Watson-K factor

CHAPTER ONE: INTRODUCTION

Viscosity (μ) is the resistance of a fluid to shear stress (Heidemann et al., 1987) and, in Newton's law of viscosity, is defined in terms of the velocity (u) gradient and shear stress (τ_{xy}) as follows:

$$\tau_{yx} = -\mu \frac{\partial u_x}{\partial y} \tag{1.2}$$

The shear stress is the cause for the momentum transfer and the viscosity is the proportionality constant between the driving force and the resulting velocity gradient. A high viscosity fluid will experience a lower velocity gradient at a given shear stress.

Viscosity, along with thermodynamic and thermophysical properties, is essential to the modeling of engineering processes. These processes are present in all aspects in petroleum industry; ranging from the recovery of reservoir fluids and natural gases from the reservoir to their ultimate conversion to final end-user products such as fuels and lubricants. The value of viscosity at given pressure, temperature and density is required to estimate the driving forces for the flow of fluid. Hence, hydraulic calculations for process facilities and fluid transportation systems (compressors pumps and pipelines) as well as the modeling of the flow in porous media depend on the prediction of fluid viscosity at process conditions. In addition, viscosity plays a role in heat and mass transfer calculations because the dimensionless groups correlating heat and mass transfer coefficients require the viscosity of the fluids of interest.

1.1 Heavy Oil and Bitumen and the Challenge of High Viscosity

In the spectrum of the petroleum fluids, viscosity is particularly important in design and development of the recovery, upgrading and refining process of heavy oils and bitumens, which comprise up to 70% of the world's oil resources (Alazard and Montadert, 1993). Heavy oils and bitumen are challenging to produce due to their high viscosity. For example, while the viscosity of the conventional oils ranges from approximately 1 mPa.s up to 10 mPa.s, the viscosity of heavy oils and bitumen can be up to more than 1 million mPa.s at ambient temperature. Heavy oils and bitumen have high viscosity either because

the source was immature or because an originally conventional deposit has been anaerobically biodegraded over geological timescales (Head et al., 2003). Heavy oils and bitumen are not recoverable by conventional methods, as they are virtually immobile and do not flow naturally toward the wellbore. Specialized recovery methods have been developed for these unconventional reservoirs which require the reduction of the viscosity prior to the production by heating, (thermal recovery methods), dilution with a solvent, or both.

Thermal recovery methods include steam flooding, cyclic steam stimulation (CSS), and steam-assisted gravity drainage (SAGD) (Butler 1997). Thermal methods are proven technologies that can achieve high oil recovery but are energy and water intensive.

Potential solvent based processes include solvent flooding and the vapor extraction process (VAPEX), (Butler and Mokrys 1989). Solvent-based methods, and in particular VAPEX, have been the subject of considerable research (Upreti, 2007) because they have the potential to reduce the energy consumption to approximately 3% of the SAGD (Singhal et al. 1996) and reduce greenhouse emission by 80% (Luhning et al. 2003). However, solvent based methods are not yet practiced in large-scale field operations.

Solvent-assisted steam processes include Expanding Solvent SAGD (ES-SAGD) (Nasr and Ayodele 2006), Solvent Aided Process (SAP) (Gupta et al. 2002, 2003), Liquid Addition to Steam for Enhanced Recovery (LASER) (Leaute 2002) and Steam Alternating Solvent Process (SAS) (Zhao 2004). These processes have the advantages of thermal methods but with reduced energy and water requirements. Field trials have commenced for several solvent-assisted steam processes (Leaute and Carey 2005, Gupta et al. 2005). Thermal solvent hybrid processes (Frauenfeld et al. 2009) have also been proposed where the injected solvent is heated by in-situ electrical heaters or small amounts of added steam.

Most surface treatment processes and transportation of the produced heavy crude oils also involve heating and dilution with solvents. For instance, dilution with condensate solvent

is often employed to meet the pipeline transportation viscosity specification of 275 mPa.s at 15°C for the produced oil.

1.2 Motivation and Knowledge Gap

The viscosity of fluids can be obtained from either measurements or viscosity models. In general, the accurate measurement of the viscosity (as a transport/flow property) is more time consuming and expensive than the measurement of the thermophysical properties such as density. In addition, petroleum fluids are multi-component mixtures ranging from natural gases to bitumens and they can undergo phase transitions and compositional changes during the recovery, production and refining processes. The measurement of viscosity for petroleum fluids over the wide range of pressures, temperatures, and compositions encountered in the industry is not practical in most cases. Therefore, reliable and accurate models (generally to within the experimental uncertainties) are required to estimate the petroleum viscosity in both liquid and gas phases.

Given the increased use of the reservoir and process simulators for design and optimization, an accurate viscosity model suitable for use with simulators is essential. A suitable viscosity model for this purpose must: 1) trace continuously the full range of single phase properties in the gas, liquid, critical, and supercritical regions; 2) be fast; 3) predict both pure-component and mixture viscosities; 4) be compatible with the fluid characterization used for the phase behavior model.

The current approach for modeling the viscosity in the reservoir and process simulators is to use of the models developed either for special types of reservoir fluids or devoted only to one phase. The viscosity correlations for natural gases and “Black Oils” are examples of the models implemented in reservoir simulators for limited applications. These models do not account for drastic compositional changes and cannot be used to model heavy oil dilution or crude oil fractionation. Process simulators generally use separate models for the viscosity of each hydrocarbon phase. For instance, HYSYS (Aspen Technology, 2005) uses a viscosity model based on the corresponding states (CS) theory for vapor phase viscosity. However, the liquid phase viscosities are calculated using methods such

as CS models or Twu's correlation (Twu and Bulls 1981, Twu 1985) based on the properties of the hydrocarbon system of interest.

In current compositional reservoir simulators, compositional viscosity models are imbedded in simulator packages as an alternative to the previous models. These models such as the LBC method (Lohrenz et al. 1964) and its modifications and CS model by Pedersen et al. (1984) (both reviewed in Chapter 2) commonly fulfill the four criteria presented above; however, both are biased towards natural gas mixtures and conventional crude oils. To date, simplistic approaches such as viscosity correlations and viscosity mixing rules with adjustable parameters are still in use for the recovery studies of the heavy oil and bitumen (Computer Modeling Group, 2011). However, with current increasing trend toward solvent-aided recovery methods of the heavy oils and bitumens and subsequent complex phase behavior of these systems, the use of compositional viscosity models is inevitable. Any potential model for this purpose must fulfill the four criteria.

1.3 Objectives

The objective of this study is to develop a compositional viscosity model for petroleum industry applications. The model must fulfill the four criteria presented above and be applicable to all aspects of the petroleum industry including natural gas processing, refining, conventional oil and gas recovery, heavy oil recovery, and bitumen extraction. The recently developed Expanded Fluid viscosity correlation (Yarranton and Satyro 2009) for hydrocarbons has the potential to meet all of these requirements but requires some development and testing. Hence, the detailed objectives of this study are defined as follows:

I. To test the applicability of the Expanded Fluid (EF) viscosity correlation to hydrocarbon mixtures; particularly asymmetric mixtures composed of the hydrocarbon compounds which are largely different in terms of the molecular size and chemical family. This test provides the required assurance that the EF correlation provides the accurate viscosity predictions for both pure components and mixtures based on state conditions; that is, pressure, temperature, and density.

II. To extend the EF correlation to non-hydrocarbons commonly encountered in petroleum industry applications. These compounds are either constituent components of the recovered petroleum fluid (water, carbon dioxide, nitrogen, hydrogen sulphide, and helium.) or used for the surface treatment of the recovered fluids (mainly organic alcohols used in natural gas processing applications). The model predictions are then assessed for natural gas mixtures.

III. To generalize the parameters of the EF correlation for hydrocarbon compounds as functions of the readily available physical properties. This development will reduce the need for the experimental viscosity data to tune the predictions of the EF correlation for hydrocarbon compounds. Hence, the model can be made predictive for ill-defined petroleum fluids such as petroleum distillation cuts and pseudo-components of the characterized crude oils.

IV. To propose a methodology to apply the EF viscosity correlation to crude oils characterized as mixtures of the defined components and pseudo-components. The methodology will use the generalized parameters of the EF correlation to provide viscosity predictions for the crude oils and is the basic of a new compositional viscosity model for the process and reservoir simulator applications. The predictions of the EF correlation with the proposed methodology are then assessed for characterized conventional crude oils, heavy oils, and bitumens.

V. To evaluate the performance of the EF viscosity correlation for the diluted heavy oil and bitumen systems. The predictions are assessed against viscosity data of the diluted heavy oil and bitumen with several solvents. The required density and viscosity data are collected using the in-house capillary viscometer with in-line density-meter.

1.4 Outline

Chapter 2 reviews current viscosity models in the literature which are either used in petroleum industry or have the potential to be used. The complex chemistry of the petroleum fluids is also briefly reviewed along with common analytical approaches to characterize them. Published viscosity and density data of the heavy oils and bitumens and their mixtures with solvents are summarized along with the modeling approaches to these systems.

Chapter 3 presents a description of the apparatus and procedures for the measuremet of viscosity and density of the heavy oil and bitumen systems in this study. The chemicals and materials used and the preparation of the dead oil samples, live oil samples, and diluted samples are reviewed. This chapter is related to Objective V.

Chapter 4 summarizes the basics of the Expanded Fluid (EF) viscosity correlation and its previously studied applications. This correlation is adapted for further developments in the subsequent chapters to fulfill the objectives of this thesis.

Chapter 5 addresses Objective I and the EF correlation is used to predict the viscosity of asymmetric hydrocarbon mixtures. A set of new mixing rules are developed for the EF correlation based on the mass fraction of the components which replaces the previously proposed volume fraction-based mixing rules.

In *Chapter 6*, Objective II is addressed and the EF correlation is extended to non-hydrocarbons. The framework of the correlation is modified to apply to compounds with significant hydrogen bonding. The predictions of the EF correlation are also evaluated for the sweet and sour natural gas mixtures and aqueous solutions of the methanol and glycols.

In *Chapter 7*, a methodology is proposed to predict and model the viscosity of the characterized crude oils (Objective IV) based on new correlations for the parameters of

the EF correlation as functions of the molecular weight and specific gravity (Objective III).

Chapter 8 addresses Objective V and evaluates the performances of the EF correlation along with two other compositional viscosity models in predicting the viscosity of the mixtures of heavy oil and bitumen with several solvents. Data used in this chapter are measurements based on the experimental methodology described in *Chapter 3*.

Finally, *Chapter 9* is a summary of major conclusions and recommendations for future research and developments on the EF viscosity correlation.

Note, the scope of this study is limited to Newtonian fluids as the most hydrocarbon compounds are in the operational temperature conditions in the petroleum industry. Recall that Newtonian fluids obey Newton's law of viscosity, Equation 1.1. For these fluids, the viscosity is fixed at a given temperature, pressure, and composition and is independent of the applied shear stress, its history, and the velocity gradient (shear rate). Non-Newtonian fluids do not obey the Newton's law of viscosity. Their viscosity depends on the applied shear stress and shear rate in addition to the state conditions. The viscosity of the non-Newtonian fluids can also vary with time. Heavy oils and bitumens may become non-Newtonian below room temperature and some modifications to the model may be required at low temperatures.

Also note, "viscosity" is also only used to refer to the dynamic viscosity (Equation 1.1) as opposed to the kinematic viscosity defined as the ratio of dynamic viscosity and density of the fluid. The unit of the viscosity used throughout this thesis is mPa.s (10^{-3} Pa.s) which is equivalent to the common unit of cP (10^{-2} Poise=10^{-2} $g.cm^{-1}.s^{-1}$) in petroleum industry.

CHAPTER TWO: LITERATURE REVIEW

This chapter presents a brief review of petroleum chemistry and the common analytical methods to determine the composition of the petroleum fluids. A summary is given of the available viscosity models in the literature with previous or potential application to petroleum industry processes. Finally, experimental and modelling studies on the viscosity of heavy oil/bitumen and solvent mixtures are summarized.

2.1 Petroleum Overview

Petroleum reservoir fluids are multi-component complex mixtures of hundreds of thousands of naturally occurring hydrocarbon compounds, organic compounds containing nitrogen, oxygen and sulphur, non-hydrocarbons, and trace amounts of metallic constituents such as nickel, vanadium and iron (Speight, 2007). Petroleum reservoir fluids from different sources vary considerably in terms of the composition; hence, their properties such as density, viscosity and volatility are different.

Petroleum is found in the reservoir as a liquid crude oil or as a natural gas. Also, when the pressure of a crude oil is reduced, the light hydrocarbons and non-hydrocarbons separate from the liquid petroleum reservoir fluids as a gas phase. Natural gas mixtures are mainly composed of light alkanes (methane to n-butane) and non-hydrocarbons such as nitrogen (N_2), carbon dioxide (CO_2), hydrogen sulfide (H_2S) and Helium (He) and traces of water vapor (Kidnay et al. 2011). Natural gas mixtures may also contain small amounts of heavier hydrocarbon components, other gaseous non-hydrocarbons, and inert gases. Therefore, the physical properties of both liquid and gas phase petroleum fluids are required for process modeling.

Several approaches are common to classify petroleum reservoir fluids. The primary classification is based on the volatility of the fluid which is related to the specific gravity (°API) and the amount of the dissolved gas (GOR) at reservoir conditions. Five types of reservoir fluid are defined: black oil, volatile oil, gas condensate, wet gas, and dry gas (McCain, 1990). Liquid petroleum reservoir fluids (crude oils) can also be classified

based on their specific gravity (API definition), Table 2.1, or on their density and viscosity (UNITAR definition), Table 2.2.

Table 2.1: Classification of crude oils based on the API definition.

Crude Oil Type	Density (kg/m³)	°API
Light	< 870	> 31.1
Medium	870−920	22.3−31.1
Heavy	920−1000	10.0−22.3
Extra Heavy	>1000	< 10.0

Table 2.2: UNITAR definition of heavy oil and bitumen.

Crude Oil Type	Viscosity (mPa.s)	Density (kg/m³)	°API
Light	< 100	< 934	> 20
Heavy	100-100000	934−1000	10−20
Bitumen	>100000	>1000	< 10

Crude oils are also classified according to their recovery method, into conventional oils and unconventional oils. Conventional oils are light and medium oils with relatively lower viscosities and are produced by traditional recovery methods such as primary production and water-flooding. Unconventional crude oils are either high viscosity heavy and extra heavy oils and bitumens or light oils in very low permeability reservoir rocks. Bitumen and heavy oils are usually produced using thermal recovery methods or open pit mining. The production of the tight oils requires extensive hydraulic fracturing.

2.1.1 Petroleum Chemistry

Methane, commonly referred to as C_1, is the simplest hydrocarbon found in the petroleum fluids and is the main constituent of the natural gas mixtures. The term C_n is widely used to name the hydrocarbons with equivalent "*n"* carbon atoms. Hence, C_2 and C_3 refer to ethane and propane, respectively. C_4 refers to normal and iso- butanes and C_5 represents the normal, iso- and neo- pentane. The number of isomers increases rapidly as the

number of carbon atoms increase above 6 in the molecule. Therefore, it is not practical to individually distinguish the higher molecular weight compounds. Conventionally, these compounds are represented as C_n (n>6) components and the sum of them is called C_{7+} fraction. The constituent compounds of C_n (n>6) components are mainly from the following chemical classes of hydrocarbons: paraffins, naphthenes, aromatics and heterocompounds (Altgelt and Boduszynski, 1993).

Paraffins are saturated hydrocarbons with straight or branched chains (normal and isoparaffins, respectively). The carbon atoms in paraffins are bonded with single covalent bonds.

Naphthenes are cycloparaffins; that is molecules containing a saturated ring structure. The saturated ring may have five, six or occasionally seven carbon atoms (cyclopentanes, cyclohexanes and cycloheptanes, respectively). Most naphthenes in petroleum have paraffinic side chains and may have more than one ring in the molecule; for example, mononaphthenes, dinaphthenes, and trinaphthenes. The rings can also be non-fused or fused if they share more than one carbon atoms.

Aromatics are hydrocarbon compound with at least one benzene ring. Aromatics are classified by the number of the aromatic rings in the molecule; for example, monoaromatics, diaromatics, and triaromatics. Aromatics in petroleum commonly have paraffinic side chains and may include naphthenic rings. The aromatic and naphthenic rings in this class of compounds can be fused or non-fused. The complexity of aromatic compounds increase greatly as the number of the rings increases due to multiple possibility of the relative arrangements of naphthenic and aromatic rings and side chains.

Heterocompounds are hydrocarbons from the above groups in which one or more heteroatoms (N, S, O, V, Ni, Fe) form part of the molecule (Altgelt and Boduszynski, 1993). The presence of the heteroatoms and their functionality adds to the complexity of the structural arrangements of the hydrocarbon compounds. Heterocompounds are commonly part of high molecular weight fractions of the petroleum fluids.

The percentage content of the first paraffinic (P), naphthenic (N) and aromatic (A) components in a petroleum fluid is often called the PNA distribution. Conventional light and medium oils have higher content of paraffins and naphthenes whereas heavy oils and bitumens are mostly composed of aromatics and heterocompunds.

2.1.2 Crude Oil Characterization

The distribution of the chemical classes of the constituent components of the crude oils is required to estimate the outcome of distillation processes in the refinery. It is also required to model any complex phase behavior of crude oils in both upstream (reservoir) and downstream (surface facility and refinery) processes. The challenge is how to simply but sufficiently represent the composition of a crude oil which is a mixture of hundreds of thousands compounds.

The light constituent compounds of the crude oils, including N_2, He, H_2S, C_1, C_2, C_3, iC_4, nC_4, iC_5 and nC_5, are identifiable by gas chromatography (GC). The heavier components are analyzed using crude oil assays. The most common assays for conventional crude oils are based on distillation and gas chromatography. Since the heavy oils and bitumens are composed mainly from non-distillable high molecular weight compounds, a full compositional analysis is not possible with conventional assays. Hence, chemical separation methods, such as SARA analysis, are more common for these crudes. These methods are summarized below.

2.1.2.1 Boiling Point Distillation Methods

Boiling point methods characterize the crude oil based on the relative volatility (relative vapor pressure) of the constituent compounds and is the most useful characterization for vapour-liquid separation processes such as distillation. The crude oil is divided into physical fractions or cuts in TBP (true boiling point at atmospheric pressure) distillation based on boiling point ranges. The cut properties, such as average molecular weight, density (specific gravity), and viscosity, are measured or estimated from correlations.

Note, the molecular weight of a given family of hydrocarbons increases monotonically with increasing boiling point. However, petroleum includes a large number of chemical

families and the variety of structures and boiling points at any given molecular weight increases as the molecular weight increases. Therefore, higher molecular weight or boiling point cuts contain a broader and broader distribution of components and corresponding properties, Figure 2.1. However, for practical reasons, the TBP fractions are commonly treated as pseudo-components each with a unique boiling point, molecular weight, density, and critical properties.

ASTM D-2892 is the current recommended TBP distillation method for the conventional crude oils (API 1997) with a final boiling point of 400ºC. This procedure specifies the equipment specifications, sample size, and calculations necessary to construct a TBP curve, a plot of the cumulative volume percent versus normal boiling point. In this procedure, distillation starts at atmospheric pressure but a vacuum up to 40 mmHg is gradually applied as the distillation proceeds. After the distillation, the sub-atmospheric boiling points are converted to the normal boiling points using inter-conversion methods such as the Maxwell and Bonnell (1957) vapor pressure correlation. ASTM D-86 is a fast, simple and inexpensive alternative to ASTM D-2892. This procedure utilizes batch atmospheric distillation and is applicable to light crude oils. Empirical correlations are used to convert D-86 data to a TBP curve (API 1997).

To extend the applicability distillation assays to heavier crudes, vacuum distillation methods were developed. ASTM D-5236 and ASTM D-1160 can be considered as extensions of ASTM D-2892 and ASTM D-86 to further distil their residues to boiling points as high as 525ºC. The ASTM D-5236 procedure is performed at pressures as low as 1.0 mmHg. However, this procedure does have limited applicability due to lack of standard conversion methods to TBP. ASTM-D1160 is performed using the exact setup of ASTM D-86 and can attain vacuum pressure of 10 mmHg. API (API 1997) provides recommendations to convert the ASTM-D1160 data to a TBP curve.

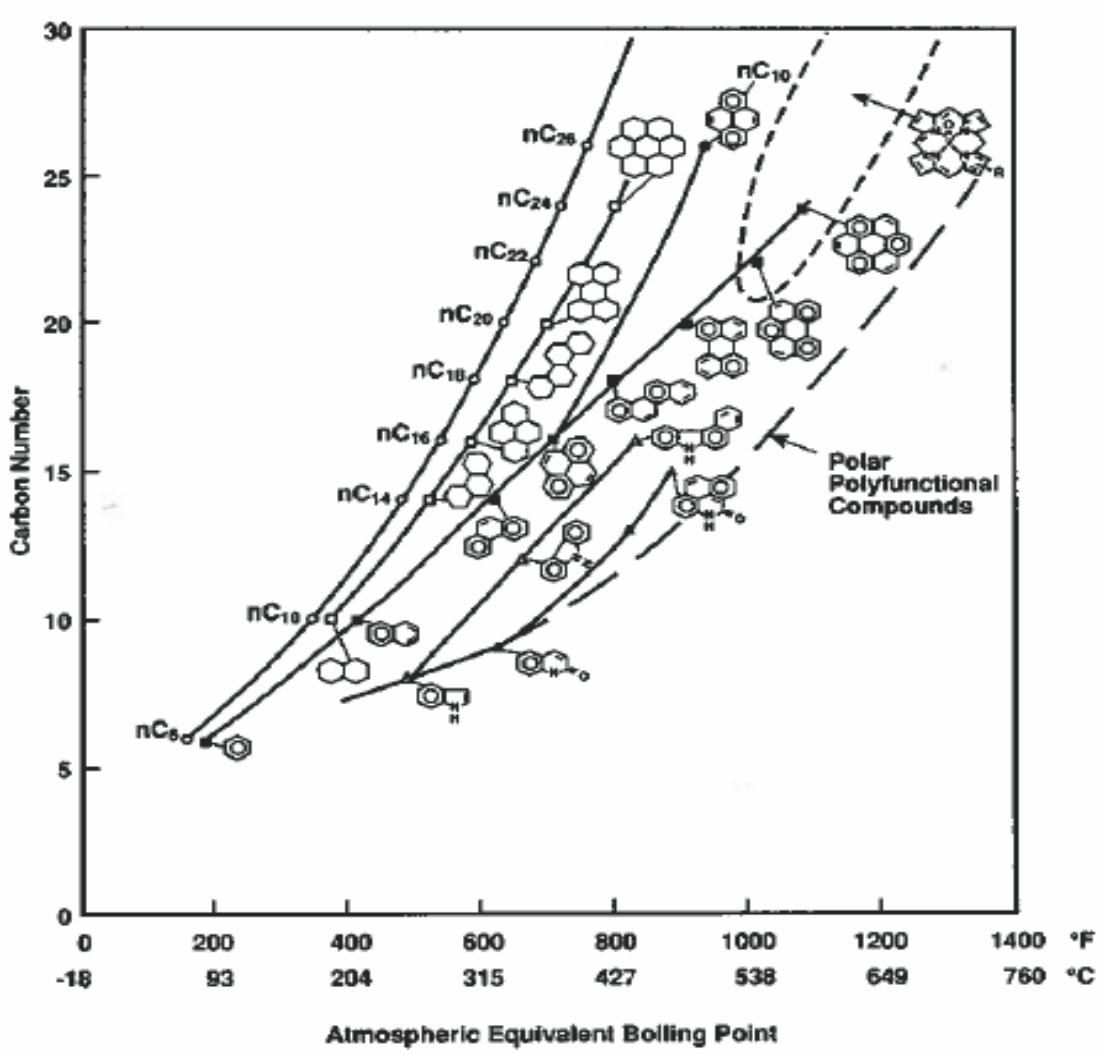

Figure 2.1: The effect of the molecular structure and size on the atmospheric equivalent (normal) boiling point; adapted from Altgelt and Boduszynski (1993).

2.1.2.2 Gas Chromatographic Methods

Gas chromatographic (GC) methods are used to determine the composition of gaseous samples as well as liquid crude oils based on the partitioning of individual species between a mobile gas phase and an immobile stationary phase. For both applications, helium is commonly used as the carrier gas unless other considerations require use of nitrogen or hydrogen. In general, GC analysis has higher resolution than the distillation-based methods. A perfect analytical distillation column may have a separating power of 50 theoretical plates in comparison to GC columns with about 500 equivalent theoretical

plates per foot (i.e. 15000 theoretical plates for a 10 meter capillary column). Therefore, GC is preferred and widely used as an alternative to the distillation-based methods as it also requires smaller sample size and is considerably faster.

The use of the GC for crude oils is based on the observation that retention time of the hydrocarbon compounds from general non-polar column is directly related to their boiling point. Hence, the low boiling point compounds elute first and so on. The response of the flame ionization detectors (FID) of the GC for crude oils is almost proportional to the mass of the eluted compounds passing through the detector. These reproducible relationships are the basis of the correlating the retention time to the boiling point in order to create a simulated distillation (SIMDIST) (Speight, 2007). To preserve the high resolution of the capillary columns and prevent flooding with too much injected sample, the crude oil sample is diluted with a volatile solvent. The common diluent is CS_2 as it completely dissolves all petroleum components and has almost no signal in FID detectors.

A gas chromatogram of crude oil is composed of many peaks which are individually identifiable and resolvable for light hydrocarbons up to approximately C_7. However, the peaks for higher molecular weight compounds of the crude oils are not resolvable as they overlap and form a continuous spectrum. Therefore, the tip of the peaks for identified known heavy n-paraffin are used to quantify the GC analysis. Since the paraffinic peaks become generally faint for heavier crude oils, a timing run is performed by spiking the sample with n-paraffins standard to correctly identify the times of elution. To quantify the GC chromatogram, the boiling point curve of the crude oil is calculated based on the boiling points of the successive members of the n-paraffin homologous series; that is, single carbon number (SCN) fractions. The mass of the fraction of the oil with boiling points between the boiling points of nC_{i-1} to nC_i, SCN fraction of "n", is calculated as the area under chromatogram from the end of the response peak of nC_{i-1} to the end of the response peak of nC_i.

A common GC assay analysis is composed of three runs: 1) empty or solvent-only run to account for zero shift caused by stationary phase elution at high temperatures; 2) the crude oil sample for analysis, and 3) the sample spiked with a known mass of "standard" which can be completely be eluted during the GC run. The result of the first runs is used to correct the measured mass of the SCN fractions. Since the GC injection techniques are not able to vaporize the entire crude oil, the heaviest compounds are not on the chromatogram and left as the residue. Based on the measured mass of the "standard" from the third run, the non-eluted mass of the crude oil is estimated and then the calculated mass of the eluted SCN fractions are scaled up. The main drawback of the GC analysis is the lack of the physical distillation cuts; thus, properties such as molecular weight and specific gravity are not provided by the analysis for each SCN fraction. These values are commonly assigned by standard correlations such recommended values of Katz and Firoozabadi (1978). Also, the method can be biased toward paraffins for aromatic fluids as the response of the detectors are calibrated against the standard n-paraffins samples (VMG, 2009).

There are three standard GC assay procedures: ASTM D-2887, ASTM D-3710, and ASTM D-7169. ASTM D-2887 is the most common procedure and provides data for the range of hydrocarbons from C_5-C_{44} corresponding to maximum boiling point of 538ºC. ASTM D-3710 is recommended for characterization of gasolines (API, 1997) with final boiling points less 260 ºC. ASTM D-7169 is the high temperature simulated distillation procedure for a final boiling point of 750ºC corresponding to elution of C_{120}. Although API (1997) provides correlations to convert data from ASTM D-2887 and ASTM D-3710 to TBP curves, their reliability is less proven (VMG, 2009). In general, checking the accuracy of the SIMDIST above C_{25} is difficult because C_{25} is the upper limit of reliable TBP distillation data for n-paraffins (Whitson and Brule, 2000). Although GC assay can be used to analyze the samples to higher SCNs, systematic losses begin to occur above about C_{22} and increase at higher carbon numbers. An arbitrary limit of C_{25} or C_{30} is used in many laboratories, but some routinely produce analyses thorough C_{50+}.

2.1.2.3 Chemical Separation Methods

Chemical separation methods are used to determine the composition of the crude oils based on the relative amount of the compounds from different chemical families. PNA analysis is one of these methods and is based on the gas chromatography with series of different columns. This method is only applicable to crudes with final boiling points of 200 ºC.

SARA analysis is another chemical separation method based on solubility and polarity of the constituent compounds of the non-volatile oils. SARA stands for Saturates, Aromatics, Resins and Asphaltenes. Saturates are non-polar compounds and include paraffins and naphthenes. Aromatics, resins and asphaltenes form the continuum of monoaromatic and polyaromatic compounds with increasing molecular weight, aromaticity, polarity, and heterocompound content. Resins are dark brown liquid at room temperature and are soluble in most hydrocarbon solvents but insoluble in acetone. Asphaltenes form a dark solid brown powder at room temperature and include the most aromatic and the most polar compounds of the crude oil with the highest molecular weight, density, and heterocompound content. Asphaltenes are insoluble in paraffinic solvents such as n-heptane and n-pentane but soluble in aromatic solvents such as benzene and toluene. Asphaltenes are known to self-associate forming macromolecules of approximately 6-10 molecules (Speight, 1999). There is no clear distinction between the properties of the aromatics, resins, and asphaltenes fractions and their relative amounts and properties depend on the method used to separate them.

Figure 2.2 shows a simplified diagram of SARA analysis procedure based on ASTM D-2007. SARA analysis of a dead crude oil starts by topping the oil to remove the relatively volatile compounds up to either C_8 or C_{14}, depending on the procedure of the laboratory. Then, the asphaltenes were separated using excess volumes of a paraffinic solvent, commonly n-pentane or n-heptane. The de-asphalted oil, called maltenes, is recovered by evaporating the excess solvent. Then, the maltenes is further separated into saturates, aromatics and resins fractions using liquid chromatography. The chromatography column composed of two parts: the upper column containing Attapulgus clay to adsorb resins and

the lower column containing silica gel to adsorb aromatics. Saturates pass through without being adsorbed. Aromatics and resins are later recovered using different mixtures of solvents. The SARA composition is determined from the mass of the recovered SARA fractions. The average molecular weight and density of SARA fractions are readily measurable. However, this type of the characterization of the crude oils is relatively coarse as millions of compounds are lumped into four fractions. There is no standard method of constructing a TBP curve based on the SARA analysis.

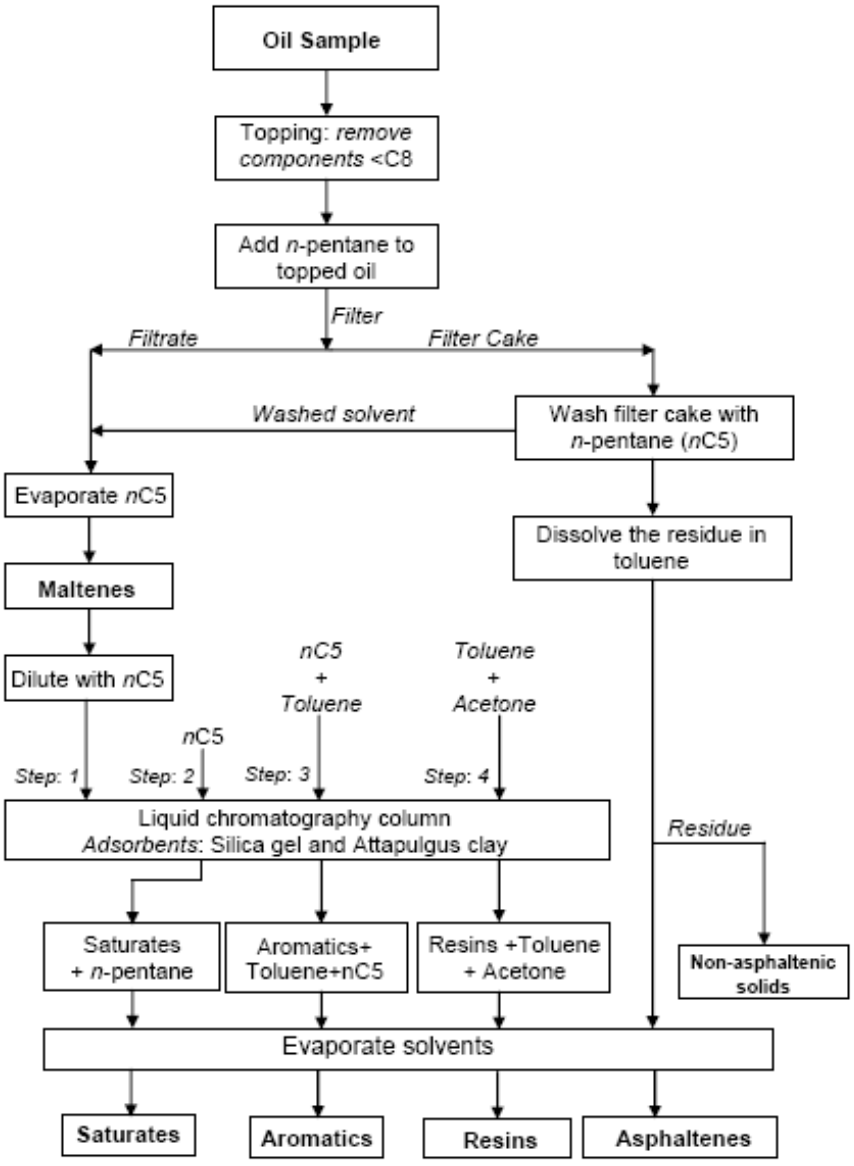

Figure 2.2: Procedure of SARA analysis method based on separation of C_5 asphaltenes; adapted from Tharnivasan (2012).

2.2 Viscosity Models

Viscosity models describe the change in the viscosity of fluid as the pressure, temperature and composition change. Numerous viscosity models are available in the literature. Poling et al. (2000) and Reid et al. (1987) provided critical reviews of the viscosity models developed for pure gases and liquids and mixtures. An extensive summary of the models was also prepared by Monnery et al. (1995). Mehrotra et al. (1996) reviewed the models developed particularly for liquid hydrocarbons and petroleum fluids.

Viscosity models can be divided into three main groups: theoretical, semi-theoretical and empirical models. Theoretical models are based on gas kinetics theory and statistical mechanics, and viscosity is related to the intermolecular potential functions. Semi-theoretical models have a theoretical basis such as the corresponding states theory or applied statistical mechanics, but they commonly have adjustable parameters for each fluid. These parameters are determined from experimental viscosity data of the fluid. Empirical methods are the correlations developed based on the experimental observations and relate the viscosity to pressure, temperature, and density.

Some of the viscosity models were developed only for one phase, either gas or liquid, while others are applicable to all fluid phases. The viscosity of the fluids in gas phase is mainly due to the momentum transfer within the fluid from two-body collisions and interactions. Theoretical and semi-theoretical models based on the kinetic theory of gases were successfully developed to predict the viscosity of the dilute gases. However, for dense gases and liquids, multi-body interaction of the closely packed molecules dominates the momentum flux between within the fluid. A theoretical viscosity model for dense fluids must take into account both short and long range interactions of the molecules, including short range repulsion and hydrogen bonding and long range attractive force fields and polar-polar interaction, as well as the statistical description of the multi-body collisions. These interactions are simplified differently in different models and, consequently, there is no widely accepted theoretical model for the viscosity of the dense fluids. Semi-theoretical models are more convenient for these fluids in which the model is tuned for the effects of the interactions using some viscosity data of the fluid.

A summary of the models widely used for the viscosity of the hydrocarbons and non-hydrocarbons commonly encountered in the petroleum industry is provided below. Although, the objective of this thesis is to develop a full phase viscosity model, single-phase liquid viscosity models are also reviewed as they are commonly used in modelling studies in petroleum engineering. In addition, the dilute gas viscosity models are important as they are usually an input to the full-phase models based on the residual viscosity concept. They also are basis of some of the full-phase viscosity models.

2.2.1 Gases and Vapors

2.2.1.1 Low Pressure Pure Gas Viscosity

The viscosity of the pure gas at dilute condition based on the elementary kinetic theory of gases (Reid et al., 1987) is expressed as follows:

$$\mu_o = 26.69\times10^{-4}\frac{(MW.T)^{1/2}}{\sigma^2} \tag{2.1}$$

where dilute gas viscosity (μ_o) is in mPa.s, MW is the molecular weight in g/mol, T is temperature in K, and σ is the hard sphere diameter of the molecules in Angstroms. In this model, the molecules are assumed to be rigid spheres which move randomly and collide but do not otherwise interact. Note, the dilute gas condition is the range of temperature and pressures where the gas viscosity is independent of density (high temperatures and low pressures). At these conditions, the dilute gas viscosity increases with temperature and is independent of pressure.

The effect of molecular interactions (attraction and repulsion during the collision) on the dilute gas viscosity is typically included via the collision integral (Ω_v) as follows:

$$\mu_o = 26.69\times10^{-4}\frac{(MW.T)^{1/2}}{\sigma^2\Omega_v} \tag{2.2}$$

This expression is known as the Chapman-Enskog theory and was derived with the following assumptions: 1) only binary collisions of molecules occur; 2) classical mechanics govern the collisions; 3) the collisions are elastic; and 4) the intermolecular force fields are symmetrical. The collision integral is solved for a specified intermolecular potential function.

Many authors developed equations to estimate the collision integral for different intermolecular potential functions (Reid et al., 1987). For example, Neufeld et al. (1972) developed an empirical correlation for the collision integral based on the Lennard-Jones intermolecular potential, given by:

$$\Omega_{\upsilon} = 1.16145\left(T^{*}\right)^{-0.14874} + 0.52487\exp\left(-0.7732\,T^{*}\right) + 2.16178\exp\left(-2.43787\,T^{*}\right) \tag{2.3}$$

where T^{*} is the dimensionless temperature and is related to characteristic energy of the potential function ε as follows:

$$T^{*} = \frac{kT}{\varepsilon} \tag{2.4}$$

Equations 2.1, 2.2 and 2.4 require numerical values of ε and σ which must be obtained from a simultaneous regression of experimental viscosity data for each fluid. However, as Reid et al. (1987) emphasised, there is more than one acceptable set of ε and σ that can describe the dilute gas viscosity of any given compound as long as the temperature range is not too broad. In addition to this difficulty of obtaining unique set of the parameters, the simplified assumptions of the theory limit its application to spherically symmetric monatomic molecules at high temperatures. Therefore, many authors (Chung et al., 1984; Lucas, 1980; Reichenberg, 1975 and 1979) opted to develop empirical or semi-theoretical dilute gas viscosity models based on more easily quantifiable parameters of the compounds.

Chung et al. (1984) developed the following empirical modification of the Chapman-Enskog theory:

$$\mu_{o} = 40.785\frac{F_{c}\sqrt{MW.T}}{v_{c}^{\,2/3}\Omega_{\upsilon}} \tag{2.5}$$

where *MW* is molecular weight in g/mol, *T* is temperature in K, v_c is the critical volume in cm^3/mol which replaced the hard-sphere diameter ($v_c \sim \sigma^3$). The viscosity collision integral is given by the correlation developed by Neufold et al. (1972), Equation 2.3. The parameter ε in Chapman-Enskog theory is related to the critical temperature of the compound and the dimensionless temperature is redefined as follows:

$$T^* = 1.2593\frac{T}{T_c} \tag{2.6}$$

F_c in the Equation 2.5 is an empirical correction factor accounting for the molecular shape, polarity, and association of the dilute gas molecules and is given by:

$$F_c = 1 - 0.2756\omega + 0.05903\left(I_d^*\right)^4 + \kappa \tag{2.7}$$

where ω is the acentric factor, κ is empirical association parameter to be regressed from experimental data, and I_d^* is dimensionless dipole moment given by:

$$I_d^* = 131.3\frac{I_d}{\sqrt{v_c T_c}} \tag{2.8}$$

where I_d is dipole moment in debyes. For largely non-polar hydrocarbons, Equation 2.8 reduces to:

$$F_c = 1 - 0.2756\omega \tag{2.10}$$

Reduced coordinates for viscosity can be defined based on Equation 2.1. Since v_c is proportional to σ^3 and to RT_c/P_c, the dimensionless reduced dilute gas viscosity is defined as follows:

$$\mu_{or} = \xi\mu_o$$

$$\xi = 1760\left(\frac{T_c}{MW^3 P_c^4}\right)^{1/6} \tag{2.11}$$

where ξ is the viscosity reducing parameter in $(\text{mPa.s})^{-1}$ and T_c and P_c are critical temperature and pressure in K and bars, respectively. Several authors have proposed expressions for the reduced viscosity as function of the reduced temperature (Stiel and Thodos, 1961). For example, Lucas (1980) proposed the following expression:

$$\mu_r = \left[0.807\,T_r^{0.618} - 0.357\exp\left(-0.449\,T_r\right) + 0.34\exp\left(-4.058\,T_r\right) + 0.018\right]F_P^o F_Q^o \tag{2.12}$$

where F^o_P and F^o_Q are correction terms with temperature dependent expressions for the polarity and the quantum effects (the latter only for He, H_2 and D_2), respectively. Once

the reduced viscosity is defined, the actual dilute gas viscosity is determined from Equations 2.11 and 2.12.

In an alternative approach, Yaws (1999, 2008) used a third degree polynomial equation to represent the dilute gas viscosity as a function of temperature:

$$\mu_o = A + B\,T + C\,T^2 + D\,T^3 \tag{2.13}$$

where *A*, *B*, *C* and *D* are compound specific coefficients which are provided by Yaws (1999, 2008). The numerical values of the coefficients were determined by regression from the available experimental data for several hydrocarbon and non-hydrocarbon compounds. In the absence of the experimental data, the coefficients were regressed to data generated by the semi-theoretical dilute gas viscosity models such as Chung et al. (1984).

Reid et al. (1987) studied the accuracy of the Chung et al. (1984) and Lucas (1980) methods against the experimental viscosity data of 29 compounds. The average absolute deviations of the methods were 1.9% and 3%, respectively. Although the accuracy of the regressed correlation of Yaws was not studied, it is more convenient than other models for practical applications. Note that none of these models are applicable to calculate the gas viscosity in the vicinity of the critical region where pressure is relatively high.

2.2.1.2 Low Pressure Gas Mixture Viscosity

Although the Chapman-Enskog theory was extended to dilute gas mixtures (Hirschfelder et al., 1954), the final expressions are complicated and less convenient to use. Instead, several simplified extensions of the theory were given in the form of interpolative mixing rules. These mixing rules describe the dilute gas mixture viscosity as a function of the composition and individual dilute gas viscosity of the components. The most consistently accurate mixing rule was developed by Reichenberg (1979) which incorporates elements of gas kinetic theory. However, the method is very complicated and requires several properties of the components in addition to the dilute gas viscosity at the given temperature. Simplified mixing rules in the following form are more common:

$$\mu_{o,mix} = \sum_i \frac{x_i \mu_{o,i}}{\sum_j x_j \varphi_{ij}} \tag{2.14}$$

Herning and Zipperer (1936) defined the φ_{ij} as:

$$\varphi_{ij} = \sqrt{\frac{MW_j}{MW_i}} \tag{2.15}$$

Alternatively, Wilke (1950) defined the φ_{ij} as:

$$\varphi_{ij} = \frac{\left[1+\left(\mu_{o,i} / \mu_{o,j}\right)^{0.5}\left(MW_i / MW_j\right)^{0.25}\right]^2}{\left[8\left(1+MW_i / MW_j\right)\right]^{0.5}} \tag{2.16}$$

Authors such as Chung et al. (1984) and Lucas (1980) also proposed mixing rules to use with their own models. In this group of mixing rules, the critical and other properties of the mixture are estimated from the pure component properties and composition. Then, the dilute gas viscosity model for pure component is used to estimate the dilute gas viscosity of the mixture.

Reid et al. (1987) compared the performance of different mixing rules and models against the viscosity data of 10 randomly selected binary gas mixtures. The mixing rule of Reichenberg (1979) was found as the most accurate one with AARD of 1.7%. The AARD of the predictions from the mixing rules of Equations 2.14 and 2.15 were 3.5% and 3.0%, respectively. The predictions with the approaches proposed by Chung et al. (1984) and Lucas (1980) were less accurate with AARD of 4.1% and 3.5%, respectively.

2.2.1.3 High Pressure Gas Viscosity

Unlike the monotonic increase of the viscosity of the dilute gases with temperature, the viscosity of dense gases can increase or decrease with temperature depending on the pressure, due to differences in the momentum transfer mechanisms. The momentum transfer in dense gas occurs over the collision distances of the molecules bigger than their hard-sphere diameter. The collision rate is, in fact, a direct function of the number density

of the molecules. Hence, as the temperature increases at constant pressure, the density and the collision rate decrease and so does the viscosity of the dense gases.

Enskog (1922) developed one of the few theoretical approaches to model the viscosity of dense gases. His development was an extension to the hard sphere dilute gas model with empirical modifications to account for the finite size of the molecules, non-zero collision diameter, and the density dependence of the collision rate.

A number of the dense gas viscosity models were used as the basis for the full-phase viscosity models and will be discussed in Section 2.2.3. These models include the hard sphere model of Enskog (1922) and the residual viscosity model of Jossi et al (1962). Most of these viscosity models empirically relate viscosity to pressure and temperature. Lucas (1980) and Reichenberg (1979) extended their dilute gas viscosity models to the dense gas by including temperature-dependent effects in the reduced pressure. Chung et al. (1988) also extended their technique to dense gas by including density dependent corrections to Equation 2.5. Poling et al. (2000) evaluated the performance of the Reichenberg, Lucas and Chung methods against data of 6 hydrocarbon and polar/non-polar hydrocarbons and found similar accuracies with AARDs of 5.7%, 4.5% and 3.7%, respectively.

Whitson and Brule (2000) recommended the method of Lucas to estimate the viscosity of petroleum reservoir gases. They also mentioned that most PVT laboratories report estimated gas viscosities using the empirical correlation of LGE (Lee-Gonzalez-Eakin). The LGE method (Lee et al., 1966) is based on 3000 natural gas viscosity data points and relates the viscosity to the molecular weight and the density of the gas using an exponential expression. The accuracy of the method is generally within 4% of the measurements (Lee et al., 1966; McCain, 1990), but can be up to 20% for gas condensate fluids.

2.2.2 Liquids

As discussed before, there is no widely accepted simple theoretical model for the viscosity of liquids. Rather empirical viscosity models are developed to describe the change in the viscosity of the liquids with temperature. For most of the liquids, the logarithm of the viscosity varies almost linearly with the inverse of temperature (Reid et al., 1987) from the freezing point up to the normal boiling point (about the reduced temperature of 0.7). Above the normal boiling point, this observation is no longer valid as the viscosity of the liquid tends to merge to the viscosity of the gas at the critical point. A summary of the main correlations for liquid viscosity is provided below.

2.2.2.1 Andrade Equation

The Andrade equation (1934), first proposed by de Guzeman (1913), can be considered as the most well-known empirical correlation for the viscosity of the liquids and is given by:

$$\ln \mu = A + \frac{B}{T} \tag{2.17}$$

Although the correlation was proposed empirically based on observation, the form of the correlation and the description of the parameters were later suggested by the less rigorous semi-theoretical reaction rate theory by Eyring (1936). Nonetheless, the Andrade correlation is most commonly used by regression of the constants to experimental liquid viscosity data. Alternatives to the Andrade equation are also available which simply add extra parameters to the same basic functional form to more accurately regress the available viscosity data over a broader range of temperature. For example, the three-parameter Vogel (1921) equation is given by:

$$\ln \mu = A + \frac{B}{T + C} \tag{2.18}$$

Reid et al. (1987), Viswanath and Natarajan (1989) and Duhne (1979) provided tabulated values and recommended temperature ranges of the regressed parameters of Equations of 2.17 and 2.18 for several pure compounds. Similarly, API (1997) and Yaws (2008) used the following extension of the Andrade equation to represent the liquid viscosity of hundreds of hydrocarbons and non-hydrocarbons with tabulated regressed parameters:

$$\ln \mu = A + \frac{B}{T} + C \ln T + D\, T^{E} \tag{2.19}$$

Several authors tried to generalize the parameters of the Andrade and Vogel equations to make the equations predictive rather than completely correlative. The developments were mostly correlations of the parameters to the structure of the molecules based on group contributions. van Velzen et al. (1972) related the parameters of the Andrade equation to a newly introduced property, the equivalent chain length. This property was defined as the sum of the total carbon atoms of the compound and the equivalent contribution of the structural/configurational groups. The correlations were developed using a database of liquid viscosity of 314 compounds and an average deviation of less than 15% was obtained for 272 of the compounds. The van Velzen method requires complicated calculations of the group contributions and commonly predicts the viscosity of the lighter compounds of the homologous series with higher deviations. Orrick and Erbar (1974) developed another group contribution method to estimate the parameters of the Andrade equation using the molecular weight and density at 20 ºC of compound as scaling parameters. Their method was developed and tested on a database of 188 organic compounds with overall AARD of 15%. Reid et al. (1978) independently compared the predictions of both methods against the experimental liquid viscosity data of 35 compounds with AARDs of 16% and 10.8%, respectively.

Allan and Teja (1991) correlated the parameters of the Vogel equation to the number of the carbon atoms for the n-alkanes homologous series from ethane to n-eicosane. They developed a one-parameter Vogel equation requiring determination of the effective carbon number of the organic compound using one single datum of the liquid viscosity. The AARD of the predicted viscosities with this method when applied to fifty hydrocarbon compounds were all less than 10%. However, Gregory (1992) showed that the use of the method for compounds with effective carbon number higher than 22 results in unrealistic viscosity behavior.

2.2.2.2 Walther (ASTM) equation:

The Walther equation is another two parameter empirical correlation to model the viscosity of liquid compounds, especially hydrocarbons and petroleum fluids. The equation was initially proposed by Walther (1931) to correlate the kinematic viscosity (υ) of the liquids to temperature as follows:

$$\log\left(\log\left(\upsilon+0.95\right)\right)=-m.\log\left(\frac{T}{T_o}\right)+\log\left(\log\left(\upsilon_o+0.95\right)\right) \tag{2.20}$$

Subsequently, several modifications of the equation were developed and used to model both the kinematic and dynamic viscosity. In 1932, ASTM used the following version of the equation to develop standard charts of the kinematic viscosity versus temperature:

$$\log\left(\log\left(\upsilon+0.8\right)\right)=b_1+b_2\log\left(T\right) \tag{2.21}$$

At the time, these charts were based on data at temperatures up to 533 K and kinematic viscosities down to 0.3 cSt. With the availability of data over a broader range of temperatures, Wright (1969) modified the Walther equation to allow the linearization of the variation of the kinematic viscosity at broader ranges of temperature (200-645 K). This version of the Walther equation was used in updated viscosity-temperature charts of ASTM (1981). Twu (1985) pointed out that this modified version becomes equivalent to Equation 2.21 (with constant 0.7 instead of 0.8) for kinematic viscosities higher than 2 cSt. A review of different modifications of the Walther equation for kinematic viscosity along with a new development was provided by Seeton (2006).

Mehrotra and co-workers extensively used the Walther equation in the form of Equation 2.21 to model the dynamic and kinematic viscosity of pure hydrocarbons and petroleum fluids. The equation was initially used for bitumens (Svrcek and Mehrotra, 1988) and will be discussed in section 2.3.2. Following a study on the applicability of the equation to middle-east crude oils (Mehrotra 1990a), Mehrotra applied it to atmospheric dynamic viscosity (μ) data of 273 pure heavy (Mehrotra 1991a) and 89 pure light and medium hydrocarbon compounds (Mehrotra 1991b). The parameters b_1 and b_2 were regressed for all compounds with an overall AARD and maximum AARD of 1.1% and 16% for pure heavy HCs and 2.7% and 6.6% for light and mediun HCs, respectively. Based on the observed linear cross-correlation between parameters b_1 and b_2, a one-parameter version

of the correlation was also developed. The single-parameter *b* was then regressed for all compounds with an overall AARD and maximum AARD of 7.1% and 56.6% for pure heavy HCs and 9.4% and 37.9% for light and medium HCs, respectively.

The parameter *b* of the one-parameter correlation was generalized for each family of the compounds to physical and thermodynamic properties such as molecular weight and boiling point at 10 mmHg for heavy HCs and molecular weight, boiling point at 760 mmHg, acentric factor, and critical temperature for light and medium HCs. Detailed error analysis was not provided for viscosity predictions with the generalized *b* parameter. Mehrotra (1994) also utilized the concept of the effective carbon number by Allan and Teja (1991) and correlated the parameter *b* to the effective carbon number (ECN) for 70 liquid hydrocarbons with overall AARD of 5%.

2.2.2.3 Free Volume Theory

Batschinski (1913) introduced the concept of the free volume by demonstrating linear plots of fluidity ($1/\mu$) versus specific volume for non-associating liquids at atmospheric pressure. This observation was modeled by Hildebrand (1971) with the following expression relating fluidity to the expansion from an intrinsic molar volume (v_∞):

$$\frac{1}{\mu} = \frac{E\left(v - v_\infty\right)}{v_\infty} \tag{2.22}$$

Hildebrand considered the fluidity as the result of the relative expansion of the fluid and the energy transfers during the collisions of the neighboring molecules, represented by parameter *E*. Regressed values of the parameters v_∞ and *E* were reported by Hildebrand and Lamoreaux (1972) for CO_2 and several hydrocarbons. The values of v_∞ for each compound were found approximately one third of the critical volume whereas the parameter *E* was found to be linearly related to the molecular weight of n-alkanes. However, Hildebrand's formulation has limited applicability at reduced temperatures below 0.46 (Ertl and Dullien, 1973) where the viscosity deviates positively from the trend suggested by the model.

Another model for the dependence of fluidity on free volume was developed empirically by Doolittle (1951) and is given by:

$$\frac{1}{\mu} = A\exp\left(\frac{-d\, v_{\infty}}{v - v_{\infty}}\right) \tag{2.23}$$

where *A* and *d* are fluid-specific constants. Doolittle (1952) showed that the parameter *A* can be considered as a general fixed constant for the n-alkane homologous series from n-hexane to n-heptadecane, based on the atmospheric viscosity data. The parameter *d* was also found to depend on the molecular weight of the n-alkanes, in the form log(*d*) proportional to $MW^{1/20}$. Doolittle's formulation provided an excellent fit to the isothermal high-pressure viscosity data of glass forming liquids at high compression ratios (Cook et al. 1993, Herbst et al. 1994). However, this formulation lacks the ability to differentiate the independent effects of pressure and temperature changes on liquid viscosity. Hence, some authors developed modified versions of the model with temperature and pressure dependent parameters (Yasutomi et al. 1984, Bair et al. 2001).

2.2.2.4 Black Oil Viscosity Correlations

This group of the empirical viscosity correlations were developed for petroleum reservoir fluids to use with "black oil" fluid characterizations. Black oil fluid models represent the liquid reservoir fluid as a mixture of dead (gas free) oil as the solution gas. The oil density and the amount of dissolved solution gas are presented as functions of pressure at a fixed temperature. The viscosity is then correlated to black oil properties including the gas-oil ratio, bubble point pressure, API gravity, gas specific gravity and the viscosity at standard conditions. Examples are the correlations of Chew and Connally (1959), Beggs and Robinson (1975), Khan et al. (1987), Petrosky and Farshad (1995). Most of these models are based on the experimental dead and live reservoir fluid data from specific geographical regions and may not apply to other regions.

2.2.2.5 Viscosity Correlations for Petroleum Fractions

This group of empirical correlations are specifically developed for predicting the kinematic viscosity of petroleum fractions and distillation cuts at two temperatures; 100 ^{o}F and 210 ^{o}F. Examples of this approach are the Twu (1985) and API (1997)

correlations. Both correlations characterize the petroleum cut with a boiling point and specific gravity. Both methods recommend the ASTM (1981) modification of Walther equation to calculate the kinematic viscosities at any other temperatures. The API has limited range of applicability in terms of average boiling point and specific gravity compared with the Twu method. The parameters of these correlations were regressed using the kinematic viscosity data of several petroleum fractions (but not the same dataset) with overall AARDs of 8% and 16%, respectively. Bergman and Sutton (2012) compared both correlations along a group of other correlations against 9024 viscosity data points of crude oils and petroleum fractions with API gravity range of 5-80 at temperature range of 35-500 ºF. They found the overall average absolute deviations of the Twu and API correlations to be 20.4% and 19.4%, respectively. Bergman and Sutton (2012) then modified constants of Twu's correlation and reduced the average deviations to 16.6%.

In another approach, Beg et al. (1988) developed a generalized correlation for the kinematic viscosity of petroleum fractions based on the Andrade equation. The parameters *A* and *B* were related to the average boiling point and specific gravity of the cuts. The proposed method evaluated against more than 250 kinematic viscosity data points of several crude oils and provided fits/predictions within 15% of the measurements.

2.2.2.6 Viscosity of Liquid Mixtures

Empirical viscosity methods for liquid mixtures are either interpolative mixing rules or pure component viscosity models where the parameters of the model are calculated using mixing rules applied to the parameters of the mixture constituents. There are relatively few of the latter methods and they will be discussed later in the Full-Phase Models section. The former methods are more common and all assume the viscosity of the pure component constituents of the liquid mixture are known at the given temperature and pressure. Similar to the empirical pure liquid viscosity equations, the mixing rules are usually valid up to approximately the normal boiling point (T_r=0.7) of the pure component constituents of the mixture (Reid et al., 1987).

2.2.2.6.1 Well-Defined Mixtures

The first proposed mixing rules were mole, mass, or volume averages of a function of the viscosity of the components as follows:

$$f(\mu_{mix}) = \sum z_i \ f(\mu_i) \tag{2.24}$$

The most commonly used function is the logarithm of the viscosity (Arrhenius, 1887). Other examples are the inverse of viscosity or fluidity (Bingham, 1914) and the cube root of the viscosity (Kendall and Monroe, 1917). The latter mixing rule is recommended by API (API, 1997) for mixtures of pure hydrocarbons (viscosity ratio of 1 to 100), but is not reliable for higher viscosity ratio mixtures (Shu, 1984).

Irving (1977a and 1977b) reviewed more than 75 liquid viscosity equations including the above and other newer developed methods and evaluated them against experimental data for 318 binary mixtures. He found that the simple predictive interpolative methods in the form of Equation 2.24 are only effective for the mixtures of the similar components with the viscosities of the same magnitude. Among the other mixing rules with adjustable constants, Irving (1977a) concluded that the most effectual yet simple methods are the additive parabolic equations with one adjustable constant. One of the recommended mixing rules is the method of Grunberg and Nissan (1949) given by:

$$\ln\left(\mu_{mix}\right) = \sum_i x_i \ln(\mu_i) + \frac{1}{2}\sum_i \sum_j x_i x_j G_{ij} \tag{2.25}$$

where μ_i and x_i are the liquid viscosity and mole fraction of the component *"i"*. G_{ij}'s are the set of the adjustable parameters, the so called the binary interaction parameter between the components *"i"* and *"j"* with $G_{ij}=G_{jj}=0$. Equation 2.25 was shown to fit the experimental data of nonpolar+nonpolar, nonpolar+polar, polar+polar and aqueous mixtures with the root mean square (RMS) of 2.3%, 3.0%, 8.9% and 24%, respectively (Irving 1977a and b).

The values of the interaction parameters depend on the binary compounds and are generally considered to be pressure and temperature dependent. Isdale et al. (1985) proposed a complex group contribution method to estimate the G_{ij} values at 298 K. They found that the binary interaction parameter is independent of temperature for alkane-

alkane mixtures and for mixtures of associating/non-associating compounds. However, the data suggested that G_{ij} is slightly temperature dependent for other hydrocarbon mixtures and mixtures of associating compounds. Isdale et al. (1985) suggested that, for the latter binaries, the calculated value of G_{ij} at 298 K increases linearly toward G_{ij}=1 at 573 K. Similar alternatives to the Grunberg and Nissan method are the predictive UNIFAC-VISCO method (Chevalier et al., 1988; Gaston-Bonhomme et al., 1994), the multi-parameter McAllister (1960) mixing rule, and the mixing rule of Teja and Rice (1981a).

Teja and Rice (1981a) developed the following model for liquid viscosity prediction based on the analogy to the corresponding-states treatment for mixture compressibility factor (Teja and Rice 1981b):

$$\ln\left(\mu_{mix}\xi_m\right) = \ln\left(\mu_1\xi_1\right) + \frac{\omega_m - \omega_1}{\omega_2 - \omega_1}\left[\ln\left(\mu_2\xi_2\right) - \ln\left(\mu_1\xi_1\right)\right] \tag{2.26}$$

where subscript 1 and 2 refer to two reference fluids. ω is the acentric factor and ξ is the viscosity reducing parameter defined as:

$$\xi = \frac{V_c^{2/3}}{T_c^{1/2} MW^{1/2}} \tag{2.27}$$

The composition of the mixture determines the mixture viscosity by virtue of the mixing rules developed to calculate the molecular weight, critical temperature and volume and acentric factor of the mixture. Embedded in these mixing rules are two types of binary interaction parameters of order of unity to fit the available experimental data. Although any two liquid compounds with available viscosity data can be chosen as two reference fluids, Teja and Rice (1981a) suggested selecting them as two main components of the mixture. With this choice of the reference fluids, the equation 2.26 reduces to the following for the binary mixtures:

$$\ln\left(\mu_{mix}\xi_m\right) = x_1 \ln\left(\mu_1\xi_1\right) + x_2 \ln\left(\mu_2\xi_2\right) \tag{2.28}$$

Using the above mixing rule and adjusting one of the binary interaction parameters, Teja and Rice (1981a) could fit the experimental data of nonpolar+nonpolar, nonpolar+polar, polar+polar and aqueous binary mixtures in the database of Irving (1977a and b) with the root mean square (RMS) of 1.0%, 2.9%, 2.5% and 12%, respectively. Sun and Teja

(2003) also used equation 2.28 in terms of mass fractions and fitted the viscosity data of aqueous solutions of glycols by adjustment of two binary interaction parameters with overall AARD and MARD of 2.4% and 8.3%, respectively. Although the model of Teja and Rice (1981a) was developed for the liquid mixtures, it is used (Computer Modeling Group, 2011) to predict the viscosity of the pseudo-components of the reservoir fluids with the choice of ethane and n-eicosane as two reference fluids.

2.2.2.6.2 Ill-Defined Mixtures of Petroleum Fluids

The application of the simple additive mixing rules of to petroleum blends are commonly not successful (Shu, 1984) due to the extremely high viscosity ratios of the components of these mixtures. Also, these mixtures are ill-defined in terms of the detailed knowledge of the constituents of the petroleum fluids. Hence, mixing rules with binary interaction parameters estimated by group contribution methods or requiring critical constants of the components are not applicable.

A number of mixing rules have been proposed to determine the viscosity of the blends of the petroleum fluids (Lederer, 1933; Cragoe, 1933; Chrinos et al., 1983; Mehrotra et al., 1989; Twu and Bulls, 1981; Miadonye et al., 2000). Since these mixing rules were developed for diluted petroleum fluids with solvents, most of them are only applicable to binaries. For example, Lederer (1933) modified the Arrhenius mixing rule as follows:

$$\ln(\mu) = x'_A \ln(\mu_A) + x'_B \ln(\mu_B) \tag{2.29}$$

where:

$$x'_A = \frac{\alpha x_A}{\alpha x_A + x_B} \tag{2.30}$$

$$x'_B = 1 - x'_A \tag{2.31}$$

and α is the so called degree of association and must be determined using the experimental viscosity data of mixture. Lederer (1937) argued that association of molecules occurs in the mixtures deviating from Arrenhius mixing rule. Consequently, the actual molecular weights of the components and their mole fractions in the mixture

differ from nominal and calculated values. This mixing rule provided excellent fit to the experimental data of 26 petroleum blends (Rahmes and Nelson 1948).

Shu (1984) examined the experimental data of 17 blends of bitumens, heavy oils, and petroleum fractions. He replaced mole fraction with volume fraction in Equation 2.30 and generalized the parameter α as a function of density and viscosity of the binary pairs, as follows:

$$\alpha = \frac{17.04(\rho_A - \rho_B)^{0.5237} \rho_A^{3.2745} \rho_B^{1.6316}}{\ln\left(\frac{\mu_A}{\mu_B}\right)} \tag{2.32}$$

where component *A* is the more viscous component of the mixture. Barrufet and Setiadarma (2003) also developed the following expression for alpha using experimental data of n-decane diluted heavy oil:

$$\alpha = 0.35242695\, x_B^{-0.71154} \tag{2.33}$$

where x_B is the mole fraction of the solvent. Both developments were validated with literature data and provided predictions within one order of magnitude.

Another group of the mixing rules widely used in the refinery industry to calculate the kinematic viscosity of the petroleum blends are based on the Viscosity Blending Index (VBI) concept. These mixing rules are in the form of the additive mixing rules of Equation 2.24 but utilize slightly more complex functions of the kinematic viscosity. For instance, the Ruftas Index method (Baird, 1989) determines viscosity as the mass fraction based average of the blending indexes of the components, given by:

$$VBI_i = 10.975 + 14.534 \ln\left[\ln\left(\upsilon_i + 0.8\right)\right] \tag{2.34}$$

Another mixing rule known as Cheveron equation (Riazi, 2005) uses a volume fraction average and a VBI defined as follows:

$$VBI_i = \frac{\log \upsilon_i}{3 + \log \upsilon_i} \tag{2.35}$$

These methods are usually reliable in the range of their application in the refinery industry. Al-Besharah et al. (1987) used the Ruftas Index method and predicted the

viscosity of ternary blends of the three crudes (14.8-36 °API, kinematic viscosity of 9.51 to 887.9 cSt at 20°C) at temperature from 10 to 60°C to within 30% of the measured values.

2.2.3 Gases and Liquids

Full-phase viscosity models encompass the gas, liquid, and supercritical phases. These models are generally semi-theoretical or empirical and relate viscosity to temperature and density, temperature and pressure, or density and pressure. The only theoretical approach to the full-phase modeling of viscosity is through molecular dynamics (MD) simulation. The predictions by MD simulations, as discussed by Cummings and Evans (1992), are strongly dependent on the definitions of the intermolecular potential functions. In addition, the MD simulations are computationally intensive and are not practical for rapid viscosity calculations in process or reservoir simulation. However, they can be used as "numerical experiments" for fluids at the conditions for which experimental data are scarce or non-existent (Galliero et al. 2007).

The full phase viscosity models applied to or with potential for the petroleum industry include: the LBC method, methods based on the Corresponding States concept, Friction Theory, Viscosity Equations of State, and Hard Sphere (Enskog) models. A summary of these models is provided below. The Expanded Fluid correlation is another full-phase model; it is the subject of this thesis and will be reviewed in detail in Chapter 4.

2.2.3.1 Empirical Residuals-LBC method:

The residual viscosity model, known as the LBC method in petroleum industry, is mainly based on the empirical correlation developed by Jossi et al. (1962) for the dense fluid viscosity of non-polar compounds. The residual viscosity concept is based on the empirical observation that the difference of the dense fluid and dilute gas viscosity of a compound at a fixed temperature is primary due to its density. Jossi et al. (1962) showed that the reduced liquid and dense gas viscosity data of 11 non-polar components, mainly hydrocarbons with n-pentane as the heaviest, fall approximately on a single curve in the range of reduced densities of 0.1-3. However, they observed that the polar components

such as water and ammonia do not follow the same trend observed for "normally behaving" substances. Jossi et al. (1962) developed the following correlation relating the viscosity to reduced density (ρ_r) of "normally behaving" substances through a fourth degree polynomial:

$$\left[\left(\mu-\mu_o\right)\lambda+10^{-4}\right]^{1/4}=0.10230+0.023364\rho_r+0.058533\rho_r^{\,2}-0.040758\rho_r^{\,3}+0.0093324\rho_r^{\,4} \tag{2.36}$$

where μ_o is the dilute gas viscosity determined by the correlation of Stiel and Thodos (1961). λ is a characteristic parameter to reduce the viscosity and is defined as below:

$$\lambda=T_c^{\,1/6}MW^{-1/2}P_c^{\,-2/3} \tag{2.37}$$

Similar formulations were also developed by Stiel and Thodos (1964) for polar compounds. Poling et al. (2000) assessed the accuracy of this method on dense gas viscosity data of 6 hydrocarbon and polar/non-polar non-hydrocarbon compounds and found an overall AARD of 3.9%.

The contribution of Lohrenz, Bray and Clark (Lohrenz et al. 1964) was to demonstrate the applicability of the empirical residual viscosity method to reservoir fluids. They used the Herning and Zipperer (1936) mixing rule, Equation 2.15, for the dilute gas viscosity and molar average mixing rules for calculation of the critical constants of the mixture. The input density to the model was taken as either measured values or values estimated by method of Alany and Kennedy (1960). For the critical volume of the undefined C_{7+} fractions, the following correlation was developed (Lohrenz et al. 1964) based the viscosity data of 236 reservoir fluids at their bubble point:

$$v_c\big|_{C7+}=21.573+0.015122\,MW_{C7+}-27.656\,SG_{C7+}+0.070615\,MW_{C7+}.SG_{C7+} \tag{2.38}$$

Lohrenz et al. (1964) found that the model predicted the viscosity for 260 reservoir fluids at pressures higher than the bubble point pressure to within ±16% and ±12.6% of the measurements using the calculated and experimental input densities, respectively.

Since the original model of Jossi et al. (1962) was developed based on the measured density, it's accuracy strongly depends on the reliability of the input density. Also, it was

shown (Dandekar et al. 1993, Al-Syabi et al. 2001) that the model predictions (Equation 2.36) at reduced densities higher than 2.5 are not reliable even when using the measured density as an input. Heavy hydrocarbons at room temperature conditions can have reduced densities above this threshold. Barrufett et al. (1997) verified the previous reports of the unreliable performance of LBC method for mixtures of reservoir fluids and carbon dioxide by showing the deterioration of the predicted viscosities for mixtures of pure hydrocarbon compounds and CO_2. Also, negative deviations up to 100% were reported for viscosity estimations by the LBC method for the reservoir fluids when the input densities were calculated by cubic equations of state such as SRK and PR (Pedersen et al. 1984, Quinones-Cisneros et al. 2001b). This latter error can be partly attributed to under-prediction of fluid density by the cubic equations of state.

Several attempts were made to improve the performance of the LBC method. Dandekar et al. (1993) and Al-Syabi et al. (2001) developed temperature and molecular weight dependent expressions for the constants of Equation 2.36 to improve the performance of model for heavier hydrocarbons at reduced temperature above 2.5. Also, Xu et al. (1996) modified Equation 2.36 to introduce an addition term in form of an exponential function of the reduced density.

Despite the limitations of the original LBC method, it is used widely in compositional reservoir simulators due to simplicity and fast execution in computer code (Danesh, 1998). A common approach is to tune the model to experimental viscosity data of petroleum fluids by adjusting the critical volumes of the C_{7+} fractions (Computer Modeling Group, 2011; Schlumberger, 2005). The adjustment of the constants of the equation 2.36 is also an option in general regression of PVT and transport properties data of the reservoir fluids (Computer Modeling Group, 2011). The implementation of modified LBC in PVTi, the PVT package of the Eclipse reservoir simulator, utilized an enhancement similar to the modified form of Equation 2.36 by Xu et al. (1996). A general multiplier in form of exponential function of the reduced density is applied to the constants of Equation 2.36 at higher reduced densities (Schlumberger, 2005).

2.2.3.2 Corresponding States (CS) Methods:

Corresponding state theory is one of the best known semi-theoretical methods to estimate the physical and transport properties of fluids. This theory is based on the observation that properties of fluids vary consistently in relation to their critical point. Therefore, reduced properties of fluids map on top of each other when plotted in reduced coordinates; where a reduced property/coordinate is a property/coordinate divided by its value at the critical point.

Pitzer (1939) used statistical mechanics to derive a theoretical framework for the two-parameter corresponding states of thermodynamic properties. Similarly, Helfand and Rice (1960) demonstrated the theoretical basis of the law of two-parameter corresponding states for transport properties. According to the two-parameter corresponding states principle, energy (ε/k) and distance/size (σ) are the two characterizing parameters for each fluid and they are assumed to be proportional to the critical temperature, T_c, and the critical molar volume, v_c, respectively. Therefore, the appropriate reduced coordinates are the reduced temperature and volume. For the fluids completely obeying the corresponding states theory, the reduced viscosity of fluid "i" is equal to the reduced viscosity of the reference fluid "o" at the same reduced temperature (T_r) and volume (v_r) as follows:

$$\mu_{r,i}(v_{r,i}, T_{r,i}) = \mu_{r,o}(v_{r,o}, T_{r,o}) \tag{2.39}$$

The viscosity of the fluid "i" at the critical condition is defined as follows:

$$\mu_{c,i} = \frac{MW_i^{1/2} R^{1/2} T_{c,i}^{1/2}}{N_A^{1/3} v_{c,i}^{2/3}} \tag{2.40}$$

where R and N_A are universal gas constant and the Avogadro number. Since most fluids do not exactly follow the two-parameter corresponding states theory, several variations of the models based on the theory have been developed. Some methods utilize one fluid as the reference fluid with correction factors (Ely and Hanley, 1981; Pedersen et al., 1987), but others use two fluids as the references (Letsou and Stiel, 1973; Teja and Rice, 1981a; Teja and Thurner, 1986; Wu and Asfour, 1992; Aasberg-Petersen et al., 1991; Moharam and Fahim, 1995). The two reference models follow an analogy of the approach used by

Pitzer et al. (1955) and Lee and Kesler (1975) for the three-parameter corresponding states models of the compressibility factor. Okeson and Rowley (1991) used three fluids as the reference in an attempt to account for the polar effects on viscosity. A summary of the most well known methods based on the corresponding states theory with one reference fluid is provided below.

Hanley (1976) developed the first working framework of the corresponding state theory for the viscosity of the pure components and mixtures. He substituted Equation 2.40 into Equation 2.39 to relate the viscosity of the fluid "i" at given density and temperature to the viscosity of the reference fluid "o", as follows:

$$\mu_i(\rho,T) = \mu_o(\rho h_{i,o}, T / f_{i,o})(MW_i / MW_o)^{1/2} h_{i,o}^{-2/3} f_{i,o}^{1/2} \tag{2.41}$$

where:

$$h_{i,o} = \frac{\rho_{c,o}}{\rho_{c,i}} \phi_{i,o} \tag{2.42}$$

$$f_{i,o} = \frac{T_{c,i}}{T_{c,o}} \theta_{i,o} \tag{2.43}$$

where $\phi_{i,o}$ and $\theta_{i,o}$ are shape factors with a default value of unity in the two-parameter corresponding states model . However, most fluids are not conformal to the two-parameter corresponding states and the above formulation does not apply to polyatomic fluids and mixtures. The extended corresponding states approach (Rowlison and Watson, 1969; Leland and Chappelear, 1968) accounts for the non-conformality by variable shape factors as general functions of the reduced temperature, reduced density and the acentric factor. The required information to use the CS model include: an equation of state and viscosity correlation for the reference fluid, the critical temperature and density, and the acentric factor and molecular weight of the reference fluid and the fluid(s) of interest.

Hanley (1976) selected methane as the reference fluid due to the interest in LNG and light hydrocarbons and also because extensive viscosity and density data were available for methane. A novel equation of state (Goodwin, 1974) and an empirical correlation (Hanley et al., 1975) were used to calculate density and viscosity of methane,

respectively. The proposed mixing rules of Mo and Gubbins (1974) were used to calculate the reducing parameters $h_{i,o}$ and $f_{i,o}$ and the molecular weight for the mixtures. Shape factors obtained from thermodynamic properties (Mollerup, 1979) were used in this study, but Hanley (1976) concluded that these shape factors do not sufficiently represent the viscosity of the non-conformal fluids at higher reduced densities.

Later, Ely and Hanley (1981 a,b) replaced the original mixing rule for the molecular weight of the mixture with a new statistical mechanics based rule to improve the model for asymmetric mixtures. They used the empirical expressions of Leach et al. (1968) for pure n-alkanes (C_1-C_{15}) to calculate the shape factors as functions of the reduced temperature and density of the fluid of interest. However, Ely and Hanley (1981) encountered a difficulty using methane as the reference fluid over a full range of temperatures because it freezes at a reduced temperature of 0.48 which is higher than the reduced freezing temperature of other heavier hydrocarbons. To overcome this problem, they developed a pseudo-methane reference for low temperatures using corresponding states theory on data from other n-alkanes. A 32-term BWR type equation of state and an empirical viscosity correlation were developed to represent the reference fluid (methane) down to 40 K (T_r=0.2). These developments led to a computer program (1981 b) known as TRAPP (TRAnsport Properties Prediction). Note that although the two coordinates in Equation 2.41 are density and temperature, the viscosity estimations were done at the given pressure and temperature. Therefore, iterative solutions of Equation 2.42 were required to calculate the density of the fluid of interest before the viscosity estimation. The model predictions for the viscosity of 35 pure hydrocarbon and carbon dioxide had an overall AARD of 8.4%. However, the performance of the model greatly deteriorated for branched alkanes and cycloalkanes with an AARD of 49% observed for cyclohexane. The overall AARD of the model predictions for mostly paraffinic binary mixtures was 7%.

Ely (1982) proposed propane as the reference fluid and developed the required equations for its density and viscosity. Since then, several authors tried to modify and improve the method including studies on the reference fluid, property equations, and shape factors

(Ely, 1984; Younglove and Ely, 1987; Monnery et al., 1991; Huber and Ely, 1992 and 1993). The latest version of TRAPP called SUPERTRAPP (Huber and Hanley, 1996) uses propane as the reference fluid with 32-term MBWR equation of state and viscosity correlation developed by Younglove and Ely (1987). The shape factors are determined by matching the reduced saturation pressures and statured liquid densities of the reference fluid and the fluid of interest (Ely and Huber, 1990). Simple density-independent correlations were proposed for the shape factors in case the saturation pressure and statured liquid density data for the fluid of interest are not available (Erickson and Ely, 1993). The predictions for the mixture were also improved by inclusion of the Enskog correction term (Ely 1984). The predictions for the naphthenes and highly branched compounds were improved by introduction of the concept of mass shape factor (Ely and Magee, 1989). The mass shape factor incorporates the known value of the viscosity of the fluid of interest at an indicated state point. The mass shape factor simply provides the option to tune model predictions for pure components and has a default value of unity when data are not available.

Baltatu (1982) used the by Ely and Hanley (1981a) corresponding states viscosity model to predict the viscosity of petroleum distillation fractions of the light crude oils with an AARD of 6.4%. The required critical properties and molecular weight of the distillation cuts were calculated using the Riazi and Daubert (1980) correlation based on their average boiling point and specific gravity. Baltatu et al. (1996 and 1999) also used the later versions of the CS model with propane reference fluid to model the viscosity of a larger dataset of petroleum fractions covering broader range of boiling points and specific gravities. They found that the model under-predicted the viscosity of more aromatic fractions at high reduced densities. Therefore, an aromaticity correction (Baltatu et al., 1996) or mass shape factor (Baltatu et al., 1999) was introduced to the model as a density dependent parameter and correlated to the Watson-K factor of the distillation cuts using the available viscosity data. The AARD of the model tested on the development dataset was 17.4% for both approaches. The extended corresponding states model was also used to model the viscosity of bitumens and dilute bitumen mixtures, but required major

modifications (Johnson et al., 1987; Mehrotra and Svrcek, 1987) .These studies will be discussed later in section 2.3.2.

Pedersen and co-workers (Pedersen et al., 1984; Pedersen and Fredenslund, 1987) adapted the formulation of Tham and Gubbins (1970) for the corresponding states model in which pressure and temperature are the corresponding coordinates as follows:

$$\mu_{r,i}(P,T) = \frac{\alpha_i}{\alpha_o}\mu_{r,o}(P_o,T_o) \tag{2.44}$$

where:

$$P_o = \frac{P.P_{c,o}\alpha_o}{P_{c,i}\alpha_i} \tag{2.45}$$

$$T_o = \frac{T.T_{c,o}\alpha_o}{T_{c,i}\alpha_i} \tag{2.46}$$

α in the above equations is the Tham and Gubbins (1970) rotational coupling coefficient and accounts for the density dependent reduced intra-molecular degrees of freedom for polyatomic fluids, especially in the liquid phase.

Pedersen et al. (1984) used methane as the reference fluid with the original correlation of Hanley et al. (1975) for its viscosity. An empirical equation was developed to relate the parameter α to molecular weight and reduced density of the fluids. Mixing rules were proposed to calculate the pseudo-critical properties of the mixtures. Pedersen et al. (1984) proposed that larger molecules make a higher contribution to the mixture viscosity; hence, the effective molecular weight of mixture should be greater than the number average molecular weight. They found the mass average molecular weight to be too large for this purpose and proposed an empirical linear weighted average of these two values as the effective molecular weight of the mixture. All the empirical developments were based on a least squares fit of the model predictions to the experimental viscosity data of the crude oils with an overall AARD of 5%. Although the method was based on crude oil data, it was shown that it provides reliable viscosity predictions (comparable to TRAPP) for pure hydrocarbons (up to C_{18}) as well as carbon dioxide and binary hydrocarbon mixtures. The overall AARD of the predictions of the method for all studied fluid except

n-C15, n-C18 and cyclohexane was 8.1% compared to 5.4% with TRAPP. The method performed better for n-C15, n-C18 and cyclohexane than TRAPP with AARD of 29.1% and 43.1, respectively. The overall AARD of the method and TRAPP for binary mixtures were 6.4% and 8.6%, respectively.

Pedersen and Fredenslund (1987) broadened the range of the applicability of the model by adding an extra term to the Hanley et al. (1975) viscosity model using viscosity data of oil mixtures and distillation fractions below T_r of 0.4. The empirical equations for the parameter alpha and the effective molecular weight of the mixture were also modified. These modifications resulted in improved viscosity predictions for the light components (ethane, propane and carbon dioxide) and petroleum fluids at reduced temperatures below 0.4.

Although the modifications of Pedersen and Fredenslund (1987) enabled the prediction of viscosity of fluids at temperature below the freezing temperature of methane, Lindeloff et al. (2004) reported that the model is not applicable at temperatures below the corresponding methane reference temperature of 60 K. The reason given was that, according to the equation of state, at these conditions the methane density (and viscosity) becomes invariant to pressure changes. They concluded that oil viscosities higher than 10 mPa.s cannot be modeled with the corresponding states model with methane as the reference fluid. Despite this limitation, the Pedersen et al. model is implemented in most compositional reservoir simulators and is used widely without any limitations on the oil viscosity.

Lindeloff et al. (2004) proposed a new addition to the Pedersen et al. model to extend it to heavy oil applications. An exception was made to the original methodology so that methane was not used as the reference fluid at a methane reference temperature below 60 K. Instead, a semi-empirical viscosity correlation (Ronningsen, 1993) of stabilized crude oils at atmospheric condition was proposed to estimate viscosity as a function of temperature and molecular weight of the oil. A logarithmic relationship between the reference crude oil viscosity and pressure was used to capture the pressure effect on

viscosity. A criterion based on the ratio between the number average molecular weight and the weight average molecular weight of the crude oil was used to distinguish between live oils and stabilized oils. The effective molecular weight of the live oils was calculated with the proposed empirical equation with two adjustable coefficients to match live oil data. The proposed modification provided viscosity predictions within 25% of the experimental values for oils with viscosities less than 20 mPa.s. The applicability of the proposed method was also tested for heavy oils with viscosities as high as 8000 mPa.s and predictions were found to be generally within a factor of 3 of the measurements. However, the method showed limited applicability in complete fitting a full dataset of live and dead oil of given crude oil over a broad range of temperature.

2.2.3.3 Friction Theory:

Friction theory (F-theory) is one of the most recently developed methods to estimate the viscosity of the fluids. This method follows the concept of the residual viscosity and relates the increase in the viscosity of the dense fluid from the viscosity of the dilute gas (μ_o) to the frictional viscosity (μ_f) contribution as follows:

$$\mu = \mu_o + \mu_f \tag{2.47}$$

The frictional viscosity term was related to the friction between the moving fluid layers arising from the normal stress as described by Coulomb's friction law in classical mechanics. The normal stress was assumed to be the isotropic total pressure of the fluid at rest which is due to the short range repulsive and long range attractive intermolecular forces. Based on van der Waals fluid theory, the total pressure has contributions from the repulsive and attractive pressure components. It was then hypothesized that the drag force (τ) between moving fluid layers has attractive and repulsive components which are analytical functions of the attractive and repulsive pressure terms as follows:

$$\tau = \sum_i \tau_{a,i} P_a^i + \sum_i \tau_{r,i} P_r^i \tag{2.48}$$

where $\tau_{a,i}$ and $\tau_{r,i}$ are the i^{th} order terms in the Taylor expansion of τ, and are proportional to the i^{th} order derivatives of the attractive and repulsive drag components. Quinones-Cisneros et al. (2000) showed that only first order attractive term and first and second order repulsive terms are required to accurately describe the viscosity of methane up to

pressures as high as 1000 MPa. Equation 2.48 was substituted into Newton's law of viscosity to obtain the frictional viscosity contribution, given by:

$$\mu_f = \frac{\tau_{a,1}P_a + \tau_{r,1}P_r + \tau_{r,2}P_r^2}{du/dy} \tag{2.49}$$

Quinones-Cisneros et al. (2000) expressed the Equation 2.49 in a more convenient form as follows:

$$\mu_f = \kappa_a P_a + \kappa_r P_r + \kappa_{rr} P_r^2 \tag{2.50}$$

where κ_a, κ_r and κ_{rr} are the first order attractive and the first and second order repulsive viscous friction coefficients. These coefficients were defined to be temperature dependent only, implying the proportionality of the Amontons-Coulomb friction coefficients in Equation 2.49 to *du/dy,* contrary to the Coulomb's friction law in classical mechanics.

Quinones-Cisneros et al. (2000) used the SRK (Soave, 1972) and the modified PR by Stryjek and Vera (1986) equations of state to calculate the repulsive and attractive pressure terms. Analytical relationships were then developed for each of the friction coefficients as functions of reduced temperature with a total of 5 fluid-specific parameters. These parameters were determined for the first 10 n-alkanes to use with each equation of state by least squares fitting of the model to viscosity data with an overall AARD less than 3%. Mixing rules were then proposed to determine the viscous friction coefficients for mixtures. The predictions of the model were evaluated against 6 binary mixtures of hydrocarbons with overall AARD and MARD of 3% and 17%, respectively.

Quinones-Cisneros et al. (2001a) developed a one-parameter F-theory model using the reduced form of the frictional viscosity term given by:

$$\hat{\mu}_f = \frac{\mu_f}{\mu_c} \tag{2.51}$$

where μ_c is the characteristic critical viscosity of the fluid. The reduced frictional viscosity was then given in terms of the reduced attractive and repulsive pressure terms as follows:

$$\hat{\mu}_f = \hat{\kappa}_a \hat{P}_a + \hat{\kappa}_r \hat{P}_r + \hat{\kappa}_{rr} \hat{P}_r^2 \tag{2.52}$$

where $\hat{\kappa}_a$, $\hat{\kappa}_r$ and $\hat{\kappa}_{rr}$ are dimensionless viscous friction coefficients. Each of these coefficients was formulated as the sum of the critical friction coefficient with the temperature dependent residual friction coefficients vanishing at the critical temperature. The values of the critical friction coefficients were determined as three common parameters for all fluids. The residual friction coefficients were formulated as functions of the reduced temperature utilizing 13 common parameters for all fluids.

Quinones-Cisneros et al. (2001a) determined the numerical values of the parameters to use with SRK, PR and PRSV equations of state by fitting the correlation to experimental viscosity data of the first 18 members of the n-alkanes series with overall AARD and MARD of 2% and 16%, respectively. The only fluid-specific adjustable parameter in the one-parameter F-theory model is the characteristic critical viscosity. This parameter must be determined from experimental data of the pure fluid of interest and was tabulated for the first 18 members of the n-alkanes series (Quinones-Cisneros et al. 2001a). The model predictions for viscosity data of 9 other hydrocarbons, carbon dioxide, and nitrogen had AARDs less than 8%. Using the proposed mixing rules for the dimensionless viscous friction coefficients, the viscosities of 14 mixtures of hydrocarbons were predicted with an overall AARD of 4%.

Quinones-Cisneros et al. (2001b, 2003) extended the one-parameter F-theory to reservoir oil systems using the PR equation of state to calculate the attractive and repulsive pressure terms. The characteristic critical viscosities of the pseudo-components of the oil were estimated as follows:

$$\mu_c = K_c \frac{MW^{1/2} P_c^{2/3}}{T_c^{1/3}} \tag{2.53}$$

where K_c is an adjustable common parameter to fit the predictions of the correlation to the viscosity data of the live oils at pressures above saturation pressure. A comprehensive characterization approach was recommended (Quinones-Cisneros et al. 2003) to define the pseudo-components of the oil; including extrapolation of GC into plus fractions using a Chi-Square distribution function to determine the molecular weights of the pseudo-components and correlations to determine the critical properties. Quinones-Cisneros et al.

(2003) showed that the correlation fitted the high pressure data of 5 live oils (with viscosities within 0.4-12 mPa.s at saturation pressure and temperature) with AARDs less than 6% and predicted the atmospheric dead oil viscosity within 35% of the measurements. However, the predictions of the model for the live oils were within 25% of the experimental values when K_c was determined using the atmospheric dead oil data point.

For heavy crude oils with molecular weights higher than 200 gr/mol, the F-theory model failed to correctly match the experimental viscosity data (Quinones-Cisneros et al., 2004). The poor match was attributed to the limitations of van der Waals type cubic equations of state in predicting the repulsive pressure terms of high molecular weight fluids. To correct for this inadequacy, a single parameter as the volume translation (ζ) was introduced to shift the volume used in the equation of state to calculate the repulsive and attractive pressure terms. As the composition of the reservoir fluid varies with pressure below the saturation pressure, the following mixing rule was proposed for the volume translation parameter:

$$\zeta = K_Z \sum_i x_i MW_i^{1/3} \tag{2.54}$$

where K_z is an adjustable parameter and x_i and MW_i are the mole fraction and molecular weight of the pseudo component *i* of the oil. Quinones-Cisneros et al. (2004) showed that the model fitted the viscosity data of 6 live heavy oils (with viscosities within 5-1500 mPa.s at saturation pressure and temperature) within the accuracy of the measurements. Similar to the previous studies, the model predicted the viscosity at pressures below saturation pressure with higher deviations. These deviations were attributed to less accurate viscosity measurements at these conditions.

In summary, the one-parameter f-theory model requires determination of the parameters K_c and K_z to fit the viscosity data of each reservoir fluid at fixed temperature. However, Zuo et al. (2008) introduced temperature dependence into these two parameters to more accurately model the viscosity of the characterized reservoir fluids oils at different temperatures. The temperature dependency of the parameters K_c and K_z for each reservoir

fluids was also briefly discussed by Quinones-Cisneros et al. (2005). In a later study of non-Newtonian behavior of reservoir fluids, Quinones-Cisneros et al. (2008) observed that the one-parameter framework of the F-theory model does not suit the heavy pseudo-components of reservoir oils because it was developed based on a database of pure hydrocarbon compounds at reduced temperatures above 0.4. Hence, Quinones-Cisneros et al. (2008) proposed a temperature dependent correlation for the parameter K_c which reduces to fixed K_c at higher temperature. The proposed modification has four adjustable parameters, but empirical correlations were determined for three of the parameters using viscosity data of 8 reservoir oils.

2.2.3.4 Hard Sphere (Enskog) Theory:

Enskog (1922) extended the hard sphere viscosity model to dense gases by assuming that the higher viscosity of dense gases is due to higher collision rates between the molecules. Two factors were assumed to contribute to the higher collision rate. First, the distance molecules travel between successive collisions is reduced in closely-packed dense fluid. Second, the non-zero diameter of the molecules is comparable to the travel distance and results in additional reductions. The higher collision rates affect the momentum transfer upon the collision of the molecules over non-zero collision diameters. The latter becomes significant as the density increases. Enskog (1922) obtained the expression for the viscosity of the dense gas as follows:

$$\frac{\mu}{\mu_o} = \frac{1}{g(\sigma)} + \frac{0.8\,b}{v} + 0.761\,g(\sigma)\left(\frac{b}{v}\right)^2 \tag{2.55}$$

where σ and $g(\sigma)$ are the hard-sphere diameter and the radial distribution function accounting for the increased collision rates. μ_o is the dilute gas viscosity; b is the excluded volume as $2/3\pi N_A\sigma^3$ and v is the molar volume. The increase in the collision rate is related to the pressure, which is proportional to the rate of momentum transfer, as below:

$$\frac{Pv}{RT} = 1 + \frac{b\,g(\sigma)}{v} \tag{2.56}$$

Since the molecules of the real fluid are not hard spheres and attract each other, Enskog proposed the modified Enskog theory (MET) (Chapman and Cowling, 1952) to replace *g(σ)* with pseudo-radial distribution function *(ğ(σ))* as follows:

$$\frac{v}{R}\left(\frac{\partial P}{\partial T}\right)_v = 1 + \frac{b\,\breve{g}(\sigma)}{v} \tag{2.57}$$

To use the above formulations, it is necessary to assign a value to the core diameter or the hard sphere diameter. Unlike hard spheres, the core diameter for real molecules can be assumed to be temperature-dependent because high energy molecules at higher temperatures collide (~maximum repulsion) with each other at shorter diameters. The difficulties in determining this value and the limitations of the simplified assumptions of the Esnkog theory led Dymond (1973) to propose the following reduced quantity of viscosity:

$$\mu^* = \frac{\mu}{\mu_o}\left(\frac{v}{v_0}\right)^{2/3} \tag{2.58}$$

where v_0 is the volume of close-packing of the molecules. By substituting the definition of the dilute gas viscosity in the above equation, Chandler (1975) and Dymond (1976) also included a roughness factor (R_μ) to account for the non-spherical molecules to rewrite Equation 2.58 as follows:

$$\mu^* = 6.619\times10^2\,\frac{\mu\, v^{2/3}}{R_\mu\left(MW.T\right)^{1/2}} \tag{2.59}$$

The roughness factor (R_μ) is unity for single atom molecules but takes values greater than one for polyatomic fluids. Based on molecular dynamics simulations, μ^* was shown to be independent of the molecular diameters and only a function of v/v_0 (Alder et al. 1970).

Following several studies by Dymond and co-workers (1974, 1975, 1976, 1977, 1979, and 1987), Assael et al. (1992a) established the following universal curve for viscosity as a function of molar volume (density):

$$\log\left(\mu^*\right) = \sum_{i=0}^{7} a_i \left(\frac{v}{v_0}\right)^{-i} \tag{2.60}$$

where a_i (i=0 to 7) are universal constants. Assael et al. (1992a) used an extensive viscosity dataset of n-alkanes from methane to n-hexadecane to determine the values of v_0 and R_μ by curve fitting. The fitted values of R_μ were generalized as a monotonically increasing function of carbon number. The values of v_0 were generalized as a function decreasing with temperature and increasing with carbon number. Using the generalized values, the viscosities of n-alkanes were estimated with RMS deviation of 2.8%.

Assael et al (1992b) used the same approach and correlated the viscosity of aromatic hydrocarbons. No definite trend was observed for the values of R_μ. However, the values of v_0 were generalized as function of carbon number and temperature, and the viscosity of the studied aromatics were fitted with less than 3% of the predictions deviating by more than 5%. Similar studies were also conducted to correlate the viscosity of organic alcohols (Assael et al. 1994) and refrigerants (Assael et al. 1995).

Assael et al. (1992c) proposed mole fraction based linear mixing rules to calculate the values of v_0 and R_μ for mixtures. The viscosity of 32 binary, 2 ternary and 3 quaternary mixtures of n-alkanes were then estimated within the uncertainties of the measurements (only 7% of the predictions deviating by more than 5%). However, the predictions with the aforementioned mixing rules for mixtures containing aromatic compounds were highly deviated (Assael et al. 2009). Hence, a fixed-value binary interaction parameter was introduced to the mixing rule of R_μ and its value determined by fitting experimental data for 19 mixtures. The fit of the correlation to data was within the accuracy of the data with predictions for only 7% of 518 data points deviating by more than 7%. Although this model has great ability in fitting the viscosity data of pure compounds and extrapolates well to extreme conditions, its applicability to the reservoir fluids and ill-defined petroleum mixtures has not yet been studied.

2.2.3.5 Cubic Viscosity Equations of State:

Philips (1912) was the first to observe the similarity between the *P-v-T* and *T-μ-P* surfaces of carbon dioxide. Little and Kennedy (1968) developed the first cubic equation of viscosity based on the form of the van der Waals equation of state by interchanging

pressure (P) and temperature (T), replacing molar volume (v) with viscosity (μ) and the gas constant and parameters a and b with fluid-specific empirical parameters.

Lawal (1968) proposed a cubic viscosity equation of state based on the Lawal-Lake-Silberberg equation of state. In this development, the parameter replacing the gas constant is a monotonically decreasing function of pressure and temperature. The parameter replacing the co-volume in cubic equations of state is also temperature-dependent and approximately represents the dilute gas viscosity of the fluid. Lawal (1968) generalized both parameters as functions of the acentric factor and molecular weight of the fluid. Hence, the equation has two adjustable parameters for each pure compound to be determined using the experimental viscosity data.

Mixing rules were also proposed to calculate the parameters of the viscosity equation of state from the values of the mixture components. Similar to the cubic equation of states, the viscosity equation of state can have up to 3 real roots. Lawal (1968) reported the criteria to choose the correct root for the liquid and vapor phases of pure compounds and mixtures. The proposed method was developed and tested against the viscosity data of normal n-alkanes up to nC_{20}, light branched alkanes, carbon dioxide and nitrogen with an AARD of 5.9%. Lawal evaluated the predictions of the model against data of several binary and multi-component mixtures including natural gas mixtures with an AARD of 3.5%. The predictions for light reservoir oils (viscosity up to 3.5 mPa.s) were within ±8% of the experimental values.

Guo et al. (1997) developed cubic viscosity equations of state based on the form of the Patel-Teja (PT) and Peng-Robinson (PR) equations of state. The parameters replacing the gas constant and co-volume were related to the reduced temperature and pressure through similar functionalities as the equations of Lawal (1986). In addition, Guo et al. (1997) included pressure dependency in the replacing parameter of the co-volume. These viscosity equations of state, unlike the model of Lawal (1968), do not have any adjustable parameters because the other parameters of the equations were related to the critical constants of the pure compounds.

Mixing rules were also proposed to calculate the parameters of the Guo et al. viscosity equations of state from the values of the mixture components. The proposed equations were developed and tested against the viscosity data of normal n-alkanes up to nC_{12}, light branched alkanes, benzene, carbon dioxide and nitrogen, with an overall AARD of 6.2%. The predictions of both equations were evaluated against the viscosity data of the binary mixtures of methane with propane, n-butane and n-decane with AARDs of 14 %, 18% and 7%, respectively. The PT-based viscosity equations also provided viscosity predictions for reservoir oils with an overall AARD of 15%, but no detailed results were given.

Guo et al. (2001) proposed modifications to PR-based viscosity equation to improve predictions for mixtures. The modifications include changes in the mixing rules and functional forms of the parameters for the pure compounds. The new equation was tested against data of 22 reservoir oils with overall AARD of 14% and maximum AARD of 46%. It was also shown that the equation provides reliable predictions for hydrocarbon mixtures with carbon dioxide. Overall AARDs of 7% and 12.6% were reported for a binary mixture of CO_2 and nC_{10} and two CO_2-injected reservoir oil systems (viscosity up to 2.5 mPa.s), respectively. No application of cubic viscosity equations of state to heavy petroleum fluids was found.

2.3 Viscosity Measurement and Modeling of Extra Heavy Oil/Bitumen Systems

The density and viscosity of the extra heavy oil/bitumen systems have been studied extensively. The AOSTRA Journal of Research is a main resource for summaries of the data and models. The following is a summary of some of the experimental measurements and modeling approaches of the viscosity of heavy oils/bitumens as well as their mixtures with solvents.

2.3.1 Summary of Experimental Studies

Clark and Ward (1950) were the first to provide a complete study of the viscosity and density of Athabasca bitumen. Based on measurements with a capillary viscometer, they observed that the viscosity of bitumen changes greatly with temperature, but behaves

essentially as a Newtonian fluid. They also concluded that the viscosity of Athabasca bitumen varies depending on the sampling region and vertical sampling depth, extraction methods, and thermal treatments.

Jacobs (1978) performed viscosity measurements on dead (gas free) Athabasca bitumen at atmospheric pressure and 6.9 MPa using a DC44 Contraves rotating cylinder flow-through viscometer and a cone and plate viscometer. In addition, Jacobs (1978) and Jacobs et al. (1980) published viscosity data of the Athabasca bitumen saturated with CO_2, N_2 and CH_4. They found that the dissolved CO_2 dramatically reduces the viscosity of the bitumen at low temperatures. The effect of the dissolved methane was less pronounced (but appreciable) while nitrogen had negligible impact. However, the reported data of Jacobs and co-workers did not include solubility measurements.

Mehrotra and Svrcek modified the apparatus of Jacobs (1978) to perform density and solubility measurements in addition to the viscosity measurements for bitumen systems. In a series of papers, Mehrotra and Svrcek (1982, 1984, 1985a, 1985b, 1985c, 1988) published viscosity data for several dead bitumens from Western Canada at atmospheric pressure and temperatures from 15-120ºC. They also reported viscosity, density, and solubility data for bitumens saturated with CO, CO_2, N_2, CH_4 and C_2H_6 at the saturation pressures and temperatures. Similar data for the saturated Athabasca, Peace River and Cold Lake bitumens with synthetic solution gas and combustion gas mixtures were also published (Mehrotra and Svrcek 1982 and 1988, Svrcek and Mehrtora 1989). Mehrotra and Svrcek described the relative effects of the dissolved gases on the bitumen viscosity as below:

$$N_2 < CO < CH_4 << CO_2 < C_2H_6$$

Svrcek and Mehrotra (1989) also observed slightly non-Newtonian behavior for Peace River bitumen at low temperatures (T<15 ºC) and low shear rates (< 0.5 s^{-1}).

Mehrotra and Svrcek were only able to perform measurements at saturation conditions. Hence, the effect of the pressure and temperature were not studied on the viscosity and density of under-saturated bitumen mixtures. Also, the measurements at saturation

conditions represent the combined effects of pressure and temperature on solubility as well as the density and viscosity of the mixture. Without having the data for the compressed dead bitumen, it is not possible to differentiate the effect of the dissolved gases on the density and viscosity. Although Mehrotra and Svrcek (1982) stated that the viscosity of the dead bitumen "remains more or less unchanged" with pressure, their measurements on the compressed Athabasca (Mehrotra and Svrcek, 1986) and Cold Lake (Mehrotra and Svrcek, 1987) bitumens proved a significant increase (up to a factor of 2) in viscosity with an increase in pressure. These sets of the viscosity measurements were performed at gauge pressure range of 0-10 MPa using nitrogen gas to provide the pressurized atmosphere. They found a more significant effect of pressure on bitumen viscosity at lower temperatures. They also concluded that the less dense the bitumen, the smaller the increase in its viscosity upon compression. Viscosity data were also published for vacuum distillation fractions of the Cold Lake bitumen (Mehrotra et al., 1989), binary blends of the fractions (Eastick and Mehrotra, 1990), atmospheric mixtures of the fractions with toluene (Mehrotra, 1990b), and saturated mixtures with CO_2 (Eastick, 1989).

Shramm and Kwak (1988) studied the rheological properties of an Athabasca bitumen samples and its mixtures with naphtha using a Haake Rotovisco viscometer and an Ostwald capillary viscometer. Although some non-Newtonian behavior was reported by Dealy (1979) for Athabasca bitumen at very low shear rate regimes of 0-1 s^{-1}, their bitumen sample exhibited Newtonian behavior over a temperature range of 15-80ºC. The Newtonian behavior was also observed for the diluted bitumen samples with naphtha in the composition range of 10 to 90% at a temperature range of 5-90ºC.

Badamchizadeh et al. (2009a and 2009b) measured the viscosity and density of the binary mixtures of Athabasca bitumen with propane (temperature range of 10-90 ºC) and ternary mixtures of Athabasca bitumen with propane and carbon dioxide (temperature range of 10-25ºC) as part of phase behavior study for VAPEX applications. The viscosity and density were measured with an in-line ViscoPro2000 Cambridge viscometer and an Anton Paar DMA 5000 density-meter, respectively. In similar studies, Yazdani and Maini

(2010) measured the viscosity of saturated binary mixtures of Frog Lake heavy oil and n-butane at room temperature using a capillary viscometer. Li et al. (2011) and Li and Yang (2012) measured the viscosity of the Lloydminster heavy oil diluted with propane, a mixture of propane and carbon dioxide and four mixtures of propane and n-butane using a capillary viscometer at saturation conditions. They also measured the viscosity of the dead Lloydminster heavy oil in temperature range of 25-100 ºC using a cone and plate viscometer.

Kokal and Sayegh (1993) measured the viscosity of saturated mixtures of dead Canadian heavy oil with carbon dioxide at 21ºC and 140ºC using a capillary viscometer. Similar measurements were also conducted for the corresponding de-asphalted oil and its two constitutive light and heavy fractions by distillation. The viscosities of the mixtures were found to decrease with increasing solubility of the carbon dioxide with pressure. However, this trend stopped for all mixtures, except the diluted light fraction of the de-asphalted oil, at a pressure near 6 MPa at 21 ºC since the maximum solubility of CO_2 was reached.

2.3.2 Summary of Modeling Studies

Jacobs (1978) evaluated the applicability of number of empirical correlations to gas-free Athabasca bitumen and found both the Andrade and the Vogel equations were not adequate to fit the viscosity data versus temperature. However, Jacobs et al. (1980) developed correlations in the form of Andrade equation to represent the viscosity data of CO_2 saturated bitumen versus temperature at fixed saturation pressure conditions.

Johnson et al. (1987) attempted to model the viscosity of the Athabasca bitumen using by Ely and Hanley's (1981a and 1981b) extended corresponding states model. The bitumen was modeled as a mixture of pseudo-components with critical properties calculated with Lee-Kesler correlations. Johnson et al. (1987) attributed the convergence problems and paraffinic trend of the predicted viscosities to the inadequacy of the shape factors and the non-correspondence of the bitumen pseudo-components with methane as the reference fluid. Therefore, "1,2,3,4,5,6,7,8-octahydrophenanthrene" was chosen as the new

reference fluid which has high molecular weight and is aromatic-naphthenic in nature. New shape factor multipliers were then determined by matching the density data. Then, the viscosity of the Athabasca bitumen was predicted with AARD of 6% over the temperature range of 20-130 ºC.

Johnson et al. (1987) used their modified extended corresponding states model with a new set of shape factors for the dissolved gases and predicted the viscosity of CO_2, CH_4 and N_2 saturated Athabasca bitumen with AARDs of 19%, 29% and 7%, respectively. Johnson et al. (1987) also tested the predictions of the mixing rules of Teja and Rice (1981a) for gas saturated bitumen and concluded that the dissolved gases must be assumed as "pseudo-liquids" for satisfactory viscosity predictions. The pseudo-liquid approach requires estimating the dissolved gas viscosity at the reduced temperature and pressure of the gas free bitumen. Mehrotra and Svrcek (1987) followed the methodology of Johnson et al. (1987) and fitted the viscosity of four gas free Alberta bitumens with AARDs within 20% of the measurements by adjusting the molecular weight and specific gravity of the pseudo-components.

Following the studies of Jacobs (1978), Khan (1982) and Sarkar (1984), Svrcek and Mehrotra (1988) fitted the experimental viscosity data of 7 Canadian gas free bitumens using the Walther equation and generalized it as a one-parameter correlation as follows:

$$\log\log(\mu + 0.7) = b - 3.63029\log(T) \tag{2.61}$$

where b is fitting parameter determined for each bitumen separately. Later, it was shown that a form of the equation with constant 0.8 instead of 0.7 is applicable to bitumen, diluted bitumen (Mehrotra, 1990b), and bitumen fractions (Eastick and Mehrotra, 1990), middle-East crude oils (Mehrotra 1990a), and pure hydrocarbons as discussed previously. Mehrotra et al. (1989) proposed the following mixing rule to predict (B_{ij}=0) the viscosity of the Cold Lake bitumen based on the viscosity of its fractions with an AARD of 38%:

$$\log(\mu_{mix} + 0.8) = \sum_i \varpi_i \log(\mu_i + 0.8) + \sum_i \sum_j \varpi_i \varpi_j B_{ij} \tag{2.62}$$

where:

$$\varpi_i = x_i \left(\frac{MW_i}{MW_{mix}} \right)^{0.5} \tag{2.63}$$

x_i is the mole fraction and B_{ij} was defined as the interaction parameter between two components. Later applications of Equation 2.62 for pseudo-binary mixtures of bitumens and solvents (Mehrotra 1990b, 1992a and 1992b) showed that non-zero interaction parameters were required in most cases. The prediction with B_{ij}=0 were found to be within an order-of-magnitude of the experimental values. However, the predictions were improved to within 15% of all data points when B_{ij} values were correlated with temperature for each pseudo-binary pair. The general correlations of B_{ij} were determined empirically by matching individual data points.

Shramm and Kwak (1988) fitted their viscosity data for Athabasca bitumen using the Andrade equation. They also used the mixing rule of Lederer with the modification of Shu (1984), Equations 2.29 to 2.32, to predict the viscosity of naphtha diluted bitumen at 20 and 80 ºC using the density and viscosity of unmixed bitumen and naphtha as the inputs. Both the fitted Andrade equation and predictions of the Shu mixing rule were found to be within the uncertainties of the measurements.

Badamchizadeh et al. (2009a and 2009b) fitted the viscosity data of Athabasca bitumen with the Walther equation. They used the mixing rule developed by Lobe (1973) to predict the kinematic viscosity of the mixture knowing the volume fraction and kinematic viscosity of the components. The predictions were found within an order of magnitude of the measurements for the binary mixtures. Better results were achieved for the ternary mixtures where the predicted values were within factor of two of the measured data.

Yazdani and Maini (2010) fitted the viscosity data of nC_4 saturated heavy oil using the power-law mixing rule of Kendall and Monroe (1917), Equation 2.24, by adjusting the exponent to 0.09 from the default value of 1/3. Yazdani and Maini (2010) reported that the compositional viscosity models implemented in Winprop such as LBC model (Section 2.2.3.1) and CS model of Pedersen (Section 2.2.3.2) had limited success in

providing reliable predictions for n-butane saturated heavy oil mixtures. They also studied the performance of some predictive mixing rules from the literature and found that Shu's (1984) mixing rule provided the most satisfactory predictions (within 20% of the measurements).

Li and co-workers (Li et al. 2011, Li and Yang 2012) fitted Lloydminister heavy oil data with the Walther equation. Then, the viscosity of solvent saturated mixtures of the heavy oil (details in Section 2.3.1) were predicted with common predictive mixing rules from literature. They found that the predictions of the Lobe's mixing rule were within a factor of two of the measurements, but the mixing rule of Shu (1984) significantly over-predicted the mixture viscosity. The latter modeling result is in contradiction with the findings of the Yazdani and Maini (2010) despite of the similar trends in the measured viscosity values of the n-butane diluted heavy oils.

Kokal and Sayegh (1993) fitted the viscosity of the dead heavy oil, de-asphalted oil and its fractions with the Walther equation. Then, the Lederer mixing rule, Equations 2.29 to 2.31, was used to fit the measured data for the CO_2 saturated mixtures with an overall AARD of 8%. The value of parameter α was adjusted for each binary at each temperature. Although the value of α was found to be function of temperature (density) and viscosity ratio, a generalized relationship was not developed. Kokal and Sayegh (1993) reported that the generalized α proposed by Shu (1984), Equation 2.32, did not provide acceptable viscosity predictions, but detailed evaluations was not reported.

Loria et al. (2009) used a modified version (Sheng et al. 1989) of the Enskog theory for dense fluids (Section 2.2.3.4) to model the viscosity of the Athabasca bitumen. They used the Peng-Robinson equation of state to calculate the radial distribution function in Equation 2.57. The constant 0.8 in Equation 2.55 was also replaced with an empirical parameter (A_p). The values of A_p were determined by fitting the experimental data of the bitumen and linearly correlating them with temperature to give an overall AARD of 7% for the fitted model. However, Loria et al. (2009) did not study the applicability of their approach to predict the viscosity of mixtures of bitumen and solvents.

2.4 Summary

Development of viscosity models for petroleum industry has been the subject of research for decades. The theoretical models are only successful in describing the viscosity of gases in dilute condition; hence, semi-theoretical and purely empirical models are mostly suitable for dense gases and liquids. Some of the models are only applicable for either gas or liquid phases; but few full-phase viscosity models are also developed covering gas, liquid and supercritical fluid phases. Most of the single phase viscosity models rely on the interpolative viscosity mixing rules to calculate the viscosity of the mixtures. The full-phase viscosity models commonly utilize specific mixing rules to calculate the values of the essential parameters of the model for the given mixture based on the composition and the values of the parameters for the components. The reviewed full-phase viscosity models in this chapter relate the viscosity to state conditions; either temperature and density or pressure and density. The most widely used full-phase viscosity models in compositional reservoir simulators for natural gases, condensates and light conventional oils are LBC model and the corresponding state model by Pedersen and co-workers.

The common approach to model the viscosity of heavy oils and bitumens is to fit data with empirical viscosity correlations for liquids. The interpolative mixing rules are also commonly used to predict the viscosity of diluted heavy petroleum fluids or to fit the available mixture viscosity data. Few studies showed the inapplicability of the full-phase viscosity models for these fluids. The main issue is the high critical temperature of these fluids resulting in the considerably low reduced temperatures in common applications in petroleum industry. Hence, the full-phase models developed based on viscosity behaviour of pure hydrocarbon compounds at higher reduced temperatures are found inapplicable. The only exceptional performance among the reviewed full-phase viscosity models is reported for the Friction Theory viscosity model with applicability to wide range of petroleum fluids from natural gases to live heavy oils. However, the performance of this model to diluted heavy oils and bitumens is not yet studied.

CHAPTER THREE: EXPERIMENTAL METHODS

In this chapter, the experimental methods used in this thesis are presented including the chemicals and materials used in the experiments, the preparation techniques for the dead and live oil test samples, and the procedures for the gas-oil ratio, viscosity, and density measurements.

3.1 Materials

Two dead (gas free) crude oils from Western Canada were used for the experimental measurements. The first sample, WC-HO-S1 was an extra heavy crude oil with API gravity of 10.4. The second sample was a bitumen from the Peace River area and was provided in three batches; WC-B-B1, WC-B-B2 and WC-B-B3 with API gravities of 7.4, 7.4 and 7.2, respectively. Although the batches were from the same source reservoir, their viscosities were notably different. All samples were distilled and centrifuged by the provider to remove water and solids. The vaporized hydrocarbons were condensed and recombined with the crude oils but some losses of light ends occurred. The residual water content was less than 1 wt%. Two synthetic solution gas mixtures, with the compositions reported in Table 3.1, were purchased from Praxair Inc. Canada and were used to prepare live oil samples. Solution Gas Mixtures 1 and 2 were specified to match the reported native solution gas compositions of WC-HO-S1 and WC-B-B1, respectively. Note, the composition of the dissolved gas in recombined live oils, Table 3.1, was different than that of the synthetic solution gas mixtures due to the mixing process. This inconsistency will be discussed later.

The solvents used for the preparation of the diluted heavy oil and bitumen samples were a condensate, carbon dioxide, and pure n-paraffins including ethane, propane, *n*-butane, *n*-pentane, and *n*-heptane. The condensate was a multi component hydrocarbon mixture, with an API gravity of 69.8 and a calculated molecular weight of 90 g/mol based on the GC assay composition, Table 3.2. The condensate was provided by Shell Canada. Pressurized liquid carbon dioxide (purity of 99.5%), ethane (purity of 99%), liquid propane (purity of 99.5%) and liquid n-butane (purity of 99.5%) were purchased from

Praxair Canada Inc. Liquid atmospheric n-pentane (purity of 99.5%) and n-heptane (purity of 99.5%) were also obtained from VWR.

Reverse osmosis (RO) water supplied by the University of Calgary water plant and nitrogen (purity of 99.9%) purchased from Praxair Canada Inc. were used for the density-meter calibration. Viscosity standards S20, S30000, and N450000, purchased from Cannon Instruments, were used for the calibration and accuracy check of the viscometer. Technical grade acetone and toluene purchased from VWR were used to clean the containers, transfer vessels, viscometer, and density-meter.

Table 3.1: Composition of the synthetic solution gas mixtures used to prepare live oils and the actual dissolved gas in live oils.

Component	**Composition in Mass Fraction**			
	Gas mixture 1		**Gas mixture 2**	
	original	**dissolved**	**original**	**dissolved**
nitrogen	0.0092	0.0057	0.0691	0.0081
carbon dioxide	0.8085	0.8721	0.1609	0.1676
methane	0.1823	0.1222	0.5435	0.3475
ethane			0.0273	0.0468
propane			0.0640	0.1605
n-butane			0.0646	0.1119
i-butane			0.0610	0.1285
n-pentane			0.0003	0.0002
i-pentane			0.0093	0.0083

Table 3.2: GC assay of condensate used for the diluted heavy oil and bitumen studies.

Component	MW (g/mol)	Mass fraction ($\times 10^{-2}$)	Component	MW (g/mol)	Mass fraction ($\times 10^{-2}$)
CO_2	44.01	0	C_9	121	2.74
H_2S	34.08	0	C_{10}	134	2.41
N_2	28.01	0	C_{11}	147	1.54
methane	16.04	0	C_{12}	161	1.33
ethane	30.07	0	C_{13}	175	1.38
propane	44.1	0	C_{14}	190	1.41
i-butane	58.12	0.03	C_{15}	206	1.44
n-butane	58.12	0.96	C_{16}	222	1.23
i-pentane	72.15	15.05	C_{17}	237	1.03
n-pentane	72.15	18.33	C_{18}	251	0.84
C_6	84	18.73	C_{19}	263	0.56
methylcyclo-pentane	84.16	2.56	C_{20}	275	0.31
			C_{21}	291	0.19
benzene	78.11	1.17	C_{22}	305	0.12
cyclohexane	84.16	2.88	C_{23}	318	0.09
C_7	96	9.94	C_{24}	331	0.07
methylcyclo-hexane	98.19	3.58	C_{25}	345	0.07
			C_{26}	359	0.09
toluene	92.13	1.97	C_{27}	374	0.06
C_8	107	5.85	C_{28}	388	0.05
ethylbenzene	106.17	0.27	C_{29}	402	0.04
xylenes	106.17	1.29	C_{30+}	500	0.36

3.2 Apparatus Description

Density and viscosity measurement were carried out in a capillary viscometer, which was designed and built in-house and equipped with an in-line density-meter. A schematic of the apparatus is shown in Figure 3.1. The apparatus consists of two transfer vessels, an Anton Paar DMA HPM density-meter, and two capillary tubes which are connected with 0.25 inch AutoClave fittings. The apparatus is enclosed in a Blue M POM-136B-1 air bath to maintain a fixed temperature during the measurements. A Quizix SP-5200 pump system provides the required fluid flow to the capillary viscometer. The main

components of the apparatus and the theoretical basis of the measurements are described below.

3.2.1 Capillary Viscometer

The capillary viscometer consists of the capillary tubes, pressure transducers, transfer vessels, and the Quizix SP-5200 pump system. Two capillary tubes out of four calibrated capillary tubes, listed in Table 3.3, are installed for the series of the measurements for each test fluid. The pressure transducers are used to measure the pressure difference between the inlet and the outlet of the capillary tubes. For each experiment, both installed capillary tubes and pressure transducers are filled with the test fluid but only one combination is used for each viscosity measurement. The range of the viscosity measurements possible with each combination of capillary tube and pressure gauge is reported in Table 3.3.

3.2.2 Fluid Displacement System

A Quizix SP-5200 pump system is used to provide the required fluid flow for the apparatus. The fluid displacement is indirect so that the test fluid is not in contact with the pump system. The working fluid is hydraulic oil which conveys the flow to the test fluid by means of the transfer vessels. For the viscosity measurements, the test fluid is displaced from one transfer vessel to the other through the capillary tube. To do so, the pump system withdraws the hydraulic oil from the hydraulic oil reservoir and delivers it to the first vessel. The discharged oil from the second vessel passes through the back pressure regulator and returns to the oil reservoir. The back pressure regulator controls the outlet pressure which is the effective pressure during the measurements.

3.2.3 Anton Paar Density Meter

The in-line Anton Paar DMA HPM density-meter cell is installed in parallel to the capillary tubes. The density meter has a built-in temperature sensor which is used to measure the air bath/experiment temperature. The density meter cell is connected by an interface module to an Anton Paar mPDS 2000V3 evaluation unit. The real-time

measured oscillation period and the temperature are displayed by the evaluation unit. The precision of the oscillation period measurements are ±0.001 micro seconds.

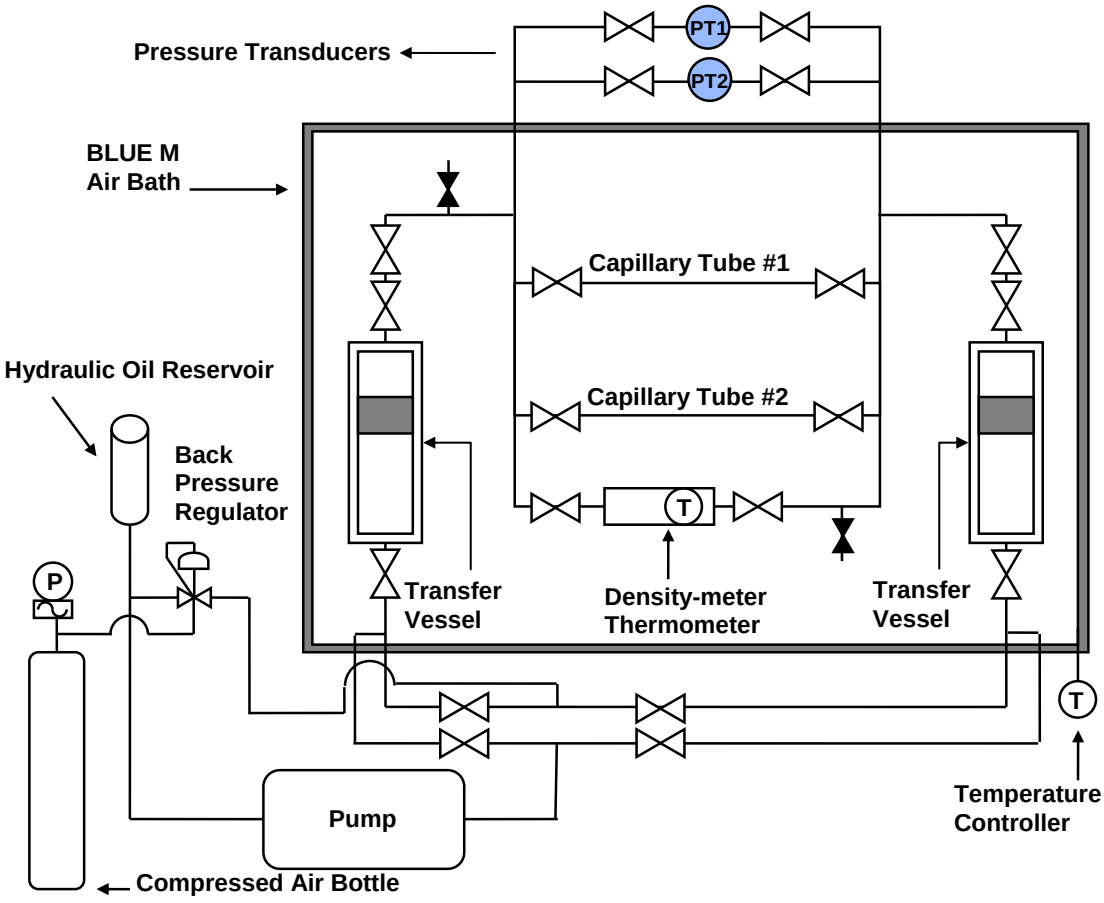

Figure 3.1: Schematics of the capillary viscometer and in-line density-meter apparatus.

Table 3.3: Summary of the calibrated capillary tubes available for the viscosity measurements. The maximum measurable pressure differences by the 1151 and 3051S gauges are 39.3 and 2200 kPa, respectively.

Capillary Tube	Nominal Outer Diameter (in.)	Calibration Fluid/ Temperature (K)	k (kPa.s/mPa.s.cm^3)	Pressure transducer	Approximate viscosity range (mPa.s)
1	0.25	S30000 at 323.15, 353.15, 373.15	0.3601	3051S	800 - 300000
				1151	20 - 6500
2	0.125	S30000 at 353.15, 373.15 S20 at 323.15, 353.15, 373.15	19.671	3051S	4 - 3200
				1151	0.4 - 100
3	0.125	S30000 at 353.15, 373.15 S20 at 323.15, 353.15, 373.15	49.268	3051S	2 - 1300
				1151	0.2 - 50
4	0.0625	S20 at 323.15, 353.15, 373.15	921.697	3051S	0.3 - 67
				1151	0.1 - 2.5

3.2.4 Control and Measurement System

The temperature and pressure of the measurements are maintained and measured by the following components:

Pressure Control: The pressure of the test fluid in the apparatus during the measurements is controlled using the back pressure regulator (BPR) on the return line of the hydraulic oil. The set pressure of the BPR is maintained using compressed air pressure. A Bourdon pressure gauge with a precision of ±0.05 MPa is used to monitor this pressure.

Temperature Control: The temperature of the air bath during the measurements is controlled by a self-tuning temperature controller. This controller unit regulates the input power to the heating unit of the air bath to maintain the temperature with a precision of ±0.1°C. The air bath is equipped with a fan to prevent the development of temperature gradients inside the air bath.

Temperature Measurement: The temperature of the test fluid in the apparatus during the measurements is recorded using the high accuracy temperature sensor of the Anton Paar density-meter with a precision of ±0.01 °C.

Differential Pressure Measurement: To measure the pressure difference between the inlet and outlet of the capillary tubes, two pressure transducers are available. The first pressure transducer is a Rosemount 1151 with a precision of ±0.01 psi and an operational range up to 5.70 psi which is preferable for low viscosity fluids. The other pressure transducer is a Rosemount 3051S with a precision of ±0.1 psi and an operational range of up to 333.3 psi, suitable for higher viscosity fluids.

3.2.5 Theoretical Basis of the Density and Viscosity Measurements

3.2.5.1 Density by Harmonic Oscillations:

The Anton Paar density-meter measures the period of harmonic oscillation of a quartz U-tube. The density of the contained test fluid in the U-tube alters the total mass of the U-tube and subsequently affects the oscillation period. The U-tube can be described as un-

damped oscillation of a mass suspended from a spring (Lagourette et al., 1992). The period of oscillation for an oscillator with one degree of freedom is given by:

$$\Lambda = 2\pi\sqrt{\frac{E}{M}} \tag{3.1}$$

where Λ is the oscillation period, E is the elasticity constant of the spring, and M is the total mass of U-tube and the test fluid as:

$$M = M_0 + \rho.V_0 \tag{3.2}$$

where M_o is the mass of the U-tube, and V_o and ρ are the volume and density of the test fluid in the U-tube. Equation 3.2 is substituted into Equation 3.1 to obtain the density of the test fluid, given by:

$$\rho = \frac{E}{4\pi^2 V_0}\Lambda^2 - \frac{M_0}{V_0} \tag{3.3}$$

The mechanical and geometrical properties of the U-tube are grouped into general constants to obtain the following linear relationship between the density of the test fluid and the square of the oscillation period:

$$\rho = D_A.\Lambda^2 - D_B \tag{3.4}$$

Since the pressure and temperature can affect the mechanical and geometrical properties of the U-tube, the constants D_A and D_B are generally temperature and pressure dependent. Two calibration fluids with known density at given temperature and pressure are required to determine the numerical values of D_A and D_B.

3.2.5.2 Capillary Viscometery

Capillary viscometery is based on the Hagen-Poiseuille equation (Brodkey and Hershey, 2003) which describes fluid flow through a circular pipe in laminar flow regime as follows:

$$Q = \frac{\Delta P}{128\mu L}\pi d^4 \tag{3.5}$$

where Q is the volumetric flow rate, ΔP is the pressure difference between the inlet and outlet of the pipe, d is the pipe diameter, μ is the viscosity of the fluid, and L is the

length of the pipe. The main assumptions in Hagen-Poiseuille equation are: 1) steady state flow; 2) fully developed flow; 3) constant viscosity of the fluid; and 4) laminar flow. The geometrical properties of the pipe are grouped into a proportionality constant, *k*, and Equation 3.5 is rearranged to obtain the following expression for viscosity:

$$\mu = \frac{\Delta P}{k\,Q} \tag{3.6}$$

Hence the viscosity of test fluid can be determined by measuring the pressure difference between the inlet and outlet of the tube with pre-determined *k* at known flowrate. More accurate measurements can be achieved by averaging the calculated viscosity from the multiple measurements at different flowrates. The values of *k* must be pre-determined using a calibration fluid with known viscosity.

3.2.5.3 Effect of High Differential Pressure on Viscosity Measurement

The assumption that the viscosity of the fluid is uniform along the length of the tube is invalid when considerable pressure drops occur along the tube. As the pressure decreases along the capillary tube, the viscosity of the fluid also decreases. Hence, the apparent viscosity of the fluid calculated using the Hagen-Poiseuille equation will be higher than the actual viscosity at the outlet pressure, the pressure at which the viscosity is typically reported. To correct the effect of high pressure drops on viscosity measurements, the following modifications to the method were developed.

Over the pressure ranges of the capillary viscometer experiments, viscosity is expected to be linearly related to pressure with a slope, α, defined as follows:

$$\alpha = \frac{\mu - \mu_0}{P - P_0} \tag{3.7}$$

where μ_0 is the viscosity in reference pressure P_0 (typically outlet pressure). The governing equation for laminar flow through a circular pipe then becomes:

$$\Delta P = \frac{\exp(\alpha k \mu_0 Q) - 1}{\alpha} \tag{3.8}$$

A linear form of flow Equation (3.8) is:

$$Y = X\mu_0 \tag{3.9}$$

where:

$$X = \alpha k Q \tag{3.10}$$

$$Y = Ln(1+\alpha\Delta P) \tag{3.11}$$

Hence, the slope of the line fitted to the plot of Y versus X with intercept of zero is the actual viscosity of test fluid at the outlet pressure. Since α is typically unknown, the correction of the measured viscosity data is made using an iterative procedure, Figure 3.2. Note that the maximum pressure drops during the measurements were controlled below 1000 kPa to hold the assumption of Equation 3.7 valid.

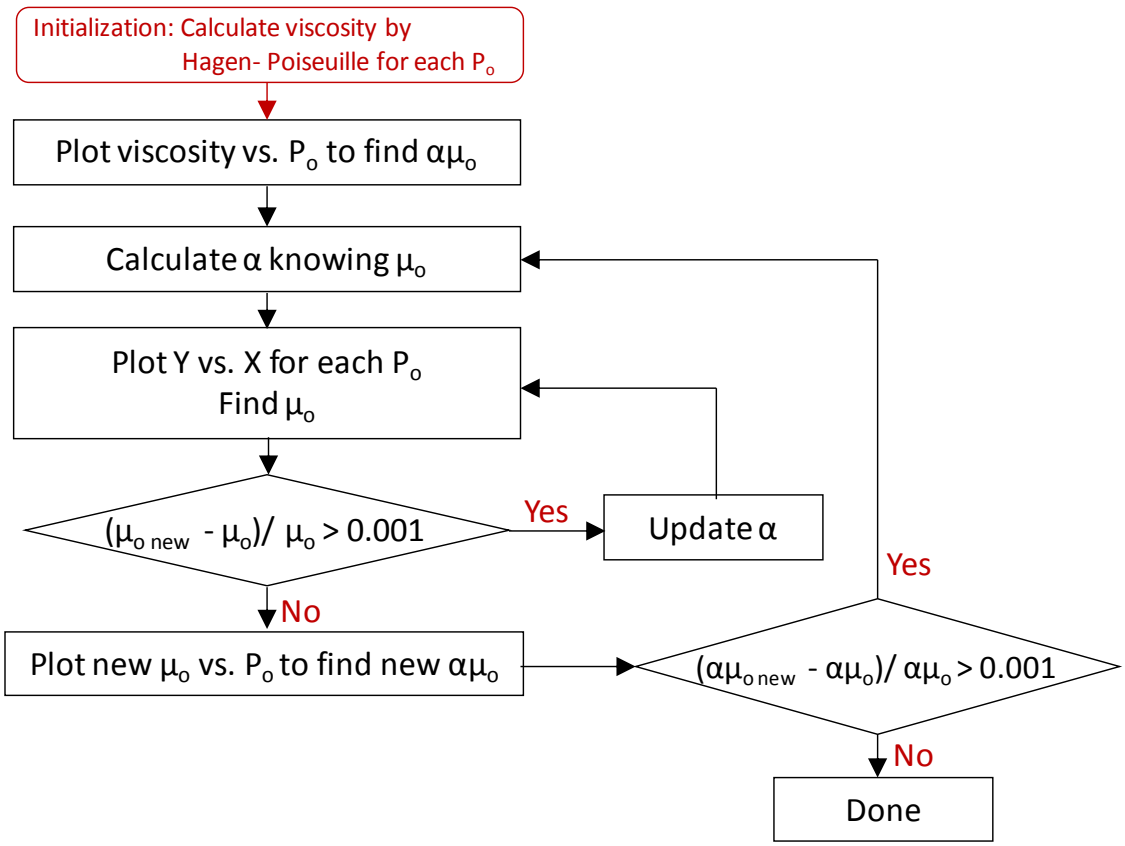

Figure 3.2: Iterative procedure to correct the effect of high differential pressure on viscosity measurements.

3.3 Experimental Procedures

3.3.1 Sample Preparation

The density and viscosity measurements were done for 28 fluids. Among these fluids, the condensate, base dead crude oils, and their mixtures with liquid solvents (condensate, n-pentane and n-heptane) are liquids at ambient conditions. The rest of the test fluids have saturation pressures above atmospheric pressure and required a high-pressure preparation procedure. The preparation procedures at ambient and pressurized conditions are described below.

3.3.1.1 Atmospheric Sample Preparation

Dead Crude Oils and Condensate: The condensate, dead WC-HO-S1 and three batches of the bitumen were simply poured into the intended transfer vessel for the measurements. Enough settling time were provided for the trapped air bubbles in the test fluids to liberate under moderate vacuum.

Dead Oils Diluted with Liquid Solvent: To prepare a mixture, the masses of the dead crude oil and the solvent were measured gravimetrically as they were placed in a container. The container was capped to prevent evaporation losses. Then, the fluid was mixed continuously for 4 hours in a rotary mixer at 6 RPM and poured into a transfer vessel for the measurements.

3.3.1.2 Pressurized Sample Preparation

Pressurized samples were prepared using an in-house mixing apparatus, Figure 3.3. The main component of the apparatus is the contactor which consists of a horizontal cylindrical vessel with two moving pistons on either sides of a perforated disks fixed in the middle of the vessel. To mix the test fluid, it is displaced back and forth through the perforated plate. The pistons provide enclosed variable volumes up to 600 cm^3 inside the vessel to contain the test fluid. The apparatus is equipped with Quizex SP-5200 pump system with hydraulic oil as the working fluid. Temperature is controlled to within ±0.5 °C using heating tapes. Pressure is monitored and controlled using a back pressure regulator (BPR) on the return line of the hydraulic oil.

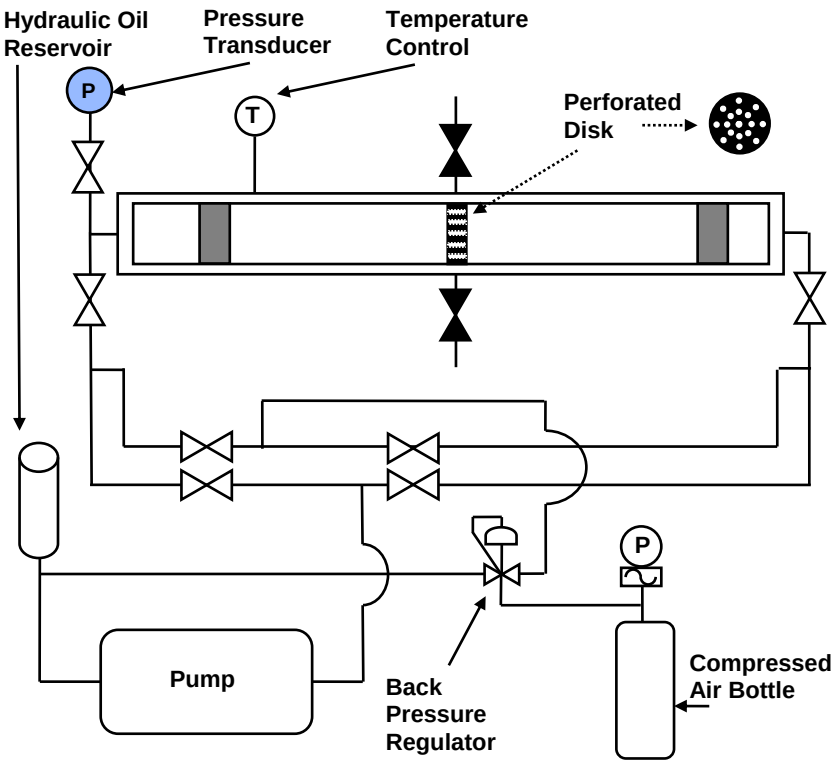

Figure 3.3: Schematics of the mixing apparatus used for the preparation of the pressurized samples.

Live Crude Oils: To prepare live crude oils, the contactor was initially filled with 600 cm^3 of the synthetic solution gas at 17 °C. Then, 430 g of heavy oil/bitumen were displaced into to the contactor though the injection port by means of an external transfer vessel. The dead crude and solution gas were mixed for 2 to 3 days at 50 °C and 10 MPa. Then the pressure and temperature were set to the desired equilibrium condition for 10 days. During this period, the expansion of the enclosed volume was monitored by the pump system to ensure the equilibrium. After equilibration, the excess solution gas cap was removed at constant pressure. The live crude oil was then displaced into the intended transfer vessel at pressures higher than the bubble pressure of the live oil. The sample in the transfer vessel was then connected to the capillary viscometer apparatus for the viscosity and density measurements.

Live Oils Diluted with Condensate: The condensate-diluted live heavy oil/bitumen samples were prepared by mixing known masses of the condensate with live crude oils. Initially, a known mass of the condensate was placed inside the intended transfer vessel. The piston was moved up by the pump system to minimize the vacant volume of the vessel. Then, a known volume of the live crude oil was pumped into the vessel at the pressure well above the bubble pressure. The displacement pressure was controlled by the BPR set on the outlet hydraulic line of the transfer vessel. The volume of the displaced live crude oil was determined from two independent measurements: 1) from the pump displacements and 2) from the displaced hydraulic oil out of the transfer vessel. Using the measured density data of the live oil and the displaced volume, the mass of live oil added to the transfer vessel and the composition of the mixture were calculated. Then, the transfer vessel was connected to the capillary viscometer apparatus for the density and viscosity measurements.

Dead Oils Diluted with Gaseous Solvent: The mixtures of bitumen with light n-paraffins or carbon dioxide were also prepared in the contactor. First, the pistons were fully moved in opposite direction to have the maximum enclosed volume of 600 cm^3 inside the contactor. The inside volume was evacuated and the contactor was weighed. Then the light gaseous or pressurized liquid solvent was filled into the vessel through one injection port. The contactor was weighed again and the extra solvent was released to have the required mass of the solvent inside the contactor. Afterwards, the required amount of the bitumen to reach the intended composition of the mixture was injected into the contactor using one transfer vessel and the pump system. The volume of the injected bitumen was determined by the pump displacement and converted to mass using the measured density data of the bitumen. The mass of the injected bitumen was confirmed subsequently after weight measurement of the contactor containing the bitumen and solvent. The bitumen and solvent were mixed following the procedure described before for the live oils. The equilibrium of the mixture was confirmed by monitoring the pressure and volume of the mixture after 4 days of mixing. The mixture was considered to be equilibrated when there was no longer any volume or pressure change. The prepared pressurized test fluid was then displaced to the transfer vessel for the density and viscosity measurements.

3.3.1.3 Homogeneity of Mixtures

For all mixtures, before any density and viscosity measurements, the mixture was flowed back and forth through the capillary viscosity to ensure complete mixing. The mixture was considered to be homogeneous when the density and pressure drop were consistent for the entire displacement.

3.3.2 Apparatus Preparation

Prior to transfer of the test fluid to the transfer vessels, the transfer vessels were cleaned and rebuilt. All the O-rings were also replaced with new replacements to ensure leak-free vessels.. Both transfer vessels were pressure tested with compressed air up to 13 MPa to ensure no leakage. To prepare the apparatus for the experiment, the appropriate capillary tubes were selected based on the viscosity range of the test fluid (Table 3.3) and installed. Two transfer vessels containing the test fluid were connected to either end of the apparatus. Then, the apparatus was filled with compressed air to pressure-test up to 13 MPa. After securing any probable leakage sites, the apparatus was evacuated for two hours with vacuum pump. Then, the test fluid was injected to the apparatus by pumping the hydraulic oil to the second transfer vessel at the highest flow rate of the pump (15 cm^3/min) to minimize the separation of the light components from the test fluids. Once the apparatus was filled up, the test fluid was flowed through the apparatus back and forth with BPR set to ensure all the flow paths were filled and to confirm the homogeneity of the test fluid.

3.3.3 Viscosity and Density Measurement

Density and viscosity measurements of the test fluid at each pressure and temperature condition were taken simultaneously. Prior to each measurement, the temperature of the air bath was set to the test temperature. Also the set pressure of the BPR was maintained at the test pressure (which is greater than the bubble pressure of the test fluid) using the compressed air bottle. While the temperature equilibrated, the test fluid was flowed back and forth through the apparatus. The apparatus and test fluid was assumed to be equilibrated at the test temperature when the temperature reading by the Anton Paar temperature sensor maintained at fixed value for at least two hour within ±0.05°C. Note

that, for the room temperature measurements, the air bath was closed to equilibrate for 12 hours but the heating unit was not used.

Before collecting data for each viscosity measurement at a given pressure and temperature, the zero-shift value of the pressure transducer at no flow condition was recorded. Then, the test fluid was flowed from one vessel to other though one of the installed capillary tubes at a fixed flow rate. Once the flow reached a steady state condition, the pressure difference between its inlet and outlet was recorded and corrected for the zero-shift value. The differential pressure readings were averaged over a time interval of 1 min and were precise to within either ±0.2 or ±0.03 psi depending on the pressure transducer.

To ensure that the flow regime in the tube was laminar, the Reynolds number of the flow was calculated using the flow rate, nominal tube diameter, and the estimated density and viscosity of the fluid. The data were only used if the Reynold's number was below 2000. This procedure was repeated at 5 different flow rates and the differential pressure values were recorded. The viscosity of the test fluid at the test pressure and temperature was calculated as the average of the calculated viscosities at the 5 flow rates. The measured viscosities were corrected following the procedure described in Section 3.2.5.3 if the measured maximum differential pressure was higher than 200 kPa (30 psi).

To measure density, the test fluid was flowed through the capillary tube at the low flow rate of 0.001 cm^3/min to maintain the test pressure set by BPR throughout the apparatus. Once the flow reached a steady state condition, the measured oscillation period by Anton Paar evaluation unit was recorded. Then, the density of the test fluid at the test pressure and temperature was calculated by the oscillation period and the corresponding calibration constants of the density-meter. Note, during the measurements, there was no flow through density-meter. Only one valve was open to the density meter so that the pressure of the test fluid inside the density-meter was equal to the set pressure of BPR.

3.3.4 Apparatus Clean-up

Once the measurements were completed at all the specified pressure and temperature conditions, the hydraulic oil was pumped to both transfer vessels to discharge the test fluid out of the apparatus through the discharge port. Then, the compressed air was connected to the apparatus and was used to blow out the residual test fluid. The compressed air was also used to displace the piston of the transfer vessel back to the bottom of the vessel. The transfer vessel was then filled with clean toluene. The pump system was then used to fill up the apparatus with the toluene. All the flow paths through the apparatus were individually swept with the high pressure flow of toluene; then, toluene was discharged and replaced with clean toluene. The toluene wash was repeated multiple times until the discharged toluene was clear and colorless. The final toluene wash was done at high temperature-high pressure conditions to dissolve any residual bitumen inside the apparatus. Once the cleaning was completed and the toluene was discharged, the air bath temperature was set to 150°C to evaporate the residual toluene. Afterwards, all the flow paths through the apparatus were blown out by compressed air. Finally, the apparatus was evacuated by vacuum pump for 2 hours to completely withdraw the toluene vapor.

3.4 Calibration and Accuracy Check

3.4.1 Capillary Viscometer:

The calibration of the capillary viscometer required determination of the proportionality constant (k) of the capillary tubes using fluids with known viscosity. Viscosity standards S20 and S30000 by Cannon Instruments were used as the calibration fluids. The viscosity and density of these fluids are provided by manufacturer versus temperature at atmospheric pressure (see Apendix A).

Differential pressure data were collected for viscosity standards at 5 flow rates at temperatures of 323.15, 353.15 and 373.15 K for each combination of the capillary tunes and pressure transducers. The proportionality constant was determined as the slope of the line (with intercept of zero) fitted to the data of normalized differential pressure values versus flow rate, as shown in Figure 3.4 for Tube 3. The normalized differential pressure

was calculated as the ratio of differential pressure divided by the known viscosity of the given calibration fluid. The calibration standards used and calibrated proportionality constants of the capillary tubes are reported in Table 3.3. Note that the proportionality constants of the tubes are independent of the calibration fluid, temperature, and pressure transducer used for the calibration.

The normalized differential pressure data used for the calibration were generally scattered around the best fit line to within 4%, as shown for Tube 3 in Figure 3.4. To assess the consistency of the reference data used to calibrate the capillary tubes, the viscosity of the viscosity standards were back-calculated using the calibrated proportionality constants reported in Table 3.3. The errors in the measured viscosity of the standards are reported in Table 3.4. The relative error of the back-calculated viscosity values of the standards ranges from 0.23 to 3.73 percent. There was no systematic inconsistency in the data.

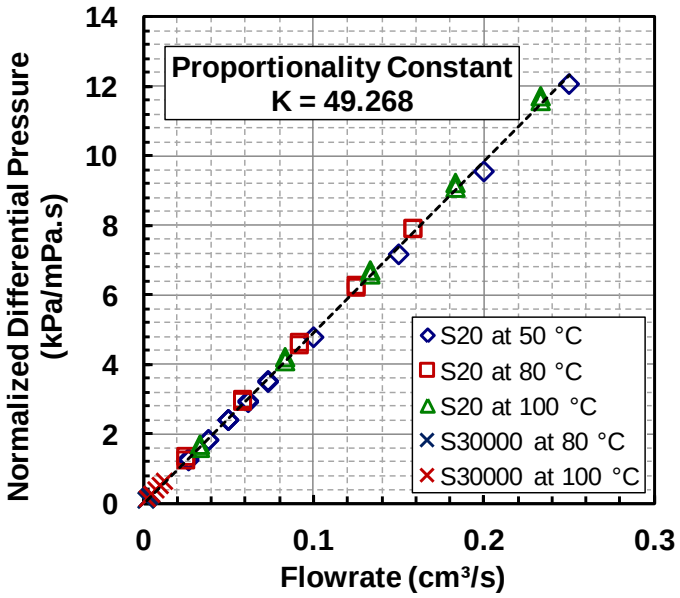

Figure 3.4: Proportionality constant of Tube 3 determined from plot of normalized differential pressure data versus flowrate.

Table 3.4: Consistency check of the data used for the calibration of the capillary tubes.

Capillary Tube	Reference Fluid	Temperature (K)	Reference Viscosity (mPa.s)	Pressure Transducer	Measured Viscosity (mPa.s)	Error %
1	S30000	323.15	9625	1151	9266	-3.73
				3051S	9400	-2.34
	S30000	353.15	1443	1151	1437	-0.45
				3051S	1440	-0.23
	S30000	373.15	530.6	1151	535.2	+0.86
				3051S	531.9	+0.24
2	S20	323.15	10.68	1151	10.62	-0.56
				3051S	10.59	-0.84
	S20	353.15	4.614	1151	4.692	+1.69
				3051S	4.663	+1.06
	S20	373.15	3.035	1151	3.074	+1.29
				3051S	2.956	-2.61
	S30000	353.15	1443	3051S	1447	+0.25
	S30000	373.15	530.6	3051S	545.2	+2.75
3	S20	323.15	10.68	1151	10.36	-2.96
				3051S	10.39	-2.72
	S20	353.15	4.614	1151	4.667	+1.14
				3051S	4.707	+2.01
	S20	373.15	3.035	1151	3.096	+2.00
				3051S	3.050	+0.50
	S30000	353.15	1443	3051S	1458	+1.06
	S30000	373.15	530.6	3051S	541.4	+2.04
4	S20	323.15	10.68	1151	10.32	-3.41
				3051S	10.39	-2.69
		353.15	4.614	1151	4.564	-1.09
				3051S	4.574	-0.86
		373.15	3.035	1151	3.046	+0.37
				3051S	3.053	+0.61

To assess the accuracy of the viscosity measurements, the viscosity of pure n-heptane, pure toluene, and the viscosity standard N450000 were measured. The measured values are compared to literature data (NIST, 2008) for pure n-heptane and toluene in Figure 3.5 and Figure 3.6, respectively. The relative errors of the measured values by the capillary viscometer range from 0.1% to 11% with overall average of 3.3%. The highest deviations were observed for viscosity measurements for n-heptane with Tube 2 at higher temperatures. Note that the viscosity values of the n-heptane at these conditions are out of the recommended application range of Tube 2 where the resolution of the pressure gauge is comparable to the measured differential pressure and can cause biased measurements.

The viscosity of the N450000 at 408.15 K was also measured with three combinations of the capillary tubes and pressure transducers as follows: 2693 mPa.s with Tube 1 and 3051S, 2708 mPa.s with Tube 1 and 1151 and 2705 mPa.s with Tube 3 and 3051S. The relative deviations of these measurements from the reference value of 2606 mPa.s are 3.3%, 3.9% and 3.8%, respectively. The deviation is within the 4% consistency range of the data used for the calibration of the tubes. The repeatability of the viscosity measurements for heavy oil and bitumen samples was also assessed as ± 3%.

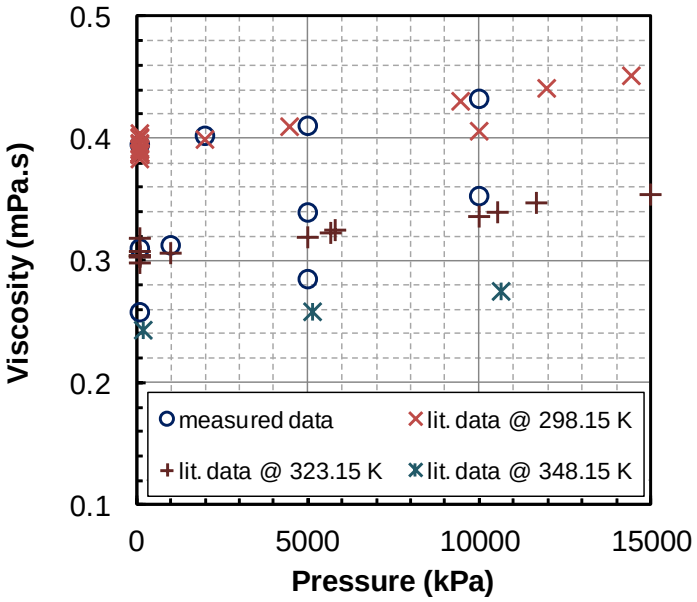

Figure 3.5: Comparison of measured viscosity of n-C_7 with Tube 2 and literature values (NIST 2008). Note, the repeatability of the measurements is within the size of the symbols.

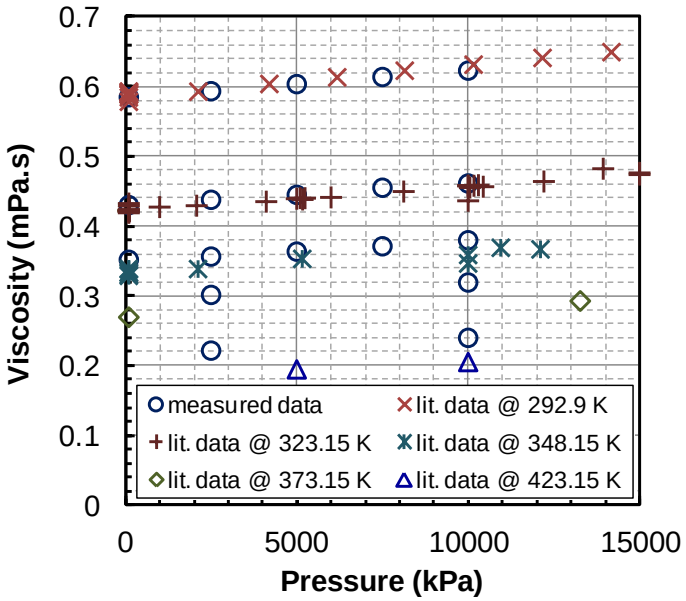

Figure 3.6: Comparison of measured viscosity of toluene with Tube 3 and literature values (NIST 2008).

3.4.2 Anton Paar Density Meter:

The calibration of the Anton Paar density-meter required the determination of the two density meter constants, D_A and D_B versus temperature and pressure. Nitrogen and degassed RO water were used as the calibration fluids with reference density values compiled from the DMA HPM instructional manual. Oscillation period data were collected for the calibrations fluids at six temperatures; 323.15, 348.15, 373.15, 398.15, 423.15 and 448.15 K and five pressures; 100, 2500, 5000, 7500 and 10000 MPa at each temperature. The density-meter constants were then calculated for each temperature and pressure condition, Table 3.5. Note that linear extrapolation/interpolation must be used to estimate the density-meter constants for the pressure and temperature conditions not listed in Table 3.5.

The accuracy of the density measurements with calibrated density-meter was evaluated against the known density of the pure hydrocarbons and the viscosity standards. Figures 3.7, 3.8 and 3.9 compare the measured densities with the literature data (NIST, 2008) for n-pentane, n-hexane, and toluene, respectively. The relative deviations of the measurements are all less than 0.5% from the average of the literature values. The average absolute deviation is 0.8 kg/m^3 with standard deviation of 0.9 kg/m^3. The maximum absolute deviation of 3 kg/m^3 occurred for the room temperature measurements where the temperature control is least satisfactory. The deviations are wihtin the scatter of the literature data (±1.5 kg/m^3). The measured density of the viscosity standards S20 and S30000 at 323.15, 353.15 and 373.15 K are in better agreement with the reference values with all deviations less than 0.3 kg/m^3. The repeatibility of the density measurements for heavy oil and bitumen samples were also assessed as ± 0.3 kg/m^3.

Table 3.5: Calibrated density-meter constants versus pressure and temperature.

Temperature (K)	Pressure (MPa)	$D_A \times 10^3$ (kg/(m³.μsec²))	D_B (kg/m³)
323.15	100	2.366985	15895.44
323.15	2500	2.368264	15905.06
323.15	5000	2.368571	15907.45
323.15	7500	2.370213	15919.30
323.15	10000	2.366521	15893.17
348.15	100	2.348682	15877.76
348.15	2500	2.351924	15901.38
348.15	5000	2.350966	15894.71
348.15	7500	2.352136	15903.40
348.15	10000	2.350877	15894.63
373.15	100	2.331838	15871.16
373.15	2500	2.333395	15882.69
373.15	5000	2.335017	15894.70
373.15	7500	2.336017	15902.17
373.15	10000	2.332473	15876.80
398.15	100	2.313624	15855.68
398.15	2500	2.314228	15860.33
398.15	5000	2.314857	15865.18
398.15	7500	2.314519	15863.04
398.15	10000	2.314435	15862.56
423.15	100	2.299477	15870.33
423.15	2500	2.297920	15859.15
423.15	5000	2.296298	15847.51
423.15	7500	2.295702	15843.47
423.15	10000	2.295471	15842.05
448.15	100	2.279382	15841.83
448.15	2500	2.278865	15838.28
448.15	5000	2.278325	15834.57
448.15	7500	2.278635	15837.06
448.15	10000	2.277278	15827.49

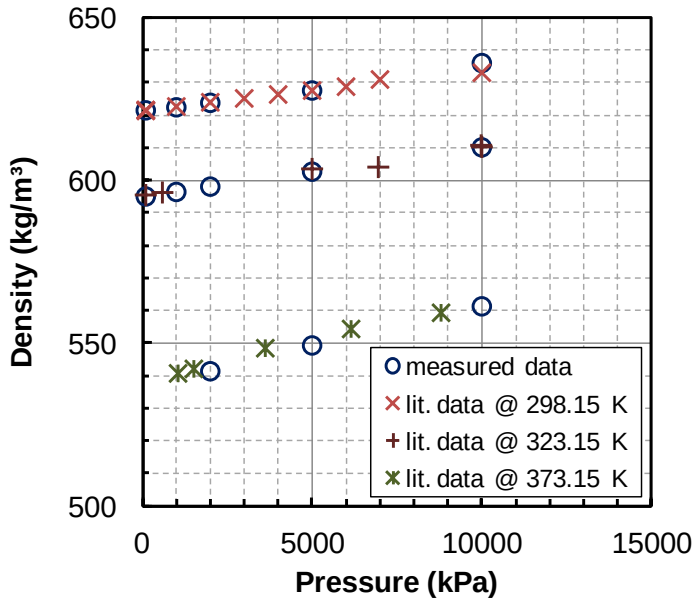

Figure 3.7: Comparison of measured density of n-pentane and literature values (NIST, 2008). Note, the repeatability of the measurements is within the size of the symbols.

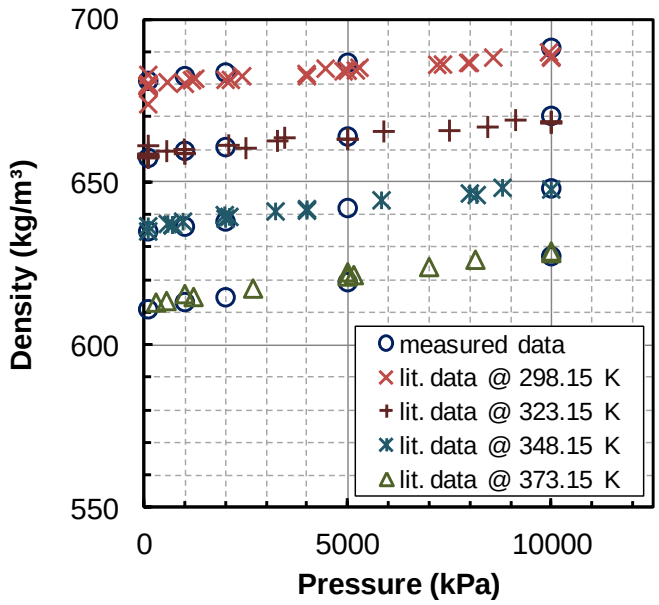

Figure 3.8: Comparison of measured density of n-heptane and literature values(NIST, 2008).

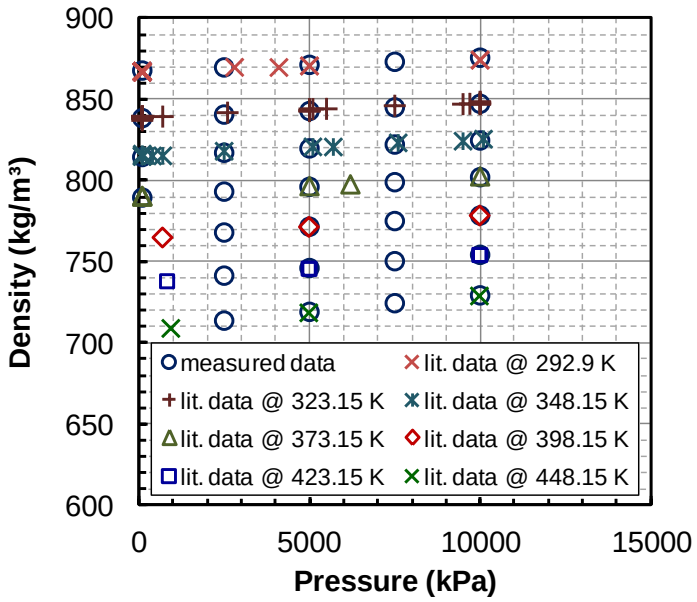

Figure 3.9: Comparison of measured density of toluene and literature values (NIST, 2008).

3.5 Live Oil GOR and Compositions Measurements

3.5.1 Gas-Oil Ratio (GOR) Measurement

After sample preparation of the live oils and before transferring the live oil to the viscometer, a small sample of the recombined live oil was also displaced into a Pycnometer for gas-oil ratio measurement. The measurement was required to determine the amount of the dissolved solution gas in the crude oil after equilibration. The Pycnometer is a small stainless steel cylindrical container with fixed volume of approximately 10 cm³. It is equipped with two injection ports to facilitate the evacuation before sampling, displacement of the live oil during sampling and cleaning up after the GOR measurement.

The pycnometer was initially cleaned and weighed. Then, it was connected to the injection port of the mixing apparatus and was evacuated along with the connecting lines using a vacuum pump. Then the injection port valve was slowly opened and the Quizix pump was used at maximum flowrate of 15 cm³/min to displace the live oil into the pycnometer. The system was allowed to reach equilibrium for 2 days at pressure of 30

MPa, well above the higher than bubble pressure of the live oil. This equilibration period ensured that the librated gas during the displacement is dissolved back into the live oil and the pycnometer is filled with a single phase liquid.

The filled Pycnometer was then weighed and moved to a JEFRI^{TM} Gasometer for GOR measurement. The JEFRI^{TM} Gasometer is a single-stage closed-system flash apparatus and is equipped with a variable-volume cylindrical container to collect the liberated gas from the test live oil. It is also equipped for the accurate measurement of the pressure, temperature, and volume of the gas. The live oil sample was flashed to the ambient condition (90 kPa and 20 °C) into a known volume. The mass of the librated solution gas from the live oil was calculated using the Ideal Gas Law (Z=1) and the gas molecular weight (calculated from its composition). The GOR in mass fraction is simply equal to the ratio of the mass of the gas and the mass of the live oil sample in the pycnometer. The measured GOR values for the live crude oils in this study are reported in Table 3.6. Note at these conditions, the error introduced to the measured GOR due to the ideal gas law assumption was at most 2%, which is within the uncertainties of the measurements.

Table 3.6: Summary of the equilibrium condition of the recombined live oils and measured gas-oil ratio.

Test Fluid		Equilibrium Condition		Measured GOR
		Pressure (kPa)	Temperature (K)	(mass percent)
WC-HO-S1	live	2100	295.55	0.8
WC-B-B1	live	2100	290.15	1.9
WC-B-B2	live	2600	290.15	2.2

3.5.2 Dissolved Gas Composition

The composition of dissolved gas in the live oils was generally different than the original composition of the synthetic solution gas mixture, due to: 1) the presence of the excess solution gas during equilibration, and: 2) different solubility of the gas components in the

heavy oil/bitumen. To confirm the composition of the dissolved gas, samples of the librated gas during the GOR measurements of Live WC-B-B1 and WC-B-B2 were sent for GC analysis by Core Laboratories Canada Ltd. The composition of the dissolved gas for Live WC-B-B2 was already reported in Table 3.1. The gas sample for Live WC-B-B1 was contaminated with air and the result of GC analysis was not reliable. However, the same gas composition as Live WC-B-B2 is a good approximate since both samples were prepared at similar equilibrium pressure and temperature conditions. The gas analysis for Live WC-HO-S1 was not performed and the reported gas composition in Table 3.1 is based on the simulation of the mixing procedure with VMGSim simulator following the methodology by Agrawal (2012).

CHAPTER FOUR: EXPANDED FLUID VISCOSITY CORRELATION

The objective of this thesis is to further study the recently developed Expanded Fluid (EF) viscosity correlation. In this chapter, the correlation is presented along with previously developed mixing rules. Sample results for application of the correlation to model the viscosity of pure hydrocarbons, heavy oil and bitumen and the relevant mixtures are also briefly reviewed. The advance developments on EF correlation in the scope of this thesis will be presented on the following chapters.

4.1 Basic Framework

The Expanded Fluid (EF) viscosity correlation is a form of free volume theory; that is, it is based on the empirical observation that, as the fluid expands, its fluidity (inverse of viscosity) increases due to the greater distance between the molecules. Several previous viscosity models based on the free volume theory (Section 2.2.2.3) attempted to formulate the observation, but found limited applicability especially at lower temperatures. This limitation is significant for heavy oils and bitumens where the viscosity increases dramatically at lower temperatures (Section 2.3.1). Yarranton and Satyro (2009) observed that the same drastic viscosity change occurs for the pure hydrocarbons at very low temperature, Figure 4.1. They used this observation to develop a free volume based viscosity correlation suitable for heavy oils and bitumens.

Yarranton and Satyro (2009) considered the fluidity as a function of the expansion of the fluid from a hypothetical state, the "compressed" state of the fluid. They assumed that, as a liquid approaches a glass or solid phase transition, its molecules become too close together to move in viscous flow; therefore, at this compressed state, the fluidity is zero and the viscosity is infinite. Utilizing the concept of the residual viscosity, Yarranton and Satyro (2009) formulated the viscosity of the fluid is as a departure from the dilute gas viscosity as follows:

$$\mu - \mu_o = c_1\left(\exp\left(c_2\beta\right) - 1\right) \tag{4.1}$$

where μ and μ_o are the fluid and its dilute gas viscosity, c_1 and c_2 are fitting parameters. β is the correlating parameter defined as follows to quantity the expansion of fluid from the compressed state:

$$\beta = \frac{1}{\exp\left\{\left(\frac{\rho_s^*}{\rho}\right)^n - 1\right\} - 1} \tag{4.2}$$

where ρ is the fluid density and ρ_s^* is the density of the fluid in the compressed state. Parameter n is an empirical exponent which was found to improve the model performance near the critical region.

The framework of the correlation is empirical and was based on a preliminary investigation of the functionality of the viscosity and density data of saturated liquid n-alkanes. There are two versions of the correlation based on the above framework: *Version 1* uses measured density values; *Version 2* uses density values calculated with the Advanced Peng-Robinson (APR) Equation-of-State (EoS) implemented in VMGSim simulator package (VMG, 2011).

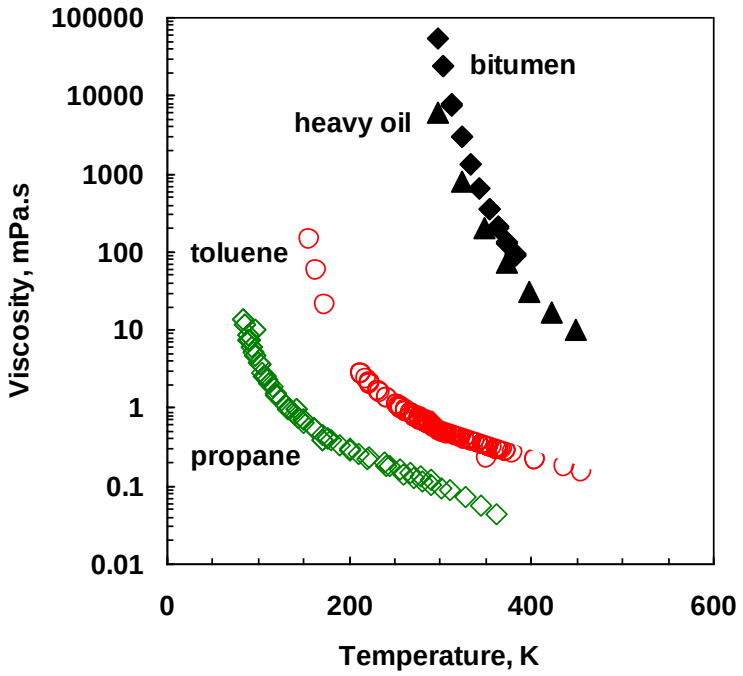

Figure 4.1: The drastic increase in the viscosity of hydrocarbons at low temperatures.

Version 1−Correlation with Measured Densities

Based on the experimental viscosity and density data for pure n-alkanes, Yarranton and Satyro (2009) fixed parameters *n* and c_1 of the correlation (Equations 4.1 and 4.2, respectively) as follows:

$$n = 0.165 \tag{4.3}$$

$$c_1 = 0.65 \tag{4.4}$$

The compressed state density was expressed as the following function of pressure to improve the correlation predictions at pressures higher than 10 MPa:

$$\rho_s^* = \frac{\rho_s^o}{\exp(-c_3 P)} \tag{4.5}$$

where ρ_s^o is the compressed state density in vacuum, c_3 is a fitting constant in kPa^{-1}, and *P* is the pressure in kPa.

For many pure hydrocarbons, the parameters c_2 and c_3 were related (Yarranton and Satyro 2009) to the viscosity of the fluid at 25°C and molecular weight as follows:

a) for all HCs except for complex aromatics:

$$c_2 = 0.241\mu_{298}^{0.13} \qquad \text{[dimensionless]} \tag{4.6}$$

b) for complex aromatics:

$$c_2 = 0.2\mu_{298}^{0.115} \qquad \text{[dimensionless]} \tag{4.7}$$

c) for all HCs:

$$c_3 = 1.68\times10^{-8} MW^{0.5} \qquad [kPa^{-1}] \tag{4.8}$$

In general, *Version 1* of the correlation requires three fluid-specific parameters for each fluid: c_2, c_3 and ρ_s^o. The inputs to the model are the measured fluid density, pressure, and the dilute gas viscosity.

Version 2−Correlation with Densities from the APR Equation of State

To eliminate the need of experimental density data, Satyro and Yarranton (2010) modified the EF viscosity correlation to use with densities calculated from an equation of state. Although any density model can be used for this purpose, the Advanced Peng-Robinson (APR) equation of state was selected as the density model due to its ability to

predict the density for gas and liquid states reasonably accurately (with volume translation) and for its consistency over the critical point and phase transitions. Also this equation of state with a large set of binary interaction parameters was already fully-implemented in VMGSim process simulator package. A detailed description of this cubic equation of state is given elsewhere (VMG, 2009) and a brief outline is provided in Appendix B, section B.2.

For *Version 2* of the EF correlation, the fixed parameters are set as:

$$c_1 = 0.4214 \qquad \text{[mPa.s]} \qquad (4.9)$$

$$n = 0.4872 \qquad \text{[dimensionless]} \qquad (4.10)$$

The previously adjustable parameter c_3 is correlated to molecular weight of the component by introducing a new parameter, c_4, which is also a function of molecular weight. The modified form of the pressure dependency of the compressed state density is given by:

$$\rho_s^* = \frac{\rho_s^o}{1 - c_4\left(1 - \exp\left(-c_3 P\right)\right)} \qquad (4.11)$$

where P is pressure in kPa and:

$$c_3 = 1.435 \cdot 10^{-6} MW^{0.4267} \qquad \text{[kPa}^{-1}\text{]} \qquad (4.12)$$

for MW <= 97:
$$c_4 = 0.015 + 0.00042\,\left|50 - MW\right| \qquad \text{[dimensionless]} \qquad (4.13)$$

for MW > 97:
$$c_4 = 0.035 \qquad \text{[dimensionless]} \qquad (4.14)$$

After fixing and correlating the parameters, *Version 2* of the correlation is left with only two fluid-specific adjustable parameters: c_2 and ρ_s^o for each pure compound. The inputs to the correlation are the fluid density from the APR EoS, molecular weight, pressure, and the dilute gas viscosity.

Dilute Gas Viscosity

Any of the low pressure gas viscosity models reviewed in Section 2.2.1.1 can be used to determine the low pressure gas viscosity for both *Version 1* and *2*. Satyro and Yarranton (2010) used Yaw's (Equation 2.13) with parameters taken from Yaws's handbook (Yaws 1999, 2008). They also used the Wilke's mixing rule (Equations 2.14 and 2.16) to calculate the dilute gas viscosity of the mixtures.

4.2 Volumetric Mixing Rules

The EF correlation treats a mixture as a single-component fluid with parameters determined from the component parameters. Yarranton and Satyro (2009, 2010) proposed volumetric mixing rules to calculate the fluid-specific parameters of the correlation. The viscosity of the mixture can then be predicted from the mixture density, dilute gas viscosity, pressure, temperature, and molecular weight (for *Version 2*).

Version 1:

The volumetric mixing rules of the correlation are:

$$\rho^{o}_{s,mix} = \sum_{i=1}^{nc}\sum_{j=1}^{nc} \varphi_i \varphi_j \frac{\left(\rho^{o}_{s,i} + \rho^{o}_{s,j}\right)}{2}\left(1-\beta_{ij}\right) \tag{4.15}$$

$$c_{2,mix} = \sum_{i=1}^{nc} \varphi_i c_{2,i} \tag{4.16}$$

$$c_{3,mix} = \left(\sum_{i=1}^{nc} \frac{\varphi_i}{c_{3,i}}\right)^{-1} \tag{4.17}$$

where i is the pure component number and nc is the number of components in the mixture. φ_i is the ideal volume fraction of component i in the mixture. β_{ij} is the binary interaction parameter between component i and j to tune the model to the available experimental viscosity data of mixture and has the default value of zero.

The volume fractions (φ) of the components are calculated at the pressure and temperature of the mixture. Hence, density data of the components at the mixture conditions are required. No correlations are provided for the binary interaction parameters (β_{ij}) and they take the default value of zero.

Version 2:

Equations 4.15 and 4.16 are used for ρ_s^o and c_2 as for *Version 1*. In *Version 2*, the values of c_3 and c_4 for the mixture are calculated based on the molecular weight of mixture and Equation 4.17 is not used. The volume fractions (φ) of the components are calculated at the standard conditions, 15.6 °C and 101 kPa.

Satyro and Yarranton (2010) found that non-zero β_{ij} were required to compensate for the errors introduced to the predictions by: uncertainties in the calculated density, the use of fixed volume fractions over the pressure and temperature range, and the inherent errors of the correlation. A general correlation was developed for interaction parameters based on the critical temperature (T_c) and Watson K-factor (WK) of the binary pair i and j:

$$\beta_{ij} = \left(1.6427 + 624.676\, f_{WK}\right) f_{Tc} \tag{4.18}$$

where f_{Tc} and f_{WK} are correlating functions defined as:

$$f_{Tc} = 1 - \frac{2\sqrt{T_{ci}T_{cj}}}{T_{ci} + T_{cj}} \tag{4.19}$$

$$f_{WK} = 1 - \frac{2\sqrt{WK_i WK_j}}{WK_i + WK_j} \tag{4.20}$$

and Watson K-factor is defined as:

$$WK = \frac{(1.8\,T_b)^{1/3}}{SG} \tag{4.21}$$

where T_b and SG are the normal boiling point and specific gravity of the compound.

4.3 Applications of the EF Correlation

The EF correlation was evaluated for several hydrocarbon systems including pure hydrocarbon compounds and binary mixtures and diluted heavy oil and bitumen systems. A review of these studies is provided below to highlight what has been done but also what remains to be done for petroleum industry applications.

Pure Hydrocarbon Compounds

Both versions of the correlation were tested for 39 pure hydrocarbons including n-alkanes, branched alkanes, alkenes, cyclics, and aromatics using the experimental density and viscosity data from NIST database (NIST, 2008). After adjusting the fluid-specific parameters of the correlation, both versions of the correlation fit the experimental data within the range of the measurement errors. The overall AARD and MARD of *Version 1* were 2.4% and 39%, respectively (Yarranton and Satyro 2009). For *Version 2*, the overall AARD was 5.8% (Satyro and Yarranton 2010). Of the more than 8000 data points, only 13% were predicted with greater than 10% deviation and only 3.5% with greater than 25% deviation. As an example, the viscosity data and model fit for toluene is shown in Figure 4.2. Table 4.1 is a summary of the fluid-specific parameters of the correlation for common hydrocarbon compounds.

Binary Mixtures of Hydrocarbon Compounds

Yarranton and Satyro (2009) and Satyro and Yarranton (2010) evaluated the predictions of the correlation against experimental viscosity data (Chevalier et al. 1990) of 64 binary liquid mixtures of n-alkanes, branched alkanes, cyclics, and aromatics at atmospheric pressure and 25°C. The predictions of the *Version 1* of the correlation were in good agreement with the measured values with overall AARD and MARD of 2.4% and 9.8%, respectively. Less satisfactory results were obtained for binaries of compounds from different HC families. For instance, the MARD for binary mixtures of naphthenes+aromatics was 10% in comparison to 3.8% for the binaries of n-alkanes.

Satyro and Yarranton (2010) found the predictions of *Version 2* to be less satisfactory than those of the *Version 1* with an overall AARD of 5.2% with default zero-valued β_{ij}. In general, a negative deviation of predictions (under-prediction) was observed for all binary mixtures. They then adjusted the interaction parameter for each binary and fitted the experimental data with an overall AARD of 0.8%. Finally, the binary interaction parameters were generalized (Equations 4.18 to 4.20) and the viscosities were predicted with an overall AARD of 3.1%.

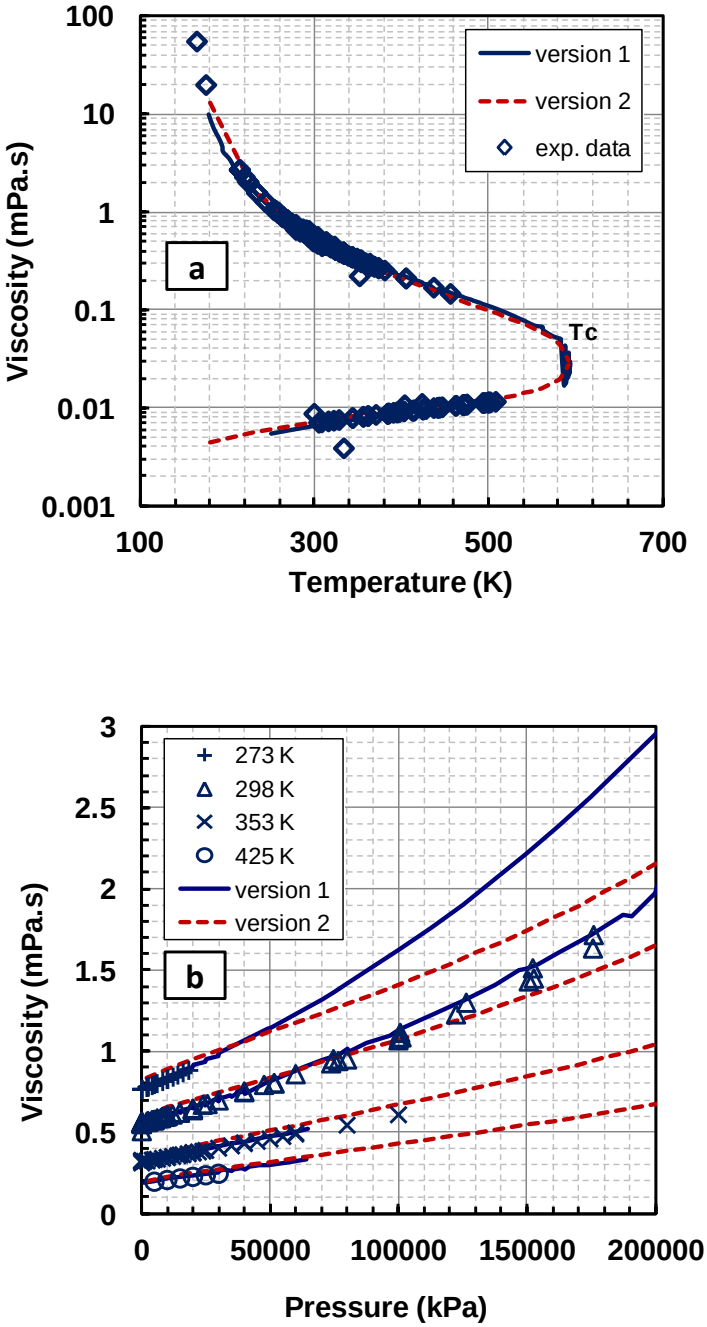

Figure 4.2: Correlation (lines) fitted to the experimental viscosity data (NIST, 2008) of toluene: a) saturated liquid and vapor; and b) compressed liquid.

Table 4.1: Summary of fluid-specific parameters of the EF correlation for selected hydrocarbon compounds from Yarranton and Satyro (2009) and Satyro and Yarranton (2010).

Component	Version 1			Version 2	
	ρ_s^o (kg/m^3)	c_2	$c_3 \times 10^6$ (kPa^{-1})	ρ_s^o (kg/m^3)	c_2
methane	540	0.1	0.1	504.33	0.0221
ethane	724	0.156	0.1	653.71	0.0324
propane	778	0.174	0.1	698.72	0.0354
n-butane	813	0.190	0.15	721.67	0.0351
n-pentane	837	0.198	0.18	744.10	0.039
n-hexane	849.1	0.205	0.18	765.44	0.0416
n-heptane	857.8	0.213	0.17	770.75	0.0400
n-octane	862.7	0.221	0.17	776.75	0.0414
n-decane	868.1	0.236	0.2	792.50	0.0445
n-dodecane	871.4	0.249	0.22	797.40	0.0462
n-tetradecane	875.5	0.265	0.24	801.88	0.0475
n-hexadecane	878.6	0.278	0.28	812.67	0.0524
cyclopentane	930	0.215	0.18	872.18	0.0526
cyclohexane	922.1	0.237	0.165	859.37	0.0589
methylcyclohexane	926	0.229	0.155	848.59	0.0490
benzene	1066.4	0.226	0.135	973.89	0.0489
toluene	1056	0.223	0.14	957.48	0.0421
o-xylene	1052.9	0.232	0.14	959.13	0.0459
p-xylene	1045.5	0.226	0.14	951.62	0.0456
ethylbenzene	1052	0.227	0.14	953.04	0.0432

Pseudo-Binary Mixtures of Heavy Oil/Bitumen and Solvents

Yarranton and Satyro (2009) and Satyro and Yarranton (2010) evaluated the predictions of the correlation against experimental viscosity data two heavy petroleum fluids and their mixtures with pure hydrocarbon compounds. The heavy petroleum fluids were treated as single component fluids and the mixtures as pseudo-binaries with the solvent as

the second component. The studied mixtures were a heavy oil with n-decane (data from Barrufet and Setiadarma, 2003) and Cold Lake bitumen with toluene (data from Eastick, 1989 and Mehrotra, 1990).

Both versions of the correlation were first fitted to the experimental viscosity data of the crude oils to determine the fluid-specific parameters of the correlation. Then, the volumetric mixing rules were used to calculate fluid-specific parameters of the correlation and predict the viscosity of the diluted crude oils. The AARDs of the correlation fitted to the data of the heavy oil and bitumen were 9% and 2% for *Version 1* and 18% and 3% for *Version 2*, respectively. The predictions of *Version 1* for both pseudo-binary mixtures were found to be within the scatter of the measurements, with an overall AARD of 18% and MARD of 50%. However, the predictions of *Version* 2 with β_{ij}=0 were highly deviated with AARDs as high as 250%. Therefore, the values of β_{ij} were adjusted for each pseudo-binary to fit the calculated viscosity values to the reported measurements. The AARDs of the fitted correlation were 16% for both the diluted heavy oil and diluted bitumen mixtures with β_{ij} values of 0.095 and -0.054, respectively. The generalized correlations of β_{ij} (Equations 4.18 to 4.20) gave a β_{ij} of 0.071 for the pseudo-binary of heavy oil and n-decane. However, the generalized correlations can only provide positive β_{ij} and therefore could not predict the negative β_{ij} for the pseudo-binary of the bitumen and toluene.

In another study, Oldenburg et al. (2010) used the *Version 1* of the correlation to model the viscosity reduction of the bitumen diluted with several low molecular weight multifunctional additives. The purpose of the study was to identify solvents which interacted with the crude oil molecules to reduce the viscosity beyond simple dilution. Although a detailed error analysis was not provided, *Version 1* predicted the viscosity of most of the diluted bitumen samples in the range of 10-90 percent volume content of additives generally to within the error of the measurements. Only aniline was found to reduce the viscosity beyond the predicted dilution effect. The authors speculated that aniline may disrupt asphaltene self-association.

While the EF correlation has the potential for petroleum industry applications, it remains to: 1) rigorously evaluate its performance for mixtures especially asymmetric mixtures containing dissolved gas components; 2) extend to non-hydrocarbon compounds; 3) develop generalized correlations for the fluid-specific parameters of the correlation; 4) study the applicability of the correlation as a compositional viscosity model for characterized conventional and unconventional crude oils; and 5) evaluate the of performance of the correlation for diluted heavy oils and bitumens with wide variety of hydrocarbon and non-hydrocarbon solvents.

CHAPTER FIVE: PREDICTING THE VISCOSITY OF ASYMMETRIC HYDROCARBON MIXTURES[1]

The objective of this study is to rigorously test the application of the EF correlation to predict the viscosity of liquid mixtures with dissolved gaseous components and asymmetric mixtures. The asymmetric mixtures are defined as mixtures of the components differ significantly in size, physical state, and/or chemical hydrocarbon family. These mixtures are found in a number of industrial applications such as crude oil production, refining and gas condensate systems. The viscosity of these mixtures can depart significantly from the viscosity predicted with existing models.

Although the EF correlation provided accurate predictions for mixtures of liquid components, volume based mixing rules have two significant disadvantages: 1) the volume fraction of each component in a mixture is not well defined for asymmetric mixtures or dissolved gases and; 2) the volume fractions are functions of temperature and pressure and must be recalculated at each change in conditions. Mass or molar based mixing rules avoid these disadvantages but are only valid if the mixture parameters are independent of pressure and temperature and are functions solely of the component parameters and the composition of the mixture. Due to the uncertainties related to the assignment of molecular masses to complex fluids, such as crude oils, this study will pursue the use of mass based mixing rules.

A number of proposed mixing rules are tested for *Version 1* of the EF correlation using experimental density and viscosity data for over 90 binary mixtures. The best performing set of mixing rule are also adopted for use with *Version 2*. The final set of mixing rules, using both measured and estimated densities, was also tested on an independent dataset of 40 binary, ternary, and multi-component mixtures of hydrocarbons as well as hydrocarbon/carbon dioxide mixtures.

---

[1] Contents of this Chapter published as: Motahhari, H.; Satyro, M. A. and Yarranton, H. W. Predicting the Viscosity of Asymmetric Hydrocarbon Mixtures with the Expanded Fluid Viscosity Correlation. *Ind. Eng. Chem. Res.* 2011, 50 (22), 12831–12843. http://dx.doi.org/10.1021/ie201415x

5.1 Pure Component Parameters

The fluid-specific parameters of the correlation for most of the pure components in this study were taken from the studies of Yarranton and Satyro (2009) and Satyro and Yarranton (2010) for use with *Version 1* and *2* of the correlation, respectively. Some of these values were reported in Table 4.1. For new components, the experimental viscosity and density data were compiled from the open literature and the parameters for the both versions of the correlation were determined by fitting the data. The detailed description of the procedure utilized for the regression is reported elsewhere (Satyro and Yarranton 2010).

Table 5.1 gives a summary of the fluid-specific parameters of the correlation for these pure components as well as the original source of the data. *Version 1* and *2* of the correlation were fitted to the data with an overall average error of 2.8% and 6.2%, respectively. The most significant deviations of the correlation occurred for 1-methylnaphthalene where the correlation fitted the data only with the maximum absolute relative deviation of 52% using the EoS estimated densities. Note, the deviations were within 8% for *Version 1* of the correlation using the measured densities. These results indicate that simple correlations of the pressure dependency parameters (Equations 4.12, 4.13 and 4.14) with molecular weight are not well suited for the complex aromatic components such as 1-methylnaphtalene. For the *Version 1* of the correlation, the maximum deviation of 20% occurred for squalane (2,6,10,15,19,23-hexamethyltetracosane).

5.2 Mixture Datasets

To develop and test the new mixing rules of the correlation, an extensive database of experimental viscosity and density data of the hydrocarbon mixtures was collected from the open literature. The database is summarized in Appendix C. The data are classified into three datasets according to their role in this study:

Dataset 1: Dataset 1 was used for the initial development and testing of the mixing rules with *Version 1* of the EF correlation. This dataset includes viscosity and density data for

methane and n-decane mixtures from two different sources (Canet et al. 2002, Audonnet and Padua 2004) over a broad range of compositions, pressure and temperature. The dataset for methane and n-decane was comprehensive and the correlation parameters for the two components are significantly different. Therefore, the trend of each parameter with composition could be computed and assessed over a wide range of conditions.

Dataset 2: Dataset 2 was used to compare the performance of different sets of mixing rules with both *Version 1* and *2* of the correlation. This dataset includes the viscosity and density data of 64 hydrocarbon liquid binaries from Chevalier et al. (1990) at atmospheric pressure and 298.15 K. These binary data were previously used (Yarranton and Satyro, 2009; Satyro and Yarranton 2010) for the assessment of the volumetric mixing rules of the correlation. To broaden the test conditions, data for an additional 29 binary mixtures of hydrocarbons, including mixtures containing light hydrocarbons and/or carbon dioxide at higher pressure and other temperature conditions, were added to the dataset.

Dataset 3: Dataset 3 was used as an independent data set to test the performance of the final proposed mixing rules. This dataset includes 40 binary, ternary, and more complex mixtures of the hydrocarbons and/or carbon dioxide. Some binary data were included in this dataset to study the performance of the mixing rules on binaries not included in Dataset 2. Also included in this dataset are mixtures that were not suitable for Dataset 2 due to: 1) limited available pure component data to determine the fluid-specific parameters of the correlation or 2) higher deviations of the fitted correlation for their pure components.

Note that for some of the mixtures, data were available for pressures as high as 500 MPa. Since the correlation parameters were determined for pure compounds using data only up to 200 MPa (Yarranton and Satyro, 2009; Satyro and Yarranton, 2010), the mixture data used in this work was limited to the pressures lower than 200 MPa.

Table 5.1: Fluid-specific parameters to use with *Version 1* and *Version 2* of the EF correlation for previously un-parameterized components.

Component	Version 1			Version 2		Data Source
	c_2	ρ_s^o (kg/m^3)	$c_3 \times 10^6$ (kPa^{-1})	c_2	ρ_s^o (kg/m^3)	
carbon dioxide	0.236	1617.7	0.187	0.0644	1572	NIST (2008), Padua et al. (1994), van der Gulik (1997)
n-tridecane	0.258	872.4	0.3	0.0475	803.4	NIST (2008), Zéberg-Mikkelsen et al. (2001a)
n-docosane	0.31	885.2	0.3	0.0668	829.2	NIST (2008)
n-tetracosane	0.335	893.2	0.3	0.0690	831.3	NIST (2008)
isocetane (2,2,4,4,6,8,8-heptamethylnonane)	0.281	889.4	0.214	0.0575	827.2	Dauge et al. (2001)
squalane (2,6,10,15,19,23-hexamethyltetracosane)	0.3035	876.9	0.377	0.0644	824.8	NIST (2008), Kumagai et al. (2006) Tomida et al. (2007)
1-methylnaphthalene	0.218	1133.9	0.167	0.0507	1069.7	Zéberg-Mikkelsen et al. (2001a)
n-heptylcyclohexane	0.272	926.8	0.24	0.0520	855.3	Baylaucq et al. (2002)
n-heptylbenzene	0.262	987.2	0.23	0.0398	895.9	Baylaucq et al. (2002)

5.3 Results and Discussion

5.3.1 Identification of Potential Mixing Rules − Dataset 1

Version 1 of the EF viscosity correlation (measured density values) has three parameters which require mixing rules: c_2, ρ_s^o, and c_3. Given that the pressure dependency parameter c_3 is the least sensitive parameter, its value is bounded in a narrow range for the pure components, and it has dimensions of 1/P, the following form of the mixing rules is proposed without further testing:

Mixing Rule C:
$$c_{3,mix} = \left(\sum_{i=1}^{nc} \frac{w_i}{c_{3,i}} \right)^{-1} \tag{5.1}$$

The first step in defining mixing rules for ρ_s^o and c_2 was to calculate optimum values for the two parameters for binary mixtures of methane and n-decane (Dataset 1). At constant composition, any mixture can be modeled as a pure component using *Version 1* of the EF correlation. Therefore, optimum values were determined by fitting viscosity data at each fixed composition over the full range of pressures and temperatures. Solid symbols in Figures 5.1 and 5.2 are the optimum values for ρ_s^o and c_2, respectively, for compositions ranging from pure methane to pure n-decane. While much of the data follow a common trend, there is considerable scatter. Therefore, the two parameters could not be fitted independently.

Instead, two potential mixing rules were defined for the compressed state density which is the most sensitive parameter in the correlation (Yarranton and Satyro 2009):

Mixing Rule A1:
$$\rho_{s,mix}^o = \left(\sum_{i=1}^{nc} \frac{w_i}{\rho_{s,i}^o} \right)^{-1} \tag{5.2}$$

Mixing Rule A2:
$$\rho_{s,mix}^o = \left(\sum_{i=1}^{nc} \frac{w_i}{\rho_{s,i}^{o\ 1/3}} \right)^{-3} \tag{5.3}$$

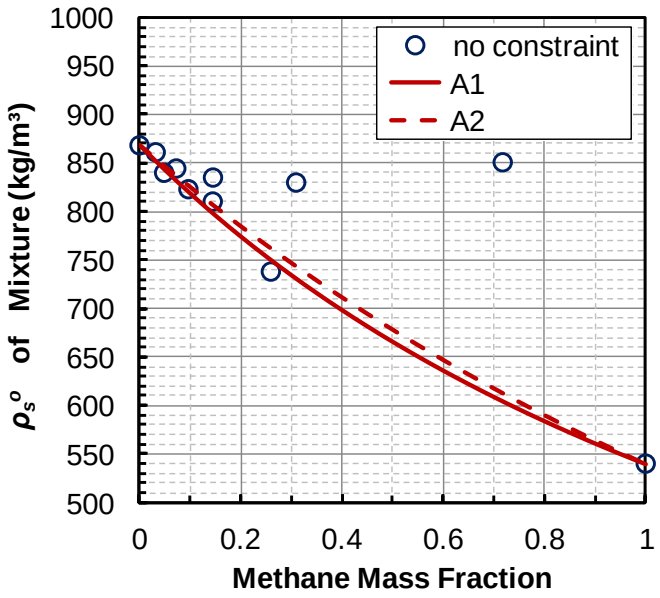

Figure 5.1: Comparison of the optimized compressed state density values for the mixtures of methane and n-decane using the experimental data points and the calculated values by Mixing Rules A1 (Equation 5.2) and A2 (Equation 5.3).

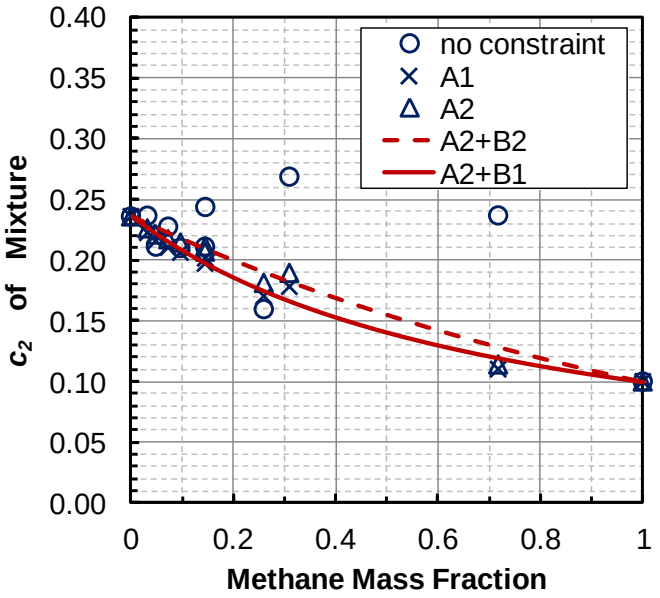

Figure 5.2: Comparison of optimized and calculated c_2 values for the mixtures of methane and n-decane. Symbols are optimized values constrained by the mixing rule indicated in the legend. Lines are calculated from the indicated mixing rules.

Mixing Rule A1 is the most natural method to mix the compressed state densities as it is identical in form to the ideal mixing rule for liquid densities that neglects excess volumes of mixing. Mixing Rule A2 is analogous to the 1/3 rule used to calculate the excluded volume parameter of an EoS and roughly approximates a molecular size based mixing rule. Figure 5.1 compares the compressed state densities determined from the two mixing rules with the optimum values determined for the methane/n-decane mixtures. Mixing Rule A2 provides a slightly better match to the optimum values but the final test is which mixing rule provides the best basis to develop a mixing rule for the c_2 parameter.

Optimum values of the parameter c_2 were then determined using the compressed state density values calculated by Mixing Rules A1 and A2. Figure 5.2 shows that, for both Mixing Rules A1 and A2, the new optimized c_2 parameters now follow a more consistent trend. Also note that the c_2 values from Mixing Rule A2 are consistently larger than from Mixing Rule A1 because Mixing Rule A2 predicted higher compressed state density values.

We can now test different mixing rules for the dimensionless parameter c_2. The simplest mixing rule is linear mass weighted mixing rule:

$$c_{2,mix} = \sum_{i=1}^{nc} w_i c_{2,i} \tag{5.4}$$

However, this mixing rule over-predicted the optimum c_2 values and was rejected without further evaluation. An alternative is to use an inverse mixing rule:

Mixing Rule B1:
$$c_{2,mix} = \left(\sum_{i=1}^{nc} \frac{w_i}{c_{2,i}} \right)^{-1} \tag{5.5}$$

Despite its simplicity, Mixing Rule B1 provided good agreement with the optimum c_2 values with Mixing Rule A1 and A2, Figure 5.2**.** Therefore, it was selected for further testing.

Another option is to introduce another variable into the mixing rule. Among the several physical and thermodynamic properties of the pure hydrocarbons, the compressed state was selected as the possible weighting factor for the mixing rules. This property is an

internal parameter to the correlation and is available for the pure components of the mixture. Also, it is a measure of the molecular size of the components in their ultimate compressed state. The following functional forms passed the preliminary screening and were selected for further evaluation:

Mixing Rule B2:
$$\frac{c_{2,mix}}{\rho^{o}_{s,mix}} = \sum_{i=1}^{nc} w_i \frac{c_{2,i}}{\rho^{o}_{s,i}} \tag{5.6}$$

Mixing Rule B3:
$$c_{2,mix} = \frac{1}{\rho^{o\ 1/2}_{s,mix}} \left(\sum_{i=1}^{nc} \frac{w_i}{c_{2,i} . \rho^{o\ 1/2}_{s,i}} \right)^{-1} \tag{5.7}$$

Mixing Rule B4:
$$c_{2,mix} = \frac{1}{\rho^{o\ 2/3}_{s,mix}} \left(\sum_{i=1}^{nc} \frac{w_i}{c_{2,i}^{1/2} . \rho^{o\ 1/3}_{s,i}} \right)^{-2} \tag{5.8}$$

5.3.2 Final Selection of Mixing Rules – Datasets 1 and 2

The initially identified mixing rules for the compressed state density and the parameter c_2 were combined into six sets of proposed mixing rules, Table 5.2. The predicted viscosities from *Version 1* of the EF correlation were evaluated for each set of mixing rules on Datasets 1 and 2. Note that the input density to *Version 1* of the EF correlation is the experimental density of the mixtures; and therefore, mixtures with missing density data or extrapolated density values were not included in this part of the study.

Table 5.3 provides a summary of the average absolute deviation (AAD), the maximum absolute deviation (MAD), the average absolute relative deviation (AARD), the maximum absolute relative deviation (MARD), and the bias of the viscosities predicted with each set of mixing rules. All six sets of mixing rules give similar overall results with an AARD of approximately 3%. Note that the predictions for the n-hexane/squalane and methane/methylcyclohexane mixtures were excluded from the error calculations due to inconsistent higher deviations in comparison to similar mixtures. For instance, the AARD for the n-hexane/squalane is 27% whereas the AARD is 13% and 7% for the binaries of squalane with n-butane and n-octane, respectively. The higher errors may be associated with the errors in the density measurements.

Table 5.2: Description of the proposed mixing rules sets for the correlation parameters.

Mixing Rules Set	$\rho^{o}_{s,mix}$	$c_{2,\,mix}$	$c_{3,\,mix}$
1	A1 (Equation 5.2)	B2 (Equation 5.6)	C (Equation 5.1)
2	A1 (Equation 5.2)	B1 (Equation 5.5)	C (Equation 5.1)
3	A1 (Equation 5.2)	B3 (Equation 5.7)	C (Equation 5.1)
4	A2 (Equation 5.3)	B2 (Equation 5.6)	C (Equation 5.1)
5	A2 (Equation 5.3)	B1 (Equation 5.5)	C (Equation 5.1)
6	A2 (Equation 5.3)	B4 (Equation 5.8)	C (Equation 5.1)

Table 5.3: Summary of the errors of the viscosity predictions for Dataset 1and 2 from *Version 1* of the EF correlation with each set of the proposed mixing rules.

Mixing Rules Set	AAD (mPa.s)	MAD (mPa.s)	AARD (%)	MARD (%)	Bias (%)
1	0.060	10.3	2.9	32.9	0.6
2	0.069	12.7	3.0	32.9	-0.3
3	0.069	12.8	2.9	32.2	-0.5
4	0.068	10.3	2.6	35.1	-0.4
5	0.079	12.8	2.9	36.8	-1.5
6	0.076	11.7	2.8	36.8	-1.3

A more revealing comparison is possible when the data are organized by carbon number or hydrocarbon family. Figure 5.3 shows that the AARD increases for binary mixtures as the difference between the carbon numbers (molecular weight) of the two components increases. However, the increase in error is significantly less with Mixing Rule Sets 1 and 4. Note that the higher error for the group C_1+C_6 is due to the slightly over-predicted viscosity values for the binaries of methane with n-hexane, benzene and cyclohexane with Mixing Rules Set 1. The larger error occurs because Mixing Rule B2 slightly over-predicts the optimum c_2 values as shown in Figure 5.2 for the similar binary of methane/n-decane. The predictions with the Mixing Rules Set 4 for the C_1+C_6 group are

in better agreement with the experimental values. For this set, the higher compressed state density values by mixing rules A2 compensates for the effect of the c_2 over-prediction. Similar results are also observed for the mixtures of methane with toluene. Also note that Mixing Rules Set 4 has higher error than the Set 1 for the group C_1+C_{30}. This group only includes the binary mixture of squalane/carbon dioxide.

Figure 5.4 shows that Mixing Rule Sets 4 to 6 (all using Mixing Rule A2) give lower AARD than Sets 1 to 3 (Mixing Rule A1) for almost all of the hydrocarbon mixtures but give significantly more error for mixtures that include carbon dioxide. Consider the binary of n-decane/carbon dioxide which is a special case because the numerical value of the c_2 parameter for carbon dioxide and n-decane are identical at 0.236. In this case, the errors in predicting the viscosity of these binary mixtures are all attributed to the compressed state density mixing rule. The AARDs with Mixing Rules A1 and A2 (Equations 5.2 and 5.3) for this binary were 4.4% and 11.1%, respectively, confirming that Mixing Rule A1 performs better for binaries involving carbon dioxide.

Overall, Mixing Rule Set 1 (Mixing Rules A1, B2, and C or Equations 5.2, 5.6, and 5.1) is selected as the preferred set of mixing rules because it is simple, gives an overall error similar to the other mixing rules, and provides the most consistent results for asymmetric mixtures.

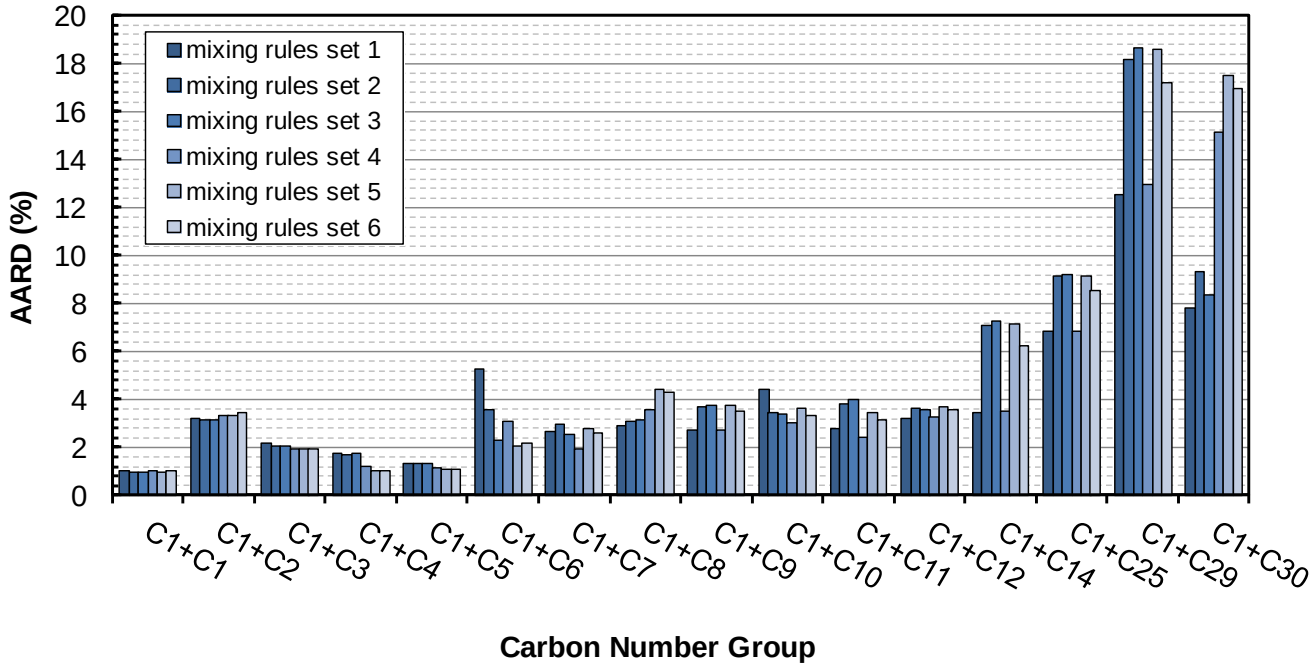

Figure 5.3: AARD of the predictions with each set of the mixing rules for the binary mixtures grouped by carbon number (molecular weight difference)**.**

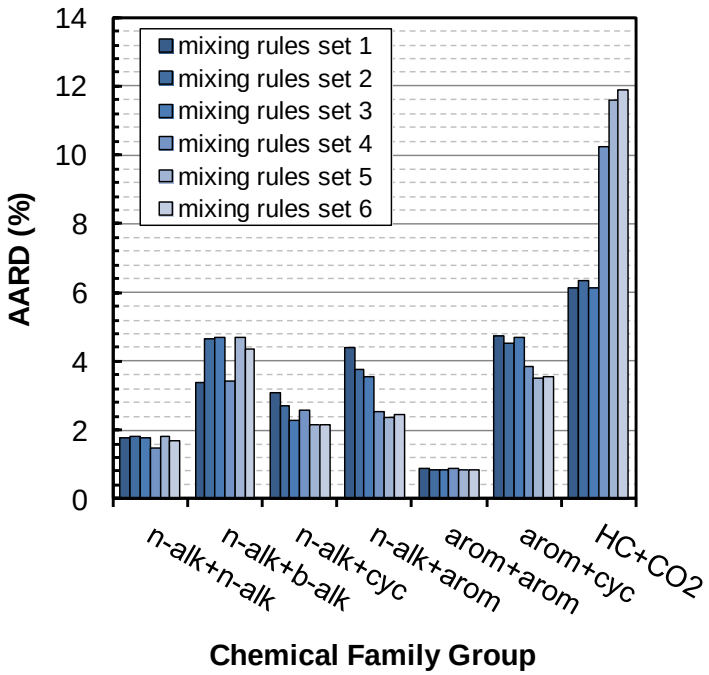

Figure 5.4: AARD of the predictions with each set of the mixing rules for the binary mixtures grouped into structural families.

Figure 5.5 and Figure 5.6 illustrate the performance of the correlation using Mixing Rules Set 1 for binary mixtures of n-decane with methane and n-hexane and o-xylene with benzene and cyclohexane, respectively. Not surprisingly, the correlation provides accurate predictions of the viscosity of mixtures composed of the similar components such as n-hexane/n-decane or o-xylene/benzene. The correlation slightly over-predicts the experimental viscosities of the asymmetric binary methane/n-decane with AARD of 8.7%. Also, the predictions for chemically asymmetric mixtures such as the binary of o-xylene/cyclohexane are less satisfactory with AARD of 3.8%, Figure 5.6. Similar results were obtained for binaries involving carbons dioxide as shown for mixtures of carbon dioxide with ethane and n-decane, Figure 5.7**.**

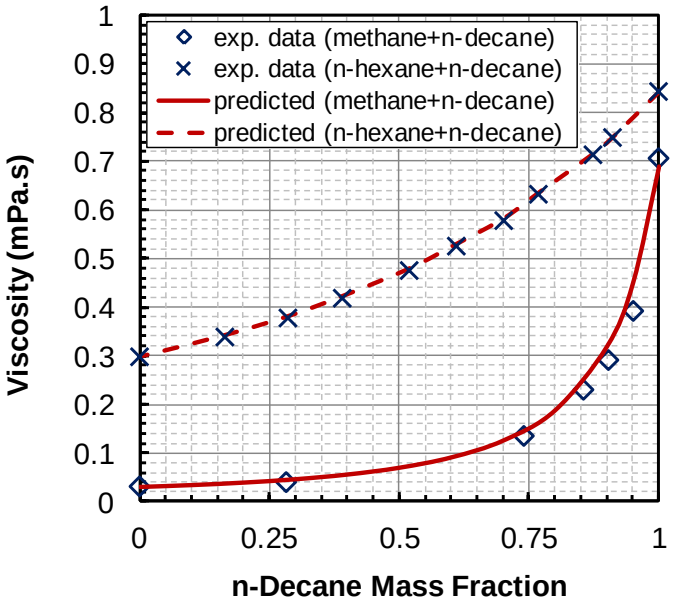

Figure 5.5: Predicted (*Version 1*) and measured viscosity (Canet et al. 2002, Chevalier et al. 1990) of methane/n-decane mixtures at 373.15 K and 60 MPa and n-hexane/n-decane mixtures at 298.15 K and 0.1 MPa. Pure component data were taken from NIST (2008).

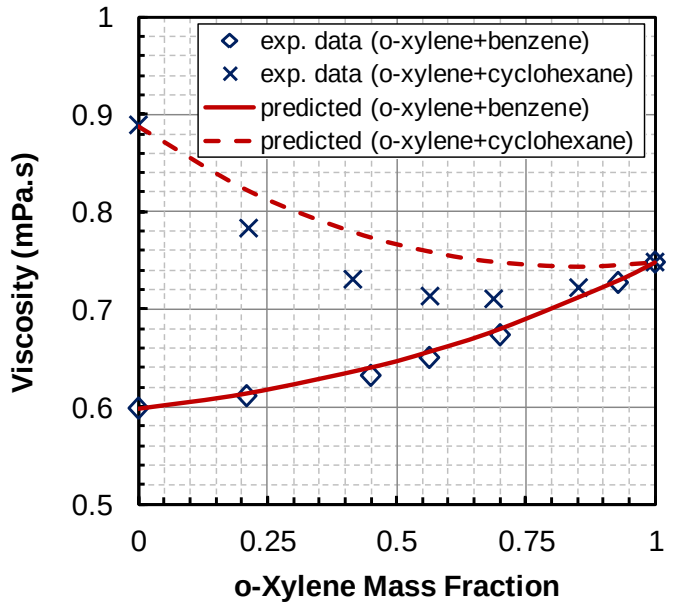

Figure 5.6: Predicted (*Version 1*) and measured viscosity (Chevalier et al. 1990) of o-xylene/benzene and o-xylene/cyclohexane binary mixtures at 298.15 K and atmospheric pressure.

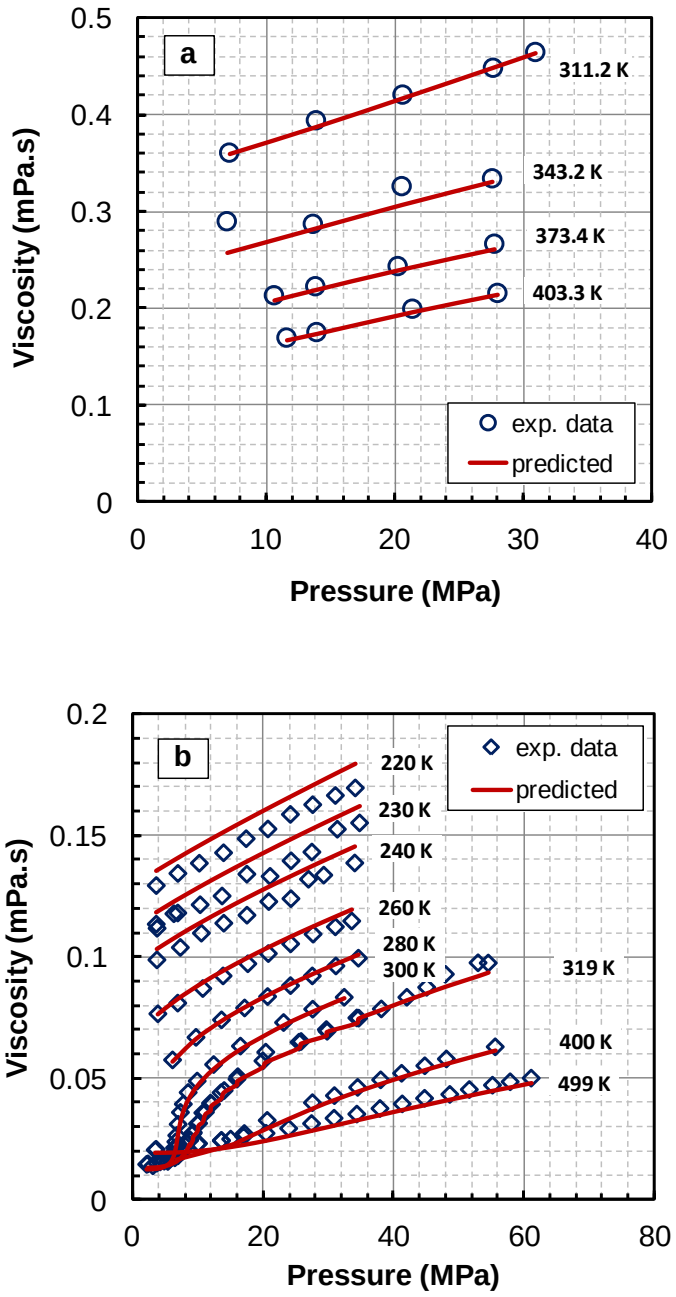

Figure 5.7: Predicted (*Version 1*) and measured (Diller et al. 1988, Cullick and Mathis 1984) viscosity of: a) 24 wt% carbon dioxide+76 wt% n-decane b) 59 wt% carbon dioxide+41 wt% ethane.

5.3.3 Extension of Mixing Rules to Equation of State Applications – Datasets 1 and 2

The performance of Mixing Rule Set 1 with *Version 2* of the correlation was evaluated using the binary mixtures of Datasets 1 and 2. Recall that, in *Version 2*, the input density values to the correlation are estimated with the Advanced Peng-Robinson (APR) EoS implemented in VMGSim. Since densities were calculated, all of the viscosity data could be used for the comparison.

Table 5.4 provides a summary of the average absolute deviation (AAD), the maximum absolute deviation (MAD), the average absolute relative deviation (AARD), the maximum absolute relative deviation (MARD), and the bias of the predicted viscosities. The overall AARD with *Version 2* of the correlation is 7.8% compared with 3% with *Version 1*. The difference is attributable to inaccurate density predictions by EoS at higher pressure-high temperature conditions. The fluid specific parameters of the correlation for pure components are skewed to compensate for the error and provide correct viscosity values for pure components. However, when used with the mixing rules, the skewed parameters results in less satisfactory predictions for mixtures. To compensate for this error, a binary interaction parameter β_{ij}, was introduced into the mixing rules as follows:

$$\rho^{o}_{s,mix} = \left(\sum_{i=1}^{nc} \sum_{j=1}^{nc} \frac{w_i w_j}{2} \left(\frac{1}{\rho^{o}_{s,i}} + \frac{1}{\rho^{o}_{s,j}} \right) \left(1 - \beta_{ij}\right) \right)^{-1} \tag{5.9}$$

and:

$$\frac{c_{2,mix}}{\rho^{o}_{s,mix}} = \sum_{i=1}^{nc} \sum_{j=1}^{nc} \frac{w_i w_j}{2} \left(\frac{c_{2,i}}{\rho^{o}_{s,i}} + \frac{c_{2,j}}{\rho^{o}_{s,j}} \right) \left(1 - \beta_{ij}\right) \tag{5.10}$$

The binary interaction parameters takes the value of zero when $i=j$. Note, when $\beta_{ij} = 0$ for all binary pairs, Equations 5.9 and 5.10 reduce to Mixing Rules Set 1 (Equations 5.2 and 5.6).

Table 5.4: Summary of the errors of the viscosity predictions for Dataset 1 and 2 from *Version 2* of the EF correlation using different values of the binary interaction parameters.

Binary Interaction Parameter (β_{ij})	**AAD (mPa.s)**	**MAD (mPa.s)**	**AARD (%)**	**MARD (%)**	**Bias (%)**
$\beta_{ij} = 0$	0.356	70.1	7.8	80.2	-3.8
tuned reference β_{ij}	0.349	174	3.6	525	2.5
Equation 5.13	0.455	266	7.8	644	5.8
Equations 5.13 and 5.15	0.162	34.7	5.4	65.4	2.1
Equation 5.14	0.218	114	6.0	203	2.5
Equations 5.14 and 5.15	0.152	30.0	4.9	60.1	0.1

A correlation for the binary interaction parameters was developed in three steps: 1) reference binary interaction parameters were determined at 298.15 K and atmospheric pressure; 2) a generalized correlation was developed for the reference values; 3) a pressure dependency was introduced into the correlation. It was decided to start with reference values because the APR EoS provides the most accurate values of mixture densities at 298.15 K and atmospheric pressure. Also, most of the data in Dataset 2 was measured at this condition. Finally, only a small adjustment was required at conditions far from the reference condition.

5.3.3.1 Reference Binary Interaction Parameters

The reference values of the binary interaction parameters, β_{ij}°, were found for 79 binary pairs by minimizing the error of the predicted viscosity values of the atmospheric mixtures at 298.15 K. Table 5.4 shows that using the adjusted β_{ij}° with no further modification reduced the overall AARD to 3.6% (now including high temperature and pressure data) although there is a considerable increase to 525% in the MARD. This increase occurred at higher pressure conditions and suggests that the reference binary interaction parameters are not suitable for the conditions beyond the reference conditions.

A generalized correlation for β_{ij}° is required to predict mixture viscosity without any mixture data available for tuning and to predict the viscosity of mixtures with more than two components. The correlation was defined to have the form:

$$\beta_{ij}^{o} = g(f_c) \quad \text{and} \quad f_C = 1 - \frac{2\sqrt{C_1.C_2}}{C_1 + C_2} \tag{5.11}$$

where g is an arbitrary function, f_C is the correlating parameter, and C is a physical property such as molecular weight, compressed state density, critical temperature, and the Watson-K factor. The Watson K-factor (WK) is defined (Riazi 2005) to classify hydrocarbons into chemical families using the measurable properties of normal boiling point (T_b in K) and specific gravity (SG) at 60 °F and is defined as follows:

$$WK = \frac{\left(1.8T_b\right)^{1/3}}{SG} \tag{5.12}$$

Note that the correlating function f_C is a convenient way of measuring differences in physical properties but it does not have any physical significance.

The correlative property that provided the clearest trend in β_{ij}° was found to be the molecular weight. Figure 5.8 shows that β_{ij}° is linearly related to molecular weight as follows:

$$\beta_{ij}^{o} = -0.319\, f_{MW} \tag{5.13}$$

Figure 5.8 also shows the reference β_{ij}^{o} values are also a weak function of the chemical families of the binary compounds. Differences in chemical families can be approximately represented by the Watson-K and therefore a second correlation is proposed as:

$$\beta_{ij}^{o} = (-0.244 - 0.45\, f_{WK}{}^{0.3})\, f_{MW} + 0.04\, f_{WK}{}^{0.3} \tag{5.14}$$

Note, aromatic-aromatic and naphthenic-aromatic binaries were not included in the evaluation due to limited number of mixtures and scattered β_{ij}°. Equation 5.14 predicts that β_{ij}° increases with f_{WK} as f_{MW} increases to 0.08 and then decreases for f_{MW} above 0.08. Since there were not enough experimental data for f_{MW} >0.08 to verify this trend reversal, Equation 5.14 is not recommended for f_{MW} > 0.08.

The improvement with Equation 5.14 is most noticeable for the *positive* binary interaction parameters of the cyclics/n-alkanes and aromatics/n-alkanes mixtures in contrast to the zero values assigned with Equation 5.13. For example, Figure 5.9a shows that Equations 5.13 and 5.14 both provide a good fit for the viscosity of mixtures of n-heptane and n-eicosane (β_{ij}° = -0.0295). However, as shown in Figure 5.9b, Equation 5.14 provides a better prediction for the viscosity of mixtures of n-hexane and p-xylene (β_{ij}° = 0.0121).

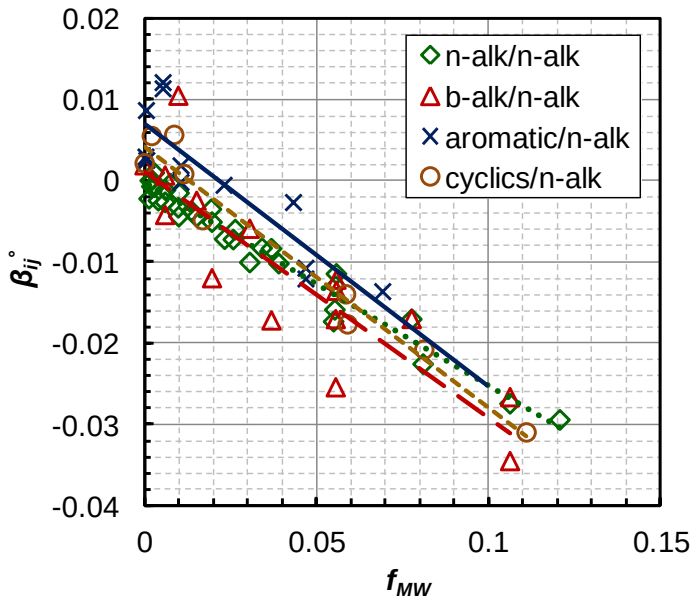

Figure 5.8: Adjusted values of the reference binary interaction parameters versus the molecular weight based correlative parameter.

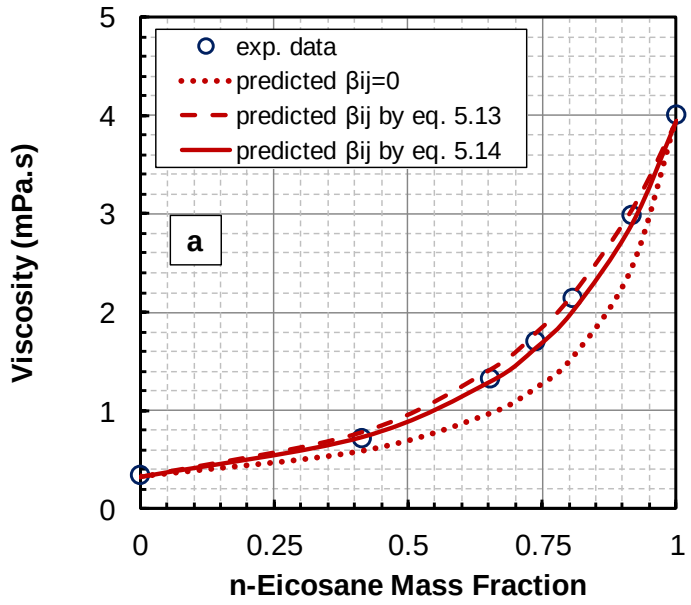

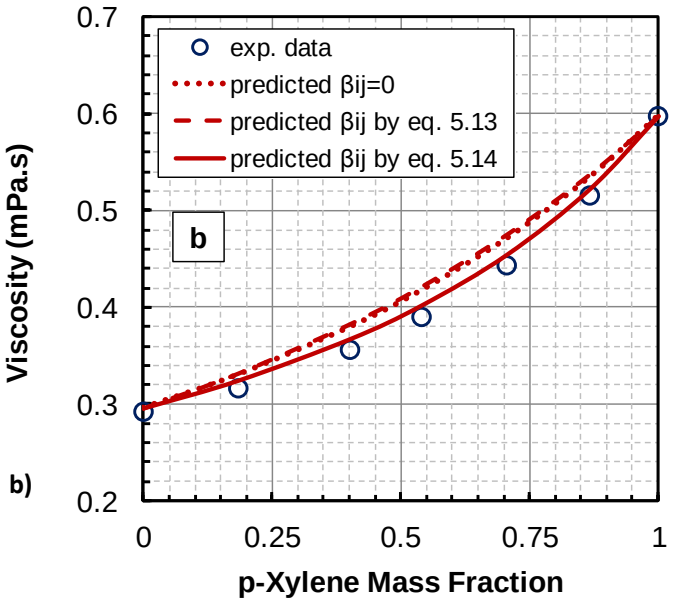

Figure 5.9: Measured and predicted (*Version 2*) viscosity of: a) n-heptane+n-eicosane at 313 K and atmospheric pressure, data from Queimada et al. (2003) and; b) n-hexane+p-xylene at 298.15 K and atmospheric pressure, data from Chevalier et al. (1990).

5.3.3.2 Extending Binary Interaction Parameters beyond the Reference Condition

Although using reference binary interaction parameters improved the overall accuracy of the correlation, for some high pressure mixtures, the viscosity predictions were worse than predictions than with interaction parameters set to zero. Figure 5.10 shows that for mixtures of cyclohexane and n-dodecane at the reference conditions, the optimized β_{ij}° provides a good fit to the data; however, this β_{ij}° leads to a poor prediction at 120 MPa and 323 K. At higher pressures, the density of the mixture components approach to the compressed state density. To provide a better match to the data, we must assume that the compressed state densities mix ideally at the compressed state conditions; that is, the binary interaction parameter must tend to zero as the fluid mixture approaches the compressed state. The following relationship is proposed:

$$\beta_{ij} = \beta_{ij}^{o} \exp(-\alpha(P - 101.325)) \tag{5.15}$$

where P is pressure in kPa and α is the decay rate of β_{ij} from atmospheric to high pressure conditions. The optimized values of α to use with Equations 5.13 and 5.14 were found to be 1.6544×10^{-5} and 1.3127×10^{-5} kPa^{-1}, respectively. Note that introducing a pressure dependant binary interaction parameters into Equation 5.9 will cause $\rho_{s,mix}^{\circ}$ to become pressure dependent. Although the pressure dependence is contrary to the definition of this parameter as the compressed state density of the mixture in vacuum, this modification is required to compensate for the errors associated with the EoS-estimated densities.

Table 5.4 also shows that using Equations 5.13 and 5.14 *without* modifications to Equation 5.15 reduces the AARD of the predictions to 7.8% and 6%, respectively. However, the MARD of the predictions are still very high (644% and 203%) similar to the MARD of using the adjusted reference binary interaction parameters at higher pressures (525%). Using Equations 5.13 and 5.14 *with* modifications to Equation 5.15 decrease the MARD of the correlation predictions to below 66% while the AARD values are less than 5.5%. Hence, Equation 5.15 is recommended for pressures beyond the reference atmospheric conditions.

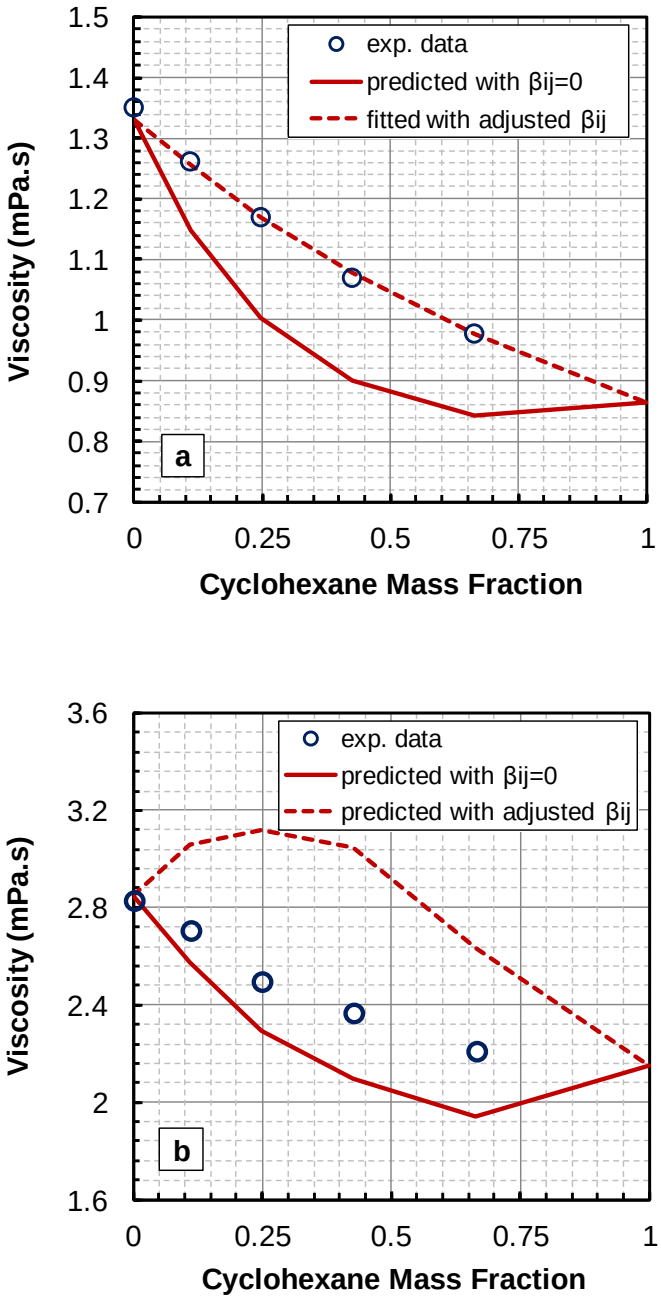

Figure 5.10: Measured (Tanaka et al. 1991) and predicted (*Version 2*) viscosity of cyclohexane/n-dodecane mixtures at: a) atmospheric pressure and 298 K, and; b) 120 MPa and 323 K.

Figure 5.11 summarizes all the results as a dispersion plot for the correlation predictions with β_{ij} =0 and with β_{ij} from Equations 5.13 to 5.15. Although use of the general binary interaction parameters improved the predictions, there are still deviations. Some of the deviations are under-predictions in the viscosity range of 3 to 30 mPa.s which correspond to the mixtures composed of squalane. The asymmetry of these mixtures is far greater than the majority of the mixtures used for the development of the general binary interaction parameters correlation (f_{MW} of ~0.3 versus maximum of ~0.1). Therefore, the generalized correlations for the binary interaction parameters do not provide the most optimum β_{ij} values for these mixtures. Another set of the deviations are over predictions in the range of 0.03 to 0.3 mPa.s for binary mixtures of methane with hydrocarbons lighter than n-decane.

Figure 5.12 shows the viscosity predictions for binary mixtures of methane/n-decane and methane/toluene with and without using generalized β_{ij}'s. The predictions with zero β_{ij}'s underestimate the viscosity of the methane/n-decane mixture and yet provide an accurate fit for the methane/toluene mixture. Similar behavior was observed for methane mixed with other hydrocarbons smaller than n-decane. The general correlation of β_{ij} improves the predications for the methane/n-decane mixture but gives poorer predictions for the methane/toluene mixture. These binaries are dissimilar to the liquid/liquid hydrocarbon binaries used for the generalization of the β_{ij}'s. First, the f_{MW} and f_{WK} of most of these binary mixtures are out of the range of the data used for the generalization and the general correlations were extrapolated for these mixtures. Second, the temperature at which the EoS volume translation of methane is set is much smaller than default value of 298 K for liquid hydrocarbons. A temperature-pressure (density) dependent generalized β_{ij} correlation may improve the predictions for these mixtures. However, this option was not studied here due to limited data at the necessary conditions.

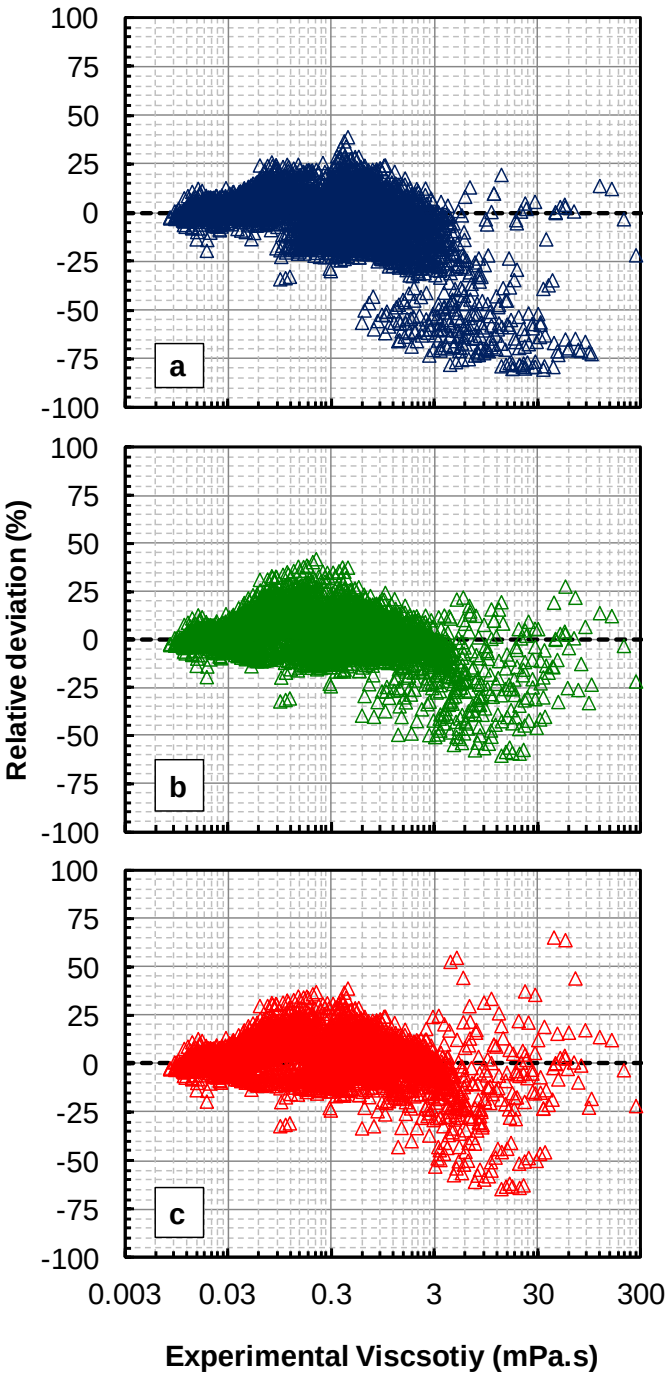

Figure 5.11: Error dispersion plots for viscosities predicted with *Version 2* of the EF correlation for binary mixtures from Datasets 1 and 2: a) β_{ij}=0; b) β_{ij} by Equations 5.13 and 5.15, c) β_{ij} by Equations 5.14 and 5.15.

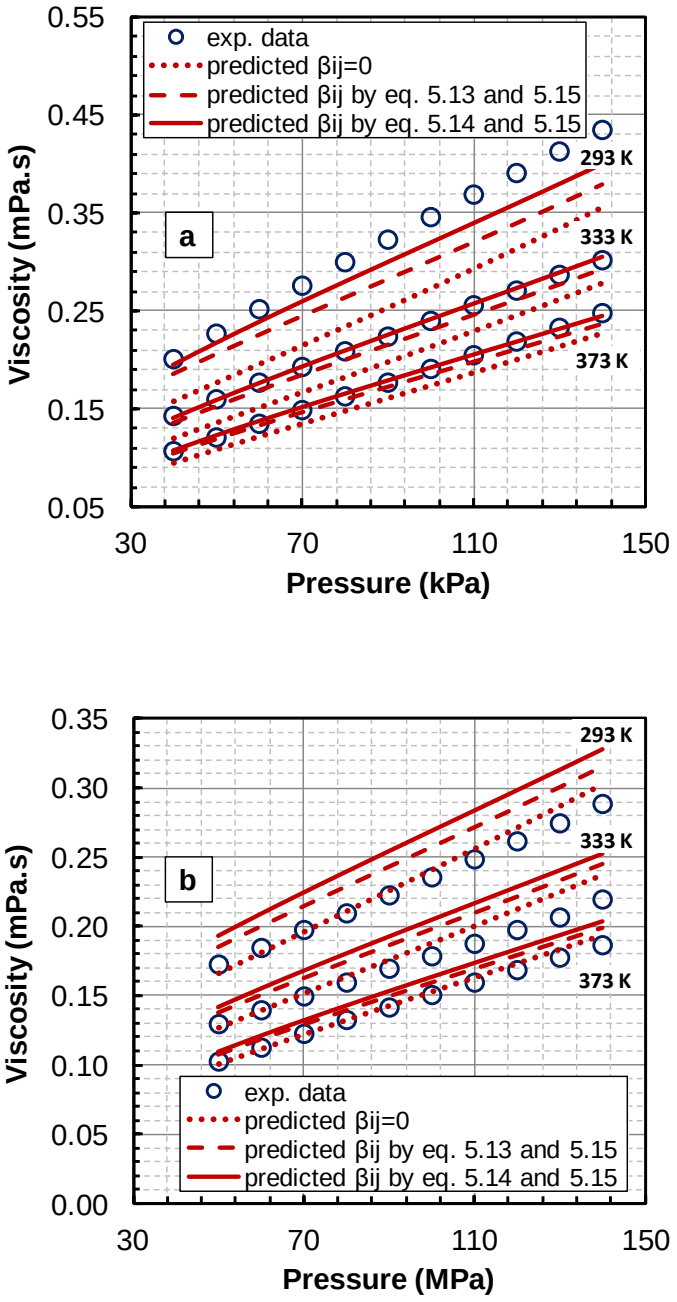

Figure 5.12: Measured and predicted (*Version 2*) viscosity for binary mixtures of :a) 26 wt% methane+74 wt% n-decane, data from Canet et al. (2002); b) 24 wt% methane+76 wt% toluene, data from Baylaucq et al. (2003).

5.3.4 Independent Assessment of the Mixing Rules – Data Set 3

As a final test, the performance of the viscosity correlation was assessed for an independent dataset, Dataset 3. *Version 1* was tested with measured densities and no interaction parameters. *Version 2* was tested using APR EoS densities with binary interaction parameters either set to zero or calculated from the proposed correlations (Equations 5.13, 5.14 and 5.15). Mixing Rules Set 1 was used in all cases. Table 5.5 provides a summary of the average absolute deviation (AAD), the maximum absolute deviation (MAD), the average absolute relative deviation (AARD), the maximum absolute relative deviation (MARD), and the bias of the predicted viscosities.

The AARD and MARD for *Version 1* were 8.4% and 65%, respectively. For *Version 2* with β_{ij} set to zero, the AARD increased to 11.6% and the MARD reduced to 51%. Using either of the proposed correlations for β_{ij} reduced the AARD and MARD to approximately 7% and 50%. While both correlations provided a similar overall performance, Equation 5.13 provided very accurate predictions for n-alkanes/n-alkanes mixtures, even for highly asymmetric mixtures such as n-heptane+n-tetracosane and n-decane+n-tetracosane. On the other hand, Equation 5.14 provided more accurate predictions than Equation 5.13 for most mixtures with aromatic and/or naphthenic components.

Table 5.5: Summary of the errors of the viscosity predictions for Dataset 3.

Correlation	**AAD (mPa.s)**	**MAD (mPa.s)**	**AARD (%)**	**MARD (%)**	**Bias (%)**
Version 1	0.127	4.88	8.4	65.4	-0.4
Version 2: $\beta_{ij} = 0$	0.209	6.83	11.6	50.9	-7.3
Version 2: estimated β_{ij} *Equations 5.13 and 5.15*	0.129	6.16	6.7	48.9	1.2
Version 2: estimated β_{ij} *Equations 5.14 and 5.15*	0.139	6.58	7.1	50.2	-2.7

The largest errors were found for mixtures containing decalin or 1-methylnaphthalene. Much of the error is caused by poor predictions of the pure component viscosity of these components at lower temperatures and pressures above 50 MPa (Satyro and Yarranton 2010). It appears that the molecular weight dependent pressure dependency parameters (c_3 and c_4) are not well suited to model the viscosity of 1-methylnaphthalene and similar components at higher pressures. It may be possible to improve the predictions of the correlation for these compounds by introducing a third pressure dependency parameter to the correlation; however, these modifications are beyond the scope of this study.

Both versions of the correlation predicted the viscosity of ternary mixtures with the same accuracy as the corresponding binary mixtures (overall AARD of 8.4% and 7.7% for binaries and ternaries, respectively). This observation suggests that the binary interaction parameters are independent of other components in the mixture and that; therefore, the model can be applied to multi-component mixtures with no further modification.

5.4 Summary

A set of mass fraction based mixing rules was developed and tested for the previously developed Expanded Fluid viscosity correlation. This set of the mixing rules replaces the original volume fraction based mixing rules of the correlation which were not suitable for the mixtures with dissolved gas components. The correlation employs two (*Version 2*) or three (*Version 1*) fluid-specific parameters to characterize each component. The mixing rules are used to calculate these parameters for the mixture from the pure component values.

After screening a number of mixing rules for the model parameters, the following rules were recommended:

$$\rho^o_{s,mix} = \left(\sum_{i=1}^{nc} \sum_{j=1}^{nc} \frac{w_i w_j}{2} \left(\frac{1}{\rho^o_{s,i}} + \frac{1}{\rho^o_{s,j}} \right) \left(1 - \beta_{ij}\right) \right)^{-1} \tag{5.16}$$

$$\frac{c_{2,mix}}{\rho^o_{s,mix}} = \sum_{i=1}^{nc} \sum_{j=1}^{nc} \frac{w_i w_j}{2} \left(\frac{c_{2,i}}{\rho^o_{s,i}} + \frac{c_{2,j}}{\rho^o_{s,j}} \right) \left(1 - \beta_{ij}\right) \tag{5.17}$$

$$c_{3,mix} = \left(\sum_{i=1}^{nc} \frac{w_i}{c_{3,i}} \right)^{-1} \tag{5.18}$$

where β_{ij} is binary interaction parameter with default value of 0. The average and maximum absolute relative deviation of the predicted viscosities for the test dataset (Datasets 1 and 2) were 2.9% and 32.9% for *Version 1* of the correlation which uses measured densities as an input parameter.

The mixing rules were also adopted and tested for *Version 2* of the correlation which uses APR EoS densities as the input. The viscosities predicted with *Version 2* of the correlation were less accurate than *Version 1* with an AARD of 7.8% using β_{ij} =0. Binary interaction parameters were determined for 79 binaries of hydrocarbons and the following correlations were proposed for the interaction parameters:

Correlation 1:

$$\beta_{ij} = \beta_{ij}^{\,o} \exp(-1.6544\times10^{-5}(P-101.325)) \qquad P \text{ in [kPa]}$$

$$\beta_{ij}^{\,o} = -0.319\, f_{MW}$$

$$f_{MW} = 1 - \frac{2\sqrt{MW_i.MW_j}}{MW_i + MW_j}$$

Correlation 2:

$$\beta_{ij} = \beta_{ij}^{\,o} \exp(-1.3127\times10^{-5}(P-101.325)) \qquad P \text{ in [kPa]}$$

$$\beta_{ij}^{\,o} = (-0.244 - 0.45\, f_{WK}^{\,0.3})\, f_{MW} + 0.04\, f_{WK}^{\,0.3}$$

$$f_{MW} = 1 - \frac{2\sqrt{MW_i.MW_j}}{MW_i + MW_j}$$

$$f_{WK} = 1 - \frac{2\sqrt{WK_i.WK_j}}{WK_i + WK_j}$$

The overall average error of the predictions with these general interaction parameters were less than 5.4%. Correlation 1 performed better for mixtures of components with a

large difference in molecular weight and Correlation 2 performed better for mixtures of n-alkanes with aromatic or naphthenic components.

The proposed mixing rules were assessed on an independent dataset (Dataset 3) consisting of 40 binary, ternary and multi component mixtures of hydrocarbons. The AARD for *Version 1* was 8.4% and the AARD for *Version 2* with the generalized β_{ij}'s was 7.1% compared with 11.6% with zero valued interaction parameters. For both versions and considering all the datasets, the AARD for 128 out of 134 individual mixtures was less than 20%. The EF correlation with the proposed mass based mixing rules is accurate, simple, robust, and executes rapidly even when coupled with an equation of state for density inputs. Hence, it is well suited for use with process and reservoir simulators.

CHAPTER SIX: VISCOSITY PREDICTION FOR NATURAL GAS PROCESSING APPLICATIONS[2]

The objective of this study is to investigate the applicability of the EF correlation for the mixtures commonly dealt with in the natural gas processing applications. Although the EF correlation fitted the experimental viscosity data of pure hydrocarbons and predicted the viscosity of hydrocarbon mixtures, its applicability for natural gas processing applications with non-hydrocarbon constituents has not been studied. Since, the correlation was built empirically based on hydrocarbon viscosity data; its validity for non-hydrocarbons has yet to be determined.

There are two categories of pure non-hydrocarbon components encountered in natural gas processing. The first category is simple non-hydrocarbons which are usually constituents of produced natural gas and include nitrogen, carbon dioxide, hydrogen sulfide and helium. These components are either non-polar and interact via London dispersion forces or polar with polar-polar interactions. The second category is associating non-hydrocarbon components normally used to treat natural gas streams such as methanol and glycols. Also included in this category is water which is a constituent of natural gas but is also an associating species. The molecules of these components are polar and form hydrogen bonds with neighboring molecules due to the presence of an O−H group.

In this chapter, the correlation is tested first for the pure non-hydrocarbon components including carbon dioxide, hydrogen sulfide, nitrogen, helium, water, methanol, ethylene glycol (EG), diethyelene glycol (DEG) and triethylene glycol (TEG). Then, the applicability of the correlation is studied for sweet and sour natural gas mixtures and aqueous solutions of methanol and glycols. Both *Version 1* (based on measured density) and *Version 2* (based on Advanced Peng-Robinson (APR) EoS density) are evaluated. *Version 2* is intended for simulator applications. However, *Version 2* is not well suited for testing model adaptations for non-hydrocarbons because errors in the EoS densities

[2] Contents of this Chapter published as: Motahhari, H.; Satyro, M. A. and Yarranton, H. W. Viscosity Prediction for Natural Gas Processing Applications. *Fluid Phase Equilib.* 2012, 322-323, pp. 56-65. http://dx.doi.org/10.1016/j.fluid.2012.03.006

may skew the interpretation. Therefore, any adaptations to the model are made with *Version 1* and then applied to *Version 2*.

6.1 Datasets

6.1.1 Pure Components

Experimental viscosity data for the interested pure non-hydrocarbon compounds were collected from open literature and summarized in Table 6.1. Density data were also compiled from the same sources but were only available for more limited ranges of pressure and temperature.

Table 6.1: Summary of the pure non-hydrocarbon experimental data used in this study.

Component	NDP[a]	Temperature (K)	Max. Pressure (MPa)	Data Source
hydrogen sulfide	18	190 - 483	4.4	Rankine and Smith (1921) Pal and Barua (1967) Pal and Bhattacharyya (1969) Bhattacharyya et al. (1970) Bhattacharyya (1970) Runovskaya et al. (1970) Nieto-Draghi et al. (2005)
carbon dioxide	520	203 - 1100	450	NIST (2008) Padua et al. (1994) van der Gulik (1997)
Helium	376	14.2-918.3	83	NIST (2008)
Nitrogen	1490	63-1989	194	NIST (2008)
Water	1795	256 - 1139	389	NIST (2008)
Methanol	575	176.1-511.1	200	NIST (2008)
ethylene glycol	95	273-428	atm.	NIST (2008)
diethylene glycol	35	273-428	atm.	NIST (2008)
triethylene glycol	24	273-428	atm.	NIST (2008)

a- number of data points

6.1.2 Mixtures

Viscosity data for 8 natural mixtures (G1 to G8) and 3 sour gas mixtures (G9 to G11), with compositions reported in Table 6.2, were compiled from open literature and used to evaluate the EF correlation. Viscosity data of the 3 sour gas mixtures include 8 data points from a molecular dynamics (MD) simulation (Galliero et al., 2007) and added to dataset to broaden the evaluation range for H_2S containing mixtures. Not included in Table 6.2 but used in this study are data for sour natural gas mixtures from Elsharkawy (2003). This dataset consists of compositions and single viscosity data points for 17 different gas samples at a given temperature and pressure.

Viscosity and density data of aqueous solutions of ethylene glycol, diethylene glycol triethyelene glycol and methanol mixtures were compiled from NIST database (NIST, 2008) and are in atmospheric pressure conditions. The temperature range of the data is 273−450 K.

6.2 Results and Discussion

The correlation is first tested for pure non-hydrocarbon components and a modification for hydrogen bonding fluids is introduced. Then, the validity of the correlation is tested by comparing predicted viscosities of mixtures commonly found in natural gas processes to experimental values.

6.2.1 Pure Component Study

The required input properties for the viscosity modeling of pure components are the dilute gas viscosity and the density at given pressure and temperature. Dilute gas viscosities of pure non-hydrocarbons were calculated using the Yaws empirical correlation (Equation 2.13) with fluid-specific constants taken from Yaws (2008). *Version 1* of the correlation is tested first using the datasets which include both measured density and viscosity. Any conceptual modifications to the correlation are introduced at this point. Then, *Version 2* of the correlation is tested using densities calculated with the APR EoS. The correlation is tested for simple and associating non-hydrocarbon compounds separately.

Table 6.2: Composition (in mole percent) of the natural gas mixtures used in this study.

Gas Mix.	N_2	CO_2	H_2S	He	n-C_1	n-C_2	n-C_3	C_4	C_5	C_6	C_7	C_8	C_9	C_{10+}	Data Source
G1	5.6	0.66	-	-	84.84	8.4	0.5	-	-	-	-	-	-	-	Assael et al. (2002)
G2	1.83	-	-	-	94.67	3.5	-	-	-	-	-	-	-	-	Nabizadeh and Mayinger (1999)
G3	-	3.2	-	-	86.33	6.8	2.4	0.91	0.22	0.1	0.04	-	-	-	Lee et al. (1966)
G4	1.4	1.4	-	0.03	71.71	14	8.3	2.67	0.39	0.09	0.01	-	-	-	Lee et al. (1966)
G5	4.8	0.9	-	0.03	80.74	8.7	2.9	1.7	0.13	0.06	0.03	-	-	-	Lee et al. (1966)
G6	0.55	1.7	-	-	91.46	3.1	1.4	1.17	0.28	0.26	0.08	-	-	-	Lee et al. (1966)
G7	0.66	2.19	-	0.01	80.01	9.31	4.96	2	0.51	0.18	0.12	0.04	0.01	0.01	Langelandsvik et al. (2007)
G8	1.39	1	-	0.02	92.2	4.34	0.54	0.33	0.07	0.06	0.04	0	0	0	
G9	-	-	0.6	-	0.4	-	-	-	-	-	-	-	-	-	Galliero et al. (2007)
G10	-	-	0.4	-	0.6	-	-	-	-	-	-	-	-	-	Galliero et al. (2007)
G11	-	0.63	0.27	-	0.1	-	-	-	-	-	-	-	-	-	Galliero et al. (2007)

6.2.1.1 Simple non-Hydrocarbons

Version 1 of the correlation was fitted to data by adjusting the fluid-specific parameters of c_2, c_3, and ρ_s^o to the values given in Table 6.3. Table 6.4 provides a summary of the average absolute deviation (AAD), the maximum absolute deviation (MAD), the average absolute relative deviation (AARD), the maximum absolute relative deviation (MARD), and the bias of the fitted correlation. The maximum deviation was observed for helium at very low temperatures. The overall AARD of 4.2% and MARD of 34% are both comparable to the deviations reported for the application of the correlation to pure hydrocarbon components. Therefore, it is concluded that the correlation framework, based on the non-polar hydrocarbon compounds data, is sufficient for these simple non-hydrocarbons.

The fluid specific parameters, c_2 and ρ_s^o, were then determined for *Version 2*, Table 6.3. Note that the general correlations of Equations 4.12, 4.13 and 4.14 were used for the pressure dependency parameters. A summary of the deviations for *Version 2* of the correlation is provided in Table 6.4. *Version 2* of the correlation fits the data with the same accuracy of the *Version 1* with overall AARD and MARD of 4.2% and 31%, respectively. However, the accuracy of the *Version 2* at elevated pressures is slightly less than *Version 1* because the pressure dependent parameters are correlated in *Version 2* but adjustable in *Version 1*. The deviation at higher pressures is shown for carbon dioxide in Figure 6.1. The fit of *Version 2* can be improved if the pressure dependency parameters (c_3 and c_4) were adjusted as well, but the generality of the correlation for mixtures would be lost.

Table 6.3: Fluid specific parameters to use with Versions 1 and 2 of the correlation for pure non-hydrocarbon components.

Component	Version 1					Version 2			
	$c_{2\infty}$	a	$b \times 10^{-3}$ (K^{-1})	ρ_s^o (kg/m^3)	$c_3 \times 10^{-6}$ (kPa^{-1})	$c_{2\infty}$	a	$b \times 10^{-3}$ (K^{-1})	ρ_s^o (kg/m^3)
hydrogen sulfide	0.188			1194.6		0.0437			1092.8
carbon dioxide	0.236			1617.7	0.187	0.0644			1572.0
helium	0.0517			300.0	0.1	0.0149			286.2
nitrogen	0.1147			1012.4	0.1	0.0244			938.4
water	0.1463	99.519	-23.1	1197.0	0.3	0.0674	35.090	-18.5	1368.2
methanol	0.1463	0.6301	-4.22	1045.0	0.449	0.0674	2.672	-10.2	1156.0
ethylene glycol	0.23			1193.7		0.1274			1201.5
diethylene glycol	0.2487			1195.0		0.1147			1175.9
triethylene glycol	0.2977			1214.3		0.1417			1189.4

Table 6.4: Summary of the errors for *Versions 1* and *2* of the EF correlation for pure non-hydrocarbon compounds.

Component	Version 1			Version 2		
	MARD (%)	AARD (%)	Bias (%)	MARD (%)	AARD (%)	Bias (%)
hydrogen sulfide	15	3.5	1.3	13	3.3	2.7
carbon dioxide	9.7	3.3	2.5	14	5.6	3.3
helium	34	4.1	-3.1	31	5.0	-0.7
nitrogen	24	5.8	-4.5	20	2.8	-0.6
water	48	5.3	2.6	25	1.9	0.2
methanol	17	2.1	0.2	30	5.4	0.4
ethylene glycol	12	3.0	0.6	54	5.8	0.8
diethylene glycol	23	5.0	-0.1	41	8.6	-0.0
triethylene glycol	7.1	4.5	-0.3	41	14	0.0

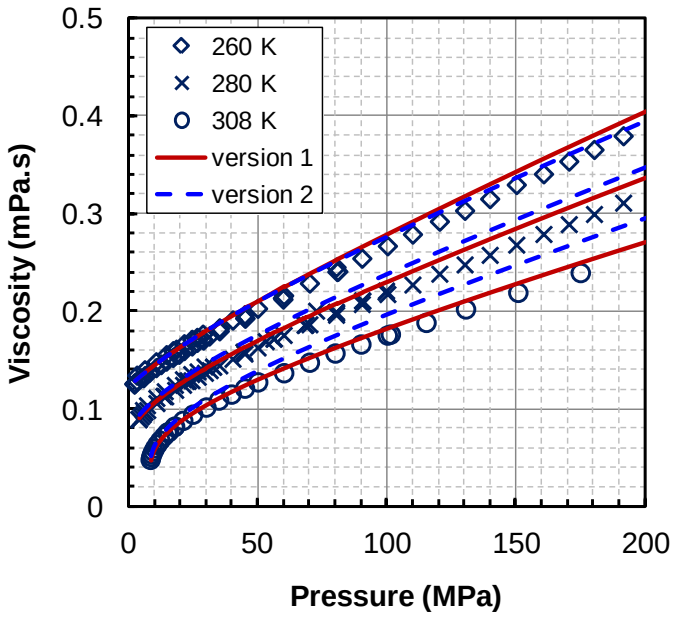

Figure 6.1: Performance of EF correlation fitted to experimental data of compressed carbon dioxide, data from NIST (2008), Padua et al. (1994) and van der Gulik (1997).

Note that both versions of the correlation were fitted to limited experimental data for hydrogen sulfide. Much of these data were calculated at the liquid-vapor coexistence curve using molecular dynamics (MD) simulation (Nieto-Draghi et al. 2005). These calculated values are reportedly in good agreement with experimental data (Schmidt et al. 2008). The only exceptions were saturated gas data which are clearly inconsistent with the experimental dilute gas data and were excluded from the analysis. Figure 6.2a shows that the fit of both versions of the correlation to the viscosity data of hydrogen sulfide on the co-existence curve. However, the correlation performs satisfactory in predicting the viscosity of H_2S at higher temperature and pressure conditions, Figure 6.2b. The symbols on this plot are measured H_2S viscosity data obtained by personal communications from Dr. Marriot in Alberta Sulphur Research Center. Note that these independent data were not used in determination of fluid-specific parameters of the both version of the correlation for H_2S.

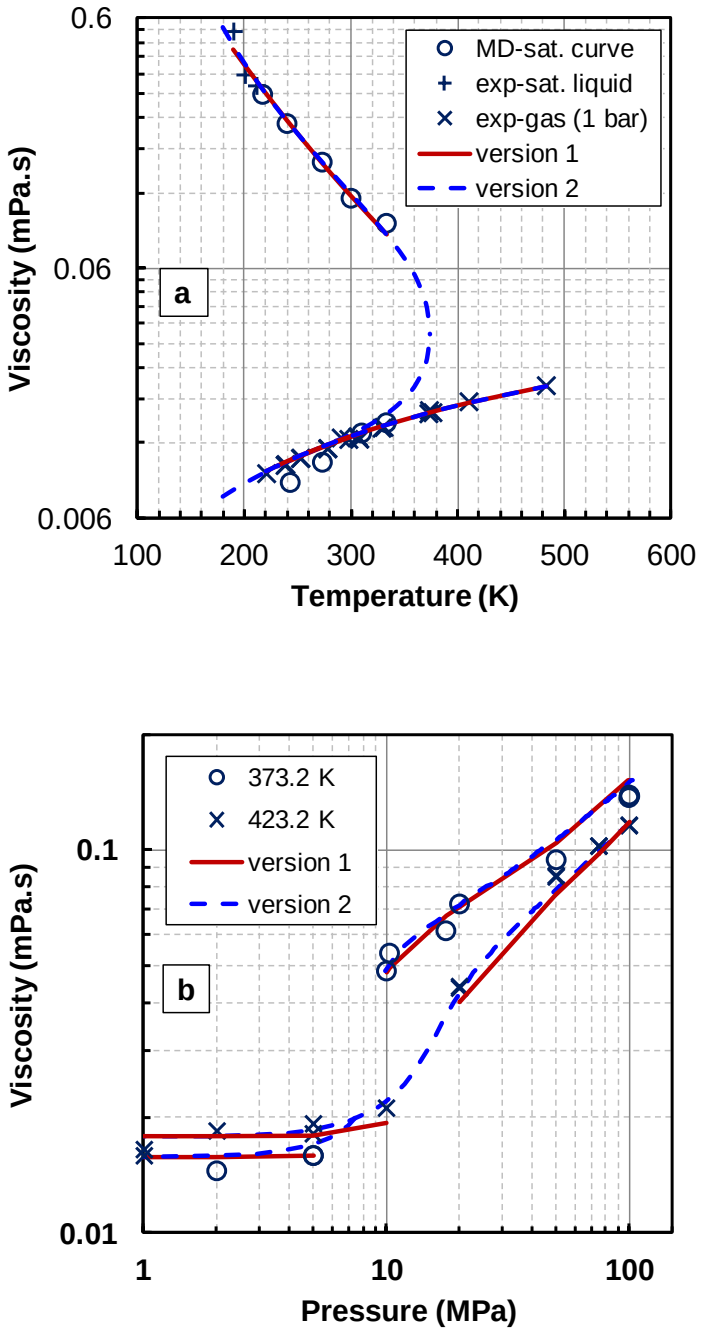

Figure 6.2: Performance of EF correlation for H2S: a) fitted to viscosity data of saturated vapor and liquid on co-existence curve, data sources reported in Table 5.1; and b) predicted and measured independent data in super critical conditions, data from Marriot and Giri (2010).

6.2.1.2 Associating non-Hydrocarbons

Unlike the simple non-hydrocarbon compounds, the fitting of *Version 1* of the correlation to viscosity data of associating non-hydrocarbon components was not straightforward. Although *Version 1* could fit the limited atmospheric data points of the glycols with AARD below 5%, it failed to adequately fit water data. Less significantly, the fitted correlation for methanol over-predicted the viscosity in the vicinity of the critical region. These results are not surprising because there is hydrogen bonding in these fluids while the correlation was originally developed for molecules interacting via dispersion forces only. The strength, length, and number of hydrogen bonds between the molecules depend on pressure and temperature (Dougherty, 1998). The response of viscosity to fluid expansion will be different than for a fluid dominated by dispersion forces. The effect of hydrogen bonding is most obvious in water. For instance, the density behavior of saturated water is different than other liquids with a maximum occurring at 4°C and negative thermal expansions at temperatures below 4°C. Also, at temperatures above ~50 °C the viscosity of water increases under compression as found with other liquids; however, at lower temperatures its viscosity decreases under compression to reach a minimum value (Yves, 2007).

A modification to the correlation was required to the model the viscosity of fluids with significant hydrogen bonding, such as water and methanol. The parameter c_2 is the proportionality of the fluid viscosity to its expansion and indirectly represents the effect of the intermolecular forces on viscosity. Hence, a temperature dependent c_2 is appropriate to model the temperature dependency of hydrogen bonding and its effect on the viscosity. The following formulation of the temperature dependent c_2 was determined to fit the data:

$$c_2 = c_{2\infty} + K_{c_2}.\exp(\gamma_{c_2} T) \tag{6.1}$$

where $c_{2\infty}$ and K_{c2} and γ_{c2} are fitting parameters. The default value for K_{c2} and γ_{c2} is zero for all components except those with significant hydrogen bonding such as water and methanol. Therefore, by definition for all hydrocarbons and simple non-hydrocarbons, the value of $c_{2\infty}$ is equal to the value of the non-temperature dependent c_2.

Version 1 of the correlation was then fitted to the experimental data of water and methanol by adjusting the parameters ρ_s^o, K_{c2} and γ_{c2} with $c_{2\infty}$ fixed at 0.1463. *Version 1* fit the limited available data of glycols with a fixed c_2 (K_{c2} and γ_{c2} set to zero). The fluid specific parameters for the associating non-hydrocarbons and a summary of the deviations of the fitted correlation are given in the Tables 6.3 and 6.4, respectively. The AARD are less than 5% while the MARD of 48% occurs for water. The correlation fits the data of water on the co-existence curve with a maximum deviation of 14%, Figure 6.3a. Figure 6.3b shows that the maximum MARD occurs for compressed liquid water at temperatures below 50°C whereas the water viscosity decreases under compression. The correlation is not able to model this behavior.

Having established the new temperature dependent expression for parameter c_2, *Version 2* of the correlation was then fitted to the experimental data of pure associating non-hydrocarbon fluids. Tables 6.3 and 6.4 report the fluid-specific parameters and model deviations, respectively, for *Version 2*. As with *Version 1*, the parameters ρ_s^o, K_{c2} and γ_{c2} were adjusted for methanol and water with $c_{2\infty}$ fixed at 0.0647. Only ρ_s^o and $c_{2\infty}$ were adjusted to fit the glycol data (K_{c2} and γ_{c2} were set to zero). The overall AARD and MARD for *Version 2* are 7.1% and 54%, respectively.

While the highest deviations in *Version 1* were observed for water, they are observed for glycol in *Version 2*, Table 6.4. The AARDs for the glycols are below 14% with *Version 2* but below 5% with *Version 1*. For instance, for diethylene glycol, the *Version 2* model viscosities deviate at higher temperatures, Figure 6.4. The main contribution to the deviations for the glycols is inaccurate density predictions by APR EoS. Using measured densities as an input to *Version 2* reduces the overall AARD for the glycols from 9.5 to 7.7%; that is, to nearly the same error as observed for *Version 1*.

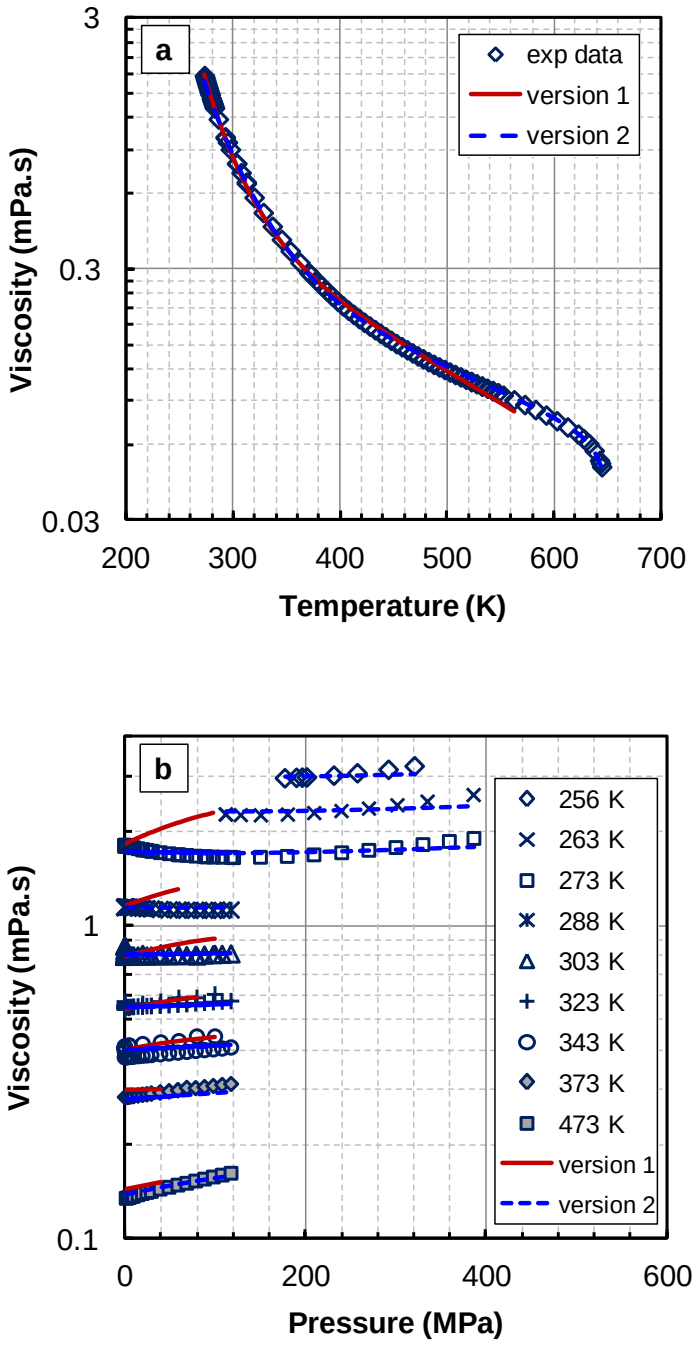

Figure 6.3: Performance of EF correlation fitted to experimental data (NIST 2008) of water: a) saturated liquid; b) compressed liquid.

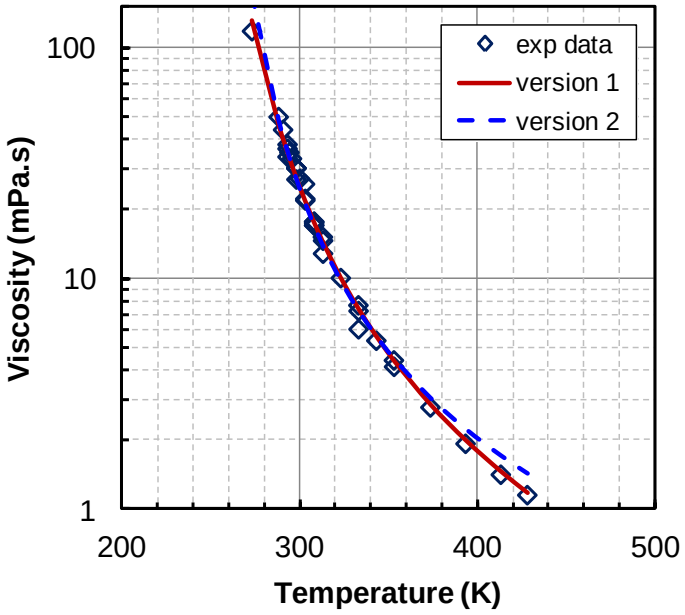

Figure 6.4: The fit of the *Version 1* and *2* of the correlation to experimental viscosity data (NIST 2008) of diethylene glycol (DEG) using fixed temperature independent c_2.

Note, *Version 2* of the correlation fit the high pressure data of water at temperatures below 50°C more accurately than *Version 1*, Figure 6.3b. The improvement is attributed to the combined effects of: 1) the form of the pressure dependency expression in *Version 2* which provides a better fit for water; 2) the underestimation of compressed liquid water density by the APR EoS which accidently compensates for the effect of the unusual density trends in water.

6.2.2 Mixture Viscosity Prediction

The required input properties for the viscosity modeling mixtures are the dilute gas viscosity and the density at given pressure and temperature. Dilute gas viscosities of mixtures at given temperature were calculated using the Wilke mixing rule (Equations 2.14 and 2.16) and the dilute gas viscosity of constituent components of the mixture by the Yaws empirical correlation (Equation 2.13) with fluid-specific constants taken from Yaws (2008). The input densities to *Version 1* and Version 2 of the correlation are measured values and estimated values with APR EoS, respectively.

6.2.2.1 Natural Gas and Sour Gas Mixtures

Viscosity predictions were made with both versions of the correlation where possible but *Version 1* is limited to mixtures with experimental density data. The fluid-specific parameters of the EF correlation for the hydrocarbon components of these mixtures were taken from Yarranton and Satyro (2009) and Satyro and Yarranton (2010) for *Version 1* and *2* of the correlation, respectively. The parameters for non-hydrocarbon components were taken from Table 6.3. Note, the sour natural gas mixtures of Elsharkawy (2003) contain plus-fractions of heavier hydrocarbons which were modeled as the equivalent n-alkanes based on their molecular weight. Although, both general correlations for β_{ij} (Equations 5.13 and 5.14) in *Version 2* were used in this study, only results with Equation 5.13 are shown since the results with Equation 5.14 were not significantly different.

Table 6.5 provides a summary of the AARD, MARD, and bias of the predictions. For sweet natural gas mixtures (G1 to G8), Figure 6.5a and b show, only for *Version 2*, that the predictions are in good agreement with the measured values over a broad range of conditions with overall AARDs of 6.4 and 2.8% for *Version 1* and *2*, respectively. Some comparisons with other models were possible. For instance, the predictions for G1 are comparable to the values estimated by Assael et al. (2001) using the relatively complex mixing rules of the Vesoic−Wakeham viscosity model (Vesoic and Wakeham 1989a and 1989b) coupled with the special density correlation of AGA8-DX92 (Jaeschke and Schley, 1996). Also, the performance of *Version 2* for the G7 and G8 mixtures is superior to the performance of the most of the models studied by Langelandsvik et al. (2007). Among these models, only LGE-3 (Lee et al., 1966; Whitson and Brule, 2000) with AARD of 1.4% and SUPERTRAPP (Huber, 2007) with AARD of 2.2% provided predictions comparable to *Version 2* with AARD of 1.9% for these two gas samples.

The predictions with *Version 1* for mixtures G1 to G8 are slightly less accurate than *Version 2*. The less accurate predictions occurred where the fluid transitions from dilute to dense gas behavior, as shown inFigure 6.6a and b for natural gas mixture G1 and methane at 323 K, respectively. *Version 1* of the correlation originally developed and tested for hydrocarbons mostly in liquid phases with limited density and viscosity data

near the critical region. Fine tuning of the parameters *n* and c_1 could improve the results for *Version 1* near the critical region but such an exercise is beyond the scope of this study as it requires revisions of all previous developments. In any case, the *Version 1* predictions are still within 15% of the measured values.

For the sour gas mixtures (G9 to G11), *Versions 1* and *2* predicted the viscosity of the binary and ternary mixtures containing H_2S with overall AARDs of 5.1% and 6.2%, respectively. All data of these mixtures are synthetic values from molecular dynamics (MD) simulations (Galliero et al. 2007). The deviations were calculated by comparing the correlation predictions to the mean of the simulated viscosity values by different intermolecular potential fields in MD simulations. The MD simulated values were scattered with an average and maximum deviations of 2.9% and 7.2% around the mean values, which are comparable to the deviations of predictions by EF correlation.

Table 6.5: Summary of the errors of the predictions by *Version 1* and *2* of the correlation for natural gas mixtures.

Mixture	Version 1			Version 2		
	MARD (%)	AARD (%)	Bias (%)	MARD (%)	AARD (%)	Bias (%)
G1	11	6.5	-6.5	3.9	1.8	-0.7
G2	8.1	3.5	-3.5	3.1	1.8	-1.8
G3	11	8.3	-8.3	5.6	3.1	-2.8
G4	15	3.2	-0.3	9.1	4.1	2.1
G5	14	8.8	-8.8	7.5	4.4	-4.3
G6	15	7.5	-7.6	11	3.5	-3.1
G7	8.6	6.3	-6.3	4.3	1.7	-1.4
G8	13	9.7	-9.7	4.6	2.1	-2.1
G9	-6.3			-5.1		
G10	-5.5			-4.0		
G11	6.8	3.5	3.5	14	9.6	9.6
Sour natural gas mix. (Elsharkawy 2003)				51	20	-9.3

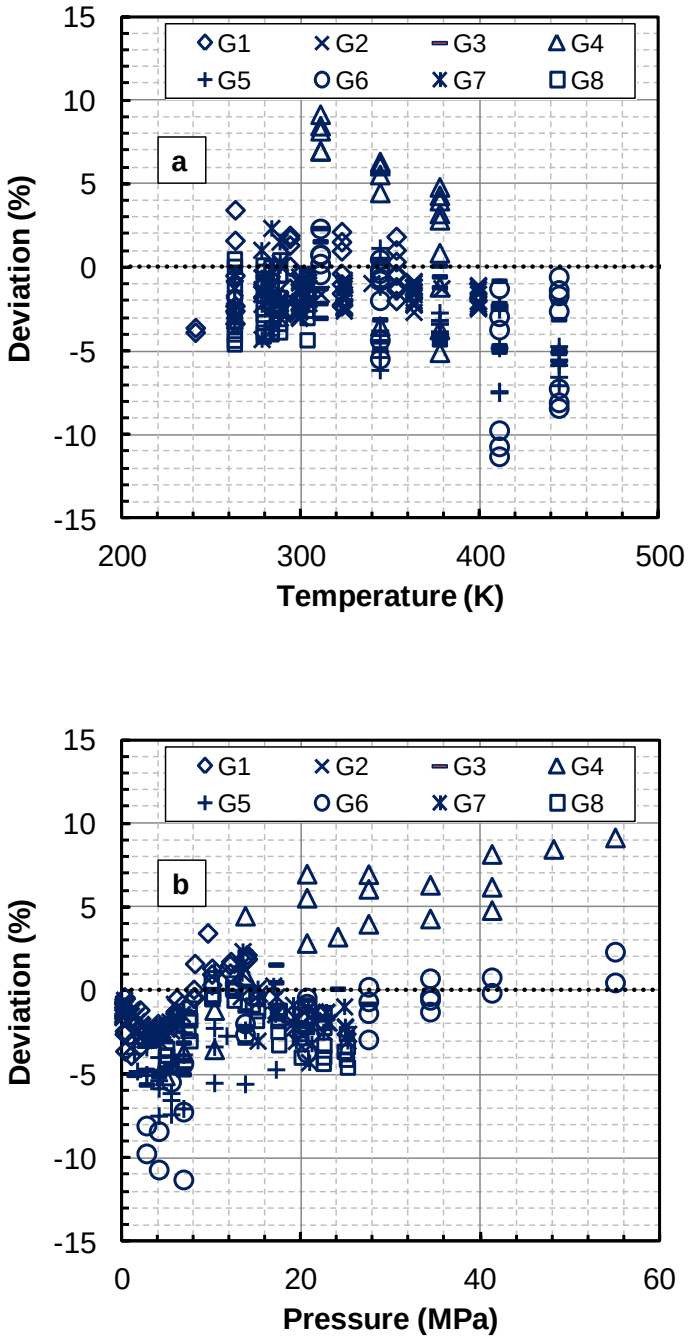

Figure 6.5: Deviations of the predicted viscosity by *Version 2* of correlation for natural gas mixtures versus: a) pressure; b) temperature.

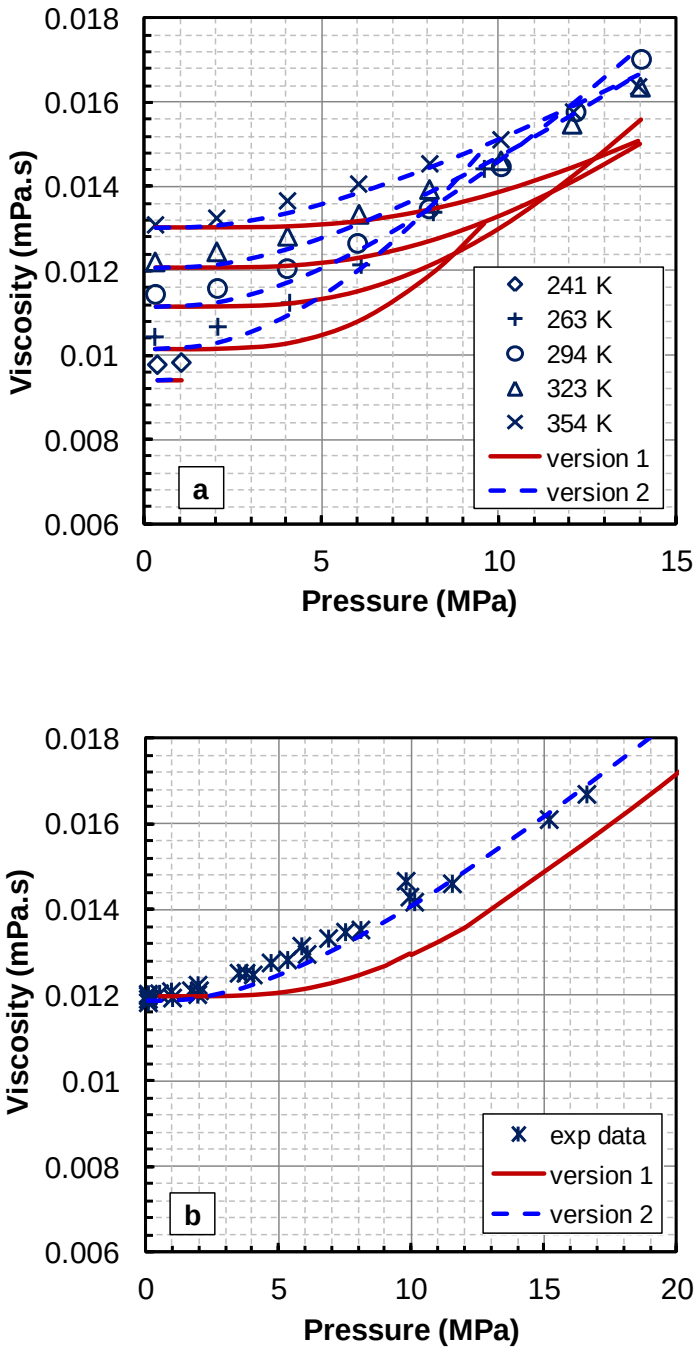

Figure 6.6: Comparison of the predictions from *Versions 1* and *2* of the EF correlation with measured viscosity data of: a) natural gas mixture G1 (Assael et al., 2001) and; b) methane at 323 K (NIST, 2008).

The predictions for gas samples of Elsharkawy (2003) were made only with *Version 2* because density data were not available. As reported in Table 6.5, the overall AARD for these mixtures is 20%, which is considerably higher than other natural gas mixtures. The higher deviations are attributable to the simplistic characterization used for the heavy plus-fractions in these mixtures. Figure 6.7 shows that the deviation of the predictions increases as the mass fraction of the plus-fraction increases. The predictions for mixtures with no plus-fraction were within 7% of the experimental values, comparable to the sweet gas mixtures.

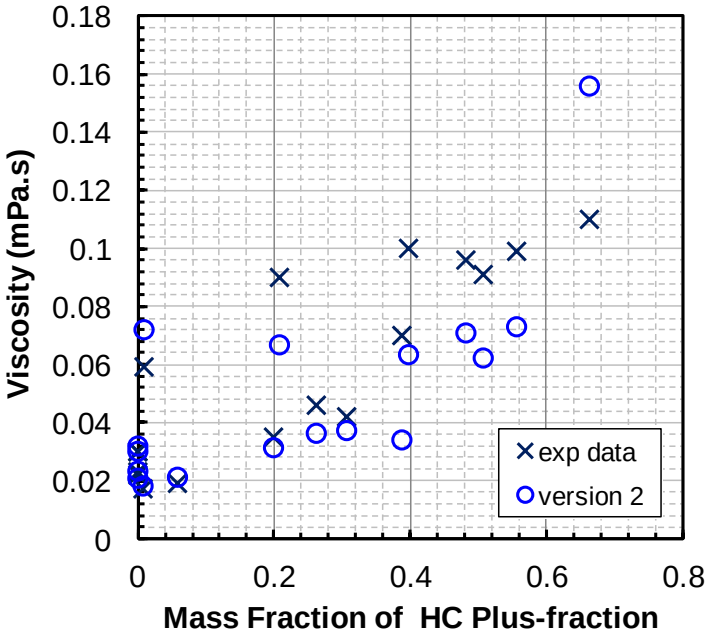

Figure 6.7: Deviation of the predicted viscosity by *Version 2* of the EF correlation for sour natural gas mixtures (Elsharkawy 2003) as a function of the heavy hydrocarbon plus-fraction content.

6.2.2.2 Associating Mixtures

The EF correlation was tested on aqueous solutions of ethylene glycol, diethylene glycol triethyelene glycol and methanol. Mixtures of these associating fluids are highly non-ideal and have significant excess volumes. Predictions from *Version 2* using untuned EoS density values are significantly skewed due to the errors in the calculated density. Therefore, it is essential to tune the EoS density calculation to achieve accurate viscosity

predictions. The APR equation of state was tuned to the experimental density data by adjusting parameters A_{ij} and B_{ij} of the volume shift mixing rule (Equation B.14 in the Appendix B). The fitted parameters are given in Table 6.6.

Table 6.7 provides a summary of the AARD, MARD, and the bias of the predictions of the correlation for these mixtures. Note, β_{ij} was set to zero unless otherwise stated. The AARDs for *Version 1* of the correlation are all less than 10% except for mixtures of water and methanol with an AARD of 21%. The deviations for *Version 2* with $\beta_{ij} = 0$ are considerably higher with an overall AARD of 26%. The reduced accuracy of *Version 2* for mixtures is consistent with results previously obtained for the hydrocarbon mixtures as observed in Chapter 5.

Version 2 was then fitted to the data using a binary interaction parameter, Table 6.7, reducing the overall AARD to 8.7%. Unfortunately, the general β_{ij} correlations developed for the hydrocarbons (Equations 5.13 and 5.14) are not applicable for these mixtures of associating species. Both equations give β_{ij} values that increase with increasing molecular weight difference. However, the optimized β_{ij} values for glycols mixtures with water have the opposite trend.

Figure 6.8a and b demonstrate the performance of the correlation for aqueous solutions of diethylene glycol and methanol, respectively. Both versions of the correlation are qualitatively correct. However, although *Version 1* correctly predicts a maximum in the viscosity of the water+methanol mixture, the maximum value is significantly under-estimated. A good fit can be obtained using a binary interaction parameter of $\beta_{ij} = -0.067$ which reduced the AARD to 4.1%. *Version 2* fitted the data using $\beta_{ij} = -0.179$ to give an AARD of 3.9%. In general for *Version 2*, tuning of binary interaction parameter is required to provide an accurate viscosity model for mixtures. For *Version 1*, the binary interaction parameter was only required for the most extreme case of hydrogen bonding, mixtures of water and methanol.

Table 6.6: Adjusted volume translation parameters of APR EoS for the aqueous solutions of glycols and methanol.

Parameter	EG (1) +water(2)	DEG (1) +water(2)	TEG (1) +water(2)	methanol (1) +water(2)
A_{12}	-0.219	-0.288	-0.348	0.0466
A_{21}	0.194	0.240	0.279	-0.051
B_{12}	4.16	1.40	0.150	1.05
B_{21}	-2.76	1.13	3.04	-1.10

Table 6.7: Summary of the errors of the predicted viscosity by the EF correlation for aqueous solutions of glycols and methanol.

Mixture	version 1				version 2 (β_{ij}=0)			version 2 with tuned β_{ij}			
	β_{ij}	MARD (%)	AARD (%)	Bias (%)	MARD (%)	AARD (%)	Bias (%)	β_{ij}	MARD (%)	AARD (%)	Bias (%)
EG+Water		29	9.8	-6.4	62	28	-26	*-0.069*	40	11	3.4
DEG+Water		17	4.6	0.4	62	26	-25	*-0.066*	24	6.8	0.7
TEG+Water		10	5.6	3.3	64	25	-18	*-0.055*	40	13	0.7
Methanol+Water		42	21	-21	52	28	-29	*-0.179*	19	3.9	-0.6
	-0.067	12	4.0	-2.3							

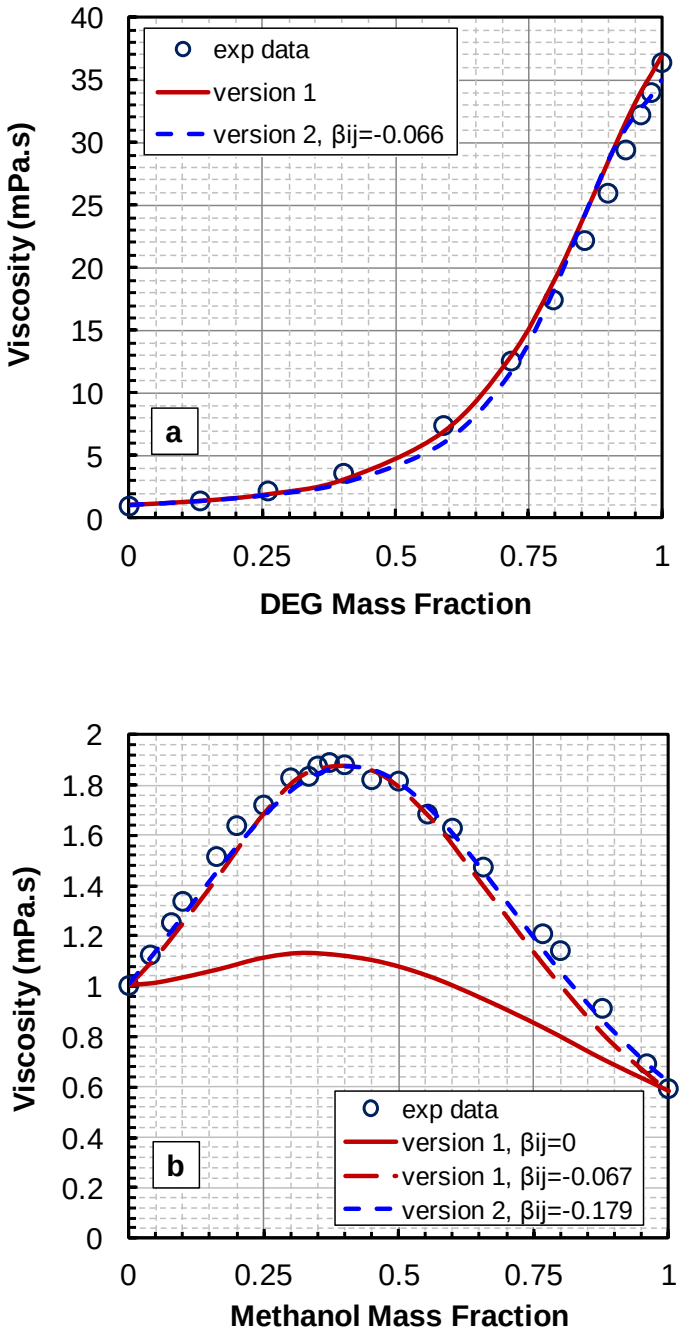

Figure 6.8: Comparison of the viscosty predictions by *Version 1* and *2* of the EF corrlelation with experimental data (NIST 2008) of: a) diethylene glycol+water at 293 K; b) methanol+water at 293 K.

6.3 Summary

The Expanded Fluid (EF) viscosity correlation was extended to natural gas processing applications; in particular, to include non-hydrocarbon components such as carbon dioxide, hydrogen sulfide, nitrogen, helium, water, methanol, ethylene glycol, diethylene glycol and triethylene glycol. Both *Version 1* (measured density input) and *Version 2* (EoS based density input) were evaluated. In both cases, for fluids with significant hydrogen bonding, such as water and methanol, the c_2 parameter of the correlation was modified from a constant to an exponential function of temperature with the following fitting parameters: $c_{2\infty}$, K_{c2}, and γ_{c2}. The default value of K_{c2} and γ_{c2} is zero for all components except those with significant hydrogen bonding.

The modified correlation was fitted to experimental data for pure non-hydrocarbons with overall average absolute relative deviations (AARD) below 6%. The maximum absolute relative deviation (MARD) for predictions with *Versions 1* and *2* were 48% and 54%, respectively. For all of the non-hydrocarbon components evaluated in this study, a fixed c_2 value (with K_{c2} and γ_{c2} equal to 0) was sufficient, except for methanol and water. *Version 1* of the correlation is not recommended for compressed water (P > 10 MPa) at temperatures below 50°C due to an unrealistic trend in the predicted viscosity values.

Version 1 and *2* of the correlation predicted the viscosity of several sweet and sour natural gas mixtures with overall AARDs of 6.3 and 5.1%, respectively. The MARDs of the predictions with *Version 1* and *2* were 15 and 51%, respectively. The higher deviations occurred for gas samples with heavy plus-fractions due to an over-simplified characterization of the plus fraction.

The viscosity of aqueous solutions of glycols and methanol were also predicted using *Version 1* of the correlation with MARD and AARD of 29 and 6%, respectively. The viscosity interaction parameter (β_{ij}) was set to zero for all binaries except for water/methanol where a single value of -0.067 was used for all temperature and compositions. The predictions with *Version 2* with $\beta_{ij} = 0$ were less accurate with MARD and AARD of 64 and 26%, respectively. Binary interaction parameters were determined

for all binaries reducing the MARD and AARD of the calculated viscosity values to 40 and 8.7%, respectively.

CHAPTER SEVEN: VISCOSITY MODELING OF CHARACTERIZED OILS[3]

The objective of this chapter is to extend the applicability of Expanded Fluid (EF) correlation to predict the viscosity of the crude oils characterized using pseudo-components. The developed framework of the EF correlation, up to now, is not predictive for hydrocarbon fluids and requires experimental viscosity data to determine the fluid-specific parameters. In addition, it has been only used for modeling the viscosity of well-defined mixtures. Its application to characterized crude oils as an ill-defined mixture of thousands of components has not yet been investigated.

It is common practice to characterize a crude oil as a mixture of some defined components and pseudo-components (Whitson and Brule, 2000). The defined components are components identifiable with analytical assays and typically include light hydrocarbons up to normal hexane and certain non-hydrocarbons such as carbon dioxide and hydrogen sulfide. Components heavier than hexane, usually termed the C_{7+} fractions, are represented by a limited number of pseudo-components (Whitson and Brule, 2000) based on assays such as TBP distillation or gas chromatography as discussed in Section 2.1.2. Each pseudo-component represents the mass fraction and average properties of either a boiling point or a molecular weight range within the overall distribution. Physical properties such as molecular weight (MW), specific gravity (SG) and normal boiling point (NBP) are measured or defined for each fraction and the critical properties and acentric factor are then estimated using well-known correlations.

In this chapter, a simple and internally consistent estimation method is developed to predict the fluid-specific parameters of the model for hydrocarbons when no experimental viscosity data are available. The model parameters are correlated as departures from an n-paraffin reference system. The validity of the viscosity predictions

---

[3] Contents of this Chapter, with some modifications, published as: Motahhari, H.; Satyro, M. A.; Taylor, S. D.; Yarranton, H. W. Extension of the Expanded Fluid Viscosity Model to Characterized Oils, *Energy Fuels*, Article ASAP. http://dx.doi.org/10.1021/ef301575n

from this method are tested against viscosity data of pure heavy hydrocarbons and distillation cuts of the crude oils. Then, the parameter correlations are used to calculate the parameters of EF model for the pseudo-components of the characterized crude oils. The viscosities of the crude oils are predicted using the measured densities as an input. A simple approach is proposed to tune the predictions to a measured viscosity. Finally, the application of the EF viscosity model to characterized crude oils using densities estimated by the Peng-Robinson equation of state is demonstrated.

7.1 Introductory Note

All developments and viscosity modeling in this chapter are done using the *Version 1* of the EF correlation. Recall that this version of the correlation is based on the measured density of the fluids. *Version 2*, based on the densities from the Advanced Peng-Robinson equation of state (APR EoS), was not further developed for the following reasons:

I. The applicability of *Version 2* is limited to APR EoS as implemented in VMGSim with specific non-adjustable volume translations as suggested by Mathias et al. (1989). *Version 2* is not valid if the volume translations are changed or improved.

II. The APR EoS only matches the density of liquid hydrocarbons at 298 K. Thus, the density is over-predicted and under-predicted at temperatures above and below 298 K, respectively. The constants of the EF correlation (n and c_1) and the fluid-specific parameters of the correlation were retuned for *Version 2* to compensate for the deviations of the density. For instance, the compressed state density of heavy hydrocarbons is smaller in *Version 2* than the actual value in *Version 1*. This difference leads in incorrect viscosity trends versus pressure at lower temperatures, especially for aromatic compounds (Satyro and Yarranton, 2010).

III. It was shown in Chapter 5 that *Version 2* tends to under-predict the viscosity of binary mixtures of well-defined hydrocarbons due to the skewed parameters of the correlation. Non-zero binary interaction parameters are required even for

simple binary mixtures with small deviations of the EoS-estimated density from measured values. It was also shown that β_{ij} would have to be pressure-dependent to adequately fit viscosity data. However, preliminary investigations indicated that introducing a density dependence of the β_{ij} adds to complexity of the model and is impractical to formulate.

The adjustment of the framework of EF correlation to work with any other cubic equation of state will encounter similar issues. Therefore, the most practical method to implement the EF correlation is to use *Version 1* coupled with an accurate full-phase density model. If density is modeled with a cubic equation of state, volume translation must be utilized and tuned to improve density predictions within the temperature range of interest, as is typically done in reservoir simulators. This approach is demonstrated in this chapter using the Peng-Robinson equation of state.

7.2 Application of EF Model to Characterized Oils

Figure 7.1 shows the proposed algorithm for the application of the EF model to characterized crude oils. First, the crude oil is represented as the mixture of defined components and pseudo-components. The numerical values of the fluid-specific parameters of the EF model (c_2, c_3 or ρ_s^o) are known for the defined components. Estimation methods are required to relate numerical values of the fluid-specific parameters of the EF model to the basic physical properties of the pseudo-components such as molecular weight, normal boiling point and specific gravity. The dilute gas viscosity of the defined components is calculated by Yaws correlation (Equation 2.13). The Chung et al. (1984) method, Equations 2.5 to 2.10 in Section 2.2.1.1, is used to estimate the dilute gas viscosity for pseudo-components and ill-defined hydrocarbons.

The fluid-specific parameters for the oil are calculated with the mixing rules and the oil viscosity is then predicted at any given pressure and temperature. The input oil density can be the measured value or the value estimated from a density model such as an equation of state. The Wilke (1950) mixing rule, Equations 2.14 and 2.16 in Section

2.2.1.2, is used to calculate the dilute gas viscosity of the crude oils as mixture of defined hydrocarbons and pseudo-components.

Finally, the model can be tuned against the experimental viscosity data if available. Single common multipliers (α_X) are applied to the estimated fluid-specific parameters of the pseudo-components as follows:

$$X_i = \alpha_X . X_{i(est)} \tag{7.1}$$

where X is any of the viscosity characterization parameters c_2, c_3 or ρ_s^o. Since the mixing rules of the EF model are linear when $\beta_{ij} = 0$, the common multiplier also applies directly to the calculated fluid-specific parameters of the crude oil. Once the oil is characterized and installed in the process or reservoir simulator, only the mass fraction and the values of the fluid-specific parameters (c_2, c_3 and ρ_s^o) are required to use the EF model.

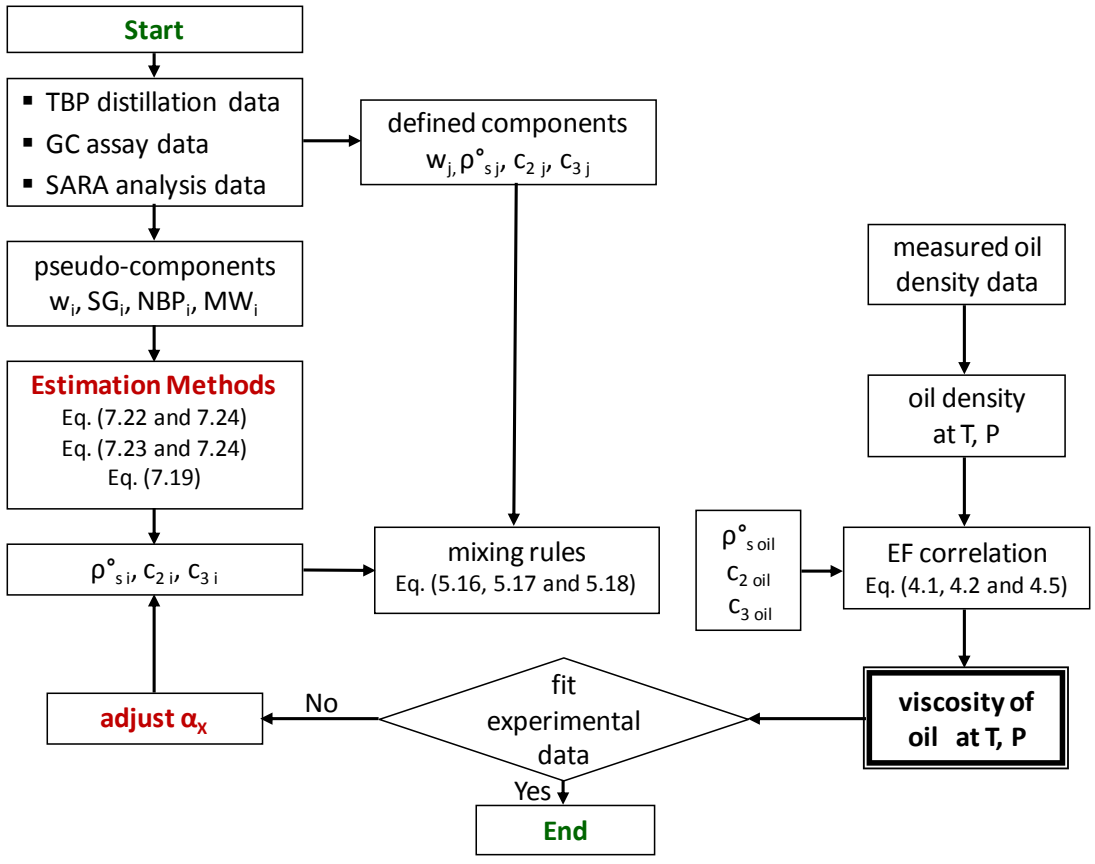

Figure 7.1: Flow diagram of the algorithm for application of the Expanded Fluid viscosity model to characterized oils.

7.3 Oil Characterization

Experimental viscosity and density data of 9 crude oils, one de-asphalted oil and one condensate were used in this study to evaluate the extension of the EF model to characterized oils. Table 7.1 gives a summary of the molecular weight and specific gravity (at standard condition) of the dead crude oils and condensate as well as the pressure and temperature ranges at which data are available. Note, the SG of the dead oil (or corresponding live oil) is required to apply the model. In this study, the SGs of dead oils were used to characterize the pseudo-components of the dead oils and the corresponding live oils except for crudes ME3a, ME1 and ME2 where the SG of the dead oil were not available. For these crudes, the live oil SG was calculated from the GC assay as reported in Table 7.1. Viscosity and density for bitumen WC-B-B1, WC-B-B2, WC-B-B3, de-asphalted oil WC-B-B3-DA,heavy oil WC-HO-S1 and condensate WC-C-B1 were measured at University of Calgary as described in Chapter 3 and the values are given in Appendix E. Data for WC-HO5 were provided by DBR Technology Centre and were collected using a similar methodology. Data for all other oils were obtained from commercial PVT studies provided by a sponsor and are from different geographical areas. The GC assays for the crude oils are given in Appendix F.

Gas chromatography (GC) assays are the basis for the oil characterizations prepared in this study. The GC assay provides the mass fractions of different compounds in the crude oil. The compounds are commonly grouped into single carbon number (SCN) fractions with assigned standard molecular weight values. Based on the GC assay technique and the style of the report, SCN data are reported up to carbon number *n-1* and the heavier hydrocarbons of the oil are usually lumped and reported as *n* plus fraction; for example, C_{7+}, C_{11+} and C_{30+}. The oils in this study were characterized up to SCN fraction of C_{29} by GC and the residue is reported as C_{30+}. The C_{30+} fraction of the oils in this dataset ranged from 0.0 to 70%, Table 7.1.

Table 7.1: Summary of the crude oils and conditions evaluated in this study.

Oil Description		mass fraction of C_{30+}	MW [a] (g/mol)	SG	Temperature (K)	Pressure (MPa)
WC-B-B1	dead	0.7	520	1.018	294-468	0.1-10
WC-B-B2	dead	0.7	520	1.018	293-448	0.1-10
WC-B-B3	dead	0.69	520	1.020	293-448	0.1-10
WC-B-B3-DA	dead	0.64	459	0.997[c]	293-448	0.1-10
WC-HO-S1	dead	0.68	424	0.997	298-448	0.1-10
WC-C-B1		0.00	90	0.703	298-448	0.1-10
WC-HO5	dead	0.67	484	1.005	298-473	0.1-8.27
EU1	dead	0.46	327	0.936	298-318	0.1
	live	0.45	238	0.900[e]	325	9.9-34.48
ME3a	live	0.33	186	0.831[d]	334-448	4.2-13.9
ME1	live	0.13	73	0.667[d]	386	27.6-37.9
ME2	live	0.66	373	0.921[d]	331-423	0.5-10
EU2	dead	0.59	362	0.903	313-423	1.6-2.1
	live	0.58	302	0.886[e]	313	4.1-15.1
	live[b]	0.58	303	0.886[e]	313	3.1-35.1
	live[b]	0.58	279	0.879[e]	303-423	7.6-20.1
AS1	dead	0.47	271	0.875	354	0.1
	live	0.39	186	0.827[d]	354	6.9-55.2

a - estimated after GC assay extrapolation except for WC-B-B2 which was measured with vapour pressure osmometry in toluene at 50°C. The MW of WC-B-B1 and WC-B-B3 is assumed equal to the MW of WC-B-B2.

b - live crude oils enriched with light n-alkanes.

c - de-asphalted oil SG calculated with Equations 7.8 and 7.9 assuming $C_f = 0.3211$ determined from SG of base WC-B-B3.

d - live oil SG calculated with Equations 7.8 and 7.9 assuming $C_f = 0.29$ and no-gas separation.

e - live oil SG calculated with Equations 7.8 and 7.9 with C_f determined from dead oil SG and the assumption of no-gas separation.

7.3.1 GC Assay Extrapolation

Given that a significant amount of the crude is lumped into the plus fraction, the GC assay must be extrapolated to estimate the heavier carbon number (CN) fractions and completely characterize the oil. For this purpose, molar distribution of the carbon number fractions in C_{30+} is assumed to follow an exponential distribution. The exponential distribution is a special form of the general three parameter gamma distribution with shape factor α=1 (Whitson and Brule, 2000) given by:

$$f(MW) = \frac{1}{MW_{C30+} - MW_{\min}} \exp\left(-\frac{MW - MW_{\min}}{MW_{C30+} - MW_{\min}} \right) \tag{7.2}$$

where MW is molecular weight, MW_{C30+} is the molecular weight of C_{30+} fraction and MW_{min} is the minimum molecular weight found in the C_{30+} fraction. The mole fraction (x_i) of carbon number fraction *"i"*, which includes the compounds with molecular weights between $MW_{b\ i-1}$ and $MW_{b\ i}$, is then given by:

$$x_i = x_{C30+} \left[f_0\left(MW_{b\ i}\right) - f_0\left(MW_{b\ i-1}\right) \right] \tag{7.3}$$

and $f_0(MW_{bi})$ is defined as follows:

$$f_0\left(MW_{b\ i}\right) = -\exp\left(-\frac{MW_{b\ i} - MW_{\min}}{MW_{C30+} - MW_{\min}} \right) \tag{7.4}$$

The mole fraction of the C_{30+} fraction is generally unknown and is estimated as follows:

$$x_{C30+} = \frac{w_{C30+} MW_{oil}}{MW_{C30+}} \tag{7.5}$$

where w_{C30+} is the mass fraction of C_{30+} fraction and MW_{oil} is the average molecular weight of the oil.

The average molecular weight of the corresponding fraction is given by:

$$MW_i = \frac{f_1\left(MW_{b\ i}\right) - f_1\left(MW_{b\ i-1}\right)}{f_0\left(MW_{b\ i}\right) - f_0\left(MW_{b\ i-1}\right)} \tag{7.6}$$

where $f_1(MW_{bi})$ is defined as follows:

$$f_1\left(MW_{b\ i}\right) = \left(MW_{b\ i} + MW_{C30+} - MW_{\min}\right).f_0\left(MW_{b\ i}\right) \tag{7.7}$$

The GC assay was extrapolated by defining 63 carbon number fractions with molecular weights evenly distributed between the molecular weight of the standard C_{29} fraction and the maximum molecular weight found in the oil. The value of the maximum molecular weight was set to 4000 g/mol. The value for MW_{min} is set as equal to upper-bound molecular weight of the last reported SCN fraction i.e. C_{29}. Thereafter, the value of the MW_{C30+} is adjusted to match the calculated average molecular weight of the oil from to the reported measured MW of the oil. If the MW of oil is not measured, the MW_{C30+} is adjusted to have a smooth transition of molar distribution of the single carbon number fractions (SCN) from C_{29} to higher SCNs.

The specific gravities of the carbon number fractions were determined from the following correlation (Sóreide 1989):

$$SG_i = 0.2855 + C_f \left(\overline{MW}_i - 66\right)^{0.13} \tag{7.8}$$

The C_f is a tuning parameter and determined by matching the calculated specific gravity of the oil to the measured value. The specific gravity of the crude is calculated as follows:

$$SG_{oil} = \left(\sum_k \frac{w_k}{SG_k} \right)^{-1} \tag{7.9}$$

where k in this summation includes all the components of the oil; that is, the C_1 to C_{29} fractions from the GC assay, the carbon number fractions from the extrapolation of the GC assay, and the defined non-hydrocarbon components such as carbon dioxide, hydrogen sulfide and nitrogen. Note, Equation (7.8) was originally proposed for the carbon number fractions heavier than C_6. Therefore, the recommended values of SG by the American Petroleum Institute (API, 1997) are used for the single carbon number fractions from C_1 to C_6. Note that the values from C_1 to C_4 are hypothetical.

7.3.2 Pseudo-Component Definition

Once the complete description of the oil was constructed as the molar distribution of the carbon number fractions and their specific gravities, the oil was divided into a number of defined components and pseudo-components. Defined components include defined non-hydrocarbons and single carbon number fractions up to C_6 which are modeled as the

corresponding normal paraffin. Each pseudo-component represents a specific molecular weight range above C_7. From 7 to 13 pseudo-components were defined for each crude oil depending on the maximum molecular weight. A set of consecutive carbon number fractions was lumped into each pseudo-component. The average properties for the pseudo-components were calculated as follows:

$$\bar{\theta}_j = \left(\sum_z \frac{w_z}{\theta_z} \right)^{-1} \tag{7.10}$$

where θ is molecular weight or specific gravity, z are the carbon number fractions lumped into the pseudo-component *"j"*.

7.4 Density Modeling

The development and testing of the estimation methods for the fluid-specific parameters of the EF model were based on measured density data. However, density predictions were required to use the EF model to predict the viscosity of the petroleum fluids lacking density data. Any density model can be used to provide the input densities for EF viscosity model; however, for general application, the density model must apply to liquid, gas, and fluid phases. Also, since the viscosity model is sensitive to density particularly near the compressed state density conditions, the density model must provide sufficiently accurate estimations of the density of the fluids; especially for saturated liquids. The modified Rackett correlation (Spencer and Danner 1972) was used to estimate the density of petroleum distillation cuts. In addition, to demonstrate the application of the viscosity model in simulation, the model was tested with densities from the Peng-Robinson equation of state instead of measured densities. Details of the density models are provided below.

7.4.1 Modified Rackett Correlation:

Spencer and Danner's (1972) well-known modification to the Rackett (1970) correlation was used to predict the density of the petroleum distillations cuts. The modified correlation is given by:

$$v_s = \frac{RT_c}{P_c} Z_{RA}^{\left[1+(1-T/Tc)^{2/7}\right]} \tag{7.11}$$

where v_s is the molar volume of the saturated liquid at temperature T, T_c and P_c are critical constants of the fluid, R is the universal gas constant and Z_{RA} is the Rackett compressibility. The numerical values of the Rackett compressibility have been regressed against saturated liquid molar volume data and are tabulated for pure components (Poling et al., 2000). There are also correlations relating this parameter to other properties of the fluids such as the acentric factor (Yamada and Gunn, 1973). However, in this study, the Rackett parameter is used as a tuning parameter to match the reported specific gravity of the petroleum distillation cuts. Note, the correlation is only valid for saturated liquids. Saturated liquid densities are sufficient to test the performance of the EF correlations for petroleum cuts which are generally studied in liquid state at atmospheric pressure where compression corrections to the saturated liquid volume are very small.

7.4.2 Peng-Robinson Equation of State

The Peng-Robinson (PR) equation of state (Peng and Robinson, 1976; Robinson and Peng, 1978) is a cubic equation of state and is widely used in process and reservoir simulators for the phase behavior modeling of the characterized oils, along with Soave-Redlich-Kwong (SRK) cubic equations of state (Soave, 1972). However, both lack the capability to accurately predict liquid molar volume. This deficiency is usually corrected using volume translation (Peneloux et al., 1982).

The detailed formulation of the PR EoS (Peng and Robinson, 1976; Robinson and Peng, 1978) is given in Appendix B. Volume translation (Peneloux et al., 1982) is introduced to improve the molar volume (i.e. density) predictions of the PR Eos as follows:

$$v = v_{EoS} - c \tag{7.12}$$

where v is the corrected molar volume, v_{EoS} is the EoS-calculated molar volume and c is the fluid-specific volume translation parameter. To improve the calculated molar volumes over a broad range of temperatures, a linear temperature dependent volume translation paramter is introduced as follows:

$$c = \gamma_0 + \gamma_1 (T - 288.75) \tag{7.13}$$

where T is temperature in K, γ_0 is the fixed volume translation parameter and γ_1 is the temperature dependency term. The values of γ_0 and γ_1 must be determined for each component by matching the predicted liquid molar volumes by the equation of state to the actual measured molar volumes of the saturated liquids at two given temperatures.

Numerical values of the γ_0 and γ_1 for the defined components of the characterized oils are given in Table 7.2. These values were determined by matching the predicted molar volumes of these compounds by equation of state to the actual molar volumes of the statured liquids (Yaws, 1999) at two temperatures, 288.75 K (60 °F) and the reduced temperature (T_r) of 0.85. For the components with $0.85T_r$ below 288.75 K, the saturated liquid molar volume at the normal boiling point was used instead of at 288.75 K.

The values of γ_0 and γ_1 for the pseudo-components of each characterized oils must be individually determined. The coefficients for each pseudo-component were adjusted to fit the EoS-estimated liquid densities to independently determined values at two temperatures, 288.75 K and 423.15 K. Following the approach of Pedersen et al. (2004), the liquid density at 288.75 K was set to the defined specific gravity of the pseudo-component while the density at 423.15 K was calculated using the ASTM 1250-80 correlation for the thermal expansion of the stable oils as follows:

$$\rho_{T_1} = \rho_{T_0} \exp\left[-A\left(T_1 - T_0\right)\left(1 + 0.8A\left(T_1 - T_0\right)\right)\right] \tag{7.14}$$

where ρ_{T1} and ρ_{T0} are liquid densities in temperatures T_1 and T_0 (288.75 and 423.15 K, respectively) and A is given by:

$$A = \frac{613.9723}{\rho_{T_0}^{\ 2}} \tag{7.15}$$

Table 7.2: Constants of temperature dependent volume translation, Equation 7.22, for defined components of the characterized oils.

Component	γ_0 (cm^3/mol)	γ_1 (cm^3/mol.K)
carbon dioxide	0.0929	0.0228
methane	2.3608	0.0364
ethane	-1.8087	0.0252
propane	-2.6827	0.0343
n-butane	-4.2303	0.0380
n-pentane	-3.3612	0.0384
n-hexane	-0.3511	0.0339

7.5 Estimation Methods for EF Model Parameters

Estimation methods are required to relate the fluid-specific parameters of the EF model to the physical properties of the pseudo-components. The obvious candidates to represent the pseudo-components of the characterized oils are petroleum distillation cuts. However, experimental viscosity data for the cuts are scarce in the open literature and the reported data do not include corresponding density measurements. Instead, pure heavy hydrocarbon compounds are selected as the model components for the pseudo-components due to their availability in the literature.

The physical properties commonly used to develop the estimation methods are the normal boiling point and specific gravity (Riazi, 2005) which roughly characterize the molecular energy and size, respectively. Normal boiling point is not readily available for the heavy hydrocarbons, but the molecular weight is. Therefore, the molecular weight and specific gravity were selected as the correlating properties (Nji et al., 2008). Note, the molecular weight and normal boiling point of the petroleum fluids are generally correlated through some well-known methods (Søreide, 1989; Twu, 1984; Lee and Kesler, 1975; Kesler and Lee, 1976).

The estimation methods of the parameters of the EF model were formulated as departure functions from a reference system. The family of n-paraffins was chosen as the reference system. The form of the departures is given by:

$$X = X_{(ref)} + \Delta X \tag{7.16}$$

where X is c_2 or ρ_s^o. The reference n-paraffin has the same molecular weight as the hydrocarbon compound or pseudo-component of interest. The departure from the paraffinic values due to the aromaticity of the hydrocarbon is formulated by a quadratic polynomial approximation given by:

$$\Delta X = A_X \ \Delta SG^2 + B_X \ \Delta SG \tag{7.17}$$

where A_X and B_X are fitting parameters and ΔSG is given by:

$$\Delta SG = SG - SG_{(ref)} \tag{7.18}$$

In this formulation, the molecular weight captures the effect of the size of the compound, while the specific gravity adds the contribution of the chemical family type of the hydrocarbon.

Note that the development of a comprehensive estimation method for parameter c_3 of the EF model is not feasible at this time due to limited availability of high pressure viscosity and density data of the heavy hydrocarbons. Therefore, the following adaptation of the original development of Yarranton and Satyro (2009) is proposed to use for the purpose of this study:

$$c_3 = \frac{2.8\times10^{-7}}{1+3.23\exp(-1.54\times10^{-2}MW)} \tag{7.19}$$

The above correlation approximates the correlation of Yarranton and Satyro (2009) and converges to a fixed value of 2.8×10^{-7} kPa^{-1} for higher molecular weight hydrocarbons. The reference system and the departure functions for c_2 and ρ_{so} are discussed individually below.

7.5.1 n-Paraffin Reference System

Experimental viscosity and density data for the family of n-paraffins from methane (n-C_1) to n-tetratetracontane (n-C_{44}) were compiled from the NIST (2008) database and API project 42 (API, 1966). The data for the n-paraffins up to n-C_{16} include measurements at higher pressures; whereas the data for heavier n-paraffins are at atmospheric conditions.

The dilute gas viscosity of n-paraffins was calculated using Equation 2.13 with parameters obtained from Yaws' Handbook (2009). Following the regression approach described in detail by Satyro and Yarranton (2010), the parameters of the EF viscosity model for these components were calculated from the experimental data. Then, the parameters were correlated as functions of the molecular weight of n-paraffin components. Also, specific gravities of reference n-paraffins were correlated to the molecular weight.

7.5.1.1 Specific Gravity (SG)

The specific gravity values of the reference n-paraffin components from C_1 to C_{20} were obtained from API (1997) handbook. SG values for heavier n-paraffins were estimated based on the experimental density data of these components. The density of water at 15.6 ºC is 999.022 kg/m³ (API 1997) and was used to convert density to specific gravity at standard condition of 15.6 ºC and 1 atm. Note, the n-paraffins from methane to n-butane (n-C_4) are in the gaseous state at standard conditions; hence, their SG were based on the standard liquid densities recommended by the API (1997).

The specific gravities of the n-paraffins were correlated as function of molecular weight (MW) as follows:

$$SG_{(ref)} = a_{0\,SG} + \frac{a_{1\,SG}}{MW^{0.5}} + \frac{a_{2\,SG}}{MW} + \frac{a_{3\,SG}}{MW^{2}} + \frac{a_{4\,SG}}{MW^{3}} \tag{7.20}$$

where a_0 to a_4 are constants of the correlation which were determined by regression and are given in Table 7.3. The value of a_0, the limiting specific gravity for the n-paraffin with infinite molecular weight was set to 0.843593 as previously used by Twu (1984) in the development of the correlation for the specific gravity of n-paraffins as function of normal boiling point. The fitted correlation is shown in Figure 7.2. The AARD and MARD of the correlated values from the experimental values are 0.5% and 2.5%, respectively.

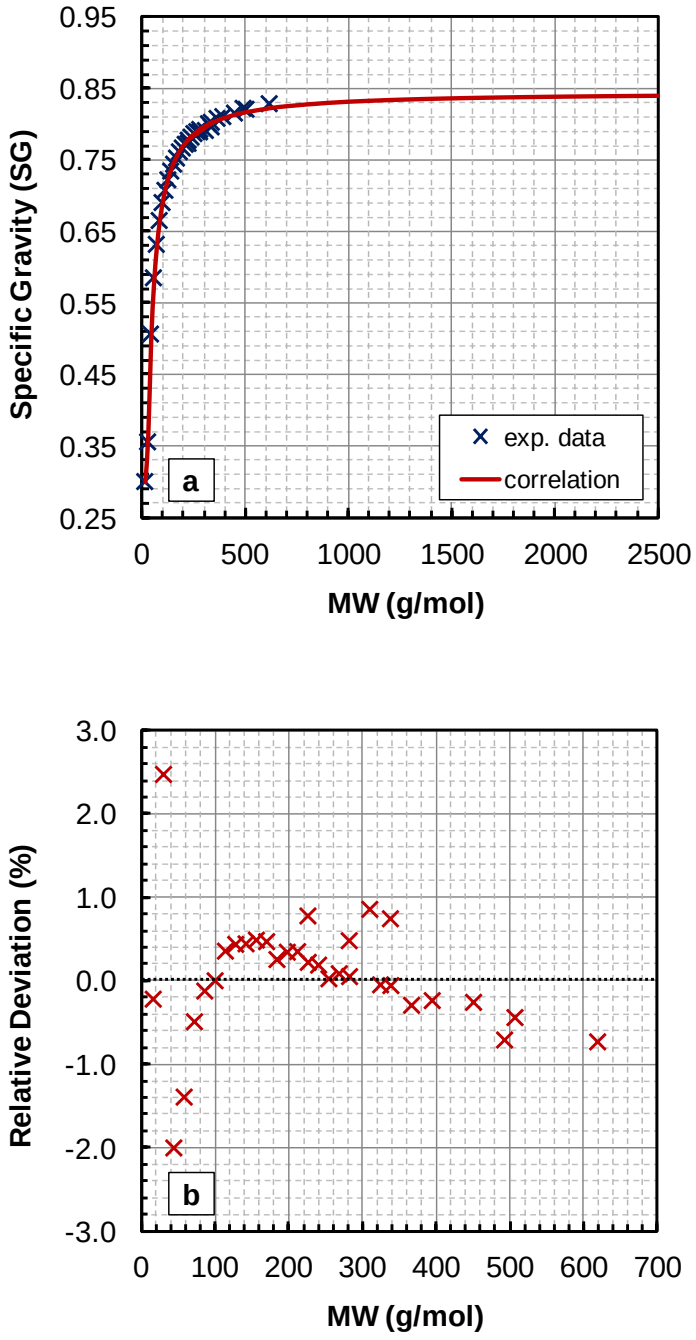

Figure 7.2: a) Correlated and measured specific gravity of n-paraffins from C_1 to C_{44}; and b) relative deviation of correlated SGs [(SGcorr-SGexp)/SGexp] versus molecular weight from C_1 to C_{44}.

7.5.1.2 Compressed State Density

The compressed state density values of n-paraffins up to n-C_{44} (618 g/mol) were obtained from fitting experimental data, Figure 7.3a. The fitted values are given in Table D.1 in Appendix D. To extrapolate to higher molecular weights, it was noted that the ratio of the compressed state density to the density of the n-paraffins at 15.6 °C reaches an asymptote at molecular weights higher than ~300 g/mol, Figure 7.3b. Hence, the assumption was made to extrapolate the compressed state density of the n-paraffins to higher molecular weights subject to the following constraint:

$$\lim_{MW\to\infty} \frac{\rho^{o}_{s\,(ref)}}{\rho_{(ref)@15.6\ ^{\circ}C}} = K \tag{7.21}$$

where K is a constant. The compressed state density of the reference n-paraffin family was then correlated to the molecular weight as follows:

$$\rho_{s}^{\ o}{}_{(ref)} = \left(\frac{a_{0\,\rho_s^{\,o}}}{MW} + a_{1\,\rho_s^{\,o}} MW^{a_{2\,\rho_s^{\,o}}} \right) \exp(a_{3\,\rho_s^{\,o}} MW) + \frac{a_{4\,\rho_s^{\,o}}}{1 + a_{5\,\rho_s^{\,o}} \exp(a_{6\,\rho_s^{\,o}} MW)} \tag{7.22}$$

where a_0 to a_6 are the constants of the correlation and are listed in Table 7.3. Figure 7.3a compares the correlated compressed state density values against the values obtained from fitting the EF model to the measured data. The regressed numerical value of constant K in Equation 7.21 was determined to be 1.12, Figure 7.3b.

7.5.1.3 Parameter c_2

The values of the parameter c_2 of n-paraffins up to n-C_{44} were obtained from experimental data (given in Table D.1 in Appendix D), Figure 7.4; but, no experimental data are available to extrapolate c_2 to molecular weights higher than 618 g/mol. Instead, the atmospheric viscosity data of the WC-B-B2 bitumen were used to guide the extrapolation of c_2. The detailed characterization of the bitumen is discussed later. Briefly, the extrapolated c_2 correlation for MW higher than 618 g/mol, coupled with the departure function (described later), was set to predict the correct viscosity of the characterized WC-B-B2 bitumen.

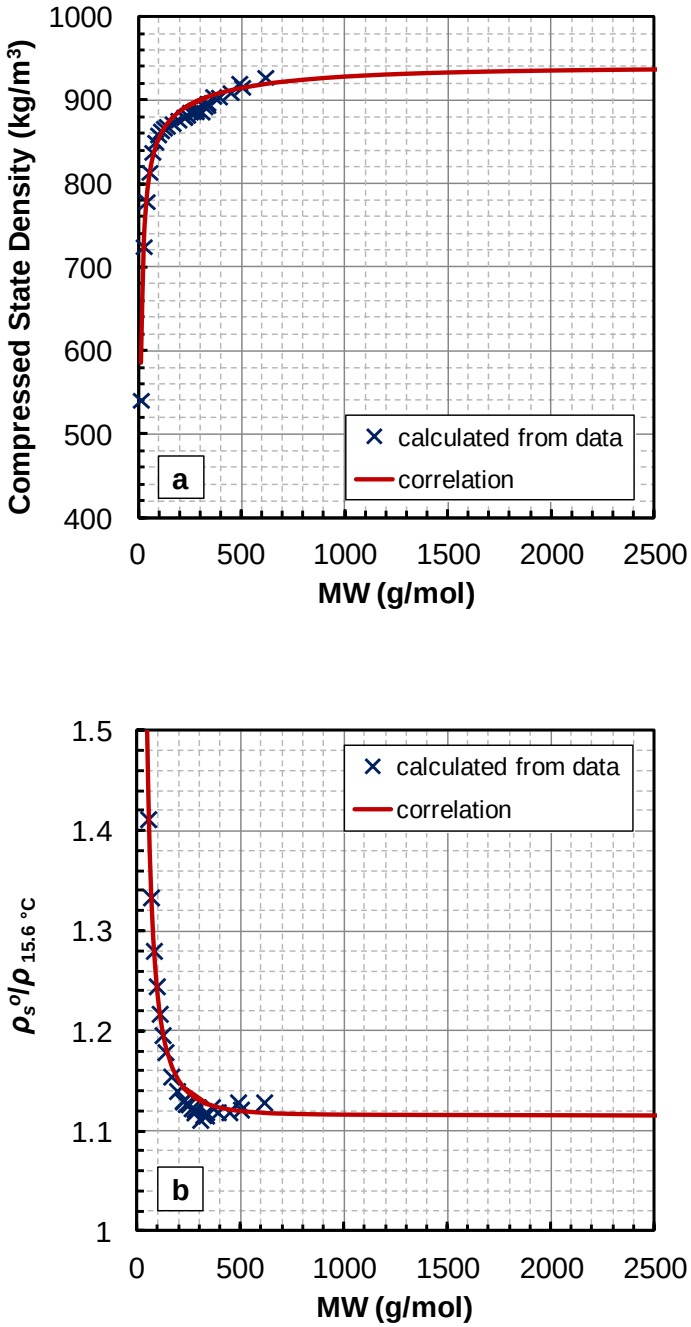

Figure 7.3: a) ρ_s^o of n-paraffins determined from fitting EF model to viscosity data (symbols) and correlated ρ_s^o (lines); and b) observation of the ratio of ρ_s^o to the density of n-paraffins at 15.6 ºC approaches to a plateau.

The final correlation of parameter c_2 to molecular weight for the reference n-paraffin family is given by:

$$c_{2(ref)} = (a_{0c_2} + a_{1c_2}.MW)\exp\left(\frac{a_{2c_2}}{MW} + a_{3c_2}.MW\right) + a_{4c_2}\ln(MW) \qquad (7.23)$$

where a_0 to a_4 are the constants of the correlation and are listed in Table 7.2. Figure 7.4 shows the extrapolation of c_2 to molecular weights above 618 g/mol. Note, the molecular weight of the heaviest pseudo-component of the characterized WC-B-B2 bitumen is 2791 g/mol. Although Equation 7.32 smoothly extrapolates to molecular weights as high as 4000 g/mol, its validity for pseudo-components with MW beyond 2791 g/mol was not studied. The application of Equation 7.32 to higher molecular weights is unnecessary as long as the high molecular weight SCN fractions are lumped into a pseudo-component with an average molecular weight lower than 2791 g/mol.

As a test, the correlations for parameters c_2 and ρ_s^o were used in the EF model to predict the viscosity of the n-paraffins from n-C_1 to n-C_{44}. The AARD and MARD were 7.4% and 65%, respectively. Note, the correlations will not be used to predict n-paraffin properties, only in the prediction of pseudo-component properties.

Table 7.3: Constants of the estimation correlations of the fluid-specific parameters of the EF correlation for the reference n-paraffin system from C_1 to C_{44} and beyond.

Property	**Equation**	**a_0**	**a_1**	**a_2**	**a_3**	**a_4**	**a_5**	**a_6**
SG	7.20	0.843593	0.1419	-16.6	-41.27	2535	-	-
ρ_s^o (kg/m^3)	7.22	-4775	3.984	0.4	-1.298×10^{-3}	938.3	8.419×10^{-2}	-1.06×10^{-3}
c_2	7.23	9.353×10^{-2}	4.420×10^{-4}	-333.4	-1.660×10^{-4}	4.770×10^{-2}	-	-

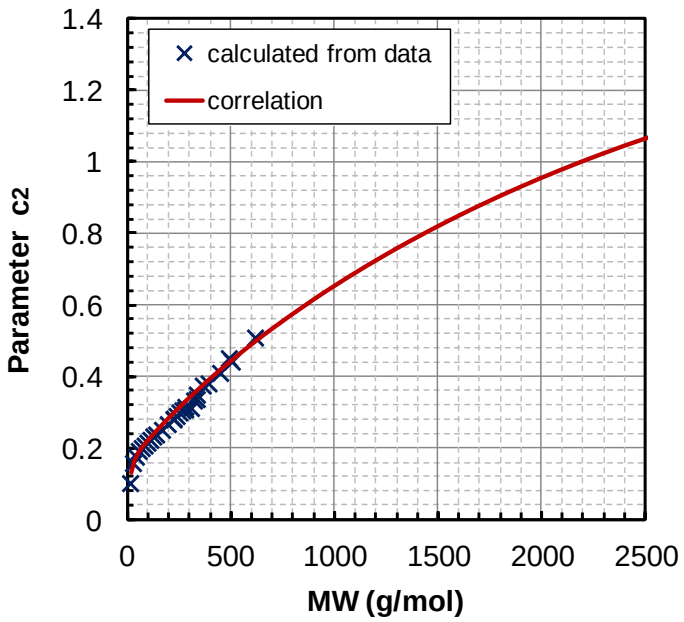

Figure 7.4: c_2 parameter of n-paraffins determined from fitting the EF model to viscosity data (symbols) and the c_2 parameter correlation (line).

7.5.2 Departure Functions for Heavy Hydrocarbons

Experimental viscosity and density data for over 170 diverse hydrocarbons including branched paraffins, aromatics and naphthenes, were compiled from the NIST (2008) database, API Project 42 (API, 1966), and the TRC (1985) handbook. Details of their chemical families are provided later in Section 7.6.1 and the compounds are listed in the Appendix D. The EF model was fitted to the data of the heavy hydrocarbons to determine the numerical values of the compressed state density and parameters c_2 for each compound. The regressed values of the parameters for each compound are given in Tables D.2 and D.3 in Appendix D. Then, the departures of c_2 and ρ_s^o for each compound from the corresponding reference n-paraffin were calculated using the reference equations (Equations 7.23 and 7.23, respectively). Note, the calculated departures of c_2 were independent of the extrapolation of c_2 for the reference n-paraffin system because the molecular weights of the pure heavy hydrocarbons in the dataset are all less than 618 g/mol.

The departures of ρ_s^o ($\Delta\rho_{so}$) increased almost monotonically with increasing ΔSG, Figure 7.5a. However, the calculated departures of c_2 (Δc_2) were significantly scattered, Figure 7.5b. The departures of c_2 were found to depend not only on specific gravity but also on the structure of the molecules; that is, on the number and types of branches, the relative positioning of the fused aromatic and naphthenic rings as well as the relative positioning of the branches and non-fused aromatic and naphthenic rings on the main chain of molecule. It is not practical to construct a correlation including structural parameters for pseudo-components which represent a mixture of unknown structures. Therefore, the departure functions were fitted to data for 24 single-ring and fused-ring naphthenic and aromatic hydrocarbons (the development group). The departures of c_2 and ρ_s^o for the development group are highlighted as the open circles on Figure 7.5 a and b. The remaining 163 heavy hydrocarbons (test group) were used to evaluate the departure functions and were not used in their development. Note, adding more components to the development group does not improve the data fitting because the correlations do not account for structural effects.

Equation 7.26 was expanded as follows to correlate the departure functions:

$$\Delta X = \left(b_0 + \frac{b_1}{MW^{b_4}} \right) \Delta SG^2 + \left(b_2 + \frac{b_3}{MW^{b_4}} \right) \Delta SG \tag{7.24}$$

where ΔX is the desired departure ($\Delta\rho_{so}$ or Δc_2), b_0 through b_4 are the fitting parameters. The values of fitting parameters were determined by simultaneous regression for both parameters and their numerical values are given in Table 7.4. The objective of the least squares regression was to minimize the deviation between the predicted viscosity (using parameters calculated from reference and departure functions) and the measured viscosity for the hydrocarbons in the development group. The AARD and MARD of the viscosity predictions for the development group were 24% and 180%, respectively.

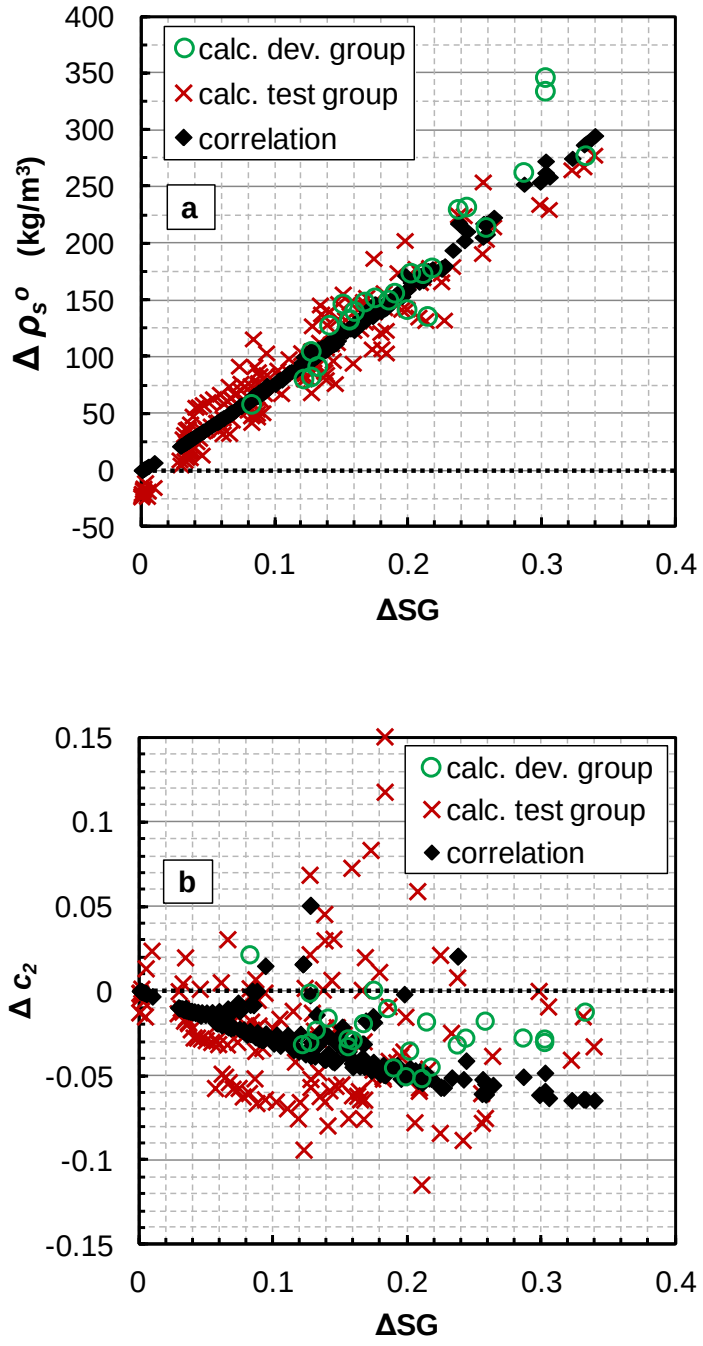

Figure 7.5: Correlated and obtained from data departures of the parameters of EF model for pure heavy hydrocarbons: a) for compressed state density; and b) for parameter c_2.

Table 7.4: Constants of the departure functions for parameters of EF model, Equation 7.24.

Property	b_0	b_1	b_2	b_3	b_4
$\Delta\rho_s^o$ (kg/m^3)		14640	739		-0.67
Δc_2	0.4925	-191900	-0.371	83930	2.67

The black solid symbols in Figure 7.5a and b represent the departure values calculated from Equation 7.32 for all 172 hydrocarbons in the test and development group. Note that the ρ_s^o departures have little dependence on molecular weight while the departures for c_2 departures depend somewhat on molecular weight at low molecular weights but not at high molecular weights. The molecular weight dependence appears as a departure from the main trend of correlation points in Figure 7.5a and b. The results for the test group are discussed later.

7.6 Application and Testing of the Model

The model was applied to a number of examples following the procedure shown in Figure 7.1. The fluid was first divided into pure components and pseudo-components as appropriate for the fluid description. Except for the pure hydrocarbon test described below, pure hydrocarbons as defined components of the crude oils were modeled using previously determined EF model parameters (Yarranton and Stayro, 2009). For pseudo-components, the EF model ρ_s^o and c_2 parameters were calculated from the departure functions (Equation 7.24 with constants in Table 7.4, coupled with Equations 7.22 and 7.23). Their c_3 parameters were calculated from Equation 7.19. At this point, the model parameters have been defined for all components. Then, the EF model parameters for the whole fluid are calculated from the mixing rules, Equations 5.16 to 5.18. The dilute gas viscosity was calculated from Equations 2.5 to 2.10 using critical properties and acentric factor values calculated from the Lee-Kesler (Lee and Kesler, 1975; Kesler and Lee, 1976) and Hall and Yarbrough (1971) correlations. Finally, the fluid viscosity was calculated from Equations 4.1 to 4.5. Example calculations are given in Appendix G.

7.6.1 Pure Hydrocarbons

The departure functions (Equation 7.24 with constants in Table 7.4) coupled with Equations 7.22 and 7.23 for the reference n-paraffin system were used to predict the viscosity of the pure heavy hydrocarbons in the test group based only on their molecular weight and specific gravity.

Table 7.5 reports the average absolute relative deviations and maximum absolute relative deviations of the predictions for each family of compounds. The predictions are evaluated against experimental atmospheric data in temperature ranges of 253 to 383 K for alkylcyclopentanes, alkylcyclohexanes and alkylbenzenes and 273 to 373 K for the rest. The predicted viscosities are within one order magnitude of the measured values with overall AARD and MARD of 31% and 334%, respectively. The predicted viscosities for the limited higher pressure data (up to 500 MPa) available for 7 of these components (NIST, 2008; API, 1966) were within the same overall AARD and MARD.

Figure 7.6a shows that, for a fixed molecular weight, the viscosity model correctly predicts the viscosity of the reference n-paraffin as well as the increasing trend of the viscosity versus specific gravity at the temperatures of 310.9 K and 372.0 K. Note that the correlation does not predict the abrupt increase of the viscosity for the three components (9-n-octyl-perhydronaphthacene, 2-n-octyl-perhydrotriphenylene, 2-n-octyl-perhydrochrysene) with the approximately similar SG of ~0.943. Although these three components are isomers with the same SG, their viscosities are significantly different due to the relative positioning of the fused saturated rings in their structures and these structural effects are not accounted for. Similar trends are observed versus molecular weight at fixed SG, Figure 7.6b. These predictions are satisfactory for our purpose which is not to obtain exact predictions for pure hydrocarbons but reasonable approximations for ill-defined pseudo-components.

Table 7.5: Summary of errors of the viscosity predictions for pure heavy hydrocarbons.

Hydrocarbon family	No. of compounds	MW range (g/mol)	SG range	MARD* (%)	AARD** (%)
branched paraffins	16	198 − 451	0.767 − 0.817	84	17
non-fused aromatics	12	168 − 351	0.860 − 1.103	334	59
fused aromatics	20	184 − 427	0.890 − 1.104	100	29
non-fused naphthenics	16	138 − 393	0.826 − 0.944	137	26
fused naphthenics	36	194 − 433	0.863 − 1.031	99	35
alkylcyclopentanes	16	84 − 294	0.754 − 0.827	75	13
alkylcyclohexanes	16	98 − 308	0.775 − 0.832	32	6.8
alkylbenzenes	16	92 − 302	0.858 − 0.874	134	49

* : $MARD = Maximum\ of\ \frac{\left|\mu_{corr\,(i)} - \mu_{\exp\,(i)}\right|}{\mu_{\exp\,(i)}} \times 100$ *for i=1 to N*

**: $AARD = \frac{100}{N}\sum_{i=1}^{N}\frac{\left|\mu_{corr\,(i)} - \mu_{\exp\,(i)}\right|}{\mu_{\exp\,(i)}}$

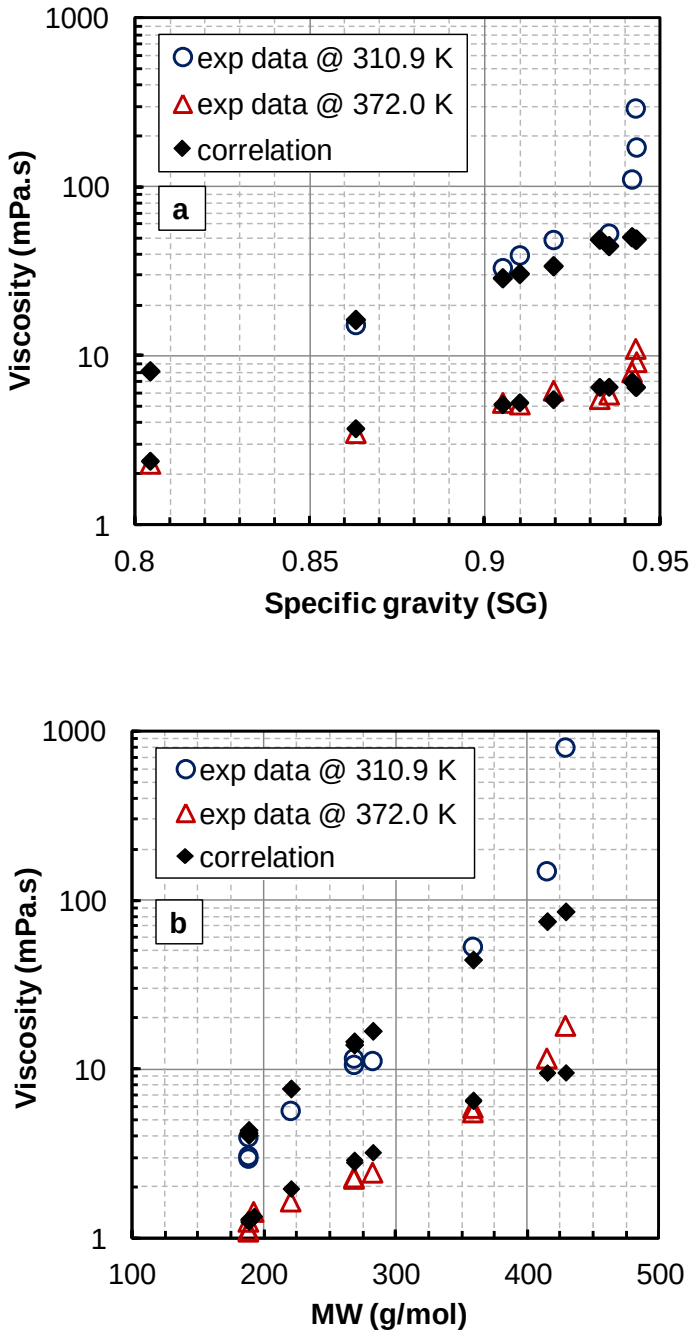

Figure 7.6: Increasing trend of viscosity with: a) specific gravity for heavy hydrocarbons of MW=360 g/mol; and b) molecular weight for heavy hydrocarbons of SG=0.935. Data are from the API Project 42 (API, 1966).

7.6.2 Petroleum Distillation Cuts

The validity of the proposed correlations for the parameters of EF model to the pseudo-components of the crudes was assessed against the viscosity data of petroleum fractions. A total of over 500 data points were compiled from the open literature (FitzSimons and Thiele, 1935; Watson et al., 1935; Beg et al., 1988; Knati et al., 1989) for the viscosity of 117 petroleum cuts at different temperatures, Table 7.6. Most of the reported data are kinematic viscosities versus temperature at atmospheric pressure for the petroleum cuts which are characterized by their average boiling point and specific gravity. The boiling point and specific gravity of these cuts vary from 327 K to 762 K and 0.660 to 1.112, respectively.

To characterize the cuts for the EF model, the molecular weight of the cuts were calculated using Twu's correlation (Twu, 1984) as a function of the boiling point and specific gravity. The required densities and dilute gas viscosities of the cuts versus temperature were estimated by the modified Rackett correlation (Equation 7.11) (Spencer and Danner, 1972) and method of Chung et al. (1988) (Equations 2.5 to 2.10) using critical properties calculated by Twu's method (Twu, 1984), respectively. The modified Rackett correlation was tuned for each cut to match the reported specific gravity. The viscosity model parameters were then calculated from the reference and departure functions. The MARD and AARD of the predicted viscosities are provided in Table 7.6. The overall AARD is 27% and the largest MARD was 100%. Note, the largest under-predictions were within one order of magnitude below the measured values and were observed for cracked materials. These results are not surprising considering the completely predictive approach of the model based on pure hydrocarbon data and the uncertainties associated with the estimated density and molecular weight. Note, the model performed similarly for the different cuts of every studied crude oil regardless of the geographical origin of the crude, Figure 7.7a and b.

Table 7.6: Summary of errors of the viscosity predictions for petroleum distillation cuts.

Petroleum Fraction	ABP[a] (K)	SG	Viscosity[b] (mPa.s)	MW[c] (g/mol)	MARD (%)	AARD (%)
Arabian light crude cuts [I]	429-560	0.740-0.867	0.3-3.8	129-212	53	27
Arabian Berri crude cuts [II]	422-672	0.755-0.888	0.4-14	126-311	31	18
Arabian Medium crude cuts [II]	422-672	0.762-0.900	0.4-15	125-305	29	17
Arabian Heavy crude cuts [II]	422-672	0.755-0.902	0.4-17	126-304	29	16
Oklahoma crude cuts [II]	411-511	0.758-0.828	0.3-4	119-176	40	23
Boscan crude cuts [II]	455-563	0.814-0.888	0.7-4	139-201	20	11
California crude cuts [II]	411-461	0.782-0.818	0.3-0.9	117-142	24	16
Pennsylvania crude cuts [II]	411-511	0.746-0.797	0.3-1.5	120-181	25	13
Wyoming crude cuts [II]	411-511	0.764-0.822	0.3-1.6	118-176	26	17
Minas crude cuts [II]	356-583	0.697-0.829	0.3-1.1	93-237	27	23
Iranian Export crude cuts [II]	363-496	0.719-0.801	0.3-1.2	95-170	39	28
Stabilized Arabian crude[II]	391-469	0.732-0.789	0.4-0.9	110-152	38	29
Midway Special crude cuts [II]	373-518	0.750-0.870	0.4-1.9	98-171	20	15
Safania crude cuts [II]	417-474	0.746-0.785	0.5-1.0	123-156	26	16
Light Valley crude cuts [II]	433-526	0.791-0.870	0.6-2.1	129-178	42	22
Waxy crude cuts [II]	398-490	0.762-0.825	0.4-1.2	111-161	36	33
Midcontinent distillates [III]	452-729	0.792-0.905	0.4-102	140-379	70	25
Smackover distillates [III]	505-676	0.860-0.928	0.7-39	165-296	56	22
distillates from cracked residue [c III]	508-691	0.925-1.059	1.8-329	153-256	91	39
Pennsylvania distillates [III]	518-705	0.809-0.866	0.7-32	184-368	47	18
Pennsylvania lube oil [III]	685-744	0.875-0.887	4.9-156	335-417	79	56
cracked residuum cuts [III]	678-762	0.998-1.112	205-1920	229-332	100	95
cuts from pressure distillate[d IV]	327-631	0.660-1.013	0.2-102	78-331	86	31
cuts from cycle stock [d IV]	366-603	0.709-0.919	0.3-8.2	96-272	47	32
Gas oils and Kerosenes [d IV]	502-580	0.816-0.851	0.6-4.7	187-266	37	30
Virgin Midcontinent naphtha cuts [d IV]	405-439	0.756-0.781	0.5-0.7	118-141	41	36
miscellaneous cuts [d IV]	534-656	0.852-0.907	1.1-21	193-337	40	29

a- ABP: average boiling point **b-** calculated from reported kinematic viscosity

c- calculated by method of Twu (1984) **d-** from midcontinent gas oil

I, II, III and **IV-** data from Knati et al. (1989), Beg et al. (1988), Watson et al. (1935) and FitzSimons and Thiele (1935), respectively.

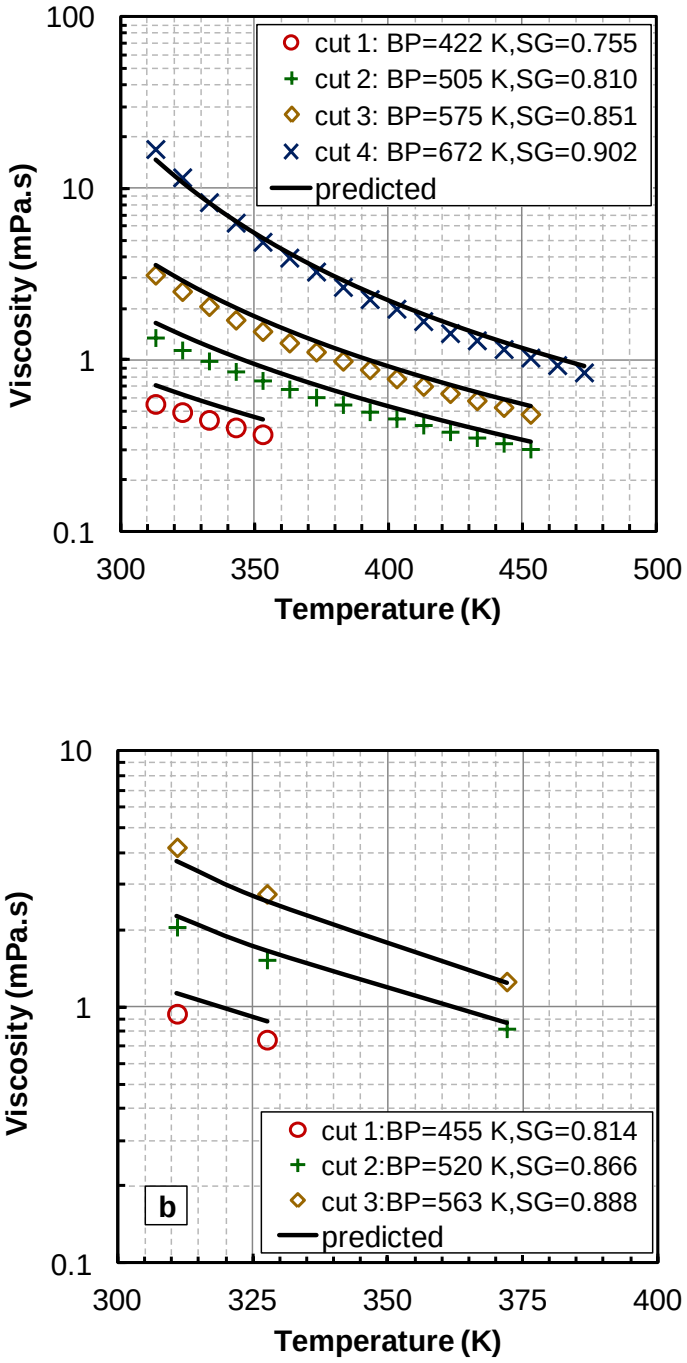

Figure 7.7: Experimental and predicted viscosity of the consecutive boiling point cuts of: a) Arabian heavy oil; and b) Boscan oil from Venezuela. data from Beg et al. (1988).

The model tended to over-predict the viscosity of the low boiling point cuts and under-predict the viscosity of the high boiling point cuts, Figure 7.8. The distillation cuts are complex mixtures of the hydrocarbons with the same vapor pressure, but are polydisperse in molecular weight. The number average molecular weight or the molecular weight from property correlations may not be the most suitable value for the viscosity model parameter correlations. An effective molecular weight (for example a mass average molecular weight) may be required. Alternatively, use of the normal boiling point and specific gravity as the characterizing properties for the estimation methods of the parameters of EF model may result in better predictions for the petroleum cuts. However, this option was not studied further due to limited reliable density and viscosity data for the petroleum cuts and normal boiling points for the pure heavy hydrocarbons.

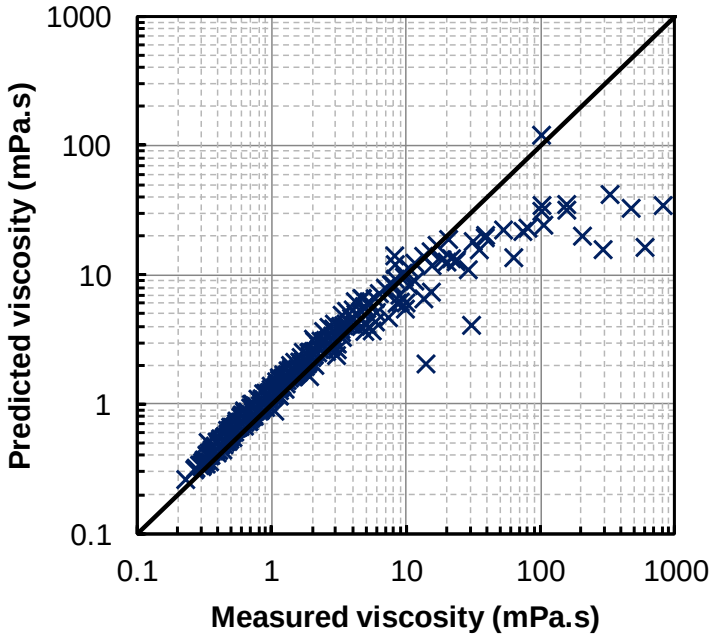

Figure 7.8: Dispersion plot of the predicted viscosity of petroleum cuts by EF model versus measured values.

7.6.3 Characterized Oils

A total of 9 different crude oils and one de-asphalted crude oil were included in this study to evaluate the application of the viscosity model with the proposed parameter correlations to characterized oils, Table 7.1. Among the fluids are three live (with solution gas) oils without data for their corresponding dead (gas free) oils. The remaining 6 crude oils are dead oils; 3 of which have data for the corresponding live oil. The WC-B-B2 bitumen was selected as the development oil to guide the extrapolation of the c_2 correlation for the reference n-paraffin system to molecular weights higher than 618 g/mol. WC-B-B1 and WC-B-B3 are different batches of the WC-B-B2 bitumen. These two fluids along the remaining oils were used as the test group to evaluate the modelling methodology.

7.6.3.1 WC-B-B2 Development Oil

The WC-B-B2 oil is a West Canadian bitumen with specific gravity of 1.018 and viscosity of 89000 mPa.s at atmospheric pressure and 20 °C. The viscosity and density of this bitumen were measured at temperature and pressures up to 175 ºC and 10 MPa. The GC assay of the bitumen, Table 7.7, is an average assay based on multiple measurements on several batches of the crude by different laboratories. The bitumen was characterized based on the extrapolated GC assay as described previously. The bitumen was represented by 13 pseudo-components, Table 7.8. Note, the characterized bitumen does not include any defined components.

The EF model parameters were then estimated using the procedure outlined in Figure 7.1. Using the measured density data as input, the viscosity of the bitumen was calculated at temperatures up to 175 °C and atmospheric pressure, Figure 7.9a, and higher pressures, Figure 7.9b. Recall that the extrapolation of the c_2 values for the reference n-paraffin system to MW higher than 618 g/mol was constrained to fit the atmospheric data points of this bitumen. The MARD and AARD of the fit is 11% and 8.1%, respectively. The viscosity predictions at higher pressure conditions are within the same range of error with MARD and AARD of 19% and 8.9%, respectively.

Table 7.7: GC assay data of the WC-B-B2, the only oil in the development group.

Component	MW (g/mol)	Mass fraction
CO_2	44.01	0
H_2S	34.08	0
N_2	28.01	0
methane	16.04	0
ethane	30.07	0
propane	44.10	0
i-butane	58.12	0
n-butane	58.12	0
i-pentane	72.15	9.20×10^{-6}
n-pentane	72.15	2.91×10^{-6}
C_6	86	9.76×10^{-5}
C_7	100	7.07×10^{-4}
C_8	114	6.21×10^{-4}
C_9	121	1.41×10^{-3}
C_{10}	134	3.70×10^{-3}
C_{11}	147	6.27×10^{-3}
C_{12}	161	8.91×10^{-3}
C_{13}	175	1.24×10^{-2}
C_{14}	190	1.48×10^{-2}
C_{15}	206	1.71×10^{-2}
C_{16}	222	1.70×10^{-2}
C_{17}	237	1.87×10^{-2}
C_{18}	251	1.89×10^{-2}
C_{19}	263	1.86×10^{-2}
C_{20}	275	1.87×10^{-2}
C_{21}	291	1.96×10^{-2}
C_{22}	305	1.81×10^{-2}
C_{23}	318	1.66×10^{-2}
C_{24}	331	1.48×10^{-2}
C_{25}	345	1.55×10^{-2}
C_{26}	359	1.48×10^{-2}
C_{27}	374	1.43×10^{-2}
C_{28}	388	1.40×10^{-2}
C_{29}	402	1.44×10^{-2}
C_{30+}	909*	7.00×10^{-1}

*: adjusted to match measured MW of WC-B-B2

Table 7.8: Properties of the pseudo-components of WC-B-B2.

Pseudo-component	**Mass fraction**	**MW (g/mol)**	**SG**	**c_2**	**ρ_s^o (kg/m³)**	**c_3 (kPa^{-1})**
#1	0.102	189	0.885	0.248	978.1	2.38×10^{-7}
#2	0.094	276	0.928	0.290	1004.0	2.68×10^{-7}
#3	0.076	343	0.951	0.323	1020.3	2.76×10^{-7}
#4	0.075	424	0.974	0.361	1036.9	2.79×10^{-7}
#5	0.093	551	1.002	0.418	1058.1	2.80×10^{-7}
#6	0.088	697	1.026	0.479	1077.6	2.80×10^{-7}
#7	0.115	875	1.051	0.549	1096.9	2.80×10^{-7}
#8	0.119	1124	1.078	0.638	1118.3	2.80×10^{-7}
#9	0.066	1385	1.101	0.722	1136.2	2.80×10^{-7}
#10	0.049	1603	1.117	0.786	1148.8	2.80×10^{-7}
#11	0.036	1822	1.132	0.845	1159.9	2.80×10^{-7}
#12	0.039	2100	1.148	0.912	1172.3	2.80×10^{-7}
#13	0.048	2791	1.183	1.050	1198.4	2.80×10^{-7}

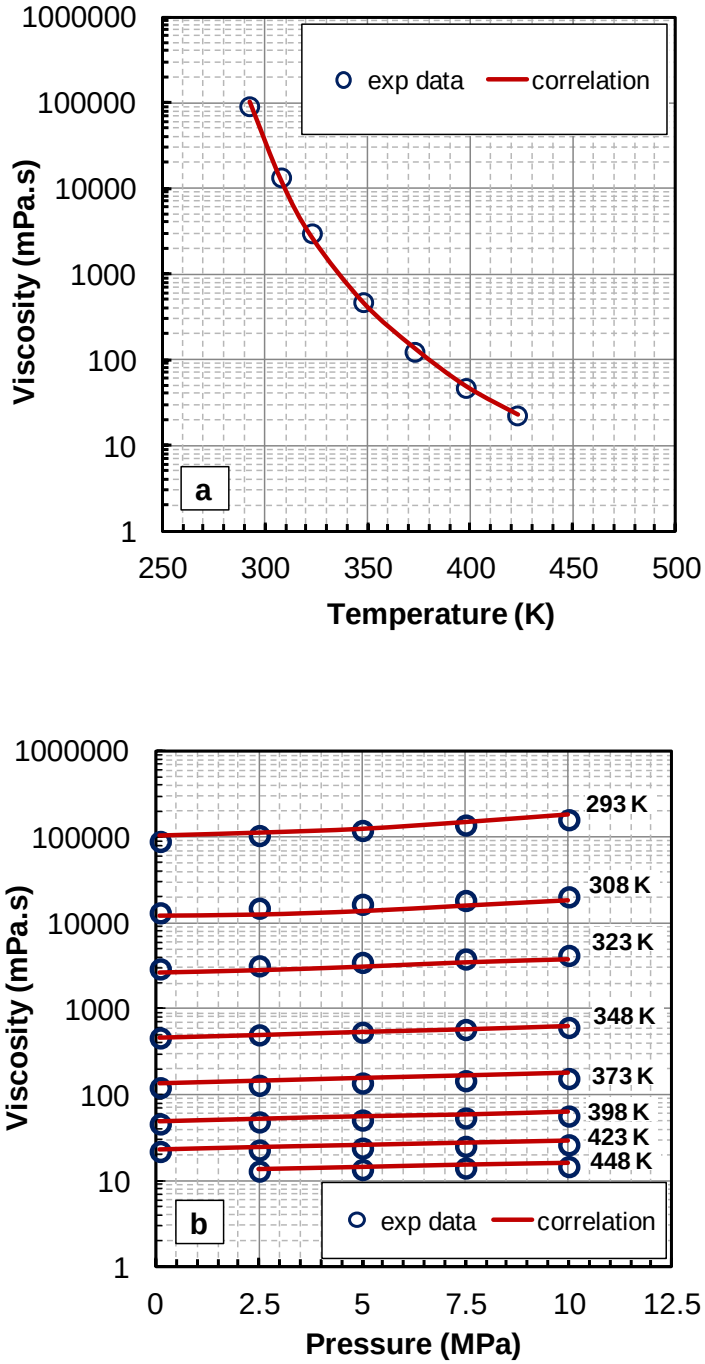

Figure 7.9: Measured and calculated viscosity of the characterized WC-B-B2 at: a) atmospheric pressure; and b) higher pressures. Dashed lines are predictions with the initial extrapolation of c_2 for the reference n-paraffins based on hypothetical viscosity data.

7.6.3.2 Test Group Predictions

The crude oils in this group (including WC-B-B1 and WC-B-B3) and the de-asphalted WC-B-B3 oil were characterized by extrapolation of their GC assays. The GC extrapolation was not required for WC-C-B1 as the C_{30+} residue is less than 1 percent of the oil. The specific gravities of the carbon number fractions of the dead and live oils were determined using Equation 7.8 and the calculated SG (Equation 7.9) was matched to the reported SG of the corresponding dead oil by adjustment of parameter C_f. For the live oils with no dead crude data (crudes ME3a, ME2 and ME1), the specific gravities were determined using the default value of 0.29 for the parameter C_f (Søreide 1989) in Equation 7.8. The specific gravity of the carbon number fractions of the WC-B-B3-DA was also calculated using C_f=0.3211 as determined from the specific gravity of WC-B-B3.

The viscosities of the crude oils were predicted using the measured density as the input at different pressure and temperature conditions. Table 7.9 reports the MARD and AARD of the viscosity predictions for all the oils of Table 7.1. Note, only a single data point was available for the AS1 dead oil; hence, no AARD was calculated. The predicted viscosities are well within a factor of 3 of the measured values; Figure 7.10. These predictive results based on the characterization of the oil by GC assay are remarkable considering no tuning of data was performed. One note of caution is that the model is only valid for Newtonian fluids. Heavy oils and bitumens at lower temperatures (typically below room temperature) or crude oils below their cloud point are non-Newtonian and the viscosity must be modeled differently. The EF model can still be used to calculate the viscosity of the continuous phase in these situations.

Table 7.9: Summary of the viscosity prediction errors for the test group of characterized oils using the measured density as input.

Oil Description		non-Tuned Model		Tuned Model		
		MARD (%)	AARD (%)	α_{c2}	MARD (%)	AARD (%)
WC-B-B1	dead	89	20	0.98	50	10
WC-B-B3	dead	24	8	1.013	23	8
WC-B-B3-DA	dead	28	12		20	13
WC-HO-S1	dead	18	11	1.011	32	8
WC-C-B1		20	13	0.881	7	2
WC-HO5	dead	73	55	1.113	45	20
EU1	dead	68	61	1.163	10	7
	live	48	47		17	12
ME3a	live	42	34	1.206	7	2
ME1	live	11	10	1.098	2	1
ME2	live	28	14	1.0197	32	11
EU2	dead	70	57	1.192	14	5
	live	71	71		19	16
	live	74	73		28	23
	live	72	61		22	18
AS1	dead	80		0.836	0	
	live	107	81		17	9

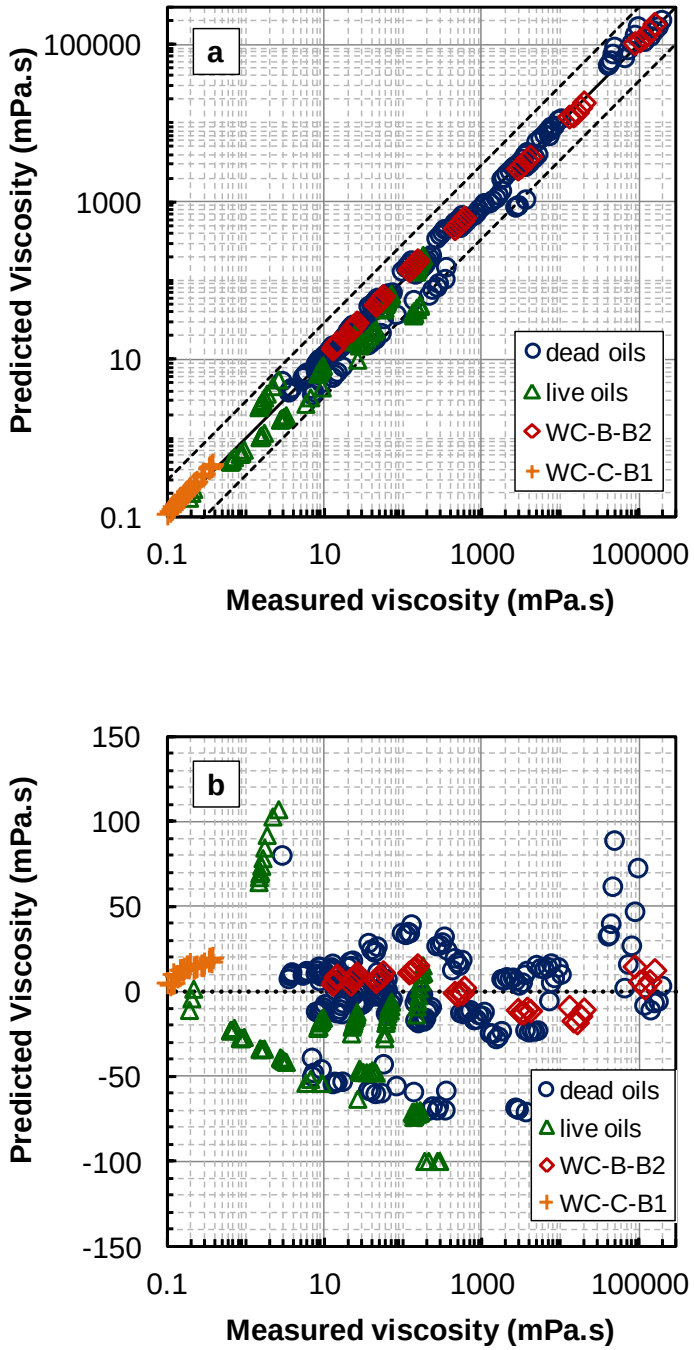

Figure 7.10: a) dispersion plot of predicted viscosity values of the oils in the development group and test group versus measured values. The dashed lines indicate a factor of 3 deviations from the measurements; b) relative deviations of the predicted viscosity values versus measured values.

7.6.3.3 Model Tuning

The model can be tuned to fit experimental data by adjusting the parameters ρ_s^o, $c_{2,}$ and c_3 for the pseudo-components. Up to three multipliers can be used (one for each parameter); however, a single multiplier applied to parameter c_2 was sufficient to fit the data for the test group oils with MARDs no greater than 50% and with AARDs less than 25%, Table 7.9. Recall that the departures of c_2 for pure heavy hydrocarbons were correlated to the specific gravity and molecular weight with less certainty than the other parameters and therefore the c_2 parameter is the most suitable candidate for adjustment when matching experimental values. The applied multiplier (α_{c2}) to the c_2 values of the pseudo-components ranged from 0.836 to 1.192. Note, when dead oil viscosities were available, the model was tuned only to the dead oil data, typically at a single pressure and temperature. The live oil viscosities predicted after dead oil tuning and were within 30% of the measurements. The results of the tuned model for the de-asphalted WC-B-B3 are also based on α_{c2} determined for the WC-B-B3. The viscosity prediction for the de-asphalted oil, the effect of an additional tuning parameter, the GC extrapolation method, and a conventional oil tuning example are discussed below.

7.6.3.3.1 Viscosity of the De-Asphalted Oil

WC-B-B3-DA is de-asphalted WC-B-B3 crude bitumen. The amount of asphaltenes removed after dilution with n-pentane was 21 wt% of the base bitumen. The GC assay of the base bitumen and the de-asphalted oil were both measured by Core Laboratories Canada Ltd. and are reported in Table 7.10. Note that the GC assay of the de-asphalted oil indicated the presence of 0.41 and 3.83 wt% n-pentane and toluene, respectively. Since the base bitumen does not have these constituents, they must gave been added to the de-asphalted oil during the preparation and measurement of the samples. The n-pentane content is the residual solvent after drying the de-asphalted oil. The toluene contamination most probably when the sample was placed in the capillary viscometer. A post-measurement investigation found that some off the cleaning toluene had been left in the apparatus before the experiment. The reported assay in Table 7.10 is the normalized assay after removing the contaminating solvents; however, the solvent contents were taken into account for the modeling.

Not surprisingly, the EF model predicted the viscosity of the WC-B-B3, as shown in Figure 7.11a and b, with accuracy comparable to the model fit to the viscosity of the WC-B-B2. The MARD and AARD of the predictions are 24% and 8%, respectively. Recall that these two crudes are different batches from the same reservoir but differ slightly in their specific gravity and considerably in their viscosity. The good agreement (MARD and AARD of 28% and 12%) between the predictions of the model for the de-asphalted WC-B-B3 and the measured values at atmospheric pressure and elevated pressures, Figure 7.11a and b, is excellent particularly given that it is based on a simple characterization of the WC-B-B3-DA from GC assay data. Note that the specific gravity of the pseudo-components of WC-B-B3-DA was calculated based on the C_f value of the base crude oil, WC-B-B3. As shown in Figure 7.11a and b, the predictions for the WC-B-B3-DA are slightly improved (MARD reduced to 20%) after tuning model to the data of the base crude oil WC-B-B3.

These predictive results (see also the results in equation of state applications) are valuable for the viscosity modeling of the solvent-aided recovery methods of the heavy oils and bitumen in which the phase splits and possible recovery of the de-asphalted oils are foreseen. Also, note that characterization approach can be still applied if the GC assay of the de-asphalted oil is not available as long as the phase compostions can be predicted. For example, a similar quality viscosity prediction was attained when the GC assay of the de-asphalted oil was constructed from the GC assay of the base crude oil. The only assumption was that all of separated asphaltenes were removed from the C30+ fraction of the base oil.

Table 7.10: GC assay of the WC-B-B3 and related de-asphalted oil, WC-B-B3-DA.

Component	MW (g/mol)	Mass fraction	
		WC-B-B3	WC-B-B3-DA
CO_2	44.01	0	0
H_2S	34.08	0	0
N_2	28.01	0	0
methane	16.04	0	0
ethane	30.07	0	0
propane	44.10	0	0
i-butane	58.12	0	0
n-butane	58.12	0	0
i-pentane	72.15	0	0
n-pentane	72.15	0	0
C_6	86	0	0
C_7	100	0	0
C_8	114	0	0
C_9	121	4.0×10^{-4}	1.04×10^{-4}
C_{10}	134	1.4×10^{-3}	2.09×10^{-4}
C_{11}	147	3.4×10^{-3}	1.36×10^{-3}
C_{12}	161	6.2×10^{-3}	3.34×10^{-3}
C_{13}	175	1.05×10^{-2}	7.41×10^{-3}
C_{14}	190	1.39×10^{-2}	1.23×10^{-2}
C_{15}	206	1.79×10^{-2}	1.82×10^{-2}
C_{16}	222	1.80×10^{-2}	2.05×10^{-2}
C_{17}	237	1.96×10^{-2}	2.35×10^{-2}
C_{18}	251	2.06×10^{-2}	2.40×10^{-2}
C_{19}	263	2.32×10^{-2}	2.52×10^{-2}
C_{20}	275	1.96×10^{-2}	2.47×10^{-2}
C_{21}	291	2.0×10^{-2}	2.53×10^{-2}
C_{22}	305	1.95×10^{-2}	2.34×10^{-2}
C_{23}	318	1.72×10^{-2}	2.26×10^{-2}
C_{24}	331	2.02×10^{-2}	2.13×10^{-2}
C_{25}	345	2.01×10^{-2}	2.05×10^{-2}
C_{26}	359	1.05×10^{-2}	2.03×10^{-2}
C_{27}	374	1.79×10^{-2}	2.01×10^{-2}
C_{28}	388	1.68×10^{-2}	2.01×10^{-2}
C_{29}	402	1.44×10^{-2}	2.05×10^{-2}
C_{30+}	a,b	6.89×10^{-1}	6.43×10^{-1}

a - MW of C_{30+} is determined as 909 g/mol to match MW of 520 g/mol for WC-B-B3.

b - MW of C_{30+} is determined as 712 g/mol for smooth transition of extrapolated GC for the WC-B-B3-DA.

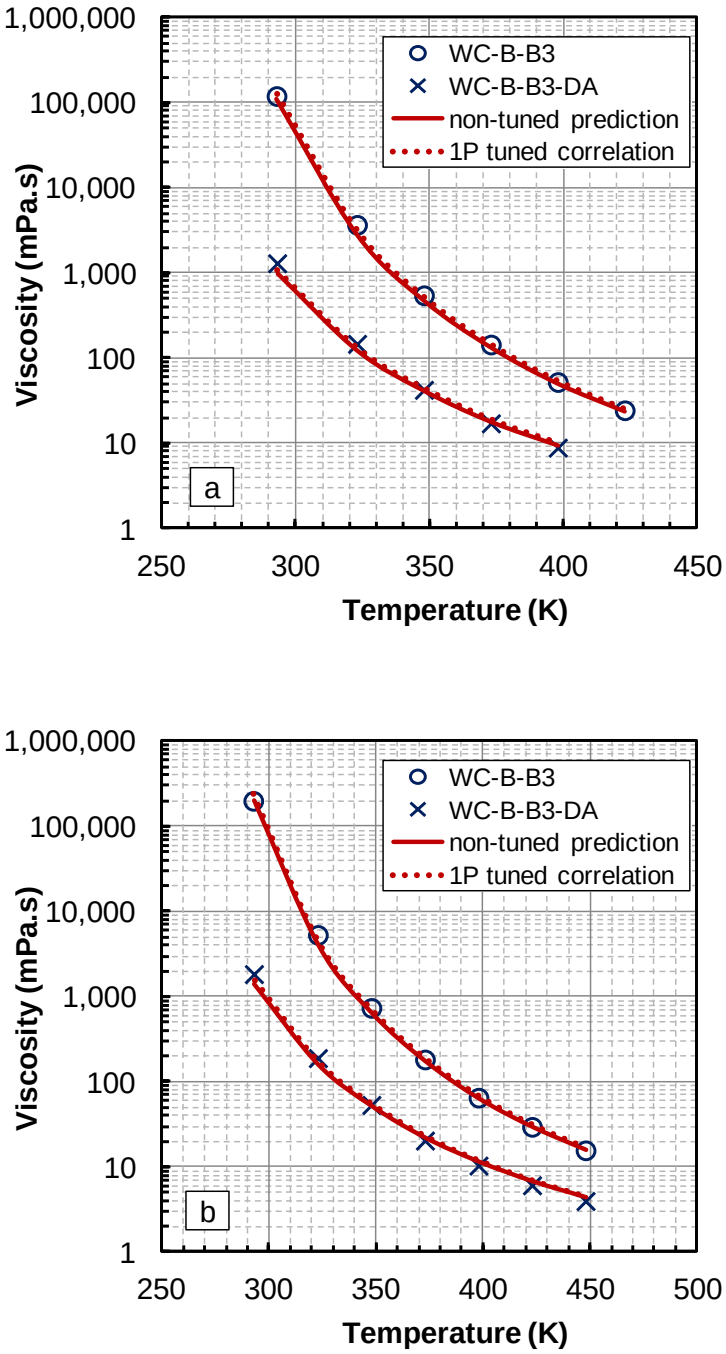

Figure 7.11: Measured and calculated viscosity of the characterized WC-B-B3 and its corresponding de-asphalted oil, WC-B-B3-DA at: a) atmospheric pressure, and b) the pressure of 10 MPa. The one-parameter (1P) tuning of the model was to match the WC-B-B3 data.

7.6.3.3.2 Two-Parameter versus One-Parameter Tuning

As an example, consider the viscosity of the WC-HO-S1, Figure 7.12a and b, which was predicted with an AARD and MARD of 11% and 18%, respectively. The model predicted the viscosity of the heavy oil at elevated pressures with the same accuracy of the atmospheric conditions. However, the model can be tuned for this oil by applying multiplier of α_{c2}=1.011 to the c_2 values of the pseudo-components, Figure 7.12a and b. The objective function was to reduce the absolute deviation of the modeled viscosity at atmospheric pressure. Although the tuned model predicted the viscosity with lower AARD of 8%, the MARD increased to 32% due to higher deviations of the tuned model at 25°C, Figure 7.13. A better approach is to fine-tune the model by applying multipliers to parameters ρ_s^o and c_2 of the pseudo-components simultaneously; that is, two-parameter tuning. Application of the multipliers as 1.005 and 1.076 to c_2 and ρ_s^o reduced the AARD and MARD to 6% and 11%, respectively. Of course, this option is only available if there are sufficient viscosity data to justify using two adjustable parameters.

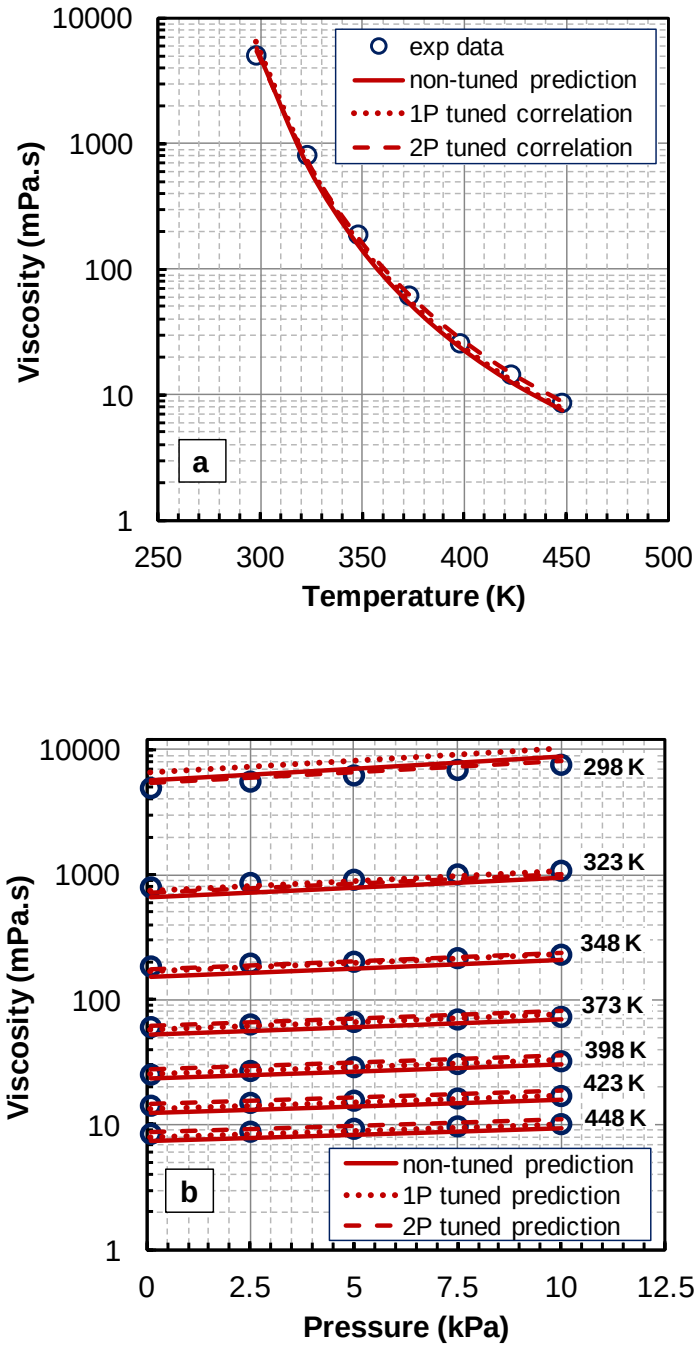

Figure 7.12: Improvement of the predictions of non-tuned model (solid line) by one-parameter tuning (dotted line) and two-parameter tuning (dashed line); comparison with experimental data of WC-B-HO1 in: a) atmospheric pressure; and b) high pressure conditions.

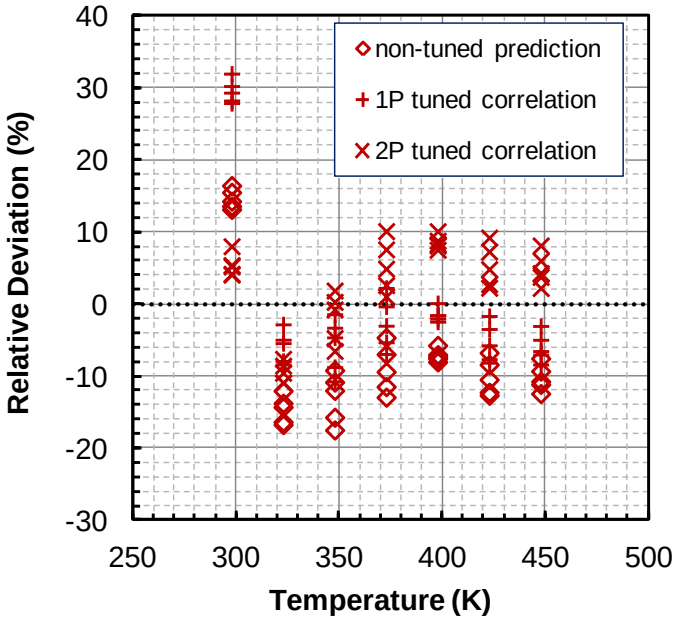

Figure 7.13: Relative deviation of the predicted viscosity of the WC-HO-S1 by non-tuned and one-parameter and two-parameter tuned EF model.

7.6.3.3.3 Effect of GC Assay Characterization

The performance of the model for heavy oil WC-HO5 is less satisfactory than for the WC-HO-S1; the predictions are considerably less than the measurements with AARD and MARD of 55% and 73%, respectively. The GC assay of this crude was extrapolated by adjusting the average molecular weight of C_{30+} to 809 g/mol to obtain a smooth molar distribution of molecular weights. The average molecular weight of the heavy oil from this extrapolation was 483 g/mol, considerably lower than the measured MW of crude as 570 g/mol using a freezing point depression method. Therefore, the heavy oil was re-characterized as follows to obtain an average molecular weight of 556 g/mol: 1) mass fraction of C_{30+} residue was assumed to be 10% higher than the reported value in GC assay (see Appendix F for "generated" GC assay); 2) the average molecular weight of C_{30+} was set equal to that of the WC-B-B2 heavy oil, 908 g/mol. The pseudo-components of the crude were re-defined including their EF model parameters. Then, the viscosity of the crude was predicted versus temperature and pressure, Figure 7.14a and b. The predictions based on the second characterization are considerably improved with an AARD and MARD of 15% and 55%, respectively, Figure 7.15.

The sensitivity of the viscosity predictions to the characterization of the oil is unavoidable because the characterization affects the molecular weight of pseudo-components which in turn determines the model parameters. The molecular weight of the plus fraction is one of the least reliable property values and is commonly used as one of the adjustable parameters in regression of the phase behavior of the reservoir fluids (Pedersen and Christensen 2007). Hence, it is not surprising that there are significant deviations in predicted viscosities that rely indirectly on C_{30+} molecular weights. One option for tuning is to adjust the C_{30+} molecular weight as above. However, the single parameter model tuning also compensates for the effects molecular weight errors. For instance, the viscosity of WC-HO5 with the original characterization was tuned to the atmospheric pressure data by applying a single multiplier of 1.113 to the c_2 parameter, Figure 7.14a. The tuned model is almost as accurate as the model with the modified characterization at all pressures, Figure 7.15, with an AARD and MARD of 20% and 45%, respectively. In general, single parameter tuning is recommended because it straightforward and easily made part of a consistent characterization methodology.

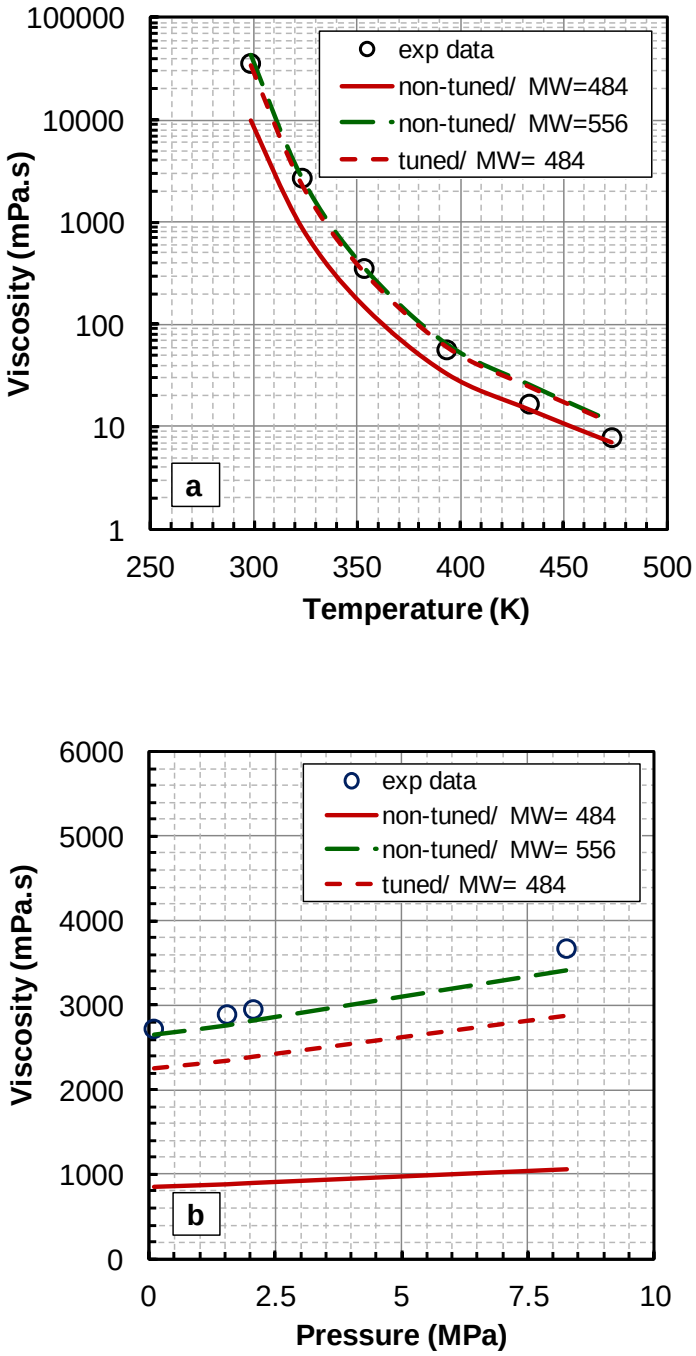

Figure 7.14: The effect of the average molecular weight of the characterized oil on viscosity predictions; comparison with experimental data of WC-HO5 in: a) atmospheric pressure; and b) high pressure conditions.

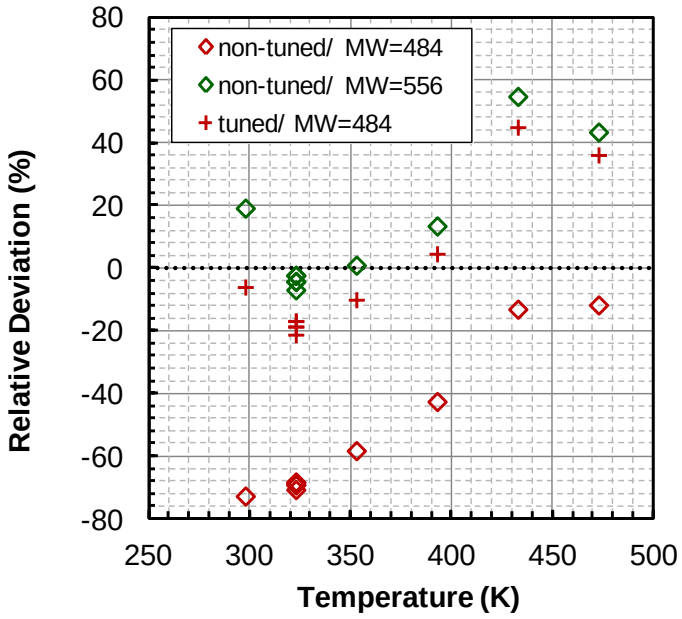

Figure 7.15: Relative deviation of the predicted viscosity of the WC-HO5 by non-tuned EF model for the characterizations based on the original and "generated" GC assay and one-parameter tuned model.

7.6.3.3.4 Conventional Oil Viscosity Modeling Example

So far all the examples presented in detail have been heavy oils. The final example is the EU1 conventional oil. The model under-predicted the viscosity of both dead and live EU1 crude oil, Figure 7.16a and b. The AARD and MARD are 61% and 68% for the dead oil and 47% and 48% for the live oil, Figure 7.17. The calculated viscosity values for the dead oil were improved by applying the single multiplier of 1.163 to the c_2 values of the pseudo-components, Figure 7.16a. Using the same value of the multiplier improved the predictions for the live oil considerably, Figure 7.16b. The AARD and MARD for the tuned model are 7% and 10% for the dead oil and 12% and 17% for the live oil, Figure 7.17. The model slightly over-predicts the live oil viscosity, possibly due to discrepancies in the GC assay data of the dead and live oils especially for the light ends. Note, the single parameter tuning is already within the accuracy of most viscosity measurements and two-parameter tuning based on three dead oil data points is difficult to justify.

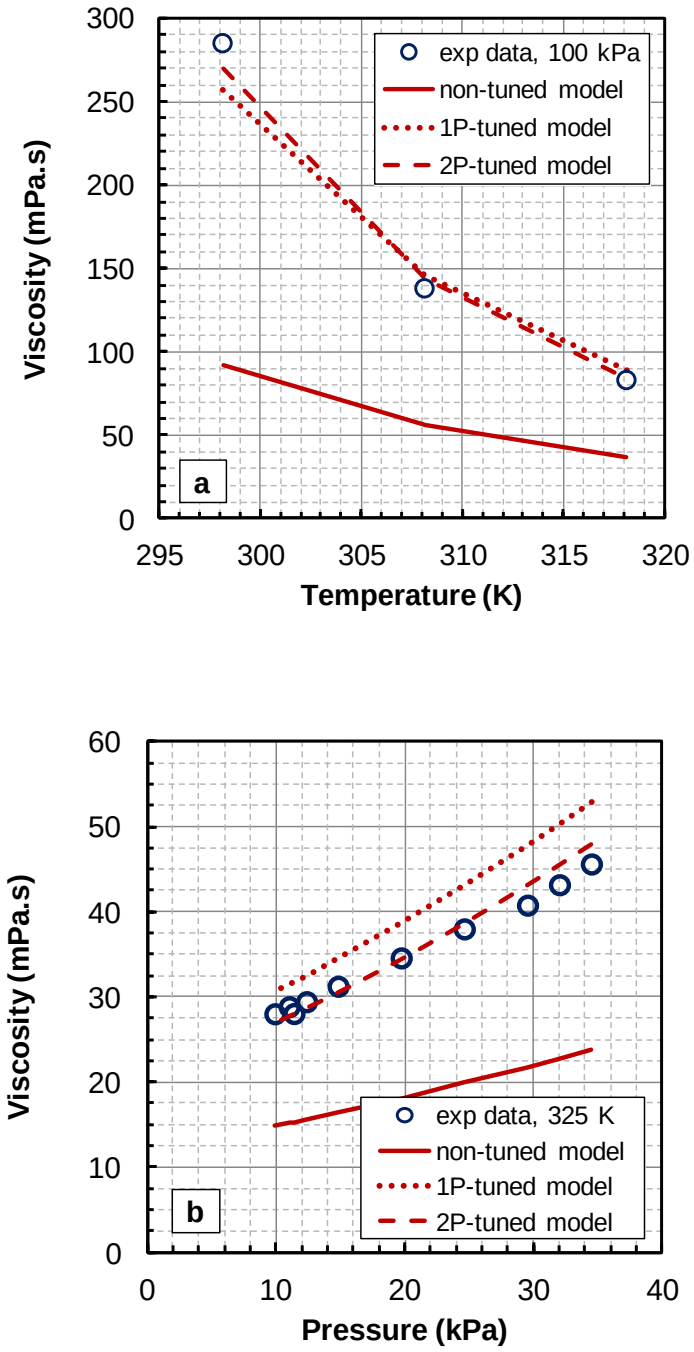

Figure 7.16: Improvement of the viscosity prediction with one-parameter tuning to dead EU1 oil data and two-parameter tuning to dead and live EU1 oil data; comparison with experimental data of: a) dead oil in atmospheric pressure; and b) live oil at 325 K.

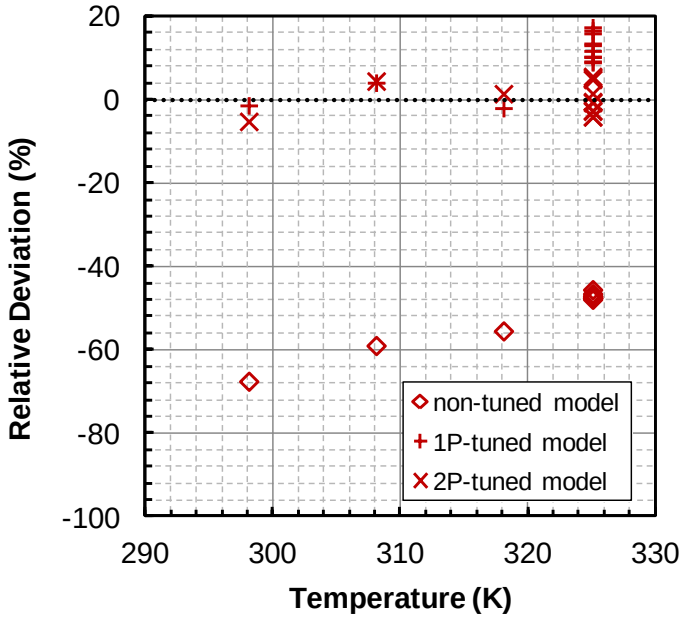

Figure 7.17: Relative deviation f the predicted viscosity by EF model for EU1 dead and live oil with non-tuned, one-parameter tuned to dead and two-parameter tuned to dead and live oil data.

However, two-parameter tuning of the model to collective viscosity data of the dead and live oil improved the model fit reducing the AARD and MARD to 4% and 5% for the dead oil and to 3% and 5% for the live oil, Figure 7.16a and b. In general, single parameter tuning is sufficient to fit the viscosity data to within typical experimental accuracy (±30%), but two-parameter fine tuning is advantageous when sufficient viscosity data are available.

7.6.3.4 Equation of State (EoS) Applications:

The EF model with the parameter estimation methods can also provide viscosity predictions for the characterized oils using the densities estimated with an equation of state. This application is demonstrated below using the original Peng-Robinson equation of state as implemented in the VMGSim process simulator. Note, temperature dependent volume translations were implemented externally to the VMGSim model to improve the density predictions, as described previously.

The required parameters for the EoS modeling of the characterized oils are the critical pressure, critical temperature, and acentric factor of the defined components and pseudo-components. The numerical values for the defined components were taken from the pure component database of VMGSim (VMG, 2011), which is partially based on the data from Yaws' handbook (1999) and the NIST database (NIST, 2008). The Lee-Kesler and Hall-Yarbrough correlations (Lee and Kesler, 1975; Kesler and Lee, 1976; Hall and Yarbrough, 1971) were used to estimate the properties of the pseudo-components. The inputs to these correlations are the normal boiling point and specific gravity. The normal boiling points for the pseudo-components were calculated using the correlation of Soreide (1989) with SG and MW as the inputs.

The densities predicted with the EoS model are in good agreement with the measured values with an AARD and MARD of 1.3% and 9.4%, respectively, Table 7.11. Note, the volume translation of the EoS model was not tuned to the measured density of the oils except for the input specific gravity. Higher deviations occurred for the characterized live oils lacking the dead oil SG data, including oils ME3a , ME1 and ME2 as shown in Figure 7.18a. The specific gravities of the pseudo-components of these oils were calculated using Equation 7.8 with the C_f parameter set equal to the default value of 0.29. The less satisfactory density predictions likely reflect the inaccuracy of using the default C_f value.

Note, the calculated compressibility of the oils at lower temperatures is slightly lower than the actual value due to the inherent limitation of cubic equations of state. Therefore, the high pressure densities are consistently lower than the measurements. The high pressure deviations were most significant for the dead extra heavy oils and bitumen. As shown in Figure 7.18b, the density of the WC-B-B2 heavy oil at lower temperatures was under-predicted because the oil compressibility was under-predicted.

The AARD and MARD of the viscosity predictions using the EoS densities as an input are 55% and 88%, respectively, Table 7.11. The predictions are less satisfactory in comparison to the predictions done using the measured density as the input (Table 7.9)

due to the errors in the predicted density. If the EoS is not tuned to the measured density of the oil, two-parameter tuning of the viscosity model is likely required by applying multipliers to the c_2 and ρ_s^o of the pseudo-components. The adjustment of ρ_s^o in addition to the c_2 adjustment is necessary mainly to compensate for the effect of the less accurate input density. Note that the tuning of the EF model for the extra heavy oils and bitumen required the application of single multiplier to the parameter c_3 for the pseudo-components, Table 7.11. The adjustment of c_3 compensates for the poor compressibility predictions from the EoS model. Note, parameter c_2 for WC-B-B2 was not adjusted because it was already used to guide the extrapolation of the reference system correlation. Also note that the tuning was done based on only the dead oil data and the viscosity of the corresponding live oils was predicted. The only exception is for crude oil AS1 whereas the model was tuned to the live oil data due to limited data for the dead oil. The AARD and MARD of the model after two-parameter tuning are 8.4% and 49%, respectively. Two-parameter tuning of the model to the dead and live oil viscosity data simultaneously is also an option as was discussed previously for the conventional oil example.

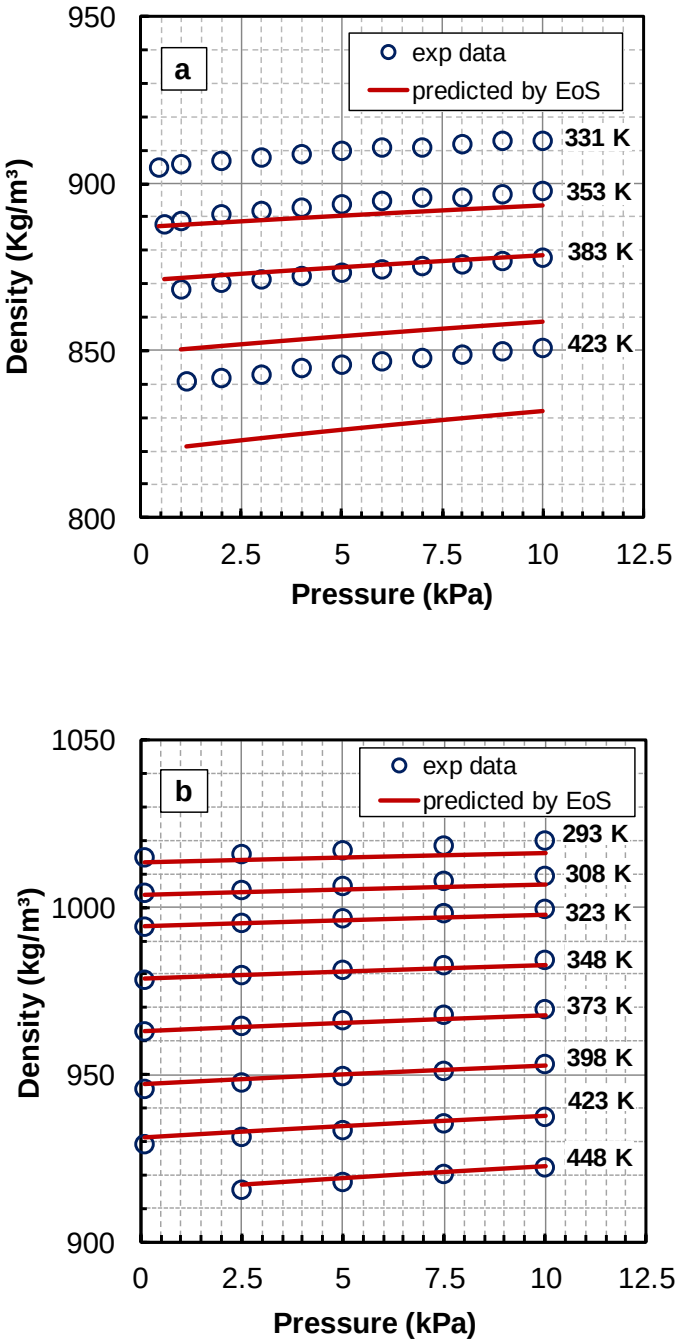

Figure 7.18: Less satisfactory density prediction by Peng-Robinson EoS for: a) live oil ME2 due to lack of dead oil SG data; and b) dead WC-B-B2 bitumen at lower temperature and high pressure conditions.

Table 7.11: Summary of the errors of the density predictions with PR equation of state and viscosity predictions with EF model using EoS-estimated density as input. The viscosity model was tuned to the dead oil data.

Oil Description		Density Prediction		Viscosity Prediction						
				Non-Tuned		Tuned Model				
		MARD (%)	AARD (%)	MARD (%)	AARD (%)	$\alpha\rho_s^o$	α_{c2}	α_{c3}	MARD (%)	AARD (%)
WC-B-B1	dead	0.44	0.19	41	21	0.995	0.916	0.17	30	8
WC-B-B2	dead	0.35	0.11	53	16	0.999		0.17	27	13
WC-B-B3	dead	0.38	0.19	60	21	0.999	1.013	0.17	14	6.6
WC-B-B3-DA	dead	0.19	0.06	35	12				33	21
WC-HO-S1	dead	0.39	0.18	38	20	1.002	1.051	0.29	13	6.0
WC-C-B1		1.90	1.16	30	21		0.823		15	4
WC-HO5	dead	1.24	0.29	79	61	0.997	1.086	0.33	7.0	3.3
EU1	dead	0.23	0.19	71	65	0.989	1.045		4.0	2.6
	live	0.29	0.19	55	52				2.7	1.4
ME3a	live	1.86	1.40	52	44	0.971	1.104		7.9	2.4
ME1	live	9.37	7.88	39	34	1.118	1.098		3.6	2.0
ME2	live	2.35	2.16	73	63	0.996	1.194		5.6	2.5
EU2	dead	1.41	0.95	82	68	0.998	1.262		12	5.2
	live	0.83	0.81	81	80				21	17
	live	1.84	1.17	83	82				33	21
	live	1.61	1.01	88	76				49	29
AS1	dead		0.50	58	58				13	13
	live	0.89	0.69	75	57	1.049	1.114	`	4.6	2.8

7.7 Summary

The Expanded Fluid viscosity model was extended to characterized crude oils. Correlations based on molecular weight and specific gravity were developed to calculate the fluid-specific parameters of the pseudo-components. The model parameters for the crude oil were calculated from the pseudo-component parameters using mass based mixing rules. The AARD and MARD of the viscosity predictions for over 150 pure hydrocarbons were 31% and 334%, respectively. The calculated viscosities of over 100 petroleum distillation cuts were within one order of magnitude of the measurements with AARD and MARD of 27% and 100%, respectively.

The proposed method was then tested on ten crude oils and one de-asphalted oil characterized based on GC C_{30+} assays. Both measured and EoS-estimated densities of the oils were used as the inputs to the EF model. The non-tuned predictions of the model with measured densities were within a factor of 3 of the measured values with AARD and MARD of 48% and 107%, respectively. The non-tuned predictions with the EoS densities were within a factor of 5 of the measurements.

A simple procedure was developed to tune the model to available viscosity data by applying up to three (one for each parameter) single multipliers to the fluid-specific parameters of the pseudo-components. The followings are the recommendations for the tuning of the model for the characterized oils:

I. Parameter c_2 is the first candidate for adjustment to match the experimental data due to higher uncertainties in its correlation. In general, tuning only the c_2 parameter was sufficient to predict viscosities (using measured densities as an input) to within 30%.

II. Tuning the c_2 parameter can compensate for the effect of inaccurate oil characterizations; for example, inaccurate molecular weights of the crude oils.

III. Fine tuning is possible when sufficient data are available to justify two-parameter tuning of the model; that is the simultaneous application of single multipliers to parameters c_2 and ρ_s^o of the pseudo-components.

IV. Two-parameter tuning is most likely required when EoS-estimated densities are used as the input to the EF model. Adjustment of ρ_s^o compensates the effect of the less accurate input densities on the predicted viscosity.

V. The adjustment of the parameter c_3 is essential if the EoS-estimated densities at higher pressures affect the viscosity predictions. This situation is unavoidable when cubic equations of state are used for extra heavy hydrocarbons at lower temperatures.

The Expanded Fluid viscosity model with the parameter correlations is a simple yet powerful tool for viscosity predictions for hydrocarbons and characterized oils with no experimental viscosity data. It was also shown that the model provides reliable and accurate viscosity predictions for the compositionally altered crude oils such as de-asphalted oils. When data are available, the model parameters can be tuned by applying up to three single-multipliers. The main shortcoming of the EF model is the need for accurate densities as an input. Therefore, if the EF model is to be used with a cubic equation of state, temperature dependent volume translation must be applied to the equation of state.

CHAPTER EIGHT: VISCOSITY OF DILUTED BITUMEN AND HEAVY OIL

The primary objective of this chapter is to evaluate the ability of the EF model to predict the viscosity of the diluted bitumen and heavy oil mixtures. Although the earlier volume fraction based mixing rules of the model were tested for limited number of diluted heavy and bitumen mixtures (Yarranton and Satyro, 2009; Satyro and Yarranton, 2010; Oldenburg et al., 2010), the performance of the newly developed mass fraction based mixing rules (Chapter 5) has not been studied for these systems. In addition, the Peng-Robinson Equation of state with the volume translations proposed in Chapter 7 has not been evaluated for the estimation of the density of diluted bitumen and heavy oil.

First, the EF correlation is evaluated against new viscosity data for bitumen diluted with single-component solvents (including n-paraffins from ethane to n-heptane and carbon dioxide). Binary interaction parameters are used to tune the model mixing rules to match the measured viscosity of the mixtures and are generalized as function of the specific gravity of the solvent. Then, the predictive capability of the correlation is evaluated for live bitumen and heavy oil and their mixtures with multi-component condensate solvent. Finally, the application of the EF viscosity correlation to diluted bitumen and heavy oils using densities estimated by the Peng-Robinson equation of state is demonstrated.

8.1 Datasets

The viscosity and density of diluted bitumen and heavy oil were measured as described in Chapter 3. Table 8.1 provides a summary of the 23 bitumen/heavy oil and solvent mixtures evaluated in this thesis as well as the pressure and temperature ranges of the measurements. The data include three main groups: 1) bitumen diluted with single-component solvents; 2) live bitumen and heavy oil; 3) diluted dead and live heavy oil and bitumen with condensate. The viscosity modeling of the fluids in each group will be discussed separately. The density and viscosity data of all the fluids in Table 8.1 are given in Appendix E.

Table 8.1: Summary of studied diluted bitumen and heavy oil mixtures and the pressure and temperature range of data. Summary of the data for the base dead bitumen and heavy oil are given in Table 7.1.

Test Fluid		Solvent Content (mass percent)	Temperature (K)	Pressure (MPa)
WC-B-B3	dead + Ethane	5.2	293.4-423.15	2.5-10
WC-B-B3	dead + propane	7.6	292-448.15	2.5-10
		16	293-423.15	2.5-10
WC-B-B2	dead + propane	11.3	288.4-423.15	0.8-10
		15.1	291.1-423.15	1.6-10
WC-B-B3	dead + n-butane	7.3	293.95-448.15	1.2-10
		14.5	293.3-448.15	2.5-10
WC-B-B3	dead + n-pentane	15	293.55-448.15	0.1-10
		30	293.3-423.15	0.1-10
WC-B-B2	dead + n-heptane	15	293.15-448.15	0.1-10
		30	292.05-398.15	0.1-10
WC-B-B3	dead + carbon dioxide	5.1	292.95-423.15	3.5-10
WC-HO-S1	live[a]		293.45-448.15	2.5-10
WC-B-B1	live[b]		291.8-448.15	2.5-10
WC-HO-S1	dead + WC-C-B1	3	298.15-448.15	0.1-10
		6	298.15-448.16	0.1-10
WC-B-B1	dead + WC-C-B1	3	298.15-448.15	0.1-10
		6	298.15-448.15	0.1-10
WC-B-B2	dead + WC-C-B1	30	293.65-448.15	0.1-10
WC-HO-S1	live[a] + WC-C-B1	3	293.55-448.15	2.5-10
		6	293.85-448.15	2.5-10
WC-B-B1	live[b] + WC-C-B1	3	292.35-448.15	2.5-10
WC-B-B2	live[c] + WC-C-B1	5.9	293.9-448.15	2.5-10

a, b, c – the solution gas content and composition is given in Table 3.7.

8.2 Fluid Characterization

Single-Component Fluids: The single-component solvents used in this thesis include ethane, propane, n-butane, n-pentane, n-heptane and carbon dioxide. Note, methane was not tested as a single component diluent but is a major component of the dissolved solution gas in the live oil samples. The hydrocarbon compounds were characterized for EF correlation by their fluid-specific parameters determined by Yarranton and Satyro (2009), Table 4.1. The fluid-specific parameters for carbon dioxide were determined in Chapter 5, Table 5.1.

The required parameters for the EoS modeling are the critical pressure, critical temperature, and acentric factor. These values for pure solvents were obtained from the pure component database of VMGSim (VMG, 2011). The volume translations for these fluids were defined following the given methodology in Section 7.4.2. The parameters γ_0 and γ_1 in Equation 7.13 are given in Table 7.2 for carbon dioxide and C_1 to n-C_5. The respective values for n-heptane are 2.5548×10^{-6} m^3/mol and 2.55×10^{-8} m^3/mol.K.

Multi-Component Fluids: The dead bitumens and heavy oil and the condensate solvent were characterized based on their GC assay data following the methodology outlined in Chapter 7. The bitumens and heavy oil are represented by 13 pseudo-components. The condensate solvent was characterized as a mixture of two defined components (n-butane and n-pentane) plus 6 pseudo-components.

The required properties for the density modeling by EoS including the critical properties and the acentric factor of the pseudo-components were estimated using the Lee-Kesler and Hall-Yarbrough correlations (Lee and Kesler, 1975; Kesler and Lee, 1976; Hall and Yarbrough, 1971). The volume translations for the pseudo-components were defined following the methodology given in Section 7.4.2. Note that the parameters γ_0 and γ_1 in Equation 7.13 were determined for the pseudo-components by matching densities at 288.75 K and 423.15 K, except for the pseudo-components of the condensate which were determined at 288.75 and 343.15 K. Figure 8.1a shows the measured and EoS-estimated densities of the bitumen, heavy oil and the condensate at 10 MPa. The MARD and

AARD of EoS-estimated densities are 1.9% and 0.4%, respectively. The highest deviations of the estimated densities were observed for the condensate solvent as the temperature range of the measurements was in the vicinity of its critical temperature.

The methodology in Chapter 7 was used to calculate the fluid-specific parameters of the EF correlation for the pseudo-components. Then, the model was fitted to the viscosity data of each dead oil and the condensate by applying three multipliers to tune the fluid-specific parameters of the pseudo-components; that is, three-parameter tuning. The parameters were tuned separately for the measured and EoS-estimated density inputs.

Since the relative composition of the pseudo-components of each oil and condensate does not change upon mixing with the solvents, the pseudo-components of each fluid were lumped into a single pseudo-component to represent the fluid for the EF correlation. The fluid-specific parameters of the EF correlation for the final representative single pseudo-component were then calculated using the mixing rules of the correlation (Equations 5.16 to 5.18 with β_{ij}=0), Table 8.2. Note that the performance of EF correlation for diluted bitumen/heavy oil will not be affected by the lumping of the pseudo-components due to the linearity of its mixing rules. Figure 8.1b shows the measured and fitted viscosities of the bitumen, heavy oil and the condensate at 10 Mpa. Table 8.2 shows that the viscosities were all fitted to within an MARD of 27% and an AARD of 10%.

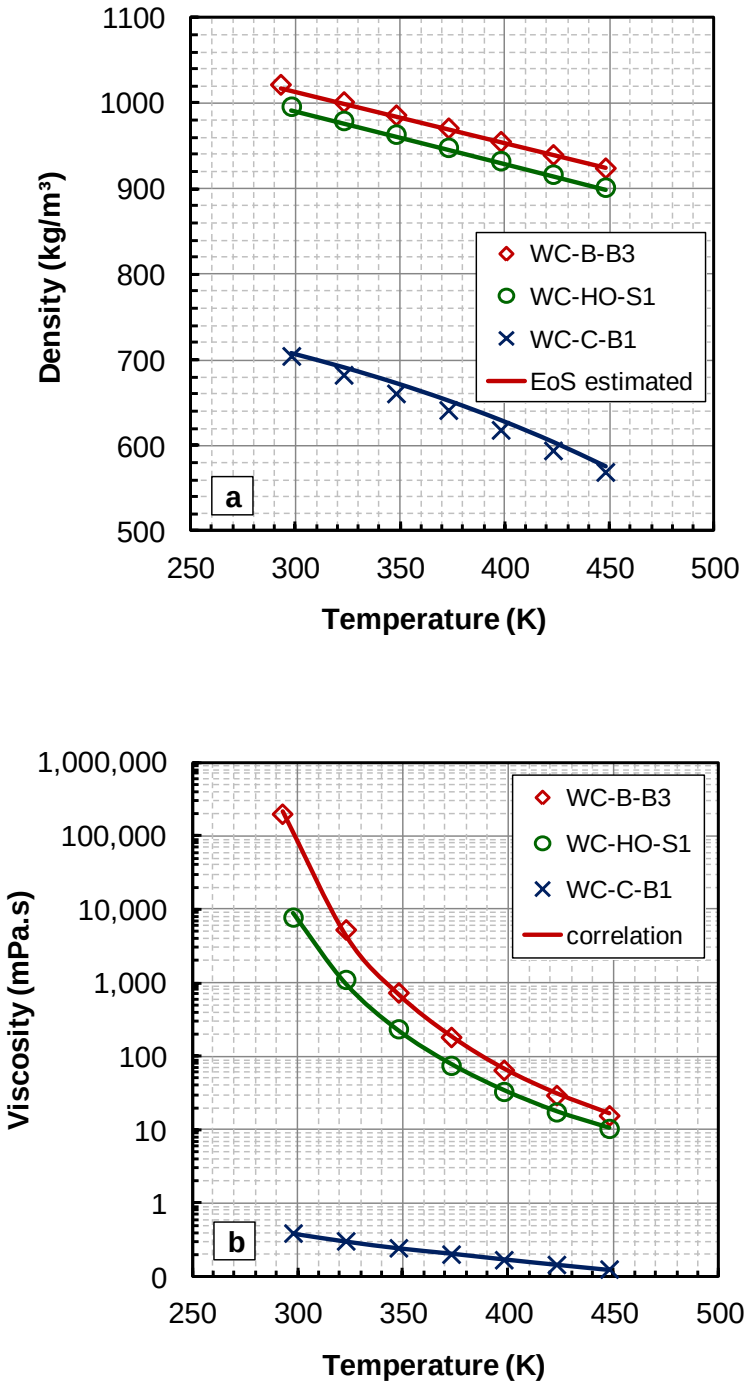

Figure 8.1: a) Measured and estimated by EoS densities of the bitumen, heavy oil and condensate solvent in pressure of 10 MPa; b) measured and fitted viscosities of the bitumen, heavy oil and condensate solvent in pressure of 10 MPa

Table 8.2: Summary of the fluid-specific parameters and deviation of the the EF model for the single pseudo-component representation of the base dead oils and the condensate solvent.

Fluid	with measured density					with EoS-estimated density				
	ρ_s° (kg/m³)	c_2	c_3	MARD (%)	AARD (%)	ρ_s°	c_2	c_3	MARD (%)	AARD (%)
WC-B-B1	1074.5	0.5016	3.1	27	10	1068.3	0.4711	1.4	17	8
WC-B-B2	1074.76	0.5148	2.8	19	9	1069.87	0.4853	1	14	4
WC-B-B3	1076.06	0.522	3.1	17	7	1071.45	0.4933	1	9	4
WC-HO-S1	1065.38	0.5198	2.8	11	6	1060.56	0.5024	1.2	10	4
WC-C-B1	879.13	0.2025	1.4	4	1	889.49	0.2034	1.4	9	4

8.3 Results and Discussion

The viscosity of the diluted heavy oil and bitumen mixtures listed in Table 8.1 were modeled using the EF correlation with both measured and EoS-estimated density as input. First, the predictions based on the measured density are discussed in detail to study the actual performance of the correlation. Then, the performance of the EF correlation in EoS applications is demonstrated.

8.3.1 Viscosity of Diluted Bitumen with Single Component Solvents

Figure 8.2a and Figure 8.3a show the measured and predicted viscosity of n-alkane diluted bitumens up to 30 wt% n-alkane at 10 MPa and 50 and 150°C, respectively. Figure 8.4a shows the measured and predicted viscosity of propane diluted bitumen from 20 to 175°C at 10 MPa. Figure 8.5a and b show similar data and predictions for CO_2 diluted bitumen. The predictions are in the same order of the magnitude of the measured values with overall AARD and MARD deviation of 19% and 63%, respectively, Table 8.3. These predictive results are remarkable considering the extreme reduction (up to 4 orders of magnitude) of the bitumen viscosity upon dilution with the solvents.

However, the EF correlation tends to under-predict the viscosities for the n-alkanes diluted bitumen. The magnitude of the under-predictions is greatest at lower temperatures, increases with the solvent content in the mixture, and depends on the type of the solvent. For instance, the under-predictions are substantial for the propane diluted bitumen but are negligible for bitumen diluted with higher n-alkanes or carbon dioxide. Figure 8.6 shows how the deviations tend to increase at the higher viscosities associated with lower temperatures.

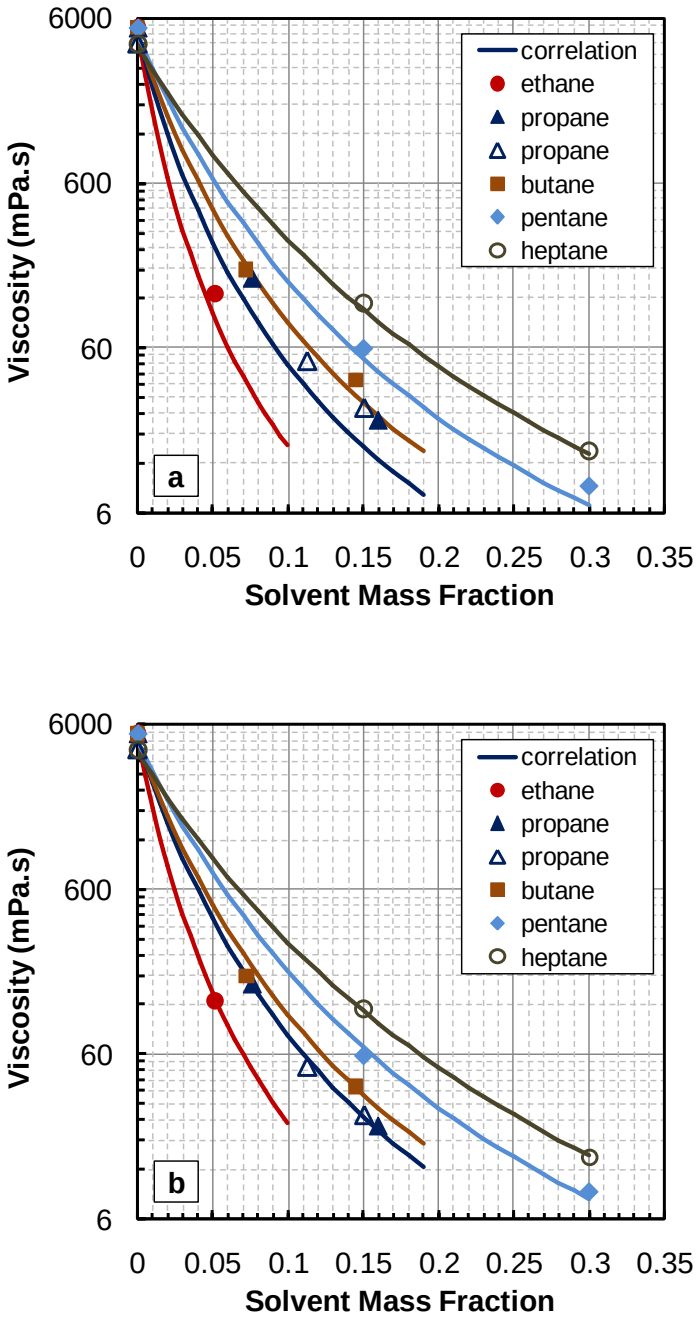

Figure 8.2: Measured and predicted viscosity of WC-B-B2 (open symbols) and WC-B-B3 bitumen (closed symbols) bitumen diluted with n-paraffin solvents and carbon dioxide at 323.15 K and 10 MPa: a) predicted viscosity; b) fitted viscosity.

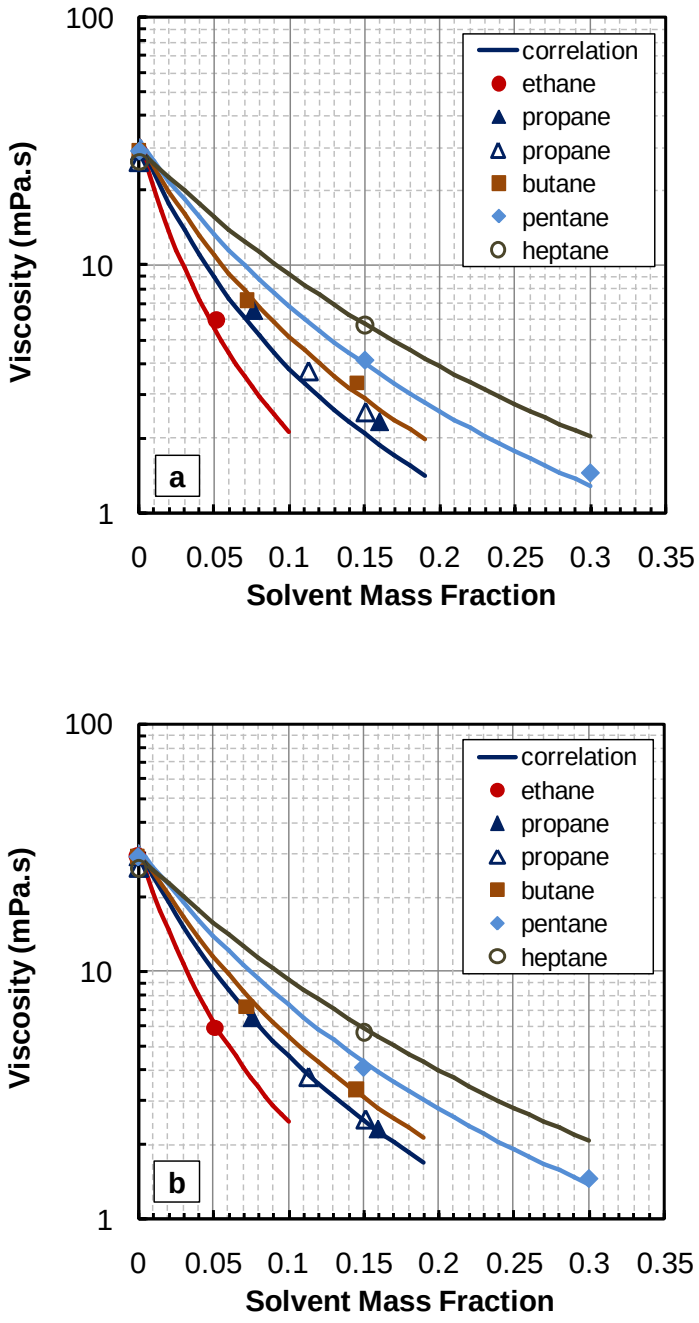

Figure 8.3: Measured and predicted viscosity of WC-B-B2 (open symbols) and WC-B-B3 bitumen (closed symbols) diluted with n-paraffin solvents and carbon dioxide at 423.15 K and 10 MPa: a) predicted viscosity; b) fitted viscosity.

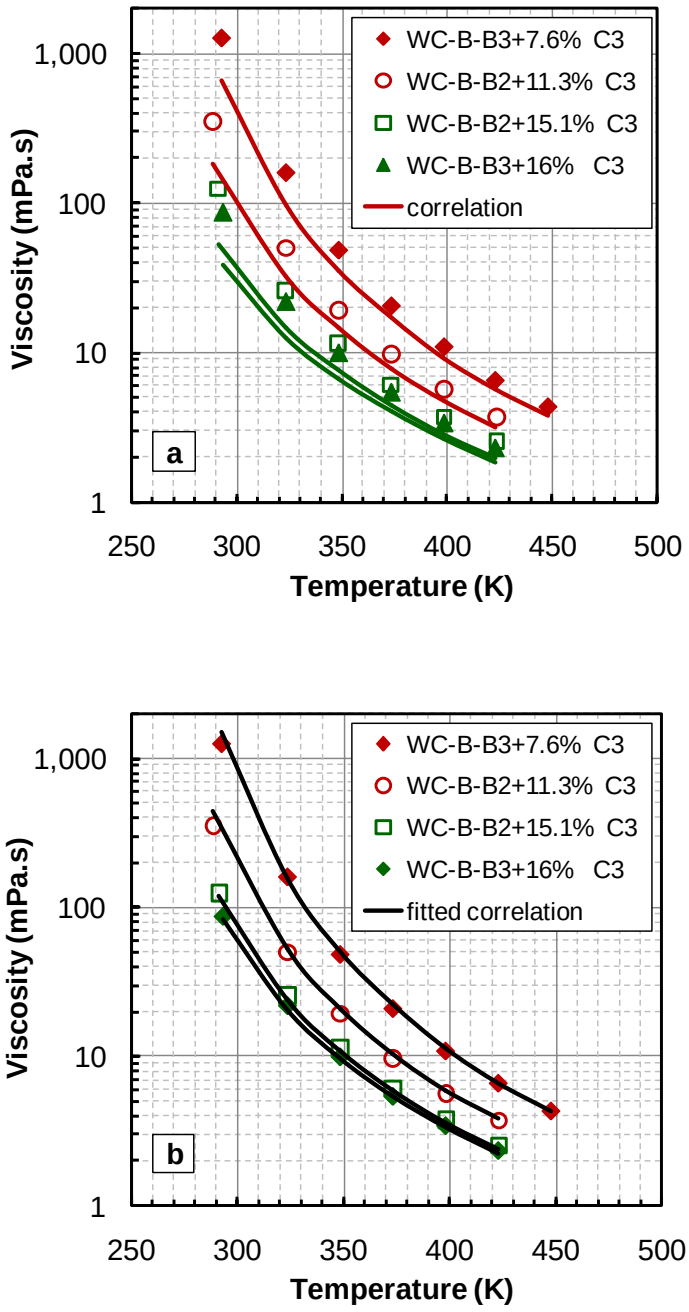

Figure 8.4: Measured, predicted (β_{ij}=0) and fitted ($\beta_{sol\text{-}oil}$=−0.046) by EF correlation viscosity of diluted mixtures of WC-B-B2 (open symbols) and WC-B-B3 bitumen (closed symbols) with propane at pressure of 10 MPa.

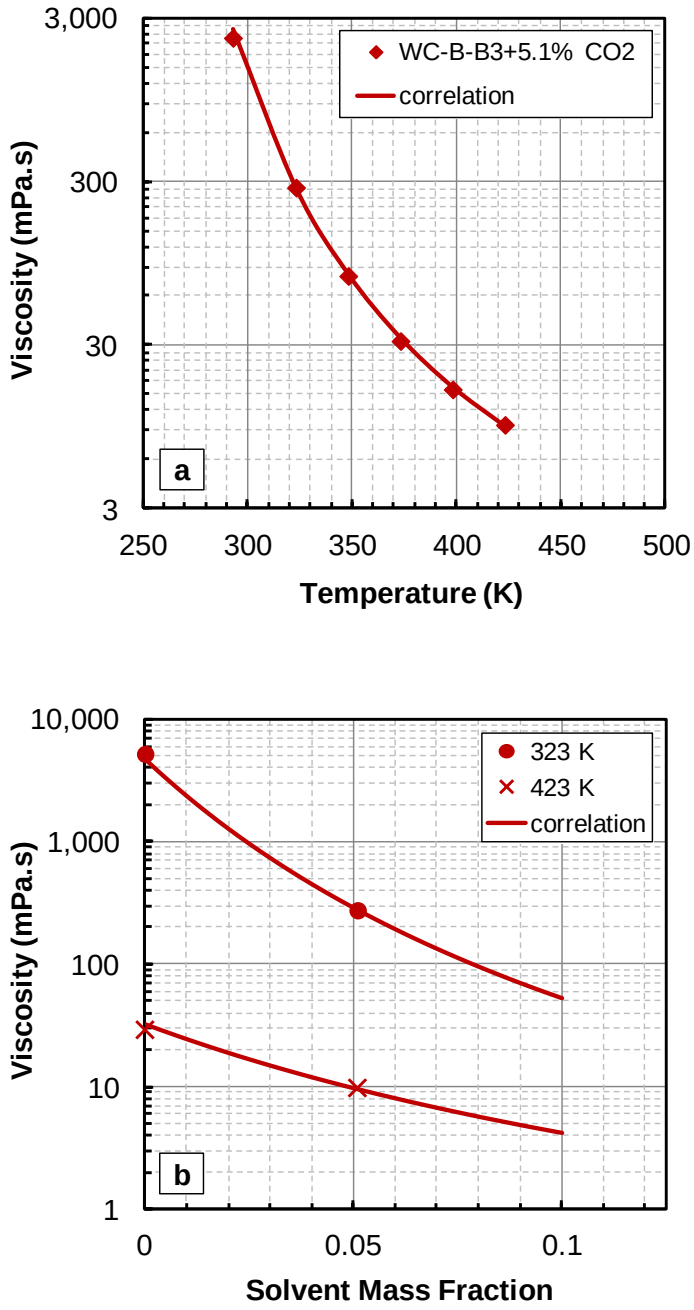

Figure 8.5: Measured and predicted (β_{ij}=0) by EF correlation viscosity of diluted mixtures of WC-B-B3 bitumen with carbon dioxide at 10 MPa: a) versus temperature; b) solvent mass fraction.

Table 8.3: Summary of the deviations of the predictions of EF model for diluted bitumens with single-component solvents. EF model is tuned by adjustment of $\beta_{sol\text{-}oil}$ to fit the all experimental data of the diluted oils with each solvent.

Diluted Bitumen Description		Predicted		Tuned		
		MARD (%)	AARD (%)	$\beta_{sol\text{-}oil}$	MARD (%)	AARD (%)
WC-B-B3	dead + 5.2 wt% C_2	46	25	-0.052	9	3
WC-B-B3	dead + 7.6 wt% C_3	52	30	-0.046	18	4
WC-B-B3	dead + 16 wt% C_3	59	38	-0.046	18	8
WC-B-B2	dead + 11.3 wt% C_3	55	33	-0.046	24	4
WC-B-B2	dead + 15.1 wt% C_3	63	40	-0.046	22	11
WC-B-B3	dead + 7.3 wt% C_4	14	4	-0.016	26	10
WC-B-B3	dead + 14.5 wt% C_4	34	15	-0.016	11	3
WC-B-B3	dead + 15 wt% C_5	23	9	-0.0154	25	8
WC-B-B3	dead + 30 wt% C_5	38	22	0.0154	20	9
WC-B-B2	dead + 15 wt% C_7	14	4	-0.0037	8	3
WC-B-B2	dead + 30 wt% C_7	19	6	-0.0037	12	3
WC-B-B3	dead + 5.1 wt% CO_2	14	4			

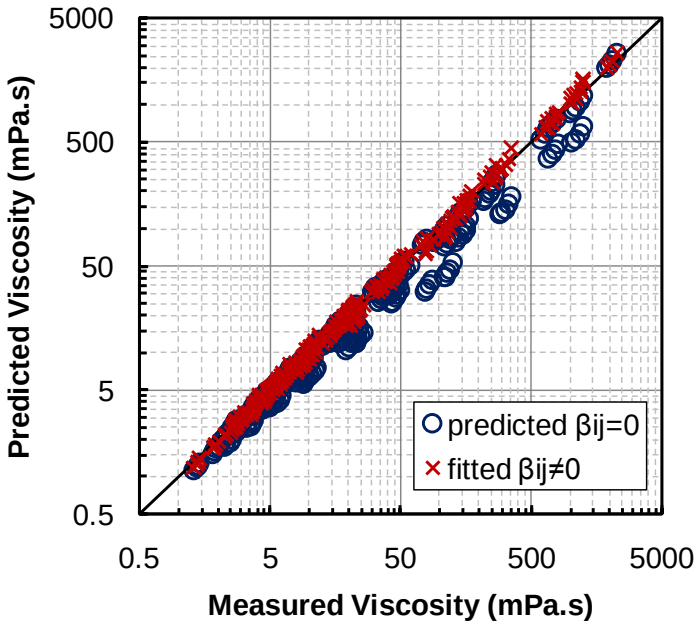

Figure 8.6: Dispersion plot of predicted (βij=0) and fitted ($\beta_{sol\text{-}oil}$≠0) viscosity values of the diluted bitumen with n-paraffin solvents and carbon dioxide versus measured values.

The trend of higher under-predictions at lower temperatures suggests that the calculated compressed state density of the diluted bitumen is the source of the deviations. In other words, the required value of the compressed state density of the mixture to correctly model the mixture viscosity is smaller than the calculated value by the mixing rule of Equation 5.16 with β_{ij}=0. Although the source of this non-ideality in mixing the compressed state density of the bitumen-solvent pair is not known, it can be compensated for in the model by using non-zero values of the binary interaction parameters (β_{ij}) for the solvent-oil binary pairs.

To minimize the number of complications introduced into the viscosity model, the β_{ij} values were assumed to be independent of temperature, pressure, and composition for each pseudo-binary pair of the solvent-bitumen. The optimum values of β_{ij} for each pseudo-binary pair were determined by fitting the EF correlation to the experimental viscosity data of diluted bitumen mixtures, Figures 8.2b, 8.3b and 8.4b. The overall MARD and AARD of the predictions of the fitted correlation are reduced to 36% and 6%, respectively, Table 8.3 and Figure 8.6.

The absolute magnitude of the adjusted values of $\beta_{sol\text{-}oil}$ approaches zero as the molecular weight of the solvent increases to 100 g/mol, Figure 8.7a. The only exception is carbon dioxide with the approximately same molecular weight as propane but $\beta_{sol\text{-}oil}$ =0. This observation suggests that the apparent non-ideal viscosity behavior of pseudo-binaries of solvent-bitumen is not only due to the difference in molecular weights but also other factors such as chemical family of the solvent.

Another approach is to relate the interaction parameters to the density difference between the components. Saryazdi (2012) correlated the interaction parameters used in excess volume of mixing determinations to the normalized difference in the liquid density of the pseudo-binaries of solvent and oil, defined as:

$$\Delta SG_{norm} = \frac{2\left|SG_{oil} - SG_{sol}\right|}{\left(SG_{oil} + SG_{sol}\right)} \tag{8.1}$$

where SG_{sol} is the calculated specific gravity of the solvent. Since viscosity is related to density, a similar approach may hold for the viscosity interaction parameters. The binary interaction parameters were plotted versus the normalized density differences, Figure 8.7b, and the following correlation proposed for the $\beta_{sol\text{-}oil}$:

$$\text{for } \Delta SG_{norm} <= 0.355: \quad \beta_{sol\text{-}oil} = 0 \tag{8.2}$$

$$\text{for } \Delta SG_{norm} > 0.355: \quad \beta_{sol\text{-}oil} = 0.055\text{-}0.155\ \Delta SG_{norm} \tag{8.3}$$

Note that the interaction parameter for CO_2 now falls on trend with the n-alkanes.

Figure 8.8 shows the dispersion of the relative deviations versus the n-paraffin solvent content of the mixtures using the binary interaction parameters calculated with Equation 8.2. The MARD and AARD of the viscosity predictions for the n-paraffin diluted bitumen were 44% and 9%, respectively. The predictions are generally within 30% of the measured values regardless of the solvent content. The maximum deviations occurred for bitumen with 7.3 wt% n-butane at room temperature and are probably due to the errors in the measurements or composition.

Note that the binary interaction parameters (β_{ij}) are also applicable to diluted bitumens characterized as mixtures of multiple pseudo-components. Since the relationship between β_{ij} and the pseudo-component properties is unknown, it is recommended to use fixed values of β_{ij} for all binary pairs of each solvent and all pseudo-components of the oil. The value of β_{ij} for all binary pairs is set equal to the $\beta_{sol\text{-}oil}$ determined for the pseudo-binary of solvent-bitumen/heavy oil. The calculated viscosity will be the same in both cases due to the linearity of the mixing rules.

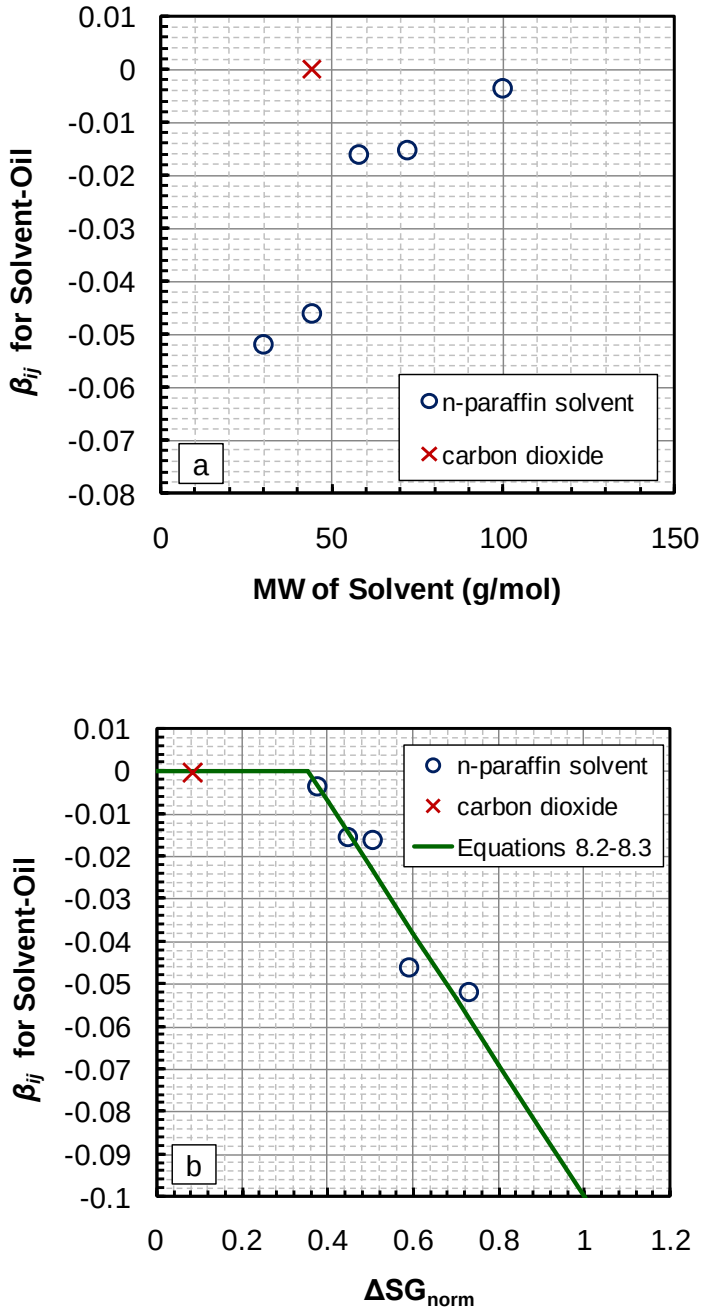

Figure 8.7: a) The binary interaction parameters of solvent-oil versus the molecular weight of the solvent; b) The binary interaction parameters of solvent-oil versus the normalized difference in the liquid density of solvent and oil.

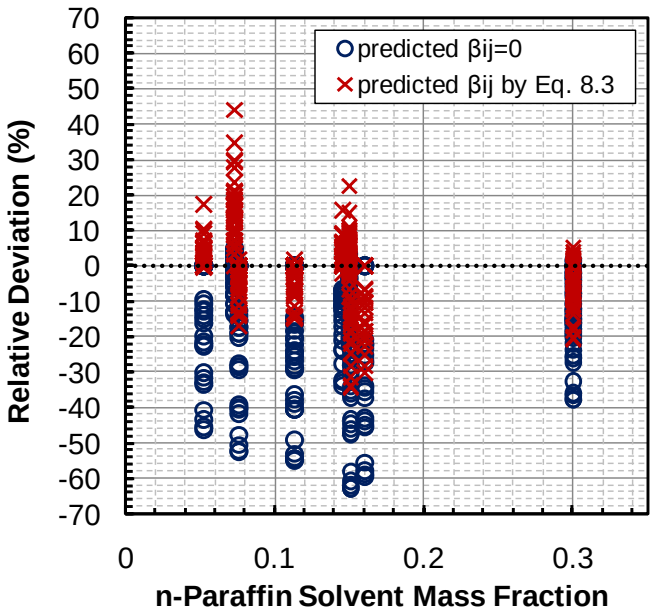

Figure 8.8: The relative deviations of the predicted viscosity with $\beta_{sol\text{-}oil}$ =0 and $\beta_{sol\text{-}oil}$ from Equation 8.3 versus n-paraffin solvent content for diluted mixtures of WC-B-B2 and WC-B-B3.

8.3.2 Viscosity of Live Heavy Oil and Bitumen

The live WC-HO-S1 and WC-B-B1 are treated multi-component mixtures consisting of the single pseudo-component dead oil and the individual components of the dissolved gas. The composition and mass fraction of the dissolved gases in the live oils are given in Table 3.1. Methane and carbon dioxide are the two main components of the dissolved gas in live WC-B-B2, but other light n-paraffins up to pentane are also dissolved in live WC-HO-S1. The addition of 2 mass percent solution gas reduced the viscosity of the dead WC-B-B1 up to one order of magnitude at room temperature, Figure 8.9a. The viscosity reduction is less pronounced for dead WC-HO-S1, Figure 8.9b.

The viscosities of the live oils were initially predicted by EF correlation with all β_{ij}=0 using the fluid-specific parameter of EF correlation for the base dead oil (Table 8.2) and the dissolved gas components (Table 3.1). The MARD and AARD of the predictions are 21% and 10% for live WC-B-B1 and 13% and 3% for live WC-HO-S1, respectively. The

predictions are slightly negatively biased, Figure 8.10a and b, as was expected from the observations presented in Section 8.3.1.

Therefore, the viscosities were predicted with non-zero β_{ij} values for the binary pairs of the dissolved gas components and the dead oil. The $\beta_{sol\text{-}oil}$ values for each n-paraffin component of the dissolved gas were determined from Equation 8.2. The predictions with non-zero $\beta_{sol\text{-}oil}$ have less negative biases, Figure 8.10a and b with AARDs of 7% and 5% for live WC-B-B1 and live WC-HO-S1, respectively. The overall deviations are within the deviations of the fitted correlation to the corresponding dead oils and generally within the uncertainties in the measurements of the amount and composition of the dissolved gases.

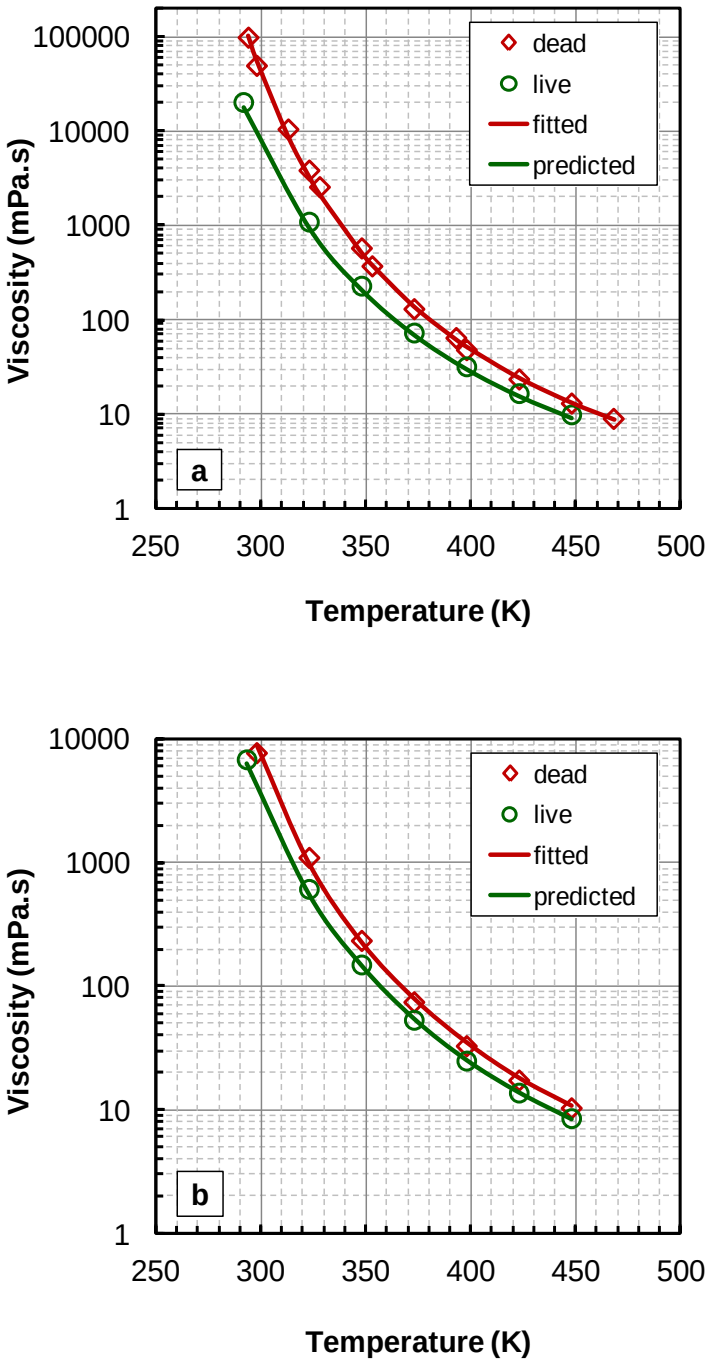

Figure 8.9: Measured and predicted (β_{ij}=0) viscosity values of the live oils versus temperature at 10 MPa: a) WC-B-B1; b) WC-HO-S1. The viscosities of the dead oils were fitted by EF correlation.

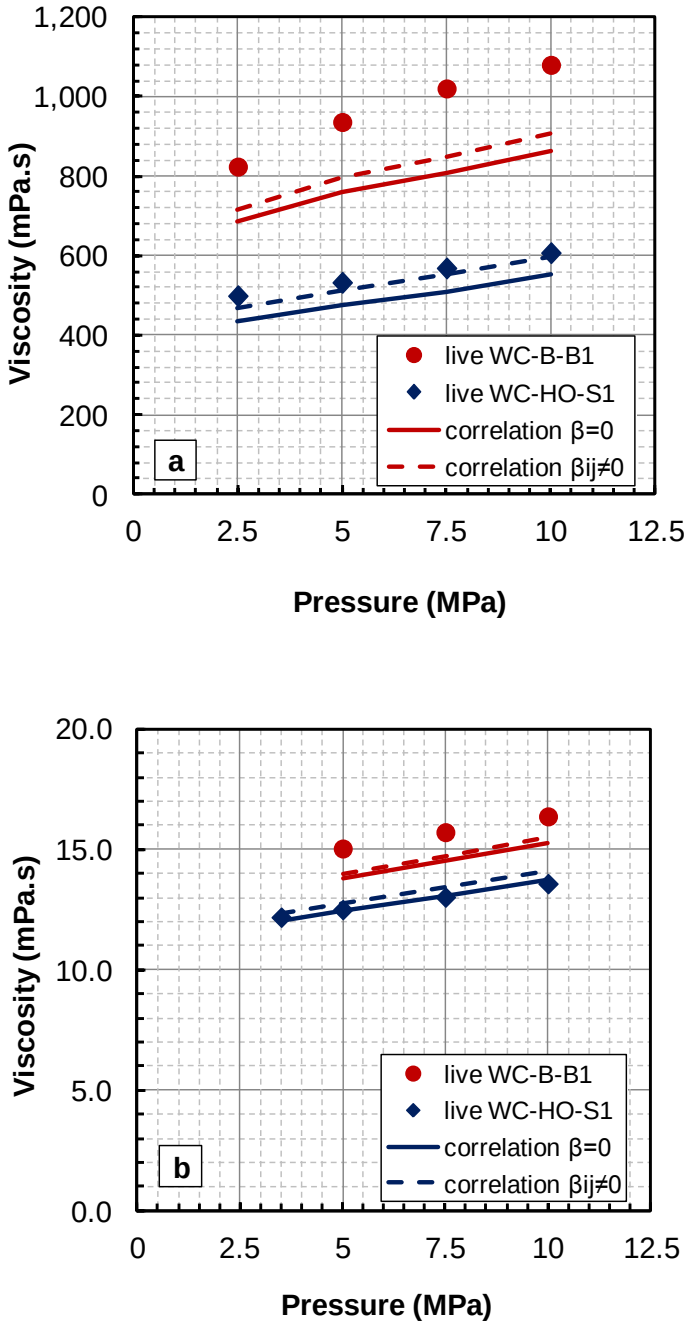

Figure 8.10: Measured and predicted viscosity of live WC-B-B1 and WC-HO-S1 at: a) 323.15 K; b) 423 K. The solid and dashed lines represent the predictions with all β_{ij}=0 and β_{ij} calculated by Equation 8.2 for binaries of solvent components and base dead oils.

8.3.3 Viscosity of Diluted Heavy Oil and Bitumen with Condensate

The final test of the EF correlation is the prediction of the viscosity of diluted dead and live bitumen and heavy oil with condensate (a multi-component solvent). Similar to the base dead oils, the condensate is included in the model as single pseudo-component with fluid-specific parameters given in Table 8.2. Note, both WC-B-B1 and WC-B-B2 were used in the measurements due to limited sample quantities. Also, the live WC-B-B2 had higher dissolved gas content than live WC-B-B1, Table 3.7. Finally, there was an error in the density for the 3% diluted live WC-B-B1 at room temperature and 5.9% diluted live WC-B-B2 and therefore these data were not included in the error analysis.

The predicted viscosities for diluted dead and live WC-HO-S1 are generally in better agreement with the measurements than the predictions for dead and live WC-B-B1; Figure 8.11 and Figure 8.12, respectively. Not included in Figure 8.12, the viscosity predictions for the 30% diluted dead WC-B-B2 at 50°C deviated as much as -21% from the data. This deviation was reduced to -18% using the $\beta_{cond\text{-}oil}$= -0.002 calculated from Equation 8.2. Table 8.4 gives a summary of the maximum absolute relative deviation (MARD) and average absolute relative deviation (AARD) of the predicted viscosities with two sets of binary interaction parameter values. Using the non-zero β_{ij} reduces the overall AARD from 8% to 7%. Directly fitting the 30% diluted WC-B-B2 data ($\beta_{cond\text{-}oil}$= -0.013) improves the overall AARD of the predicted viscosity of condensate diluted dead and live bitumen and heavy oil to 5% (dotted line on Figures 8.11 and 8.12). In summary, the predictions of the EF correlation for the condensate diluted mixtures are within the same order of magnitude of the measurements even when $\beta_{cond\text{-}oil}$=0.

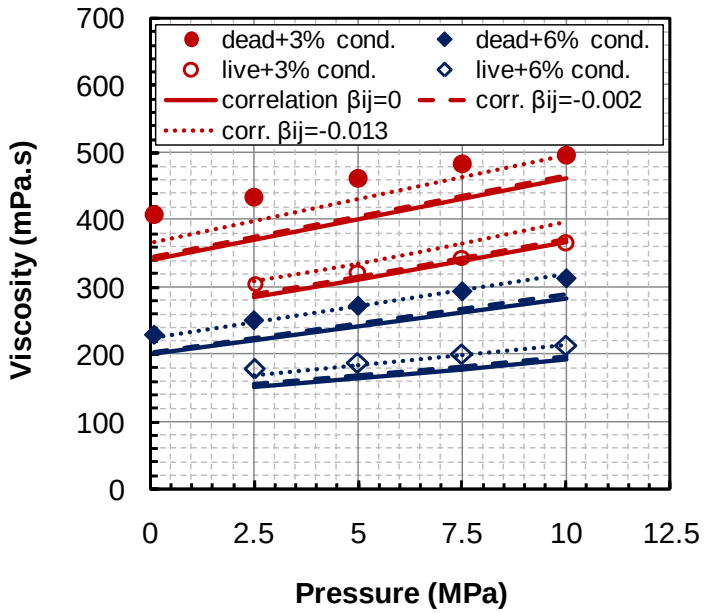

Figure 8.11: Measured and predicted viscosity of diluted mixtures of dead and live WC-HO-S1 with the condensate at 323.15 K. The dashed and dotted lines represents the predictions with $\beta_{cond\text{-}oil}$=-0.005 by Equation 8.1 and with $\beta_{cond\text{-}oil}$=-0.013 by fitting the data of WC-B-B2+30% condensate, respectively.

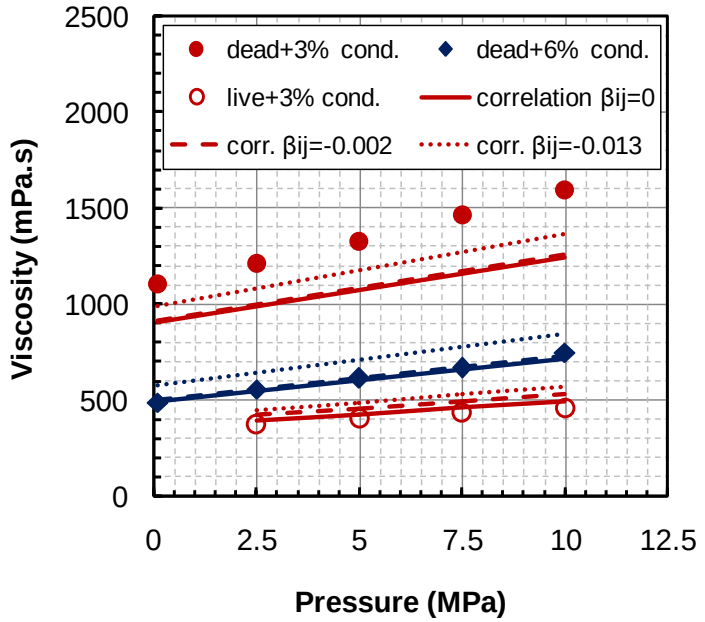

Figure 8.12: Measured and predicted viscosity of diluted mixtures of dead and live WC-B-B1 with the condensate at 323.15 K. The dashed and dotted lines represents the predictions with $\beta_{cond\text{-}oil}$=-0.005 by Equation 8.1 and with $\beta_{cond\text{-}oil}$=-0.013 by fitting the data of WC-B-B2+30% condensate, respectively.

Table 8.4: Summary of the deviations of the predictions of EF model for diluted dead and live heavy oil and bitumen with condensate solvent.

Diluted Bitumen Description	β_{ij}=0		β_{ij} by Eq. 8.2-8.3	
	MARD (%)	AARD (%)	MARD (%)	AARD (%)
WC-HO-S1 dead + 3 wt% WC-C-B1	18	8	17	7
WC-HO-S1 dead + 6 wt% WC-C-B1	14	7	13	6
WC-B-B1 dead + 3 wt% WC-C-B1	22	6	21	6
WC-B-B1 dead + 6 wt% WC-C-B1	15	4	20	5
WC-B-B2 dead + 30 wt% WC-C-B1	29	16	26	14
WC-HO-S1 live + 3 wt% WC-C-B1	8	2	6	3
WC-HO-S1 live + 6 wt% WC-C-B1	15	6	13	5
WC-B-B1 live + 3 wt% WC-C-B1	8	4	16	8
WC-B-B2 live + 5.9 wt% WC-C-B1				

8.3.4 Equation of State (EoS) Applications:

The EF correlation can also provide viscosity predictions for diluted bitumen and heavy oils using the densities estimated with an equation of state. This application is demonstrated below using the original Peng-Robinson equation of state as implemented in the VMGSim process simulator. Note, temperature dependent volume translations were implemented externally to the VMGSim model to improve the density predictions, as described previously in Section 7.4.2. The volume translations of the EoS model are tuned based only on the specific gravity of the base dead oils and the condensate and the saturated liquid density of the pure solvents at two temperatures.

Figure 8.13 compares the predicted and measured density for mixtures of WC-B-B3 with single-component solvents at 10 MPa. There is little bias in the predictions but the deviations tend to be greatest at lower temperatures and near the critical temperature of the solvent. Overall, the AARD and MARD of the EoS densities are of 0.35% and 1.0%, respectively, Table 8.5. Note that the predictions are generally in better agreement with the measurements for the live WC-B-B1 and WC-HO-S1 as they contain low amounts of the dissolved gas components.

Figure 8.14 compares the predicted and measured viscosity for the same systems as shown in Figure 8.13. In general, the deviations increase at lower temperatures. The overall AARD and MARD of the viscosity predictions using the EoS densities as an input are 21% and 70%, respectively, Table 8.5. The predictions are less satisfactory in comparison to the predictions done using the measured density (with overall AARD and MARD of 14% and 63%, respectively) as the input due to the errors in the predicted density. Note, the predictions for the live oils and the mixtures of the bitumen with lighter solvents are as good as the predictions with the measured densities; or are even improved for the diluted bitumen with ethane, Figure 8.14, due to over-predicted densities, Figure 8.13.

The predictions of the EF correlation with EoS-estimated density as input were also tuned to the measured viscosity data of the diluted bitumen and heavy oil mixtures by adjusting the values of β_{ij} for the pseudo-binary pairs of dead oils and the solvents, Table 8.5. Note that the β_{ij} value for the condensate solvent was determined by fitting only the data of WC-B-B2 diluted with 30 wt% condensate. Hence, the reported deviations for other mixtures with condensate are predicted values. The overall AARD and MARD of the fitted model are 10% and 42%, respectively. However, the performance of the fitted model is not as exact as the fitted model with measured densities due to temperature-dependent deviations in the EoS-estimated densities, Figure 8.13. Note that the adjusted values of binary interaction parameters do not follow a clear trend as they compensate for combined effects of the deviations in the EoS-estimated density and the non-ideality of the viscosity of the diluted mixtures.

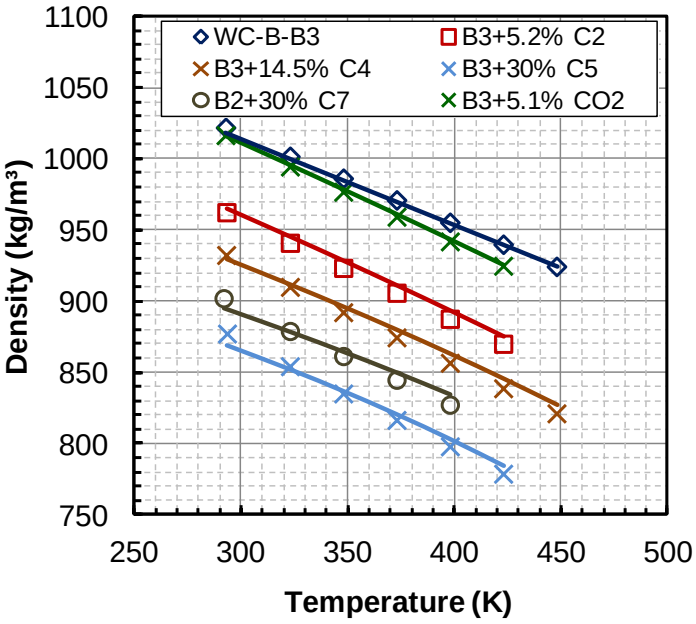

Figure 8.13: Measured and predicted by EoS density of the diluted bitumen with n-paraffin solvents and carbon dioxide in pressure of 10 MPa.

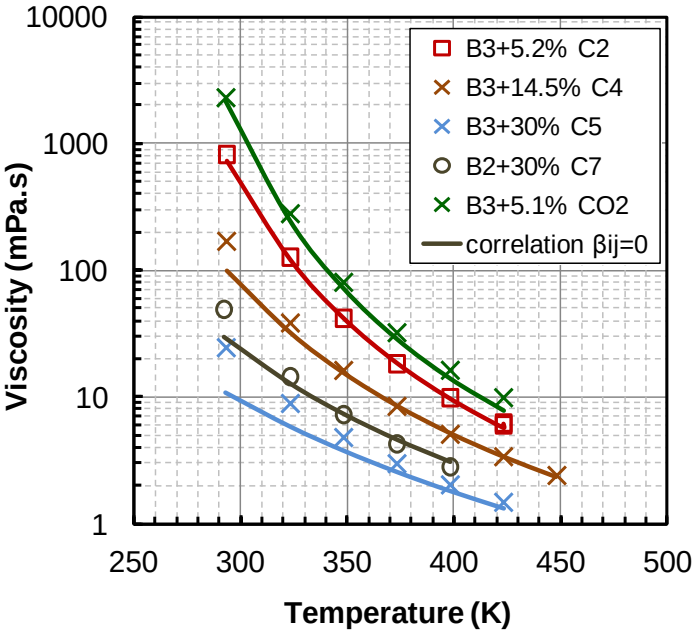

Figure 8.14: Measured and predicted by EF correlation (all β_{ij}=0) viscosity of the diluted bitumen with n-paraffin solvents and carbon dioxide in pressure of 10 MPa. The input densities to EF correlation were calculated by the equation of state, Figure 8.10.

Table 8.5: Summary of the deviations of the density predictions with PR equation of state and viscosity predictions with EF model using EoS-estimated density as input.

Diluted Bitumen Description		Density Prediction		Viscosity Prediction				
				Predicted $\beta_{sol\text{-}oil}$=0		Tuned		
		MARD (%)	AARD (%)	MARD (%)	AARD (%)	$\beta_{sol\text{-}oil}$	MARD (%)	AARD (%)
WC-B-B3	dead + 5.2 wt% C_7	0.64	0.51	25	8	-0.020	16	6
WC-B-B3	dead + 7.6 wt% C_3	0.53	0.33	54	25	-0.044	28	8
WC-B-B3	dead + 16 wt% C_3	0.62	0.37	64	37	-0.044	22	10
WC-B-B2	dead + 11.3 wt% C_3	0.50	0.30	63	33	-0.0447	29	11
WC-B-B2	dead + 15.1 wt% C_3	0.51	0.28	70	43	-0.0447	33	11
WC-B-B3	dead + 7.3 wt% C_4	0.78	0.46	25	12	-0.015	42	23
WC-B-B3	dead + 14.5 wt% C_4	0.82	0.47	46	14	-0.015	30	9
WC-B-B3	dead + 15 wt% C_5	0.70	0.38	51	16	-0.029	34	16
WC-B-B3	dead + 30 wt% C_5	0.96	0.47	59	28	-0.029	36	11
WC-B-B2	dead + 15 wt% C_7	0.70	0.70	51	15	-0.016	26	12
WC-B-B2	dead + 30 wt% C_7	0.87	0.87	44	15	-0.016	30	18
WC-B-B3	dead + 5.1 wt% CO_2	0.24	0.17	21	14	-0.016	18	8
WC-HO-S1	live	0.38	0.16	20	13			
WC-B-B1	live	0.40	0.13	11	4			
WC-HO-S1	dead + 3 wt% WC-C-B1	0.35	0.14	23	10	0.0356	11	4
WC-HO-S1	dead + 6 wt% WC-C-B1	0.54	0.30	37	24	0.0356	9	4
WC-B-B1	dead + 3 wt% WC-C-B1	0.49	0.26	32	19	0.0356	11	6
WC-B-B1	dead + 6 wt% WC-C-B1	0.76	0.51	52	30	0.0356	15	7
WC-B-B2	dead + 30 wt% WC-C-B1	0.71	0.24	59	32	0.0356	17	7
WC-HO-S1	live + 3 wt% WC-C-B1	0.57	0.39	33	17	0.0356	12	6
WC-HO-S1	live + 6 wt% WC-C-B1	0.74	0.42	48	21	0.0356	18	6
WC-B-B1	live + 3 wt% WC-C-B1	0.64	0.36	21	14	0.0356	26	8
WC-B-B2	live + 5.9 wt% WC-C-B1			50	33	0.0356	23	17

Since the viscosity predictions for the diluted heavy oil and bitumen with EF correlation is highly sensitive to the input density, its performance in EoS applications strongly depends on the volume translations for the cubic equation of state. The set of the temperature-dependent volume translations used in this study for the pure components provides satisfactory density estimations but limits the fitting capability of the EF correlation due to the temperature-dependent deviations in density. However, this method can have better performances for the diluted bitumen and heavy oil mixtures in a short temperature range of interest if the γ_0 and γ_1 in Equation 7.13 for the pure solvents are tuned accordingly. More sophisticated implementations of the temperature-dependent volume translations are required for the applications with wide temperature range of interest (see Appendix B). The evaluation of the performance of the model for diluted bitumen and heavy oil applications with any chosen set the volume translation for the equation of state is highly recommended.

8.4 Summary

The Expanded Fluid (EF) correlation was used to model the viscosity of 23 diluted bitumen and heavy oils with single-component solvents, solution gas mixtures, and the condensate solvent. Both measured and EoS-estimated density values were used as the input to the correlation.

The viscosity of dead bitumen diluted with single-component solvents including ethane, propane, n-butane, n-pentane, n-heptane were predicted using the measured density with overall AARD and MARD of 19% and 63%, respectively. Higher deviations were observed for the diluted mixtures with lighter solvents except carbon dioxide. Hence, the viscosity interaction parameters (β_{ij}) were determined for all bitumen/solvent pseudo-binaries and correlated to the normalized difference in liquid density of the oil and the solvent. The overall AARD and MARD of the predicted viscosities using the generalized non-zero β_{ij} values were 9% and 44%, respectively.

Both sets of the predicted viscosities of live WC-HO-S1 and WC-B-B1 with all β_{ij}=0 and the generalized non-zero β_{ij} values for n-paraffin and oil binaries were within the

uncertainties of the measurements and model with overall AARDs of 8% and 6%, respectively. The predictions with calculated $\beta_{oil\text{-}sol}$ for the condensate diluted dead and live bitumen and heavy oil were improved with overall AARD of 7% in comparison to 8% with $\beta_{oil\text{-}sol}$=0.

The predicted viscosities of the 23 studied diluted mixtures of bitumen and heavy oil using the EoS-estimated densities were less satisfactory with overall AARD and MARD of 21% and 70%, respectively. The performance of the EF correlation for the live oils was better because the dissolved gas content was relatively low. New β_{ij} values were determined with partially compensated for the deviations in density and the non-ideality in the viscosity of the diluted mixtures. The overall MARD and AARD of the fitted correlation to data of the diluted bitumen mixtures with single-component solvents and the condensate were 42% and 10%, respectively.

The Expanded Fluid viscosity correlation is a simple yet powerful tool to provide viscosity predictions for diluted bitumen and heavy oil with no experimental viscosity data. The main shortcoming of the EF model is the need for accurate densities as an input. Therefore, if the EF model is to be used with a cubic equation of state, temperature dependent volume translation must be applied. The binary interaction parameters in the mixing rules of the EF correlation can be used to tune the predictions of the correlation to available viscosity data of the mixtures.

CHAPTER NINE: CONCLUSIONS AND RECOMMENDATIONS

9.1 Dissertation Conclusions

The primary objective of this thesis was to develop a compositional viscosity model for petroleum industry applications including natural gas processing, refining, conventional oil and gas recovery, heavy oil recovery, and bitumen extraction. The requirements for the suitable viscosity model for implementation in process and reservoir simulators were set as: 1) trace continuously the full range of single phase properties in the gas, liquid, critical, and supercritical regions; 2) be fast; 3) predict both pure-component and mixture viscosities; 4) be compatible with the fluid characterization used for the phase behavior model. The recently developed Expanded Fluid (EF) viscosity correlation was found to have the potential to meet the above criteria; but required more development and testing as specified in the five objectives in Chapter 1 of this thesis. Objectives I and II of this thesis were fulfilled with both *Version 1* and *Version 2* of the EF correlation. However, further development of *Version 2* was not pursued for Objectives III, IV, and V due to the limited applicability of *Version 2* (details in Section 7.1). The following is a summary of the major contributions and developments on EF correlation and the conclusions drawn from this dissertation:

1- Development of Mass-Based Mixing Rules

- Mass fraction based mixing rules were developed for the fluid-specific parameters of EF correlation. The new set of mixing rules enabled the EF correlation to provide viscosity predictions for mixtures with dissolved gas components at the given pressure and temperature of interest.
- The concept of the binary interaction parameters, β_{ij}, (with default values of zero) was imbedded into the mixing rules of the EF correlation. The adjustment of the binary interaction parameters to non-zero values was proposed to tune model predictions to available viscosity data of the mixtures. The predictions of *Version 1* of the EF correlation with measured density were found to be satisfactory with all β_{ij} =0.
- It was shown that the adoption of the new set of the mixing rules (with all β_{ij}=0) to *Version 2* of EF correlation resulted in consistently under-predicted viscosities for the

mixtures. The skewed fluid-specific parameters of the EF correlation for pure components in *Version 2* were identified as the source of the deviations.

- The values of the binary interaction parameters were regressed for over 70 binaries of hydrocarbon compounds for use with *Version 2* of correlation. Generalized correlations were also developed for the binary interaction parameters.

2- Extension of the Correlation to Non-Hydrocarbons

- It was shown that the current framework of the EF correlation fit the experimental viscosity data of carbon dioxide, hydrogen sulfide, helium, nitrogen and glycols. The predictive capability of the EF correlation was confirmed by comparing calculated viscosities of hydrogen sulfide based on the fit to limited number of data points with new independent high temperature-high pressure data points.
- The EF correlation failed to fit data of associating non-hydrocarbons with strong hydrogen bonds such as water and methanol due to its empirical basis on mostly non-polar hydrocarbons. Hence, the c_2 parameter of the correlation was modified (for these compounds) from a constant to an exponential function of temperature reducing to fixed constant value at high temperatures. However, *Version 1* of the correlation was found insufficient to model the viscosity of the compressed water at temperatures below 50°C whereas the viscosity of the water, unlike other liquids, decreases upon compression.
- Both *Version 1* and *Version 2* (with generalized β_{ij}) of the EF correlation were used to predict the viscosity of several sweet and sour natural gas mixtures with overall average relative deviations (AARD) less than 6.3%.
- *Version 1* predicted the viscosity of aqueous solutions with AARDs less than 10%, except for solutions of methanol and water where the viscosity was under-predicted. The β_{ij} was regressed for the water and methanol binary to fit the viscosity data over the temperature range of the study with AARD of 4%. Similar to the hydrocarbon mixtures, the predictions of *Version 2* for all aqueous solutions were found to be negatively biased but were improved by regression of the β_{ij} values. No generalized correlation was found for the β_{ij} of hydrocarbon binaries with *Version 2*.

3- Estimation Methods for the Parameters of the Correlation

- Estimation methods were developed for the fluid-specific parameters of the EF correlation (*Version 1*) as functions of molecular weight and specific gravity for the hydrocarbon compounds. Hence, the EF correlation was made predictive for ill-defined fluids such as hydrocarbon compounds with no viscosity data, petroleum distillation cuts, and pseudo-components of characterized crude oils.
- The above estimations methods for the compressed state density and the c_2 parameter were cast as the departure functions from a reference n-paraffin system. The departure functions were correlated to the molecular weight and the difference in the specific gravity of the hydrocarbon in respect to the reference n-paraffin. The compressed state density, parameter c_2 and specific gravity of reference n-paraffin system were also correlated to the molecular weight. Due to the limited availability of high pressure viscosity data for heavy hydrocarbons, the c_3 parameter was only correlated to the molecular weight.
- The EF correlation (*Version 1*) with the estimation methods provided viscosity predictions for over 150 heavy hydrocarbon compounds at atmospheric pressure and in temperature range of 253-383 K with an overall AARD of 31%. The viscosities of over 100 petroleum distillation cuts in the temperature range of 310-373 K were also predicted with an overall AARD of 27%.
- No systematic deviations of the predicted viscosities were observed for the pure hydrocarbons. The dependence of the viscosity (mostly parameter c_2 in the EF correlation) on the molecular structure of the pure hydrocarbons was identified as the main source of the deviations of the predictions.
- The viscosities of the high boiling point distillation cuts were systematically under-predicted by EF correlation. It was speculated that the measured number-average or calculated (by correlations based on the specific gravity and boiling point) molecular weight of the cuts does not correctly represent the distillation cuts, which are polydisperse in molecular weight, for the viscosity correlation.

4- Extension of EF Correlation to Characterized Oils

- A methodology was proposed to apply the EF correlation (*Version 1*) to crude oils characterized as mixtures of defined components and pseudo-components. The EF correlation with this methodology is a compositional viscosity model suitable for process and reservoir simulator applications.
- The above estimation methods are used to calculate the fluid-specific parameters for the pseudo-components based on their molecular weight and specific gravity. Then, the parameters for the crude oil are calculated using the correlation mixing rules and the viscosity of the crude oils is predicted. A simple procedure is used to tune the predictions to available viscosity data of the crude oils by applying up to three single multipliers to the fluid-specific parameters of the pseudo-components.
- The EF correlation (*Version 1*) with the proposed methodology provided viscosity predictions for 9 crude oils (dead and live) and 1 de-asphalted oil within a factor of 3 the measured values based on measured densities and within a factor of 5 based on EoS-estimated densities. The crude oils were characterized based on the extrapolated GC assay data and the specific gravity of the dead crude oils. The EoS-estimated densities were calculated by Peng-Robinson equation of state with temperature-dependent volume translations.
- It was shown that tuning of only the parameter c_2 by applying a single multiplier was sufficient to fit (using measured densities as an input) viscosities of the studied characterized crude oils to within 30% of the measured values. In general, the parameter c_2 is the first candidate for adjustment to match the experimental data due to higher uncertainties in its estimation method. It can also compensate for the effect of inaccurate oil characterizations; for example, inaccurate molecular weights of the crude oils. Two and three-parameter tuning can also be employed when sufficient data are available to justify multi-parameter tuning of the model.
- It was shown that two-parameter tuning is usually required when EoS-estimated densities are used as the input to the EF correlation. Adjustment of the compressed state densities of the pseudo-components compensates the effect of the less accurate input densities on the predicted viscosity. In addition, the adjustment of the parameter c_3 is also essential if the EoS-estimated densities at higher pressures affect the

viscosity predictions. This situation is unavoidable when cubic equations of state are used for extra heavy hydrocarbons at lower temperatures.

5- Modeling the Viscosity of Diluted Heavy Oil and Bitumen

- Extensive viscosity and density measurements were conducted at temperature and pressure ranges of 288-448 K and 0.1-11 MPa for 23 diluted heavy oil and bitumen mixtures. The solvents include single component solvents, a multi-component solvent (condensate) and solution gas mixtures. Measurements were also performed on the corresponding dead heavy oil and bitumen (3 batches) from Western Canada.
- The viscosity of dead bitumen diluted with single-component solvents including ethane, propane, n-butane, n-pentane, n-heptane were predicted using the measured density within the same order of magnitude of measurements with overall AARD and MARD of 19% and 63%, respectively. The correlation was found to under-predict the viscosity of the mixtures, especially for lighter solvents (except carbon dioxide) and/or at lower temperatures.
- The non-ideality in the viscosity of the diluted bitumen was accounted for by use of non-zero viscosity interaction parameters (β_{ij}) for the binary pair of solvent-bitumen. The values of temperature-pressure-composition independent binary interaction parameters were correlated to the normalized difference in liquid density of the oil and the solvent. The overall AARD of the predicted viscosities using the generalized non-zero β_{ij} values was 9% .
- The viscosity of live bitumen and heavy oil and the condensate diluted dead and live heavy oil and bitumen were predicted within the uncertainties of the measurements with overall AARDs less 10% either with all β_{ij}=0 or by non-zero β_{ij} calculated by the developed general correlation.
- It was shown that Peng-Robinson EoS provides density predictions for diluted heavy oil and bitumen with MARD of 1%. The predicted viscosities by EF correlation with EoS-estimated densities as input were found within the same order of magnitude of the measurements with overall AARD of 21%. A new set of non-zero β_{ij} values were determined by fitting the data of the diluted bitumen/heavy oil mixtures with overall

AARD of 10%. This set of β_{ij} values did not follow a clear trend since they were compensating for both deviations in EoS-estimated density and non-idealities in viscosity of the diluted mixtures.

- As the viscosity predictions by EF correlation are highly sensitive to input densities, the use of temperature-dependent volume translations with cubic equations of state is necessary.

9.2 Recommendations for Future Research

The EF correlation (*Version 1*) with the aforementioned developments is a simple yet powerful tool to provide viscosity predictions for the applications in the petroleum industry. To add to robustness of the EF correlation and to broaden its application range, the following research and developments are recommended:

I. To minimize the dependence of the EF correlation on the experimental density data, a robust and accurate density model is required. The Peng-Robinson equation of state with temperature and pressure dependent volume translations (see Appendix B, Section B.3) has the potential, but requires more development. The main avenues of research are: 1) to develop methodology of determination of the parameters γ'_0 and γ'_1 for compounds with limited liquid density data and pseudo-components; 2) to generalize the excess volumes of mixing for binary pairs. Use of the modified Rackett correlation (Section 7.4.1) or the ASTM 1250-80 for the density of crude oils (Section 7.4.2) can be a starting point for the first avenue. Other options are non-cubic equations of state such as those based on the Statistical Associating Fluid Theory (SAFT).

II. The molecular structure of the hydrocarbon compounds was identified as the main contribution to the numerical values of parameter c_2 and the compressed density. The effect of molecular structure on the deviations of the predicted viscosity with the developed estimations methods based on only molecular weight and specific gravity was discussed sections 7.5.2 and 7.6.1. However, the molecular structure essentially determines the latter two physical properties of the hydrocarbon compounds. Hence, it is proposed to develop general estimation methods for the

fluid-specific parameters of the EF correlation based on group contribution methods. This approach may provide more accurate viscosity predictions than the current estimation method for well-defined hydrocarbon compounds with no viscosity data.

III. It was shown that EF correlation with the current estimation methods tends to under-predict the viscosity of the high boiling point petroleum distillation cuts. Hence, it is proposed to further study the validity of the density predictions by the modified Rackett correlation and the viscosity prediction with EF correlation for these fluids. This can be achieved by collecting viscosity and density data for petroleum distillation cuts at different temperatures. If the modified Rackett correlation is found to be reliable, the extensive database of the kinematic viscosities of distillation cuts compiled in this thesis can be used to develop new sets of the estimations methods as functions of the normal boiling point and specific gravity.

IV. More experimental viscosity and density data of diluted heavy oils and bitumens are required to confirm the trend of the viscosity interaction parameters for the pseudo-binaries of oil and solvent with normalized difference in their liquid densities. The recommended solvents are naphthenic and aromatic hydrocarbon compounds (such as cyclohexane, toluene and 1-methylnaphthalene) to verify the transition from n-heptane toward carbon dioxide and beyond. It is also recommended to conduct measurements with bitumens from different reservoirs/batches to confirm that β_{ij} values do not depend on factors other than the difference in the liquid densities.

V. It is recommended to conduct a follow-up study to compare the performance of the EF model with current viscosity models in reservoir simulators such as the Corresponding States models and/or the other promising models such as F-Theory. The proposed study would include case studies in primary production and

enhanced recoveries of conventional and unconventional reservoirs and would also compare the computational efficiency of the models.

References

Aasberg-Petersen, K., Knudsen, K., and Fredenslund, A. **1991**. Prediction of Viscosities of Hydrocarbon Mixtures. *Fluid Phase Equilib, 70*(2), 293-308.

Agrawal, P. **2012**. *Measurement and Modeling of the Phase Behavior of Solvent Diluted Bitumens*. M.Sc. dissertation, UNIVERSITY OF CALGARY.

Alani, G. H. and Kennedy, H. T. **1960**. Volume of Liquid Hydrocarbons at High Temperatures and Pressures. Trans. AIME, 219, 288.

Alazard, N. and Montadert, L. **1993**. Oil Resources for Next Century: What's Ahead?. *Natural Resources Research*. 2(3):197-206.

Al-Besharah, J. M., Salman, O. A. and Akashah, S. A. **1987**. Viscosity of Crude Oil Blends. *Ind Eng Chem Res,* 26, 2445–2449.

Alder, B., Gass, D. M. and Wainwright, T. E. **1970**. Studies in Molecular Dynamics. VIII. The Transport Coefficients for a Hard-Sphere Fluid. *The Journal of Chemical Physics*, 53(10), 3813-3826.

Allan, J. M. and Teja, A. S. **1991**. Correlation and Prediction of the Viscosity of Defined and Undefined Hydrocarbon Liquids. *Can J of Chem Eng*, 69(4), 986-991.

Al-Syabi, Z., Danesh, A., Tohidi, B., Todd, A. C. and Tehrani, D. H. **2001**. A |Residual Viscosity Correlation for Predicting the Viscosity of Petroleum Reservoir Fluids Over Wide Ranges of Pressure and Temperature. *Chemical engineering science*, 56(24), 6997-7006.

Altgelt, K. H. and Boduszynski, M. M. **1994**. *Composition and Analysis of Heavy Petroleum Fractions*. Marcel Dekker, Inc. New York.

Andrade, E. N. da. C. **1934**. A Theory of The Viscosity of Liquids. *Phil Mag, 17*, 497-511.

API. **1997**. *API Technical Data Book-Petroleum Refining*, 6th Ed. Daubert, T. E. and Danner, R. P.(Eds). American Petroleum Institute (API), Washington, DC, USA.

API. **1966**. *Properties of Hydrocarbons of High Molecular Weight*. Research Project 42, American Petroleum Institute, Washington, DC.

Arrhenius, S. A. **1887**. Uber die Dissociation der in Wasser Gelosten Stoffe. *Z Phys Chem*, 1, 631–648.

Aspen Technology, Inc. **2005**. Aspen HYSYS 2004.2.

Assael, M. J., Kalyva, A. E., Kakosimos, K. E. and Antoniadis, K. D. **2009**. Correlation and Prediction of Dense Fluid Transport Coefficients VIII. Mixtures of Alkyl Benzenes with Other Hydrocarbons. *Int J Thermophys*, 30(6), 1733-1747.

Assael, M. J.; Dalaouti, N. K. and Vesovic. **2001**. Viscosity of Natural-Gas Mixtures: Measurements and Prediction. *Int J Thermophys*, 22(1) , 61−71.

Assael, M. J., Dymond, J. H. and Polimatidou, S. K. **1995**. . Correlation and Prediction of Dense Fluid Transport Coefficients VII. Refrigerants. *Int J Thermophys*, 16(3), 761-772.

Assael, M. J., Dymond, J. H. and Polimatidou, S. K. **1994**. Correlation and Prediction of Dense Fluid Transport Coefficients VI. n-Alcohols. *Int J Thermophys*, 15(2), 189-201.

Assael, M. J., Dymond, J. H., Papadaki, M. and Patterson, P. M. **1992a**. Correlation and Prediction of Dense Fluid Transport Coefficients I. n-Alkanes. . *Int J Thermophys*, 13(2), 269-281.

Assael, M. J., Dymond, J. H. and Patterson, P. M. **1992b**. Correlation and Prediction of Dense Fluid Transport Coefficients V. Aromatic Hydrocarbons. *Int J Thermophys*, 13(5), 895-905.

Assael, M. J., Dymond, J. H., Papadaki, M. and Patterson, P. M. **1992c**. Correlation and Prediction of Dense Fluid Transport Coefficients III. n-Alkane Mixtures. *Int J Thermophys*, 13(4), 659-669.

Assael, M. J., Karagiannidis, L. and Papadaki, M. **1991**. Measurements of the Viscosity of n-Heptane+ n-Undecane Mixtures at Pressures up to 75 MPa. *Int J Thermophys,*. 12(5), 811-820.

ASTM. **1981**. Annual Book of ASTM Standards, American Society for Testing and Materials, Philadelphia, PA, 205.

Audonnet, F. And Padua, A. A. H. **2004**. Viscosity and Density of Mixtures of Methane and n-Decane from 298 to 393 K and up to 75 MPa. *Fluid Phase Equilib,* 216, 235-244.

Badamchi-Zadeh, A., Yarranton, H., Maini, B. and Satyro, M. **2009a**. Phase Behaviour and Physical Property Measurements for VAPEX Solvents: Part II. Propane, Carbon Dioxide and Athabasca Bitumen. *J Can Pet Tech*, 48(3), 57-65.

Badamchi-Zadeh, A., Yarranton, H., Svrcek, W. and Maini, B. **2009b**. Phase Behaviour and Physical Property Measurements for VAPEX Solvents: Part I. Propane and Athabasca Bitumen. *J Can Pet Tech*, 48(1), 54-61.

Bair, S., Jarzynski, J. and Winer, W. O. **2001**. The Temperature, Pressure and Time Dependence of Lubricant Viscosity. *Tribology Int.*, 34(7), 461-468.

Baird C. T. **1989**. *Guide to Petroleum Product Blending*. HPI Consultants Inc., Austin, Texas, USA.

Baltatu, M. E., Chong, R. A., Huber, M. L. and Laesecke, A. **1999**. Transport Properties of Petroleum Fractions. *Int J Thermophys,* 20(1), 85-95.

Baltatu, M. E., Chong, R. A. and Huber, M. L. **1996**. Viscosity of Defined and Undefined Hydrocarbon Liquids Calculated Using an Extended Corresponding-States Model. *Int J Thermophys*, 17(1), 213-221.

Baltatu, M. E. **1982**. Prediction of the Liquid Viscosity for Petroleum Fractions. *Ind Eng Chem Process Des Dev*, 21, 192-195.

Barrouhou, M., Zéberg-Mikkelsen, C. K., Baylaucq, A. and Boned, C. **2003**. High-Pressure Viscosity and Density Measurements for the Asymmetric Binary System cis-Decalin+2,2,4,4,6,8,8-Heptamethylnonane. *Int J Thermophys*, 24, 937-952.

Barrufet, M. A. and Setiadarma, A. **2003**. Reliable Heavy Oil–Solvent Viscosity Mixing Rules for Viscosities up to 450 K, Oil–Solvent Viscosity Ratios up to 4×105, and any Solvent Proportion. *Fluid Phase Equilib*, 213,65-79.

Barrufet, M. A., Hall, K. R., Estrada-Baltazar A. and Iglesias-Silva, G. A. **1999**. Liquid Viscosity of Octane and Pentane + Octane Mixtures from 298.15 K to 373.15 K up to 25 MP. *J Chem Eng Data*, 44, 1310–1314.

Barrufet, M. A., El-Sayed Salem, S. K., Tantawy, M and Iglesias-Silva, G. A. **1997**. Liquid Viscosities of Carbon Dioxide+Hydrocarbons from 310 K to 403 K. *J Chem Eng Data*, 41, 436–439.

Batschinski, A. J. **1913**. Investigations of the Internal Friction of Fluids. *Z Phys Chem*, 84, 643-706.

Baylaucq, A., Boned, C., Canet, X. and Zéberg-Mikkelsen, C. K. **2003**. High-Pressure (up to 140 MPa) Dynamic Viscosity of the Methane and Toluene System: Measurements and Comparative Study of Some Representative Models. *Int J Thermophys*, 24, 612–638.

Baylaucq, A., Zéberg-Mikkelsen, C. K., Dauge´, P. and Boned. C. **2002**. Dynamic Viscosity and Density of Heptylbenzene and Heptylcyclohexane up to 100 MPa. *J Chem Eng Data*, 47, 997-1002.

Baylaucq, A., Boned, C., Dauge, P. and Lagourette, B. **1997**. Measurements of the Viscosity and Density of Three Hydrocarbons and the Three Associated Binary Mixtures Versus Pressure and Temperature. *Int J Thermophys*, 18, 3-23.

Baylaucq, A., Dauge, P. and Boned, C. **1997**. Viscosity and Density of the ternary Mixture Heptane+Methylcyclohexane+1-Methylnaphthalene, *Int J Thermophys*, 18, 1089-1107.

Beg, S. A., Amin, M. B. and Hussain, I. **1988**. Generalized Kinematic Viscosity–Temperature Correction for Undefined Petroleum Fractions. *Chem Eng J*, 38, 123-136.

Beggs, H.D., and Robinson, J.R. **1975**. Estimating the Viscosity of Crude Oil Systems .*Journal of Petroleum Technology* 27, 1140-1141.

Berstad, D.A. **1989**. *Viscosity and Density of n-Hexane, Cyclohexane and Benzene and Their Binary Mixtures with Methane.* PhD Thesis, University of Trondheim-NTH, The Norwegian Institute of Technology, Institute of Inorganic Chemistry, Trondheim, Norway.

Bhattacharyya, P. K. **1970**. Viscosity of Binary Polar-Gas Mixtures: CH_3Cl-H_2S and CH_3Cl-SO2. *J Chem Phys*, 53, 893–895.

Bhattacharyya, P. K., Ghosh, A. K. and Barua, A. K. **1970**. Dipole-Dipole Interaction and Viscosity of Polar Gases. *J Phys*, 3, 526–535.

Bicher, L. B. and Katz, D. L. 1943. Viscosities of the Methane-Propane System. *Ind Eng Chem*, 35, 754-761.

Bingham, E. C. **1914**. The Viscosity of Binary Mixtures. *J Phys Chem*, 18, 157-165.

Boned, C., Zéberg-Mikkelsen, C. K., Baylaucq, A. and Dauge, P. **2003**. High-Pressure Dynamic Viscosity and Density of Two Synthetic Hydrocarbon Mixtures Representative of Some Heavy Petroleum Distillation Cuts, *Fluid Phase Equilib*, 212, 143-164.

Brodkey Robert S. and Hershey Harry C. **2003**. *Transport Phenomena: A Unified Approach*. Brodkey Publishing.

Butler, R.M., **1997**. *GravDrain's Blackbook: Thermal Recovery of oil and bitumen*.GravDrain Inc., Calgary,Alberta ISBN0-9682563-0-9.

Butler, R. M. and Mokrys, I. J. **1989**. Solvent Analog Model of Steam-Assisted Gravity Drainage. *AOSTRA Journal of Reasearch*, 5, 17.

Canet, X., Baylaucq, A. and Boned., C. **2002**. High-Pressure (up to 140 MPa) Dynamic Viscosity of the Methane+Decane System. *Int J Thermophys*, 23, 1469–1486.

Canet, X., Dauge, P., Baylaucq, A., Boned, C., Zéberg-Mikkelsen, C. K., Quiñones-Cisneros, S. E. and Stenby, E. H. **2001**. Density and Viscosity of the 1-Methylnaphthalene +2,2,4,4,6,8,8-Heptamethylnonane System from 293.15 to 353.15 K at Pressures up to 100 MPa. *Int J Thermophys*, 22, 1669-1689.

Carmichael, L. T., Berry, V. M. and Sage, B. H. **1967**. Viscosity of a Mixture of Methane and n-Butane. *J Chem Eng Data*, 12, 44-47.

Chandler, D. **1975**. Rough Hard Sphere Theory of the Self-Diffusion Constant for Molecular Liquids. *J Chem Phys*, 62(4), 1358-1363.

Chapman, S. and Cowling, T. G. **1952**. *The Mathematical Theory o f Nonuniform Gases*, Cambridge University Press, Cambridge, NY.

Chevalier, J. L. E., Petrino, P. J. and Gaston-Bonhomme, Y. H. **1990**. Viscosity and Density of some Aliphatic, Cyclic, and Aromatic Hydrocarbons Binary Mixtures. *J Chem Eng Data*, 35, 206–212.

Chevalier, J. L., Petrino, P. and Gaston-Bonhomme, Y. **1988**. Estimation method for the kinematic viscosity of a liquid-phase mixture. *Chemical engineering science*, 43(6), 1303-1309.

Chew, J. and Connally, C. A. **1959**. A Viscosity Correlation for Gas-Saturated Crude Oils. *Trans. AIME*, 216, 23-25.

Chirinos, M. L., Gonzalez, J. and Layrisse, I. **1983**. Rheological Properties of Crude Oils from the Orinoco Oil Belt and Their Mixtures with Diluents: *Rev. Tec. INTEVEP*, 3(2), 103-115.

Chung, T. H., Ajlan, M., Lee, L. L. and Starling, K.E. **1988**. Generalized Multiparameter Correlation for Nonpolar and Polar Fluid Transport Properties. *Ind Eng Chem Res*, 27(4), 671-679.

Chung, T. H., Lee, L. L. and Starling, K. E. **1984**. Applications of Kinetic Gas Theories and Multiparameter Correlation for Prediction of Dilute Gas Viscosity and Thermal Conductivity. *Ind Eng Chem Fundamen*, 23, 8-13.

Ciotta, F., Maitland, G., Smietana, M., Martin Trusler, J. P. and Vesovic, V. **2009**. Viscosity and Density of Carbon Dioxide+ 2,6,10,15,19,23-Hexamethyltetracosane (Squalane). *J Chem Eng Data*, 54, 2436-2443.

Clark, K. A. and Ward, S. H. **1950**. *Determination of the viscosities and specific gravities of the oils in samples of Athabaska Bituminous Sand*. King's Printer.

Computer Modeling Group, Ltd. **2011**. WinProp User Manual; Version 2011.

Cook, R. L., Herbst, C. A. and King Jr, H. E. **1993**. High-Pressure Viscosity of Glass-Forming Liquids Measured by the Centrifugal Force Diamond Anvil Cell Viscometer. *J Phys Chem*, 97(10), 2355-2361.

Cragoe, C. S. **1933**. Changes in the Viscosity of Liquids with Temperature, Pressure and Composition. *Proc World Pet Cong London*, 2, 529–541.

Cullick, A. S. and Mathis, M. L. **1984**. Densities and Viscosities of Mixtures of Carbon Dioxide and n-Decane from 310 to 403K and 7 to 30 MPa. *J Chem Eng Data*, 29, 393–396.

Cummings, P. T. and Evans, D. J. **1992**. Nonequilibrium Molecular Dynamics Approaches to Transport Properties and non-Newtonian Fluid Rheology. *Ind Eng Chem Res***,** 31, 1237-1252.

Dandekar, A., Danesh, A., Tehrani, D.H. and Todd, A.C. **1993**. A Modified Residual Viscosity Method for Improved Prediction of Dense Phase Viscosities, Presented at the 7th European Improved Oil Recovery (IOR) Symposium in Moscow, Russia, October 27-29.

Danesh, A. **1998**. *PVT and Phase Behaviour of Petroleum Reservoir Fluid*, Elsevier.

Dauge, P., Baylaucq, A. and Boned, C. **1999**. High-Pressure Viscosity Behaviour of the Tridecane+1-Methylnaphthalene System. *High temperatures-High Pressures*, 31, 665-680.

Dauge, P., Canet, X., Baylaucq, A. and Boned, C. **2001**. Measurement of the Density and Viscosity of the Tridecane+2,2,4,4,6,8,8-Heptamethylnonane Mixtures in the Temperature Range 293.15-353.15 K at Pressures up to 100 MPa. *High temperatures-High Pressures*, 33, 213-230.

De Guzman, J. **1913**. Relation Between Fluidity and Heat of Fusion. *Anales Soc. Espan. Fia. Y. Quim*, 11, 353-362.

Dealy, J. M. **1979**. Rheological Properties of Oil Sand Bitumens. *Can J Chem Eng*, 57(6), 677-683.

DeWitt, K. J., Thodos, G. **1966**.Viscosities of Binary Mixtures in the Dense Gaseous State: The Methane-Carbon Dioxide System. *Can J Chem Eng, 3, 148-1*51.

Diller, D.E. and Ely, J.F. **1989**. Measurements of the Viscosities of Compressed Gaseous Carbon Dioxide, Ethane, and Their Mixtures, at Temperatures up to 500K. *High Temperatures-High Pressures*, 21, 613–620.

Diller, D.E., van Poolen, L. J. and dos Santos, F.V. **1988**. Measurements of the Viscosities of Compressed Fluid and Liquid Carbon Dioxide+Ethane. *J Chem Eng Data*, 33, 460–464.

Diller, D. E. **1984**. Measurements of the Viscosity of Compressed Gasseous and Liquid methane + Ethane mixtures. *J Chem Eng Data*, 29, 215-221.

Doolittle, A. K. **1952**. Studies in Newtonian Flow. III. The Dependence of the Viscosity of Liquids on Molecular Weight and Free Space (in Homologous Series). of Applied Physics, 23(2), 236-239.

Doolittle, A. K. **1951**. Studies in Newtonian Flow. II. The Dependence of the Viscosity of Liquids on Free-Space. *Journal of Applied Physics*, 22(12), 1471-1475.

Dougherty, R. C. **1998**. Temperature and Pressure Dependence of Hydrogen Bond Strength: A Perturbation Molecular Orbital Approach. *J Chem Phys*, 109 (17), 7372−7378.

Ducoulombier, D., Zhou, H., Boned, C., Peyrelasse, J., Saint-Guirons, H. and Xans, P. **1986**. Pressure (1-1000 bars) and Temperature (20-100 °C) Dependence of the Viscosity of Liquid Hydrocarbons. *J Phys Chem*, 90, 1692-1700.

Duhne, C. R. 1979. Viscosity-Temperature Correlations for Liquids. *Chem. Eng*, 86, 15-83.

Dymond, J. H., Awan, M. A., Glen, N. F. and Isdale, J. D. **1991**. Transport Properties of Nonelectrolyte Liquid Mixtures. VIII. Viscosity Coefficients for Toluene and for Three Mixtures of Toluene + Hexane from 25 to 100 °C at Pressures up to 500 MPa. *Int J Thermophys*, 12, 275-287.

Dymond, J. H. **1987**. Corrections to the Enskog Theory for Viscosity and Thermal Conductivity. *Physica B+C*, 144(3), 267-276.

Dymond, J. H., Robertson, J. and Isdale, J. D. **1985**. Transport Properties of Nonelectolyte Liquid Mixtures- III. Viscosity Coefficients for Isooctane, and Equilmolar Mixtures of Isooctnae+n-Octane and Isooctnae +n-Dodecane from 25 to 100°C at Pressures Up to the Freezing Pressure or 500 MPa. *Int J Thermophys*, 6, 233-250.

Dymond, J. H., Robertson, J. and Isdale, J. D. **1981**. Transport Properties of Nonelectolyte Liquid Mixtures- III. Viscosity Coefficients for n-Octane, n-Dodecane, and Equilmolar Mixtures of n-Octane+n-Dodecane and n-Hexane+n-Dodecane from 25 to 100°C at Pressures Up to the Freezing Pressure or 500 MPa. *Int J Thermophys*, 2, 133-154.

Dymond, J. H. and Brawn, T. A. **1979.** Molecular Theories of Transport Properties in Dense Fluids. *Symp. Transp. Prop. Fluids. and Fluid Mixtures, Natl. Eng. Lab.*, East Kilbride, Glasgow, Scotland.

Dymond, J. H. and Brawn, T. A. **1977**. Viscosity Coefficients of Liquids Under Pressure, *Proc. 7th. Syrnp. Therrnophys. Prop.* ASME, New York, 660.

Dymond, J. H. **1976**. A Modified Hard-Sphere Theory for Transport Properties of Fluids over the Whole Density Range: I. Viscosity Coefficients of Low Molecular Weight Hydrocarbons. *Chemical Physics*, 17(1), 101-109.

Dymond, J. H. **1975**. Interpretation of Transport Coefficients on the Basis of the Van der Waals Model: II. Extension to Dilute Gases. *Physica A: Statistical Mechanics and Its Applications*, 79(1), 65-74.

Dymond, J. H. **1974**. The Interpretation of Transport Coefficients on the Basis of the Van der Waals Model: I Dense Fluids. *Physica*, 75(1), 100-114.

Dymond, J. H. **1973**. Transport Properties in Dense Fluids. *Proc. 6th Sym. Thermophys. Props.* ASME. , New York, 143-157.

Eastick, R. R. and Mehrotra, A. K. **1990**. Viscosity Data and Correlation for Mixtures of Bitumen Fractions. *Fuel Processing Tech*. 26, 25-37.

Eastick, R. R. **1989**. Phase Behaviour and Viscosity of Bitumen Fractions Saturated with CO_2, M.Sc. Thesis, University of Calgary, Calgary, Canada.

Elsharkawy, A. M. **2003**. Predicting Volumetric and Transport Properties of Sour Gases and Gas Condensates Using EOSs, Corresponding State Models, and Empirical Correlations. *J Petrol Sci Techno,*, 21, 1759−1787.

Ely, J. F. and Huber, M. L. **1990**. *NIST Standard Reference Database 4, Computer Program SUPERTRAPP, NIST Thermophysical Properties of Hydrocarbon Mixtures, Version 1.0*. National Inst. of Standards and Technology, Gaithersburg, MD.

Ely, J. F. and Magee, J. W. **1989**. Experimental Measurement and Prediction of Thermophysical Property Data of Carbon Dioxide Rich Mixtures. *Proc the 68th GPA Annual Conv*, Tulsa, OK.

Ely, J. F. **1984**. Application of the Extended Corresponding States Model to Hydrocarbon Mixtures. *GPA Proc. of 63rd Ann. Conv.*, 9-22.

Ely, J. F. **1982**. Prediction of Dense Fluid Viscosities in Hydrocarbon Mixtures. *GPA Proc. of 61st Ann. Conv.*, 9-17.

Ely, J. F. and Hanley H. J. M. **1981 a**. Prediction of Transport Properties. 1. Viscosity of Fluids and Mixtures. *Ind Eng Chem Fundam*, 20 (4), 323-332.

Ely, J. F. and Hanley, H. J. M. **1981 b,** A Computer Program for the Prediction of Viscosity and Thermal Conductivity in Hydrocarbon Mixtures (TRAPP), NBS Technical Note 1039.

Enskog, D. **1922** . Kinetische Theorie der Wärmeleitung, Reibung und Selbstdiffussion in gewissen verdichteten Gasen und Flüssigkeiten. *Kung. Svenska Vet-Ak Hanl*, 63,4-4.

Erickson, D. and Ely, J. **1993.** in Chap 12 of *Transport Properties of Fluids, Their Correlation, Prediction and Estimation*, J. Millat, J. H. Dymond, and C. A. Nieto de Castro (eds.) IUPAC, Cambridge Univ. Press, Cambridge.

Ertl, H. and Dullien, F. A. L. **1973**. Self-Diffusion and Viscosity of Some Liquids as a Function of Temperature. *AIChE J*, 19(6), 1215-1223.

Estrada-Baltazar, A., Alvarado, J. F. J., Iglesias-Silva, G. A. and Barrufet, M. A. **1998**. Experimental Liquid Viscosities of Decane and Octane + Decane from 298.15 to 373.15 K and up to 25 MPa. *J Chem Eng Data*, 43, 441-446.

Estrada-Baltazar, A., Iglesias-Silva, G. A. and Barrufet, M. A. **1998**. Experimental Liquid Viscosities of Pentane and Pentane + n-Decane from 298.15 to 373.15 K and up to 25 MPa. *J Chem Eng Data*, 43, 601-604.

Ewell, R. H. and Eyring, H. **1937**. Theory of the Viscosity of Liquids as a Function of Temperature and Pressure. *J Chem Phys*, 5, 726-736.

Eyring, H. Viscosity, Plasticity and Diffusion as Examples of Absolute Reaction Rates. *J. Chem. Phys.* **1936**, *4*, 283–291.

FitzSimons, O. and Thiele, E. W. **1935**. Molecular Weight of Cracked Distillates. *Ind Eng Chem*, 7(1), 11-14.

Fylstra, D., Lasdon, L., Watson, J. and Waren, A. **1998**. Design and use of the Microsoft Excel Solver. *Interfaces*, 28(5), 29-55.

Frauenfeld, T. W., Jossy, C., Bleile, J. and Krispin, D. **2009**. Experimental and Economic Analysis of the Thermal Solvent and Hybrid Solvent Processes. *J Can Pet Technol*, 48(11), 55-62.

Galliero, G., Nieto-Draghi, C., Boned, C., Avalos, J. B., Mackie, A. D., Baylaucq, A. and Montel, F. **2007**. Molecular Dynamics Simulation of Acid Gas Mixtures: A Comparison between Several Approximations. *Ind Eng Chem Res*, 46, 5238–5244.

Gaston-Bonhomme, Y., Petrino, P. and Chevalier, J. L. **1994**. UNIFAC—VISCO group contribution method for predicting kinematic viscosity: extension and temperature dependence. Chemical *engineering* science, 49(11), 1799-1806.

Giddings, J. G., Kao, J. T. F., Kobayashi, R. **1966**. Development of a High-Pressure Capillary-Tube Viscometer and Its Application to Methane, Propane, and Their Mixtures in the Gaseous and Liquid Regions. *J Chem Phys*, 45, 578-586.

Goodwin, R. D. **1974**. Thermophysical Properties of Methane, from 90 to 500 K at Pressures to 700 bar. *No. NBS-TN-653, National Bureau of Standards, Boulder, Colo.(USA). Cryogenics Div.*

Gregory, G. A. **1992**. Letter to Editor. Correlation and Predication of the Viscosity of Defined and Undefined Hydrocarbon Mixtures JM Allan and AS Teja, can J. Chem. Eng. 69, 986-991 (1991). J. Chem. Eng., 70(5), 1037-1037.

Grunberg, L. and Nissan, A. H. **1949**. Mixture Law for Viscosity. *Nature*, 164, 799-800.

Guo, X. Q., Sun, C. Y., Rong, S. X., Chen, G. J. and Guo, T. M. **2001**. Equation of State Analog Correlations for the Viscosity and Thermal Conductivity of Hydrocarbons and Reservoir Fluids. *J Pet Sci Eng*, 30(1), 15-27.

Guo, X. Q., Wang, L. S., Rong, S. X. And Guo, T. M. **1997**. Viscosit Model Based on Equations of State for Hydrocarbon Liquids and Gases. *Fluid phase equilib*, 139(1), 405-421.

Gupta, S. and Gittins, S. **2005**. Christina Lake Solvent Aided Process Pilot. Paper Number 2005-190 presented at the 56th Canadian International Petroleum Conference. Calgary, Alberta, June 7–9.

Gupta, S., Gittins, S. and Picherack, P. **2003**. Insights Into Some Key Issue with Solvent Aided Process. *J Can Pet Tech*, **43**(2), 54-61.

Gupta, S., Gittins, S. and Picherack, P. **2002**. Field Implementation of Solvent Aided Process. Paper 2002-299 presented at the 53rd Canadian International Petroleum Conference. Calgary, Alberta, June 11–13.

Hall, K. R. and Yarborough, L. **1971**. New Simple Correlation for Predicting Critical Volume. *Chem Eng*, 78(25), 76-77.

Hanley, H. J. M. 1976. Prediction of the Viscosity and Thermal Conductivity Coefficients of Mixtures, *Cryogenics*, 16 (11), 643-651.

Hanley, H. J. M., McCarty, R. D. and Haynes, W. M. **1975**. Equations for the Viscosity and Thermal Conductivity Coefficients of Methane. *Cryogenics* 15(7), 413-417.

Head, I. M., Jones, D. M. and Larter, S. R. **2003**. Bilogical Activity in the Deep Subsurface and the Origin of Heavy Oil. *Nature*, 426, 344-352.

Heidemann, R. A., Jeje, A. A. and Mohtadi, M. F. **1987**. *An Introduction to the Properties of Fluids and Solids*. University of Calgary Press.

Helfand, E. and Rice, S. A. **1960**. Principle of Corresponding States for Transport Properties. *J Chem Phys*, 32, 1642-1644.

Herbst, C. A., Cook, R. L. and King, H. E. **1994**. Density-Mediated Transport and the Glass Transition: High Pressure Viscosity Measurements in the Diamond Anvil Cell. *Journal of non-Crystalline Solids*, 172, 265-271.

Hernández-Galván, M. A. García-Sánchez, F. and Macías-Salinas, R. **2007**. Liquid Viscosities of Benzene, n-Tetradecane, and Benzene +n-Tetradecane from 313 to 393 K and Pressures up to 60 MPa: Experiment and Modeling. *Fluid Phase Equilib*, 262, 51–60.

Hernández-Galván, M. A., García-Sánchez, F., García-Flores, B. E. and Castro-Arellano, J. **2009**. Liquid Viscosities of Cyclohexane, Cyclohexane+Tetradecane, and Cyclohexane+Benzene from (313 to 393) K and Pressures up to 60 MPa. *J Chem Eng Data*, 54, 2831-8.

Herning, F. and Zipperer, L. **1936**. Calculation of the Viscosity of Technical Gas Mixtures from the Viscosity of the Individual Gases. *Gas u. Wasserfach*, 79, 69-73.

Hildebrand, J. H. and Lamoreaux, R. H. **1972**. Fluidity: A general theory. *Proc Natl Acad Sci*, 69(11), 3428-3431.

Hildebrand, J. H. **1971**. Motions of molecules in liquids: viscosity and diffusivity. *Science*, 174(4008), 490-493.

Hirschfelder, J. O., Curtiss, C. F. and Bird, R. B. **1954**. *Molecular Theory of Gases and Liquids*, Wiley: New York.

Huber, M. L. and Hanley, H. J. M. **1996**. Chap 12 in *Transport Properties of Fluids, Their Correlation, Prediction and Estimation*, J. Millat, J. H. Dymond, and C. A. Nieto de Castro (eds.) IUPAC, Cambridge Univ. Press, Cambridge.

Huber, M.L., and Ely, J.F. **1993**. A Predictive Extended Corresponding States Model for Pure and Mixed Refrigerants Including an Equation of State for R134a. *Int. J. Refrig.* 7, 18-31.

Huber, M. L. and Ely, J. F. **1992**. Prediction of Viscosity of Refrigerants and Refrigerant Mixtures. *Fluid Phase Equilib*, 80 , 239–248.

Iglesias-Silva, G. A., Estrada-Baltazar, A., Hall, K. R. and Barrufet, M. A. **1999**. Experimental Liquid Viscosity of Pentane + Octane + Decane Mixtures from 298.15 to 373.15 K up to 25 Mpa. *J Chem Eng Data*, 44, 1304-1309.

Irving, J. B. **1977 a.** Viscosity of binary liquid mixtures: A survey of mixture equations. National Engineering Lab. Report Number 630, East Kilbride, Glasgow, Scotland.

Irving, J. B. **1977 b.** Viscosity of binary liquid mixtures: The effectiveness of mixture equations. National Engineering Lab. Report Number 631, East Kilbride, Glasgow, Scotland.

Isdale, J. D., MacGillivray, J. C. and Cartwright, G. **1985**. Prediction of Viscosity of Organic Liquid Mixtures by a Group Contribution Method. Natl. Eng. lab. Rept., East Kilbride, Glasgow, Scotland,.

Jacobs, F. A, Donnelly, J. K., Stanislav J. and Svrcek, W. Y. **1980**. Viscosity of Gas-Saturated Bitumen, *J Can Pet Tech*, **19** (4), 46-50.

Jacobs, F. A. **1978**. Viscosity of Carbon Dioxide Saturated Athabasca Bitumen. M.Sc. Dissertation, UNIVERSITY of CALGARY.

Jaeschke, M. and Schley, P. **1996**. Calculation of the Compressibility Factor of Natural Gases According to the AGA8-DC92 Equation of State: 1. Set up of the Equation, *gwf-Gas/Erdgas*, 137 (7), 339.

Johnson, S. E., Svrcek , W. Y. and Mehrotra, A. K. **1987**. Viscosity Prediction of Athabasca Bitumen Using the Extended Principle of Corresponding States. *Ind Eng Chem Res*, 26, 2290.

Jossi, J. A., Stiel, L. I. and Thodos, G. **1962**. The Viscosity of Pure Substances in the Dense Gaseous and Liquid Phases. *AIChE J*, 8, 59-63.

Kanti, M., Zhou, H., Ye, S., Boned, C., Lagourette, B., Saint-Guirons, H., Xans, P. and Montel, F. **1989**. Viscosity of Liquid Hydrocarbons, Mixtures and Petroleum Cuts, as a Function of Pressure and Temperature. *J Phys Chem*, 93, 3860-3864.

Katz, D. L. and Firoozabadi, A. **1978**. Predicting Phase Behavior of Condensate/Crude-oil Systems Using Methane Interaction Coefficients. *J Pet Tech*, 30(11), 1649-1655.

Kendall, J. and Monroe, K. P. **1917**. The Viscosity of Liquids II: The Viscosity-Composition Curve for Ideal Liquid Mixtures. *Journal of ACS*, 39, 1787-1807.

Kesler, M. G. and Lee, B. I. **1976**. Improved Prediction of Enthalpy of Fractions. *Hydro Proc*, 55, 153–158.

Khan, S. A., Al-Marhoun, M. A., Duffuaa, S. O. and Abu-Khamsin, S. A. **1987**. Viscosity Correlations for Saudi Arabian Crude Oils. SPE 15720 presented at Fifth SPE Middle East Oil Show, Manama, Bahrain, March 7-10.

Khan, M. A. B. **1982**. Viscosity Models for Athabasca Bitumen. M.Sc. Dissertation, UNIVERSITY of CALGARY.

Kidnay, A. J., Parrish, W. R. and McCartney, D. G. **2011**.*Fundamentals of Natural Gas Processing.* CRC Press, Boca Raton, FL, USA.

Kokal, S. L. and Sayegh, S. G. **1993**. Phase Behavior and Physical Properties of CO_2 Saturated Heavy Oil and its Constitutive Fractions: Experimental Data and Correlations. *J Pet Sci Eng*, 9(4), 289-302.

Kumagai, A., Tomida, D. and Yokoyama, C. **2006**. Measurements of the Liquid Viscosities of Mixtures of n-Butane, n-Hexane, and n-Octane with Squalane to 30MPa, *Int J Thermophys*, 27(2), 376-393.

Lagourette B., Boned C., Saint-Guirons H., Xans P. and Zhou H. **1992**. Densimeter Calibration Method Versus Temperature and Pressure. *Measure Sci Technol*, 3(8), 699-703.

Langelandsvik, L. I., Solvang, S., Rousselet, M. Metaxa, I. N. and Assael, M. J. **2007**. Dynamic Viscosity Measurements of Three Natural Gas Mixtures−Comparison against Prediction Models. *Int J Thermophys*, 28, 1120−1130.

Lawal, A. S. **1986**. Prediction of Vapor and Liquid Viscosities from the Lawal-Lake-Silberberg Equation of State. paper 14926-MS presented in SPE Enhanced Oil Recovery Symposium, 20-23 April, Tulsa, Oklahoma.

Leach, J. W., Chappelear, P. S. and Leland, T. W. **1968**. Use of Molecular Shape Factors in Vapor-Liquid Equilibrium Calculations with the Corresponding States Principle. *AIChE J*, 14(4), 568-576.

Leaute, R. P. and Carey, B. S. **2005**. Liquid Addition to Steam for Enhancing Recovery (LASER) of Bitumen with CSS: Results from the First Pilot Cycle. Paper Number 2005-161 presented at the 56th Canadian International Petroleum Conference. Calgary, Alberta, Canada, June 7–9.

Leaute, R. P. **2002**. Liquid addition to steam for enhancing recovery of bitumen with CSS: evolution of technology from research concept to a field pilot at Cold lake. SPE/Petroleum Society of CIM/CHOA Paper 79011 presented at the SPE International Thermal Operations and Heavy Oil Symposium and International Horizontal Well Technology Conference. Calgary, Alberta, Canada, November 4–7.

Lederer, E. L. **1933**. Viscosity of Mixtures with and without Diluents. *Proc World Pet Cong London*, 2, 526–528.

Lee, A. L., Gonzalez, M. H. and Eakin, B. E. **1966**. The Viscosity of Natural Gases. *J Petrol Technol*, 18 (8), 997-1000.

Lee, B. I. and Kesler, M. G. **1975**. A Generalized Thermodynamic Correlation Based on Three-Parameter Corresponding States. *AlChE J*, 21, 510-527.

Leland, T.W. and Chappelear, P.S. **1968**. The Corresponding States Principle—a Review of Current Theory and Practice. *Ind Eng Chem*, 60, 15-43.

Letsou, A. and Stiel, L. I. **1973**. Viscosity of Saturated Nonpolar Liquids at Elevated Pressures. *AIChE J*, 19(2), 409-411.

Li, H. Z. and Yang, D. T. **2012**. Phase Behaviour of C3H8-n-C4H10-Heavy Oil Systems at High Pressures and Elevated Temperatures. paper 157744 presentted in SPE Heavy Oil Conference Canada, 2-14 June , Calgary, Alberta, Canada.

Li, H. Z., Zheng, S. and Yang, D. T. **2011**. Enhanced Swelling Effect and Viscosity Reduction of Solvents-CO2-Heavy Oil Systems. paper 150168 presented in SPE Heavy Oil Conference and Exhibition, 12-14 December, Kuwait City, Kuwait

Lindeloff, N., Pedersen, K. S., Ronningsen, H. P. and Milter, J. **2004**. The Corresponding States Viscosity Model Applied to Heavy Oil Systems. *J Can Petroleum Technol*, 43(9), 47-53.

Little, J. E. and Kennedy, H. T. **1968**. A Correlation of the Viscosity of Hydrocarbon Systems with Pressure, Temperature and Composition. *SPE J*, 8(2), 157-162.

Lobe, V. M. **1973**. A Model for the Viscosity of Liquid–Liquid Mixtures. M.Sc. Thesis. University of Rochester, NY, USA.

Lohrenz, J., Bray, B. G. and Clark, C. R. 1**964**. Calculating Viscosities of Reservoir Fluids from their Compositions. *J Pet Technol*, 16, 1171–1176.

Loria, H., Pereira-Almao, P. and Satyro, M. **2009**. Prediction of Density and Viscosity of Bitumen Using the Peng-Robinson Equation of State. *Ind Eng Chem Res*, 48(22), 10129-10135.

Lucas, K. **1980**. Phase Equilibria and Fluid Properties in the Chemical Industry, Dechema, Frankfurt, p.573.

Luhning, R. W., Das, S. K., Fisher, L. J., Bakker, J., Grabowski, J., Engeleman, J. R., Wong, S., Sullivan, L. A. and Boyle, H. A. **2003**. Full Scale VAPEX Process-Climate Change Advantage and Economic Consequences. *J Can Pet Technol*, 42, 29-33.

Mathias, P. M.; Naheiri, T. and Oh, E. M. **1989**. A Density Correction for the Peng-Robinson Equation of State, *Fluid Phase Equilib*, 47, 77−87.

Mathias, P. M. and Copeman, T. W. **1983**. Extension of the Peng-Robinson Equation of State to Complex Mixtures: Evaluation of the Various Forms of the Local Composition Concept, *Fluid Phase Equilib*, 13, 91−108.

Maxwell, J. B. and Bonnell, L. S. **1957**. Derivation and Precision of a New Vapor Pressure Correlation for Petroleum Hydrocarbons. *Ind Eng Chem*, 49(7), 1187-1196.

McAllister, R. A. **1960**. The Viscosity of Liquid Mixtures. *AIChE J*, 6, 427–431.

McCain, W. D. **1990**. The properties of petroleum fluids. PennWell Corporation.

Mehrotra, A. K, Monnery, W. D. and Svrcek, W. Y. **1996**. A Review of Practical Calculation Methods for Viscosity of Liquid Hydrocarbons and Their Mixtures. *Fluid Phase Equilib*, 117, 344-355.

Mehrotra, A. K. **1994**. Correlation and prediction of the viscosity of pure hydrocarbons. *Can J Chem Eng*, 72(3), 554-557.

Mehrotra, A. K. **1992a**. Mixing Rules for Predicting the Viscosity of Bitumens Saturated with Pure Gases. *Can J Chem Eng*, 70, 165-172.

Mehrotra, A. K. **1992b**. A model for the viscosity of bitumen/bitumen fractions-diluent blends. *J Can Pet Tech*, *31*, 28-28.

Mehrotra, A. K. **1991a**. A generalized viscosity equation for pure heavy hydrocarbons. *Ind Eng Chem Res*, 30(2), 420-427.

Mehrotra, A. K. **1991b**. Generalized one-parameter viscosity equation for light and medium liquid hydrocarbons. *Ind Eng Chem Res*, 30(6), 1367-1372.

Mehrotra, A. K. **1990a**. Modeling the effects of temperature, pressure, and composition on the viscosity of crude oil mixtures. *Ind Eng Chem Res*, 29(7), 1574-1578.

Mehrotra, A. K. **1990b**. Development of Mixing Rules for Predicting the Viscosity of Bitumen and Its Fractions Blended with Toluene. *Can J Chem Eng*, 68, 839-848.

Mehrotra, A. K. Eastick, R. R. and Svrcek, W. Y. **1989**. Viscosity of Cold Lake Bitumen and Its Fractions. *Can J Chem Eng*, 67, 1004-1009.

Mehrotra, A. K. and Svrcek, W. Y. **1988**. Properties of Cold Lake Bitumen Saturated with Pure Gases and Gas Mixtures. *Can J Chem Eng*, 66, 656-665.

Mehrotra, A. K., Svrcek, W. Y. **1987**. Viscosity of Compressed Cold Lake Bitumen. *Can J Chem Eng*, **65**, 672-675.

Mehrotra, A. and Svrcek, W. **1987**. Corresponding states method for calculating bitumen viscosity. *J Can Pet Tech*, 26(5), 60-66.

Mehrotra, A. K., Svrcek, W. Y. **1986**. Viscosity of Compressed Athabasca Bitumen. *Can J Chem Eng*, **64**, 844-847.

Mehrotra, A. K. and Svrcek, W. Y. **1985a**. Viscosity, Density and Gas Solubility Data for Oil Sand Bitumens. Part I: Athabasca Bitumen Saturated with CO and C_2H_6. *AOSTRA J Res*, 1(4), 263-268.

Mehrotra, A. K. and Svrcek, W. Y. **1985b**. Viscosity, Density and Gas Solubility Data for Oil Sand Bitumens. Part 11: Peace River Bitumen Saturated with N_2, CO, CH_4, CO_2, and C_2H_6. *AOSTRA J Res*, 1(4), 269-279.

Mehrotra, A. K. and Svrcek, W. Y. **1985c**. Viscosity, Density and Gas Solubility Data for Oil Sand Bitumens. Part 111: Wabasca Bitumen Saturated with with N_2, CO, CH_4, CO_2, and C_2H_6. *AOSTRA J Res*, 2(2), 83-93.

Mehrotra, A. K. and Svrcek, W. Y. **1984**. Measurement and Correlation of Viscosity, Density and Gas Solubility for Marguerite Lake Bitumen Saturated with Carbon Dioxide. *AOSTRA J Res*, 1(1), 51-62.

Mehrotra, A. K. and Svrcek, W. Y. **1982**. Correlations for Properties of Bitumen Saturated with CO_2, CH_4, and N_2, and Experiments with Combustion Gas Mixture. *J Can Pet Tech*, 21(6):95-104.

Miadonye, A., Latour, N and Puttagunta, V. R. **2000**. A Correlation for Viscosity and Solvent Mass Fraction of Bitumen-Diluent Mixtures. *Pet Sci Technol*, 18, 1–14.

Mo, K. C. and Gubbins, K. E. 1974. Molecular Principle of Corresponding States for Viscosity and Thermal Conductivity of Fluid Mixtures. *Chem Eng Commun*, 1, 281-290.

Moharam, H. M. and Fahim, M. A. **1995**. Prediction of Viscosity of Heavy Petroleum Fractions and Crude Oils Using a Corresponding States Method. *Ind Eng Chem Res*, 34(11), 4140-4144.

Mollerup, J. **1979**. *Advances in Cryogenic Engineering* 20, (Plenum Press, NY) 172.

Monnery, W. D.; Mehrotra, A. K. and Svercek, W. Y. **1995**. Viscosity: A Critical Review of Practical Predictive and Correlative Methods. *Can J Chem Eng*, 73, 3-40.

Monnery, W. D., Mehrotra, A. K. and Svercek, W. Y. **1991**. Modified Shape Factors for Improved Viscosity Predictions Using Corresponding States. *Can J Chem Eng*, 69, 1213-1219.

Nabizadeh, H. and Mayinger, F. **1999**. Viscosity of Binary Mixtures of Hydrogen and Ntural Gas (Hythane) in the Gaseous Phase. *High Temperatures−High Pressures*, 31, 601−612.

Nasr, T. N. and Ayodele, O. R. **2006**. New Hybrid Steam-Solvent Processes for the Recovery of Heavy Oil and Bitumen. Paper SPE 101717 presented at the 2006 Abu Dhabi International Petroleum Exhibition and Conference., Abu Dhabi, U.A.E., 5-8 November 2006. doi: 10.2118/101717-MS.

Neufeld, P. D., Janzen, A. R. and Aziz, R. A. **1972**. Empirical Equations to Calculate 16 of the Transport Collision Integrals Ω for the Lennard-Jones (12–6) Potential. *J Chem Phys*, 57, 1100-1102.

Nieto-Draghi, C., Mackie, A. D. and Bonet A. J. **2005**. Transport Coefficients and Dynamic Properties of Hydrogen Sulfide from Molecular Simulation. *J Chem Phys*, 123, 014505-1–014505-8.

NIST. **2008**. NIST Standard Reference Database; NIST/TRC Source Database; WinSource, Version.

NIST. **2005.** NIST ThermoData Engine. Standard Reference Database #103b, version 7.0; National Institute of Standards and Technology, Gaithersburg, MD.

Nji, G. N., Svrcek, W. Y., Yarranton H. W. and Satyro, M. A. **2008**. Characterization of Heavy Oils and Bitumens. 1. Vapor Pressure and Critical Constant Prediction Method for Heavy Hydrocarbons. *Energy Fuels*, 22(1), 455–462.

Okeson, K. J. and Rowley, R. L. **1991**. A four-parameter corresponding-states method for prediction of Newtonian, pure-component viscosity. *Int Jof Thermophys*, 12(1), 119-136.

Oldenburg, T. B. P., Yarranton, H. W. and Larter, S. R. **2010**. The Effect of Low Molecular Weight Multifunctional Additives on Heavy Oil Viscosity. Paper CSUG/SPE 137505 presented at the 2010 the Canadian Unconventional Resources and International Petroleum Conference, Calgary, Alberta, Canada, 19-21 October.

Orrick , C. and Erbar, J. H. **1974**. in Chapter 9 of *The Properties of gases and Liquids*, McGraw-Hill (1987).

Padua, A., Wakeham, W. A. and Wilhelm, J. **1994**. The Viscosity of Liquid Carbon Dioxide. *Int J.Thermophys*, 15, 767-777.

Pal, A. K. and Bhattacharyya, P. K. **1969**. Viscosity of Binary Polar-Gas Mixtures. *J Chem Phys*, 51, 828–831.

Pal, A. K. And Barua, A. K. **1967**. Viscosity and Intermolecular Potentials of Hydrogen Sulfide, Sulfur Dioxide and Ammonia. *Trans Faraday Soc*, 63, 341–346.

Pandey, J. D., Vyas, V., Jain, P., Dubey, G. P., Tripathi, N. and Dey, R. **1991**. Speed of Sound, Viscosity and Refractive Index of Multicomponent Systems: Theoretical Predictions from the Properties of Pure Components. *J Mol Liq*, 81, 123-133.

Pedersen, K. S. and Christensen, P. L. **2007**. *Phase Behavior of Petroleum Reservoir Fluids*, CRC Press, Boca Raton, FL.

Pedersen, K. S., Milter, J. and Sørensen, H. **2004**. Cubic Equation of State Applied to HT/HP and Highly Aromatic Fluids, *SPE J*, 9, 186-192.

Pedersen, K. S., Fredenslund, Aa. **1987**. An Improved Corresponding States Model for the Prediction of Oil and Gas Viscosities and Thermal Conductivities. *Chem Eng Sci*, 42, 182-186.

Pedersen, K. S., Fredenslund, Aa, Christensen, P. L. and Thoassen, P. **1984**. Viscosity of Crude Oils. *Chem Eng Sci*, 39, 1011-1016.

Peneloux, A., Rauzy, E. and Freze, R. **1982**. A Consistent Correction for Redlich-Kwong-Soave Volumes, *Fluid Phase Equilib*, 8, 7−23.

Peng, D. Y. and Robinson, D. B. **1976**. A New Two-Constant Equation of State, *Ind Eng Chem Fundam*, 15, 59-64.

Petrosky, G. E. and Farshad, F. F. **1995**. Viscosity Correlations for Gulf of Mexico Crude Oils. SPE 29468 presented at the Production Operations Symposium, Oklahama City, OK, April 2-4.

Phillips, P. **1912**. The viscosity of carbon dioxide. *Proceedings of the Royal Society of London. Series A*, 87(592), 48-61.

Pitzer, K. S., Lippmann, D. Z., Curl Jr, R. F., Huggins, C. M. and Petersen, D. E. **1955**. The Volumetric and Thermodynamic Properties of Fluids. II. Compressibility Factor, Vapor Pressure and Entropy of Vaporization. *Journal of the American Chemical Society*, 77(13), 3433-3440.

Pitzer, K. S. **1939**. Corresponding States for Perfect Liquids. *J Chem Phys*, 7, 583-590.

Poling, B. E., Prausnitz, J. M. and O'Connell, J. P. **2000**. *The Properties of Gases and Liquids*, 5th Ed., McGraw-Hill: New York.

Queimada, A. J., Marrucho, I. M., Coutinho J. A. P. and Stenby, E. H. **2005**. Viscosity and Liquid Density of Asymmetric *n*-Alkane Mixtures: Measurement and Modeling. *Int J Thermophys*, 26, 47–61.

Queimada, A. J., Quiñones-Cisñeros, S. E., Marrucho, I. M., Coutinho, J. A. and Stenby, E. H. **2003**. Viscosity and Liquid Density of Asymmetric Hydrocarbon Mixtures. *Int. J. Thermophys*, 24, 1221-1239.

Quiñones-Cisneros, S. E., Schmidt, K. A., Creek, J. and Deiters, U. K. **2008**. Friction Theory Modeling of the Non-Newtonian Viscosity of Crude Oils. *Energy & Fuels*, 22(2), 799-804.

Quinones-Cisneros, S. E., Andersen S. I. and Creek, J. **2005**. Density and Viscosity Modeling and Characterization of Heavy Oils. *Energy & Fuels*, 19, 1314-1318.

Quiñones-Cisneros, S. E., Zéberg -Mikkelsen, C. K., Baylaucq, A. and Boned, C. **2004**. Viscosity Modeling and Prediction of Reservoir Fluids: From Natural Gas to Heavy Oils. *Int J Thermophys*, 25(5), 1353-1366.

Quiñones-Cisneros, S. E, Zéberg -Mikkelsen, C. K., Stenby, E. H. **2003**. Friction theory prediction of crude oil viscosity at reservoir conditions based on dead oil properties. *Fluid Phase Equilib*, 212, 233-243.

Quiñones-Cisneros, S. E, Zéberg -Mikkelsen, C. K., Stenby, E. H. **2001**. The Friction Theory for Viscosity Modrling: Extension to Crude Oil Systems. *Chem Eng Sci*, 56, 7007-7015.

Quiñones-Cisneros, S. E., Zéberg -Mikkelsen, C. K. and Stenby, E. H. **2001**. One Parameter Friction Theory Models for Viscosity. *Fluid Phase Equilib*, 178, 1-16.

Quiñones-Cisneros, S. E., Zéberg -Mikkelsen, C. K. and Stenby, E. H. **2000**. The Friction Theory (f-theory) for Viscosity Modeling. *Fluid Phase Equilib*, 169, 249-276.

Rackett, H. G. **1970**. Equation of State for Saturated Liquids. *J Chem Eng Data*, 15, 514-527.

Rahmes, M. H. and Nelson, W. L. **1948**. Viscosity Blending Relationships of Heavy Petroleum Oils. *Analytical Chem*, 20, 912-915.

Rankine, A. O. and Smith, C. J. **1921**. The Viscosities and Molecular Dimensions of Methane, Sulphuretted Hydrogen and Cyanogen. *Philos Mag*, 42, 615–620.

Reichenberg, D. **1979**. The Estimation of the Viscosities of Gases and Gas Mixtures. *Symp. Transp. Prop. Fluids. and Fluid Mixtures, Natl. Eng. Lab.*, East Kilbride, Glasgow, Scotland.

Reichenberg, D. **1975**. New methods for the estimation of the viscosity coefficients of pure gases at moderate pressures (with particular reference to organic vapors). *AIChE J*, 21(1), 181-183.

Reid, R. C., Prausnitz, J. M. and Poling, B. E. **1987**. *The Properties of gases and Liquids*. McGraw-Hill (1987).

Riazi, M. R. **2005**. *Characterization and Properties of Petroleum Fractions*. American Society for Testing and Materials, West Conshohocken, PA, USA.

Riazi, M. R. and Daubert, T. E. **1980**. Simplify property predictions. *Hydrocarbon Process*, 59 (3), 115-116.

Robinson, D. B. and Peng, D. Y. **1978**. The Characterization of the Heptanes and Heavier Fractions. Reasearch Report 28, Gas Producers Assn., Tulsa, Oklohoma.

Ronningsen, H. P. **1993**. Prediction of viscosity and surface tension of North Sea petroleum fluids by using the average molecular weight. *Energy & Fuels*, 7, 565-573.

Rowlinson, J. S. and Watson, I. D. **1969**. The prediction of the thermodynamic properties of fluids and fluid mixtures-I The principle of corresponding states and its extensions. *Chemical Engineering Science*, 24(10), 1565-1574

Runovskaya, I. V., Zorin, A. D. and Devyatykh, G. G. **1970**. Viscosity of Condensed Volatile Inorganic Hydrides of Group III-VI Elements. *Russ J Inorg Chem*, 15, 1338–1339.

Sarkar, M. **1984**. Property prediction of gas saturated bitumen. M.Sc. Dissertation, Department of Chemical and Petroleum Engineering, University of Calgary.

Saryazdi, F. **2012**. Density Prediction for Mixtures of Heavy Oil and Solvents, M.Sc. Dissertation, Department of Chemical and Petroleum Engineering, University of Calgary.

Satyro, M. A. and Yarranton, H. W. **2010**. Expanded Fluid Based Viscosity Correlation for Hydrocarbons Using an Equation of State. *Fluid Phase Equilib*, 298, 1-11.

Satyro, M. A. **2009**. The Role of Thermodynamic Modeling Consistency in Process Simulation, 8th World Congress of Chemical Engineering, Palais des Congres, Montreal, August 23-27.

Schlumberger. **2005**. PVTi and ECLIPSE 300: An Introduction to PVT analysis and compositional simulation. Abingdon Technology Center Training.

Schmidt, K. A. G., Quinones-Cisneros, S. E., Carroll, J. J. and Kvamme. B. **2008**. Hydrogen Sulfide Viscosity Modelling. *Energy & Fuels*, 22, 3424–3434.

Schramm, L. L. and Kwak, J. **1988**. The Rheological Properties of an Athabasca Bitumen and Some Bituminous Mixtures and Dispersions. *J Can Pet Tech*, 27(1).

Seeton, C. J. **2006**. Viscosity–temperature correlation for liquids. *Tribology Letters*, 22(1), 67-78.

Sheng, W., Chen, G. J. and Lu, H. C. **1989**. Prediction of transport properties of dense gases and liquids by the Peng-Robinson (PR) equation of state. *Int J Thermophys*, 10(1), 133-144.

Shu, W. R. **1984**. A Viscosity Correlation for Mixtures of Heavy oil, Bitumen, and Petroleum Fractions. *Soc Pet Eng J*, 24(3), 277-282.

Silva, A. A., Reis, R. A., Paredes, M. L. L. **2009**. Density and Viscosity of Decalin, Cyclohexane, and Toluene Binary Mixtures at (283.15, 293.15, 303.15, 313.15, and 323.15) K. *J Chem Eng Data*, 54, 2067–2072.

Singhal, A. K., Das, S. K., Leggitt, S. M., Kasraiem M. and Ito, Y. **1996**. Screening of Reservoirs for Exploitation by Application of Steam Assisted Gravity Drainage/VAPEX Processes. paper SPE 37144 presented at the International Confernce on Horizontal Well Technology. Calgary, Alberta, Canada, 18-20 November.

Soave, G. **1972**. Equilbrium Constants from a Modified Redlich-Kwong Equation of State. *Chem.Eng Sci*, 27(6), 1197-1203.

Søreide, I. **1989**. Improved Phase Behavior Predictions of Petroleum Reservoir Fluids From a Cubic Equation of State, "Dr. Ing. Dissertation, Norwegian Inst. Of Technology,.

Speight , J. G. **2007**. The Chemistry and Technology of Petroleum, 4th Ed.. Marcel Dekker Inc., New York.

Speight , J. G. **1999**. The Chemistry and Technology of Petroleum, 3rd Ed.. Marcel Dekker Inc., New York.

Spencer, C. F. and Danner, R. P. **1972**. Improved Equation for Prediction of Saturated Liquid Density. *J Chem Eng Data*, 17, 236–241.

Stiel, L. I. and Thodos, G. **1964**. The viscosity of polar substances in the dense gaseous and liquid regions. *AIChE J*, 10(2), 275-277.

Stiel, L. I. and Thodos, G. **1961**. The viscosity of nonpolar gases at normal pressures. *AIChE J*, 7, 611-615.

Stryjek, R. and Vera, J. H. **1986**. PRSV—An improved peng-Robinson equation of state with new mixing rules for strongly nonideal mixtures. *Can J Chem Eng*, 64(2), 334-340.

Sun, T. and Teja, A. S. **2003**. Density, Viscosity, and Thermal Conductivity of Aqueous Ethylene, Diethylene, and Triethylene Glycol Mixtures between 290 K and 450 K. *J Chem Eng Data***,** 48, 198-202.

Sutton, R. anf Bergman, D. **2012**. Application of the Bergman-Sutton Method for Determining Blend Viscosity. *SPE Production & Operations*, 27(1), 106-124.

Svrcek, W. Y and Mehrotra, A. K. **1989**. Properties of Peace River Bitumen Saturated with Field Gas Mixtures. *J Can Pet Tech*, 28(2), 50-56.

Svrcek, W. Y and Mehrotra, A. K. **1988**. One Paramter Correlation For Bitumen Viscosity. *Chem Eng Res Des*, 66(4), 323-327.

Tanaka, Y., Hosokawa, H., Kubota, H. and Makita, T. **1991**. Viscosity and Density of Binary Mixtures of Cyclohexane with n-Octane, n-Dodecane, and n-Hexadecane under High Pressures. *Int J Thermophys*, 12, 245-264.

Teja, A. S. And Thurner, P. A. **1986**. The correlation and prediction of the viscosities of mixtures over a wide range of pressure and temperature. *Chem eng comm*, 49(1-3), 69-79.

Teja, A. S. and Rice, P. **1981a**. Generalized Corresponding States Method for the Viscosities of Liquid Mixtures. *Ind Eng Chem Fundam*, 20, 77-81.

Teja, A. S. and Rice, P. **1981b**. A Multifluid Corresponding States Principle for the Thermodynamic Properties of Fluid Mixtures. *Chem Eng Sci*, 36(1), 1-6.

Tham, M. J. and Gubbins, K. E. **1970**. Correspondence principle for transport properties of dense fluids. Nonpolar polyatomic fluids. *Ind Eng Chem Fundamentals*, 9(1), 63-70.

Tharanivasan, A. K. **2012**. Asphaltene Precipitation from Crude Oil Blends, Conventional Oils, and Oils with Emulsified Water. Doctoral dissertation, UNIVERSITY OF CALGARY.

Tohidi, B., Burgass, R., Danesh, A. and Todd, A. C. **2001a**. Viscosity and Density of Methane+Methylcyclohexane from 323 to 423 K at Pressures to 140 MPa. *J Chem Eng Data* , 46, 385–390.

Tohidi, B., Todd, A. C., Danesh, A., Burgass, R. W. and Gozalpour, F. **2001b**. Viscosity and Density of Methane+cis-Decalin from 323 to 423 K at Pressures to 140 MPa. *Int J Thermophys*, 22, 1661–1668.

Tomida, D., Kumagai, A. and Yokoyama, C. **2007**. Viscosity Measurements and Correlation of the Squalane + CO_2 Mixture. *Int J Thermophys*, 28, 133-145.

TRC. **1985.** *TRC Thermodynamic Tables-Hydrocarbons Volume III*. Thermodynamic Research Center, Texas A&M University, College Station, TX.

Twu, C. H. **1985**. Internally Consistent Correlation for Predicting the Liquid Viscosities of Petroleum Fractions. *Ind Eng Chem Process Des Dev*, 24 (2), 1287–1293.

Twu, C. H. **1984**. An Internally Consistent Correlation for Predicting the Critical Properties and Molecular Weights of Petroleum and Coal-Tar Liquids. *Fluid Phase Equilib*, 16, 137–150.

Twu, C. H. and Bulls, J. W. **1981**. Viscosity Blending Tested. *Hydrocarbon Processing*, 60, 217-218.

Upreti, S. R., Lohi, A., Kapadia, A., El-Haj, R. **2007**. Vapor Extraction of Heavy Oil and Bitumen: A Review. *Energy & Fuels*, 21, 1562-1574.

van der Gulik, P. S. **1997**. Viscosity of Carbon Dioxide in the Liquid Phase. *Physica A*, 238, 81-112.

van Velzen, D., Cardozo, R. L. and Langenkamp, H. **1972**. A liquid viscosity-temperature-chemical constitution relation for organic compounds. *Ind Eng Chem Fundamentals*, 11(1), 20-25.

Vesovic, V. and Wakeham, W. A. **1989**. Prediction of the Viscosity of Fluid Mixtures Over Wide Ranges of Temperature and Pressure. *Chem Eng Sci*, 44 (10), 2181−2189.

Virtual Materials Group, Inc. **2011**. VMGSim Process Simulator, version 6.5. Calgary, AB, Canada.

Virtual Materials Group, Inc. **2009**. VMGSim Version 5.0 User's Manual. Calgary, AB, Canada.

Viswanath, D. S. and Natarajan, G. **1989**. *Data Book on the Viscosity*. Hemisphere Pub. Corp., New York.

Vogel, E., Dobbert, K., Meissner, K., Ruh, U. and Bich, E. **1991**. Initial Density Dependence of Experimental Viscosities and of calculated Diffusion Coefficients of the Binary Vapor Mixtures Methanol-Benzene and Methanol-Cyclohexane. *Int J of Thermophys*, 12(3), 469-490.

Vogel, H. **1921**. Temperature Dependence of Viscosity of Melts. *Phys. Z*, 22, 645-646.

Wakefield, D. L., Marsh, K. N. and Zwolinski, B. J. **1998**. Viscosities of Nonelectrolyte Liquid Mixtures. II. Binary and Quaternary Systems of Some *n*-alkanes. *Int J Thermophys*, 9, 47-59.

Walther, C. **1931**. The Evaluation of Viscosity Data. *Erdol Teer*, 7, 382-384.

Watson, K. M., Nelson, E. F. and Murphy, G. B. **1935**. Characterization of Petroleum Fractions. *Ind Eng Chem*, 27(12), 1460-1464.

Whitson, C. and Brule, M. **2000**. *Phase Behavior*, Monograph vol. 20, Soc. Petrol. Eng..

Wilke, C. R. **1950**. A Viscosity Equation for Gas Mixtures. *J Chem Phys*, 18, 517-519.

Wright, W. A. **1969**. An Improved Viscosity-Temperature Chart for Hydrocarbons. *Journal Materials*, 4(1), 19-25.

Wu, J. and Asfour, A. F. A. **1992**. Viscometric Properties of n-Alkane Liquid Mixtures. *Fluid Phase Equilib*, 76, 283-294.

Xu, D. H., and Khurana, A. K. **1996**. A Simple and Efficient Approach for Improving the Prediction of Reservoir Fluid Viscosity. paper SPE 37011 presented at the 1996 SPE asia Pacific Oil and Gas Conference, Adelaide, Australia, 28-31 October.

Yamada, T. and Gunn, R. D. **1973**. Saturated Liquid Molar Volumes. The Rackett Equation. *J Chem Eng Data*, 18, 234–236.

Yang, C., Xu, W. and Ma, P. **2005**. Thermodynamic properties of binary mixtures of p-xylene with cyclohexane, heptane, octane, and N-methyl-2-pyrrolidone at several temperatures. *J. Chem. Eng. Data* **2005**, *50*, 732.

Yang, C., Xu, W. and Ma, P. **2004**. Thermodynamic Properties of Binary Mixtures of p-Xylene with Cyclohexane, Heptane, Octane, and N-methyl-2-Pyrrolidone at Several Temperatures. *J Chem Eng Data*, 49, 1794-1801.

Yarranton, H. W. and Satyro, M. A. **2009**. Expanded Fluid-Based Viscosity Correlation for Hydrocarbons. *Ind Eng Chem Res*, 48, 3640–3648.

Yasutomi, S., Bair, S. and Winer, W. O. **1984**. An application of a free volume model to lubricant rheology. I: dependence of viscosity on temperature and pressure. II: Variation in viscosity of binary blended lubricants. *Journal of tribology*, 106(2), 291-312.

Yaws, C. L. **1999**. *Chemical Properties Handbook: Physical, Thermodynamic, Environmental, Transport, Safety, and Health Related Properties for Organic and Inorganic Chemicals*. McGraw-Hill.

Yaws, C. L. **2008**. *Transport Properties of Chemicals and Hydrocarbons*. William Andrew Inc., Norwich, NY, USA.

Yazdani. A. and Maini, B.B. **2010**. Measurements and Modelling of Phase Behaviour and Viscosity of a Heavy Oil/Butane System. *J Can Pet Tech*, 49(2), 8-14.

Younglove, B.A. and Ely, J.F. **1987**. Thermophysical Properties of Fluids: II. Methane, Ethane, Propane, Isobutane, and Normal Butane *J. Phys. Chem. Ref. Data.* 16, 577-798.

Yves, M. **2007**. *The Hydrogen Bond and the Water Molecule : The Physics and Chemistry of Water, Aqueous and Bio Media*, Elsevier, Amsterdam, Netherlands.

Zéberg-Mikkelsen, C. K., Barrouhou, M., Baylaucq, A. And Boned, C. **2003**. High-Pressure Viscosity and density Measurements of the Ternary System Methylcyclohexane+cis-Decalin+2,2,4,4,6,8,8-Heptamethylnonane. *J Chem Eng Data*, 48, 1387-1392.

Zéberg-Mikkelsen, C. K., Barrouhou, M., Baylaucq, A. and Boned, C. **2003**. Viscosity and Density Measurements of Binary Mixtures Composed of Methylcyclohexane+cis-Decalin versus Temperature and Pressure. *Int J Thermophys*, 24,361-374.

Zéberg-Mikkelsen, C. K., Barrouhou, M., Baylaucq, A. and Boned, C. **2002**. Measurement of the Density and Viscosity versus Temperature and Pressure for the Binary System Methylcyclohexane+2,2,4,4,6,8,8-Heptamethylnonane. *High temperatures-High Pressures*, 34, 591-601.

Zéberg-Mikkelsen, C. K., Canet, X., Quiñones-Cisñeros, S. E., Baylaucq, A., Allal, A., Boned, C. and Stenby, E. H. **2001a**. Viscosity Modeling of the Ternary System 1-Methylnaphthalene + n-Tridecane + 2,2,4,4,6,8,8-Heptamethylnonane up to 100 MPa. *High Pres. Res*, 21, 281–303.

Zéberg-Mikkelsen C. K., Canet X., Baylaucq A., Quiñones-Cisneros S. E., Boned C. and Stenby E. H. **2001b**. High Pressure Viscosity and Density Behavior of Ternary Mixtures: 1-Methylnaphthalene + n-Tridecane + 2,2,4,4,6,8,8-Heptamethylnonane. *Int J Thermophys*, 22, 1691–1726.

Zhao, L. **2004**. Steam Alternating Solvent Process. paper SPE 86957 presented at the SPE International Thermal Operations and Heavy Oil Symposium and Western Regional Meeting. Bakersfield, California, USA, 16-18 March.

Zuo, J. Y., Zhang, D. D. and Creek, J. **2008**. Modeling of Phase Equilibria and Viscosity of Heavy Oils. paper 2008-392 presented and published in the Proceedings for the World Heavy Oil Congress held in Edmonton Canada, 10-12 March.

APPENDIX A: VISCOSITY AND DENSITY DATA OF VISCOSITY STANDARDS

Table A.1: Properties of the viscosity standards purchased from Cannon Instruments Inc.

Standard Description	Temp. (°C)	Viscosity (mPa.s)	Density (kg/m^3)
S20 Manufactured: 3/6/2008, Lot Number: 08201	20.00	37.37	0.8617
	25.00	29.13	0.8584
	37.78	16.69	0.8502
	40.00	15.30	0.8488
	50.00	10.68	0.8424
	80.00	4.614	0.8231
	98.89	3.099	0.8109
	100.00	3.035	0.8102
S30000 Manufactured: 2/29/2008, Lot Number: 07101a	25.00	75230	0.8939
	37.78	24710	0.8870
	40.00	20660	0.8858
	50.00	9625	0.8804
	80.00	1443	0.8644
	100.00	530.6	0.8538
N450000 Manufactured: 4/4/2008, Lot Number: 07101a	25.00	1639000	
	60.00	107100	
	135.00	2606	

APPENDIX B: PENG-ROBINSON EQUATION OF STATE AND VOLUME TRANSLATIONS

B.1 Peng-Robinson Equation of State (PR EoS)

The PR EoS is cubic equation of state is defined as follows (Peng and Robinson, 1976):

$$P = \frac{RT}{v-b} - \frac{a}{v^2 + 2bv - b^2} \tag{B.1}$$

where b is the co-volume given by:

$$b = \frac{0.0777969 RT_c}{P_c} \tag{B.2}$$

and *a* is the attractive term given by:

$$a = a_c \alpha(T) \tag{B.3}$$

$$a_c = \frac{0.457235 R^2 T_c^{\,2}}{P_c} \tag{B.4}$$

where $\alpha(T)$ is an empirical dimensionless scaling function of temperature. This empirical function is correlated to acentric factor for non-polar or slightly pure components, such as hydrocarbons, as follows:

$$\alpha = \left[1 + f_\omega \left(1 - \sqrt{T_r}\right)\right]^2 \tag{B.5}$$

where T_r is the reduced temperature and f_ω is given by (Peng and Robinson, 1976; Robinson and Peng, 1978):

for ω<0.5: $$f_\omega = 0.37464 + 1.54226\omega - 0.26992\omega^2 \tag{B.6}$$

for ω=>0.5: $$f_\omega = 0.3796 + 1.4850\omega - 0.1644\omega^2 + 0.01666\omega^3 \tag{B.7}$$

The parameters *a* and *b* are calculated for the mixtures using the following mixing rules:

$$a = \sum_i \sum_j \left(1 - k_{ij}\right) \sqrt{a_i a_j}\, x_i x_j \tag{B.8}$$

$$b = \sum_i x_i b_i \tag{B.9}$$

where x_i is the mole fraction of component *i* and k_{ij} is the interaction parameter between components *i* and *j* and determined based on experimental vapor-liquid equilibrium data.

B.2 Advanced Peng-Robinson Equation of State (APR EoS)

The Advanced Peng-Robinson equation of state (APR EoS) (Satyro 2009) is a modification of the Peng-Robinson equation of state and is implemented in VMGSim process simulator package. The APR EoS utilizes Equations B.1 to B.4 and B.8 and B.9, but the empirical dimensionless scaling function of temperature ($\alpha(T)$) is defined in the following general form (Mathias and Copemen, 1983):

$$\alpha(T)=\left[1+A'\left(1-\sqrt{T_r}\right)+B'\left(1-\sqrt{T_r}\right)^2+C'\left(1-\sqrt{T_r}\right)^3\right]^2 \tag{B.10}$$

where constants A', B' and C' are fluid-specific coefficients and are determined by fitting the vapor pressure predicted by the equation of state against experimental vapor pressure data.

The implementation of the APR EoS in VMGSim uses default values of zero for B' and C' *and* calculates A' by Equations B.6 and B.7 as function of acentric factor for non-polar and slightly polar components. For highly polar components such as water, glycols and methanol, the values of A', B' and C' are individually regressed.

To correct the deficiency of PR EoS in liquid density calculations, the volume translations are implemented in APR EoS using the method suggested by Mathias et al. (1989) as follows:

$$v^T = v^{APR} + s + f_c\left(\frac{0.41}{0.41+\delta}\right) \tag{B.11}$$

where v^T is the translated molar volume, v^{APR} is the molar volume as calculated by the APR EoS and s is the volume shift. f_c is a correction factor to match the experimental critical volume (v_c) and is given by:

$$f_c = v_c - (3.946b + s) \tag{B.12}$$

and δ is the dimensionless inverse of isothermal compressibility given by:

$$\delta = -\frac{v^2}{RT}\left(\frac{\partial P}{\partial v}\right)_T \tag{B.13}$$

The values of the volume translation (s) in APR EoS is determined by matching the experimental liquid molar volume of the compounds at 298 K or the normal boiling point

whichever is smaller. Note that the presence of parameter δ implies pressure dependency of the volume translation value. This form of the volume translations was originally proposed by Mathias et al. (1989) for light hydrocarbons and provides better density predictions for lighter compounds as shown for as propane in Figure B.1a and b. However, the APR EoS over-predicts the liquid density of heavier compounds at temperatures higher than 298 K and less than the critical temperature, Figure B.2a and b for n-heptane. The higher the critical temperature of the compound the greater is the magnitude of the over predictions.

The volume translation for the mixtures is also given by:

$$s_{mix} = \sum_i s_i x_i + s^{Excess}\left(T, \vec{x}\right) \tag{B.14}$$

$$s^{Excess}\left(T, \vec{x}\right) = \sum_{i=1}^{nc} x_i \ln \sum_{j=1}^{nc} x_j a_{ij} \tag{B.15}$$

where a_{ij} is the binary cross term and is given by:

$$a_{ij} = e^{A_{ij} + \frac{B_{ij}}{T}} \tag{B.16}$$

where A_{ij} and B_{ij} are adjustable constants that can be used to match liquid densities of mixtures. The default value of these constants are zero unless otherwise set.

B.3 PR EoS with Temperature-Pressure Dependent Volume Translation

More sophisticated form of volume translations is required to overcome the insufficiency of APR EoS in estimating the liquid density of the heavier hydrocarbons at temperatures higher than 298 K. As plotted in Figures B.1 and B.2, the temperature-dependent volume translations used in Chapter 7 also is incompetent to provide accurate density predictions, especially in the vicinity of the critical point as well as at high pressures.

One solution to improve the density estimations is to combine the form of volume translations proposed by Mathias et al. (1989) as implemented in APR EoS with temperature-dependent volume translations as used in Chapter 7. Hence, the volume

translations are defined by Equations B.11, B.12 and B13 as it is in APR EoS, but the volume shift parameter (s) is a function of temperature as follows:

$$s = \gamma'_0 + \gamma'_1 (T - 288.75) \tag{B.17}$$

where T is temperature in K, γ'_0 is the fixed volume shift and γ'_1 is the temperature dependency term. The values of γ'_0 and γ'_1 must be determined for each component by matching the predicted liquid molar volumes by the equation of state to the actual measured molar volumes of the saturated liquids at two given temperatures.

Numerical values of the γ'_0 and γ'_1 for n-paraffin compounds and carbon dioxide are given in Table B.1. These values were determined by matching the predicted molar volumes of these compounds by equation of state to the actual molar volumes of the statured liquids (Yaws 1999) at two temperatures, 288.75 K (60 °F) and the reduced temperature (T_r) of 0.85. For the components with $0.85T_r$ below 288.75 K, the saturated liquid molar volume at the normal boiling point was used instead of at 288.75 K.

Table B.1: Constants of temperature dependent volume shift, Equation B.17, for some pure compounds.

Component	γ'_0 **(cm³/mol)**	γ'_1 **(cm³/mol.K)**
carbon dioxide	-2.9697	-0.0103
methane	-4.0841	0.0018
Ethane	-5.7979	-0.0088
propane	-5.7156	-0.0063
n-butane	-6.1646	-0.0164
n-pentane	-4.4077	-0.0180
n-hexane	-1.2118	-0.0220
n-heptane	1.7921	-0.0329

This form of volume translations benefits from two strengths of volume translation method by Mathias et al. (1989): 1) it matches the experimental critical volume of the compounds; and 2) the parameter δ (Equation B.13) introduces information about the compressibility of the compound into the formulation of the volume translations. Hence, the liquid density estimations in the vicinity of the critical point as well as at higher pressure conditions are considerably improved, Figures B.1 and B.2, in comparison to the simple volume translation introduced in Chapter 7. In addition, the temperature

dependent volume shift (Equation B.17) overcomes the insufficiency of APR EoS and improves the match to saturated liquid densities.

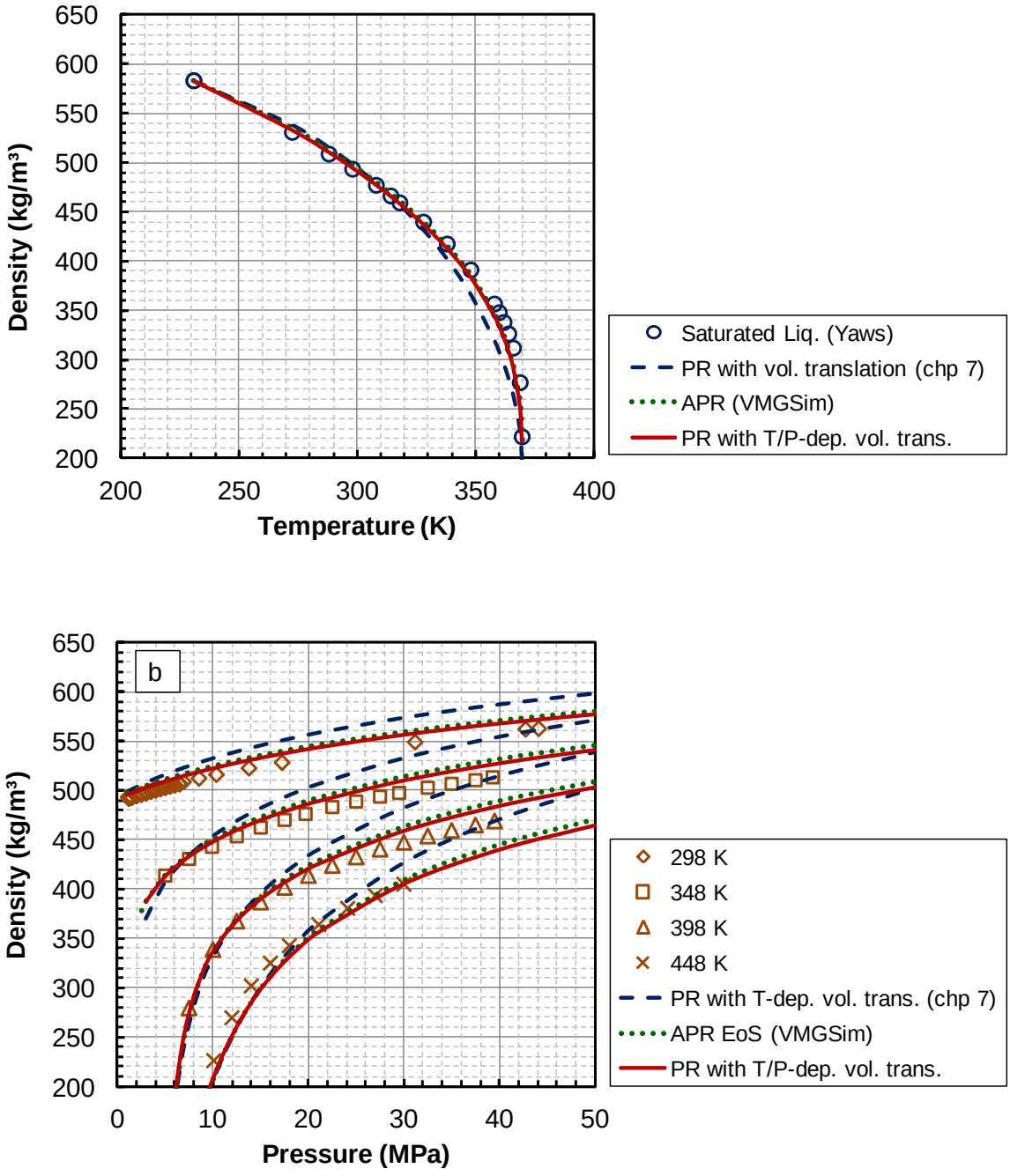

Figure B.1: Measured and predicted by EoS density of propane: a) saturated liquid density (data points calculated by Yaws (1999) correlation); and b) compressed liquid and super-critical fluid (data points from NIST (2008).

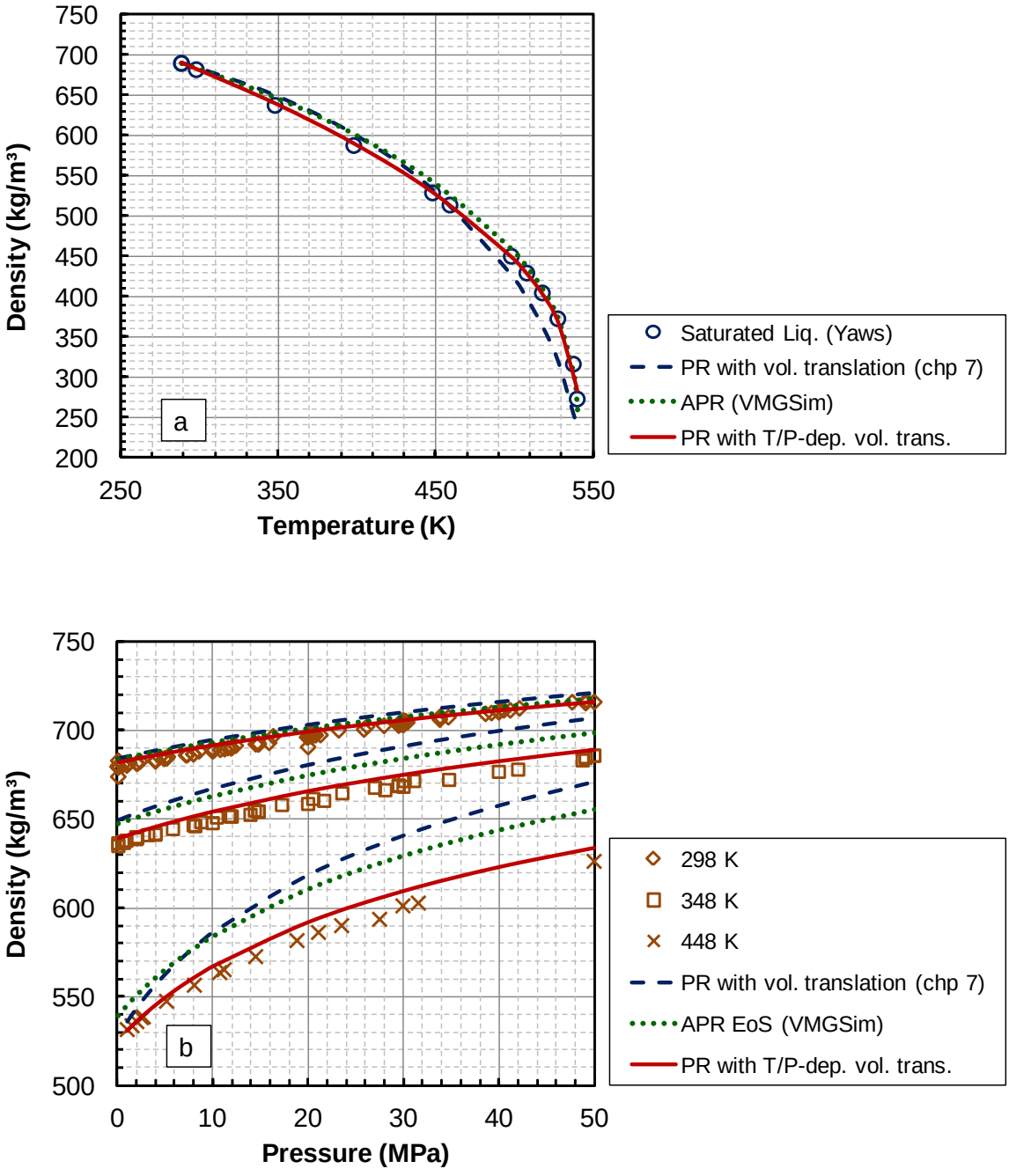

Figure B.2: Measured and predicted by EoS density of n-heptane: a) saturated liquid density (data points calculated by Yaws (1999) correlation); and b) compressed liquid and super-critical fluid (data points from NIST (2008).

Note that the PR EoS improved with the newly proposed volume translations consistently under-predicts the density of WC-B-B3 diluted with single component solvents, Figure B.3. As the predictions of the EoS model for liquid density of the pure solvents are in close agreement with experimental data, the under-predictions are due to the excess volumes of mixing (Equation B.14) which are assumed to be zero for bitumen-solvent binary pairs. Determination of the excess volumes of mixing and correlation of them to the physical properties of the binary pairs are plausible but are not pursued in this study.

Note that, in Figure B.3, the predicted densities with temperature-dependent volume translations used in Chapter 7 are greater than the predictions with newly proposed volume translations. This compensation of the excess volumes is due to over-predicted liquid densities of the pure solvents by the PR EoS with temperature-dependent volume translations, Figures B.1 and B.2.

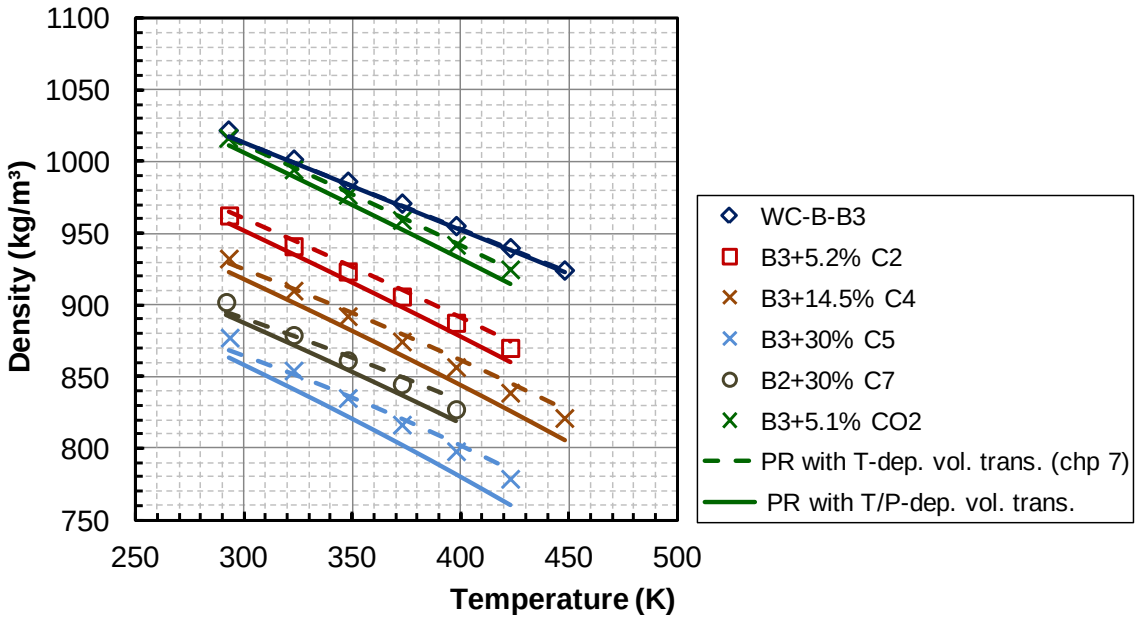

Figure 9B.3: Measured and EoS-estimated density of diluted WC-B-B3 with single component solvents at 10 MPa.

APPENDIX C: DETAILS OF HYDROCARBON MIXTURES DATASETS AND RESULTS OF CHAPTER FIVE

Table C.1: Summary of the experimental viscosity and density data of the mixtures used in Chapter 5. "*" denotes mixtures with available density data.

Mixture	Pressure (MPa)	Temp. (K)	Data Source
DATASET 1			
methane + n-decane*	10-75	303-393	Audonnet and Padua (2004)
methane + n-decane*	20-140	293-375	Canet et al. (2002)
DATASET 2			
methane+ethane*	1.5-35	100-300	Diller (1984)
methane+propane*	1.8-35	298-498	Bicher and Katz (1943)
methane+propane	0.1-55	310-410	Giddings et al. (1966)
methane+n-butane	0.14-36	277-478	Carmichael et al. (1967)
methane+n-hexane*	15-40	293-353	Berstad (1989)
n-pentane+n-octane	0.1-25	298-374	Barrufet et al. (1999)
n-pentane+n-decane	0.1-25	298-374	Estrada-Baltazar et al. (1998)
n-hexane+n-heptane*	0.1	298.15	Chevalier et al. (1990)
n-hexane+n-octane*	0.1	298.15	Chevalier et al. (1990)
n-hexane+n-nonane*	0.1	298.15	Chevalier et al. (1990)
n-hexane+n-decane*	0.1	298.15	Chevalier et al. (1990)
n-hexane+n-dodecane*	0.1	298.15	Chevalier et al. (1990)
n-hexane+n-dodecane*	0.1-178	298-373	Dymond et al. (1981)
n-hexane+n-tetradecane*	0.1	298.15	Chevalier et al. (1990)
n-hexane+n-hexadecane*	0.1	298.15	Chevalier et al. (1990)
n-hexane+n-hexadecane *	0.1-199	298-373	Chevalier et al. (1990)
n-heptane+n-octane*	0.1	298.15	Chevalier et al. (1990)
n-heptane+n-nonane*	0.1	298.15	Chevalier et al. (1990)
n-heptane+n-decane*	0.1	298.15	Chevalier et al. (1990)
n-heptane+n-decane	0.1-100	293-313	Ducoulombier et al. (1986)
n-heptane+n-dodecane*	0.1	298.15	Chevalier et al. (1990)
n-heptane+n-tetradecane*	0.1	298.15	Chevalier et al. (1990)
n-heptane+n-hexadecane*	0.1	298.15	Chevalier et al. (1990)

Mixture	Pressure (MPa)	Temp. (K)	Data Source
DATASET 2 (cont.)			
n-heptane+n-eicosane*	0.1	293-343	Queimada et al. (2003)
n-octane+n-nonane*	0.1	298.15	Chevalier et al. (1990)
n-octane+n-decane*	0.1	298.15	Chevalier et al. (1990)
n-octane+n-decane	0.1-25	297-374	Estrada-Baltazar et al. (1998)
n-octane+n-dodecane*	0.1	298.15	Chevalier et al. (1990)
n-octane+n-dodecane*	0.1-198	298-373	Dymond et al. (1981)
n-octane+n-tetradecane*	0.1	298.15	Chevalier et al. (1990)
n-octane+n-hexadecane*	0.1	298.15	Chevalier et al. (1990)
n-nonane+n-decane*	0.1	298.15	Chevalier et al. (1990)
n-nonane+n-dodecane*	0.1	298.15	Chevalier et al. (1990)
n-nonane+n-tetradecane*	0.1	298.15	Chevalier et al. (1990)
n-nonane+n-hexadecane*	0.1	298.15	Chevalier et al. (1990)
n-decane+n-dodecane*	0.1	298.15	Chevalier et al. (1990)
n-decane+n-tetradecane*	0.1	298.15	Chevalier et al. (1990)
n-decane+n-hexadecane*	0.1	298.15	Chevalier et al. (1990)
n-decane+n-hexadecane	0.1-100	313-353	Ducoulombier et al. (1986)
n-dodecane+n-tetradecane*	0.1	298.15	Chevalier et al. (1990)
n-dodecane+n-hexadecane*	0.1	298.15	Chevalier et al. (1990)
n-tetradecane+n-hexadecane*	0.1	298.15	Chevalier et al. (1990)
n-hexadecane+n-eicosane*	0.1	293-343	Queimada et al. (2003)
i-octane+n-hexane*	0.1	298.15	Chevalier et al. (1990)
i-octane+n-octane*	0.1-101	298-373	Dymond et al. (1985)
i-octane+n-decane*	0.1	298.15	Chevalier et al. (1990)
i-octane+n-dodecane*	0.1-104	298-372	Baylaucq et al. (1997)
i-octane+n-tetradecane*	0.1	298.15	Chevalier et al. (1990)
3-methylpentane+n-decane*	0.1	298.15	Chevalier et al. (1990)
3-methylpentane+n-hexadecane*	0.1	298.15	Chevalier et al. (1990)
2-methylpentane+n-hexadecane*	0.1	298.15	Chevalier et al. (1990)
2-methylhexane+n-tetradecane*	0.1	298.15	Chevalier et al. (1990)
2,3-dimethylpentane+n-tetradecane*	0.1	298.15	Chevalier et al. (1990)

Mixture	Pressure (MPa)	Temp. (K)	Data Source
DATASET 2 (cont.)			
2,2-dimethylpentane+n-decane*	0.1	298.15	Chevalier et al. (1990)
2,2-dimethylpentane+n-hexadecane*	0.1	298.15	Chevalier et al. (1990)
2,2-dimethylhexane+n-decane*	0.1	298.15	Chevalier et al. (1990)
2,2-dimethylhexane+n-hexadecane*	0.1	298.15	Chevalier et al. (1990)
2,5-dimethylhexane+n-hexadecane*	0.1	298.15	Chevalier et al. (1990)
squalane+n-butane*	0.1-30	273-333	Kumagai et al. (2006)
squalane+n-hexane*	0.1-30	273-333	Kumagai et al. (2006)
squalane+n-octane*	0.1-30	273-333	Kumagai et al. (2006)
methylcyclohexane+methane*	20-140	323-424	Tohidi et al. (2001)
methylcyclohexane+n-hexane*	0.1	298.15	Chevalier et al. (1990)
methylcyclohexane+n-heptane*	0.1-100	303-343	Baylaucq et al. (1997)
methylcyclohexane+n-decane*	0.1	298.15	Chevalier et al. (1990)
methylcyclohexane+n-hexadecane*	0.1	298.15	Chevalier et al. (1990)
cyclohexane+methane*	10-40	295-343	Berstad (1989)
cyclohexane+n-octane*	0.1-163	298-348	Tanaka et al. (1991)
cyclohexane+n-dodecane*	0.1-180	298-348	Tanaka et al. (1991)
cyclohexane+n-hexandecane*	0.1	298.15	Chevalier et al. (1990)
cyclohexane+n-hexandecane*	0.1-181	298-348	Tanaka et al. (1991)
cis-1,2-dimethylcyclohexane+n-hexane*	0.1	298.15	Chevalier et al. (1990)
cis-1,2-dimethylcyclohexane+n-hexadecane*	0.1	298.15	Chevalier et al. (1990)
toluene+methane*	20-140	293-373	Baylaucq et al. (2003)
toluene+n-hexane*	0.1-200	298-373	Dymond et al. (1991)
toluene+n-decane*	0.1	298.15	Chevalier et al. (1990)
toluene+n-hexadecane*	0.1	298.15	Chevalier et al. (1990)
benzene+methane*	12-48	293-433	Berstad (1989)
benzene+n-decane*	0.1	298.15	Chevalier et al. (1990)
benzene+n-tetradecane	0.7-60	313-393	Hernández-Galván et al. (2007)
o-xylene+n-hexane*	0.1	298.15	Chevalier et al. (1990)
o-xylene+n-decane*	0.1	298.15	Chevalier et al. (1990)
o-xylene+n-tetradecane*	0.1	298.15	Chevalier et al. (1990)
p-xylene+n-hexane*	0.1	298.15	Chevalier et al. (1990)

Mixture	Pressure (MPa)	Temp. (K)	Data Source
DATASET 2 (cont.)			
p-xylene+n-heptane*	0.1	298-343	Yang et al. (2004, 2005)
p-xylene+n-octane*	0.1	298-353	Yang et al. (2004)
p-xylene+n-decane*	0.1	298.15	Chevalier et al. (1990)
p-xylene+n-tetradecane*	0.1	298.15	Chevalier et al. (1990)
benzene+o-xylene*	0.1	298.15	Chevalier et al. (1990)
benzene+p-xylene*	0.1	298.15	Chevalier et al. (1990)
toluene+o-xylene*	0.1	298.15	Chevalier et al. (1990)
toluene+p-xylene*	0.1	298.15	Chevalier et al. (1990)
o-xylene+p-xylene*	0.1	298.15	Chevalier et al. (1990)
benzene+cyclohexane*	0.1	298.15	Chevalier et al. (1990)
benzene+cyclohexane	0.7-60	313-393	Hernández-Galván et al. (2009)
o-xylene+cyclohexane*	0.1	298.15	Chevalier et al. (1990)
toluene+methylcyclohexane*	0.1	298.15	Chevalier et al. (1990)
p-xylene+cyclohexane*	0.1	298-313	Yang et al. (2004)
carbon dioxide+methane*	3.4-70	323-474	DeWitt and Thodos (1966)
carbon dioxide + ethane*	2.1-37	210-320	Diller et al. (1988)
carbon dioxide + ethane*	1.7-62	320-500	Diller and Ely (1989)
carbon dioxide+n-decane*	7-30	310-403	Cullick and Mathis (1984)
carbon dioxide+n-decane*	7-12	311-403	Barrufet et al. (1997)
carbon dioxide +squalane*	10-20	293-353	Tomida et al. (2007)
DATASET 3			
methane+cis-decalin*	60-140	323-423	Tohidi et al. (2001)
n-pentane+n-decane*	0.2-0.5	354-402	Barrufet et al. (1997)
n-heptane+1-methylnaphthalene*	0.1-100	303-343	Baylaucq et al. (1997)
n-heptane+n-tetracosane*	0.1	313-343	Queimada et al. (2003)
n-heptane+n-docosane*	0.1	303-343	Queimada et al. (2003)
n-octane+n-tetracosane*	0.1	318-338	Wakefield et al. (1998)
n-decane+n-eicosane*	0.1	293-343	Queimada et al. (2005)
n-decane+n-docosane*	0.1	303-343	Queimada et al. (2005)

Mixture	Pressure (MPa)	Temp. (K)	Data Source
DATASET 3 (cont.)			
n-decane+n-tetracosane*	0.1	313-343	Queimada et al. (2005)
n-tridecane+1-methylnaphthalene*	0.1-100	293-353	Dauge et al. (1999)
n-tridecane+ 2,2,4,4,6,8,8-heptamethylnonane*	0.1-100	293-353	Dauge et al. (2001)
1-methylnaphthalene+ 2,2,4,4,6,8,8-heptamethylnonane*	0.1-100	293-353	Canet et al. (2001)
n-tridecane+1-methylnaphthalene+ 2,2,4,4,6,8,8-heptamethylnonane*	0.1-100	293-353	Zéberg-Mikkelsen et al. (2001b)
methylcyclohexane+ 2,2,4,4,6,8,8-heptamethylnonane*	0.1-100	293-353	Zéberg-Mikkelsen et al. (2002)
1-methylnaphthalene+methylcyclohexane*	0.1-100	303-343	Baylaucaq et al. (1997)
cis-decalin+ 2,2,4,4,6,8,8-heptamethylnonane*	0.1-100	293-353	Barrouhou et al. (2003)
cis-decalin+methylcyclohexane*	0.1-100	293-353	Zéberg-Mikkelsen et al. (2003)
cyclohexane+toluene*	0.1	283-323	Silva et al. (2009)
cyclohexane+decalin*	0.1	283-323	Silva et al. (2009)
cyclohexane+n-tetradecane	0.7-60	313-393	Hernández-Galván et al. (2009)
toluene+decalin*	0.1	283-323	Silva et al. (2009)
n-butane+n-hexane+n-decane*	0.3-0.8	324-396	Barrufet et al. (1997)
n-butane+n-hexane+n-decane+ carbon dioxide*	2.5-4.9	324-396	Barrufet et al. (1997)
n-pentane+n-octane+n-decane	0.1-25	298-373	Iglesias-Silva et al. (1999)
n-pentane+n-hexane+n-heptane+n-decane*	0.3-0.4	360-396	Barrufet et al. (1997)
n-pentane+n-hexane+n-heptane+n-decane+ carbon dioxide*	2.5-4.9	360-396	Barrufet et al. (1997)
n-pentane+n-decane+carbon dioxide*	2.5-4.9	354-402	Barrufet et al. (1997)
n-hexane+n-heptane+n-decane*	0.1	298.15	Pandey et al. (1991)
n-hexane+n-octane+n-decane+n-tetracosane*	0.1	328-338	Wakefield et al. (1998)
n-heptane+n-nonane+n-dodecane+ n-hexadecane*	0.1	303-308	Wakefield et al. (1998)
n-heptane+n-eicosane+n-tetracosane*	0.1	303-343	Queimada et al. (2003)
n-decane+n-dodecane+n-tetradecane+ n-hexadecane*	0.1-100	313-353	Ducoulombier et al. (1986)
n-decane+n-eicosane+n-docosane+ n-tetracosane*	0.1	303-343	Queimada et al. (2005)

Mixture	Pressure (MPa)	Temp. (K)	Data Source
DATASET 3 (cont.)			
n-heptane+1-methylnaphthalene+ methylcyclohexane*	0.1-100	303-343	Baylaucaq et al. (1997)
cis-decalin+2,2,4,4,6,8,8- heptamethylnonane+methylcyclohexane*	0.1-100	293-353	Zéberg-Mikkelsen et al. (2003)
cyclohexane+n-hexane+n-heptane*	0.1	298.15	Zéberg-Mikkelsen et al. (2003)
toluene+n-hexane+n-heptane*	0.1	298.15	Pandey et al. (1991)
n-hexane+n-decane+n-dodecane+ n-hexadecane*	0.1	303-308	Wakefield et al. (1998)
n-tridecane+2,2,4,4,6,8,8- heptamethylnonane+heptylcyclohexane+ heptylbenzene+1-methylnaphthalene*	0.1-100	293-353	Boned et al. (2003)
n-tridecane+heptylcyclohexane+ heptylbenzene*	0.1-100	293-353	Boned et al. (2003)

Table C.2: AARD (%) of the viscosity predictions of *Version 1* of EF correlation using proposed sets of the mixing rules (Table 5.2) for the mixtures of the datasets 1 and 2.

Binary Mixture	Mixing Rule Set					
	1	**2**	**3**	**4**	**5**	**6**
methane+ethane	5.3	4.5	4.2	4.8	4.9	4.9
methane+propane	6.7	5.9	5.2	6.1	5.0	5.1
methane+n-hexane	6.7	3.7	2.5	4.3	2.3	2.3
methane + n-decane	8.7	3.8	3.6	4.3	4.3	3.8
n-hexane+n-heptane	0.6	0.5	0.5	0.6	0.5	0.5
n-hexane+n-octane	0.5	0.4	0.4	0.5	0.4	0.4
n-hexane+n-nonane	1.4	1.1	1.1	1.4	1.1	1.2
n-hexane+n-decane	0.6	0.2	0.2	0.6	0.2	0.3
n-hexane+n-dodecane	2.0	2.9	3.0	2.0	2.9	2.7
n-hexane+n-tetradecane	1.5	1.8	1.8	1.5	1.8	1.7
n-hexane+n-hexadecane	1.8	3.7	3.8	1.9	3.7	3.2
n-heptane+n-octane	0.1	0.1	0.1	0.1	0.1	0.1
n-heptane+n-nonane	0.9	0.8	0.7	0.9	0.7	0.8
n-heptane+n-decane	0.1	0.3	0.3	0.1	0.3	0.2
n-heptane+n-dodecane	0.3	0.8	0.9	0.3	0.8	0.7
n-heptane+n-tetradecane	0.5	1.5	1.6	0.6	1.5	1.3
n-heptane+n-hexadecane	1.3	2.9	3.0	1.4	2.9	2.5
n-heptane+n-eicosane	3.5	7.1	7.3	3.5	7.2	6.3

Binary Mixture	Mixing Rule Set					
	1	**2**	**3**	**4**	**5**	**6**
n-octane+n-nonane	0.8	0.7	0.7	0.8	0.7	0.7
n-octane+n-decane	0.1	0.2	0.3	0.1	0.3	0.2
n-octane+n-dodecane	1.8	1.8	1.8	1.7	1.8	1.7
n-octane+n-tetradecane	0.7	1.4	1.4	0.7	1.4	1.2
n-octane+n-hexadecane	1.2	2.4	2.5	1.2	2.5	2.1
n-nonane+n-decane	0.6	0.6	0.6	0.6	0.6	0.6
n-nonane+n-dodecane	0.6	0.5	0.5	0.6	0.5	0.5
n-nonane+n-tetradecane	0.8	0.8	0.8	0.8	0.8	0.7
n-nonane+n-hexadecane	0.8	1.7	1.7	0.8	1.7	1.5
n-decane+n-dodecane	0.4	0.5	0.5	0.4	0.5	0.5
n-decane+n-tetradecane	0.5	0.7	0.7	0.5	0.7	0.6
n-decane+n-hexadecane	0.8	1.5	1.5	0.8	1.5	1.3
n-dodecane+n-tetradecane	0.2	0.3	0.3	0.2	0.3	0.2
n-dodecane+n-hexadecane	0.2	0.5	0.5	0.2	0.5	0.4
n-tetradecane+n-hexadecane	0.1	0.1	0.1	0.1	0.1	0.1
n-hexadecane+n-eicosane	1.5	1.4	1.4	1.5	1.4	1.4
i-octane+n-hexane	1.5	1.4	1.4	1.5	1.4	1.5
i-octane+n-octane	2.7	2.7	2.7	2.7	2.7	2.7
i-octane+n-decane	1.1	1.2	1.3	1.1	1.3	1.2
i-octane+n-dodecane	2.5	2.7	2.8	2.5	2.7	2.7
i-octane+n-tetradecane	3.4	4.5	4.5	3.5	4.5	4.3
3-methylpentane+n-decane	0.8	0.8	0.8	0.8	0.8	0.8
3-methylpentane+n-hexadecane	3.3	5.6	5.7	3.3	5.6	5.1
2-methylpentane+n-hexadecane	2.6	4.8	4.9	2.7	4.9	4.3
2-methylhexane+n-tetradecane	3.3	4.6	4.7	3.3	4.7	4.3
2,3-dimethylpentane+n-tetradecane	3.2	4.7	4.7	3.2	4.7	4.3
2,2-dimethylpentane+n-decane	0.8	1.0	1.0	0.8	1.0	1.0
2,2-dimethylpentane+ n-hexadecane	5.0	6.7	6.8	5.0	6.7	6.3
2,2-dimethylhexane+n-decane	0.5	0.6	0.7	0.6	0.7	0.6
2,2-dimethylhexane+n-hexadecane	4.1	5.6	5.7	4.2	5.6	5.3
2,5-dimethylhexane+n-hexadecane	3.3	4.3	4.4	3.3	4.4	4.1
squalane+n-butane	12.5	18.1	18.7	13.0	18.6	17.2
squalane+n-hexane	*26.9*	*30.9*	*31.1*	*27.0*	*31.0*	*30.0*
squalane+n-octane	6.8	9.1	9.2	6.9	9.2	8.5
methylcyclohexane+methane	14.9	10.9	8.3	10.6	6.5	6.7
methylcyclohexane+n-hexane	1.7	1.7	1.6	1.5	1.3	1.3
methylcyclohexane+n-heptane	1.8	1.8	1.9	2.0	2.1	2.1

Binary Mixture	Mixing Rule Set					
	1	2	3	4	5	6
methylcyclohexane+n-decane	0.4	0.4	0.4	0.4	0.4	0.4
methylcyclohexane+n-hexadecane	1.3	1.3	1.3	1.3	1.3	1.3
cyclohexane+methane	12.4	7.2	3.1	7.5	1.6	2.1
cyclohexane+n-octane	2.2	2.2	2.2	2.0	1.9	1.9
cyclohexane+n-dodecane	2.2	2.2	2.2	2.2	2.2	2.2
cyclohexane+n-hexandecane	3.2	3.6	3.5	3.2	3.7	3.6
cis-1,2-dimethylcyclohexane+ n-hexane	3.9	3.6	3.4	3.4	3.1	3.1
cis-1,2-dimethylcyclohexane+ n-hexadecane	1.4	2.1	2.0	1.6	2.4	2.2
toluene+methane	8.1	6.4	3.7	3.4	5.0	5.1
toluene+n-hexane	3.2	3.0	3.1	4.7	4.8	4.9
toluene+n-decane	4.8	4.3	4.6	3.0	2.2	2.3
toluene+n-hexadecane	5.7	3.7	4.3	3.5	1.3	1.9
benzene+methane	6.8	4.7	2.1	3.2	5.0	5.1
benzene+n-decane	4.6	4.2	4.5	2.5	1.8	1.9
o-xylene+n-hexane	3.4	3.7	3.5	1.7	1.6	1.5
o-xylene+n-decane	2.7	2.6	2.8	0.8	0.3	0.4
o-xylene+n-tetradecane	2.5	1.0	1.6	0.2	1.6	1.2
p-xylene+n-hexane	3.8	4.0	3.9	2.3	2.2	2.1
p-xylene+n-heptane	3.6	3.8	3.8	2.3	2.2	2.2
p-xylene+n-octane	3.8	3.9	4.0	2.5	2.3	2.3
p-xylene+n-decane	4.3	4.0	4.2	2.6	2.0	2.1
p-xylene+n-tetradecane	4.7	2.9	3.5	2.7	0.7	1.2
benzene+o-xylene	0.6	0.5	0.5	0.5	0.5	0.5
benzene+p-xylene	0.6	0.6	0.6	0.6	0.6	0.6
toluene+o-xylene	1.7	1.6	1.6	1.7	1.6	1.6
toluene+p-xylene	1.0	1.0	1.0	1.0	1.0	1.0
o-xylene+p-xylene	0.5	0.5	0.5	0.5	0.5	0.5
benzene+cyclohexane	6.2	5.9	6.1	5.2	4.7	4.8
o-xylene+cyclohexane	3.8	3.7	3.8	2.9	2.6	2.6
toluene+methylcyclohexane	4.9	4.8	4.9	4.2	3.9	3.9
p-xylene+cyclohexane	4.0	3.7	3.9	3.3	2.9	3.0
carbon dioxide+methane	4.3	4.1	4.7	6.7	8.1	8.9
carbon dioxide + ethane	8.0	8.1	7.9	10.4	11.0	11.8
carbon dioxide+n-decane	4.4	4.4	4.0	9.3	11.1	11.1
carbon dioxide +squalane	7.8	9.2	8.3	15.1	17.4	16.9

Table C.3: Summary of the viscosity predictions by *Version 2* of EF correlation using different binary interaction parameter (β_{ij}) values for the binary mixtures of the datasets 1 and 2. Adjusted βij values were determined by fitting data at 298 K and 101 kPa. Estimated βij values were calculated by: 1) Equations 5.13 and 5.15; 2) Equations 5.14 and 5.15. "*" denotes mixtures in conditions other than 101 kPa and 298 K.

Binary Mixture	β_{ij}	**AARD(%) with**			
	adjusted	$\beta_{ij} = 0$	β_{ij} adjusted	β_{ij} est. 1	β_{ij} est. 2
methane+ethane		4.9		6.3	5.7
methane+propane		2.6		4.3	4.3
methane+n-butane		3.8		7.3	7.5
methane+n-hexane		3.7		9.0	10.2
methane + n-decane		10.9		6.5	6.7
n-pentane+n-octane	-0.724	2.6	1.1	1.0	1.4
n-pentane+n-octane*		4.6	4.4	4.3	4.3
n-pentane+n-decane	-1.735	7.1	1.6	1.8	2.6
n-pentane+n-decane*		6.5	4.3	3.6	4.1
n-hexane+n-heptane	0.096	0.4	0.2	0.7	0.2
n-hexane+n-octane	-0.333	1.2	0.3	0.3	0.8
n-hexane+n-nonane	-0.351	1.4	0.2	1.1	0.2
n-hexane+n-decane	-1.007	4.2	0.7	0.7	1.6
n-hexane+n-dodecane	-1.590	5.7	1.0	1.6	2.0
n-hexane+n-dodecane*		10.6	12.3	8.8	9.3
n-hexane+n-tetradecane	-2.258	9.6	0.5	2.0	1.6
n-hexane+n-hexadecane	-2.746	11.2	0.4	3.4	0.7
n-hexane+n-hexadecane*		15.0	13.7	6.3	5.9
n-heptane+n-octane	-0.071	0.3	0.1	0.1	0.2
n-heptane+n-nonane	-0.036	0.2	0.1	0.9	0.5
n-heptane+n-decane	-0.444	2.3	0.5	0.6	0.6
n-heptane+n-decane*		8.8	13.7	11.0	10.7
n-heptane+n-dodecane	-0.831	3.6	0.4	1.3	0.5
n-heptane+n-tetradecane	-1.298	5.4	0.1	2.3	0.1
n-heptane+n-hexadecane	-1.706	8.3	0.2	4.6	0.9
n-heptane+n-eicosane	-2.945	16.7	2.5	7.8	2.5
n-heptane+n-eicosane*		17.8	4.4	3.0	4.0
n-octane+n-nonane	0.001	0.2	0.2	0.3	0.2
n-octane+n-decane	-0.266	1.7	0.6	0.7	1.1
n-octane+n-decane*		3.4	3.0	3.0	3.1
n-octane+n-dodecane	-0.510	2.6	0.4	0.8	0.8
n-octane+n-dodecane*		8.0	10.3	7.9	7.9

Binary Mixture	β_{ij} adjusted	AARD(%) with $\beta_{ij} = 0$	AARD(%) with β_{ij} adjusted	AARD(%) with β_{ij} est. 1	AARD(%) with β_{ij} est. 2
n-octane+n-tetradecane	-0.838	4.4	0.2	2.0	0.3
n-octane+n-hexadecane	-1.148	6.5	0.3	4.3	0.9
n-nonane+n-decane	-0.222	1.5	0.5	1.3	1.5
n-nonane+n-dodecane	-0.442	2.5	0.4	0.9	1.8
n-nonane+n-tetradecane	-0.720	4.1	0.3	0.3	1.6
n-nonane+n-hexadecane	-1.021	6.2	0.3	1.7	1.4
n-decane+n-dodecane	-0.245	2.0	0.8	1.3	1.9
n-decane+n-tetradecane	-0.374	2.8	0.9	1.0	1.4
n-decane+n-hexadecane	-0.602	4.6	0.7	2.3	1.3
n-decane+n-hexadecane*		5.9	7.6	5.5	5.2
n-dodecane+n-tetradecane	-0.080	0.8	0.4	0.4	1.0
n-dodecane+n-hexadecane	-0.152	1.6	0.4	1.8	1.0
n-tetradecane+n-hexadecane	0.006	0.2	0.2	0.9	1.0
n-hexadecane+n-eicosane	-0.116	2.1	1.8	7.1	2.0
n-hexadecane+n-eicosane*		1.5	1.7	2.3	1.5
i-octane+n-hexane	1.047	3.4	0.9	4.3	3.5
i-octane+n-octane	0.190	1.5	0.4	1.5	0.6
i-octane+n-octane*		6.6	5.5	6.6	6.1
i-octane+n-decane	-0.422	2.5	1.1	1.7	2.5
i-octane+n-dodecane	-1.200	8.8	0.4	4.2	6.4
i-octane+n-dodecane*		6.8	8.1	5.5	6.0
i-octane+n-tetradecane	-1.720	10.4	0.5	3.8	6.2
3-methylpentane+n-decane	-0.591	3.4	1.9	2.7	1.9
3-methylpentane+n-hexadecane	-2.664	15.0	1.2	6.0	1.4
2-methylpentane+n-hexadecane	-3.452	14.7	1.1	1.2	4.5
2-methylhexane+n-tetradecane	-1.704	8.7	0.2	0.5	2.3
2,3-dimethylpentane+n-tetradecane	-2.543	14.0	0.9	5.0	7.7
2,2-dimethylpentane+n-decane	-0.247	1.8	1.1	1.7	1.1
2,2-dimethylpentane+n-hexadecane	-1.702	11.3	0.4	6.7	1.7
2,2-dimethylhexane+n-decane	0.065	1.7	1.7	2.3	1.9
2,2-dimethylhexane+n-hexadecane	-1.218	9.4	1.0	5.6	1.3
2,5-dimethylhexane+n-hexadecane	-1.354	9.5	0.9	3.9	1.1
squalane+n-butane		62.0		22.3	33.3
squalane+n-hexane	-8.788	62.7	16.5	16.5	26.5
squalane+n-hexane*		58.2	71.3	9.9	16.3
squalane+n-octane	-5.449	38.5	12.1	17.2	12.9

Binary Mixture	β_{ij} adjusted	AARD(%) with $\beta_{ij} = 0$	AARD(%) with β_{ij} adjusted	AARD(%) with β_{ij} est. 1	AARD(%) with β_{ij} est. 2
squalane+n-octane*		32.6	38.0	14.0	8.1
methylcyclohexane+methane*		9.4		13.2	15.1
methylcyclohexane+n-hexane	0.550	2.2	0.7	2.5	0.7
methylcyclohexane+n-heptane	0.215	1.0	0.3	1.0	1.8
methylcyclohexane+n-heptane*		6.9	5.6	7.0	5.5
methylcyclohexane+n-decane	-0.486	2.9	1.1	1.2	3.2
methylcyclohexane+n-hexadecane	-2.079	13.4	0.5	4.5	1.4
cyclohexane+methane		17.8		26.6	28.9
cyclohexane+n-octane	0.082	0.9	0.8	2.6	1.4
cyclohexane+n-octane*		6.4	6.0	7.1	5.8
cyclohexane+n-dodecane	-1.769	11.0	0.6	1.0	4.0
cyclohexane+n-dodecane*		7.2	16.1	4.9	5.1
cyclohexane+n-hexandecane	-3.099	18.6	0.6	4.1	1.9
cyclohexane+n-hexandecane*		19.0	18.3	7.3	7.3
cis-1,2-dimethylcyclohexane+ n-hexane	0.565	2.8	0.7	3.4	1.4
cis-1,2-dimethylcyclohexane+ n-hexadecane	-1.398	8.7	1.1	3.6	1.9
toluene+methane		6.2		7.8	10.1
toluene+n-hexane	0.864	4.3	0.6	4.3	0.6
toluene+n-decane	-0.056	1.0	1.0	3.6	1.3
toluene+n-tetradecane	-1.366	8.0	0.6	6.0	1.0
benzene+methane		10.1		17.7	20.2
benzene+n-decane	-0.268	2.0	1.5	5.7	2.0
benzene+n-tetradecane		10.0		3.8	5.6
o-xylene+n-hexane	1.132	4.5	0.6	5.2	2.0
o-xylene+n-decane	-0.021	1.1	1.1	2.3	3.2
o-xylene+n-tetradecane	-1.210	8.4	0.8	2.5	3.7
p-xylene+n-hexane	1.208	4.2	0.6	4.8	2.1
p-xylene+n-heptane	0.292	1.7	1.0	1.7	2.7
p-xylene+n-heptane*		2.4	1.6	2.4	1.4
p-xylene+n-octane	0.249	1.6	0.8	1.7	3.0
p-xylene+n-octane*		2.3	1.6	2.4	1.5
p-xylene+n-decane	0.183	1.6	1.1	3.1	1.7
p-xylene+n-tetradecane	-1.078	6.0	0.7	3.5	1.5
benzene+o-xylene	0.529	3.0	0.9	4.8	2.9
benzene+p-xylene	-0.014	0.6	0.6	1.9	0.9
toluene+o-xylene	0.314	2.9	1.8	3.2	2.5

Binary Mixture	β_{ij} adjusted	AARD(%) with $\beta_{ij} = 0$	AARD(%) with β_{ij} adjusted	AARD(%) with β_{ij} est. 1	AARD(%) with β_{ij} est. 2
toluene+p-xylene	0.021	0.3	0.3	0.6	1.0
o-xylene+p-xylene	0.163	1.1	0.5	1.1	0.5
benzene+cyclohexane	2.638	12.2	0.9	12.3	9.4
benzene+cyclohexane*		17.5	5.5	17.4	15.3
o-xylene+cyclohexane	1.814	10.1	0.7	11.4	8.8
toluene+methylcyclohexane	1.734	8.3	0.9	8.3	5.6
p-xylene+cyclohexane	1.461	7.6	1.4	8.7	6.7
p-xylene+cyclohexane*		9.0	3.0	10.0	8.3
carbon dioxide+methane		7.4		8.0	8.1
carbon dioxide + ethane		6.0		6.2	5.6
carbon dioxide+n-decane		14.8		10.5	10.5
carbon dioxide +squalane		55.1		42.4	33.2

Table C.4: AARD (%) of the viscosity predictions by *Version 1* and *2* of EF correlation for the mixtures of the dataset 3 using measured and EoS-estimated densities as input, respectively. Estimated βij values were calculated by: 1) Equations 5.13 and 5.15; 2) Equations 5.14 and 5.15.

Mixtures	Version 1	Version 2		
		$\beta_{ij} = 0$	β_{ij} est. 1	β_{ij} est. 2
methane+cis-decalin	10.3	10.8	10.7	10.6
n-heptane+n-docosane	8.7	25.0	5.1	9.5
n-heptane+n-tetracosane	7.9	28.0	4.4	9.5
n-octane+n-tetracosane	5.2	26.5	3.1	9.7
n-decane+n-eicosane	2.7	13.3	4.5	1.6
n-decane+n-docosane	4.3	20.0	2.7	5.0
n-decane+n-tetracosane	10.6	26.9	3.1	9.7
n-pentane+n-octane+n-decane		3.4	4.2	3.6
n-hexane+n-heptane+n-decane		1.1	3.8	2.8
n-heptane+n-eicosane+n-tetracosane	7.4	23.6	4.0	7.4
n-decane+n-eicosane+n-tetracosane	2.7	15.3	5.4	2.4
n-hexane+n-octane+n-decane+ n-tetracosane	4.6	19.7	4.7	8.3
n-hexane+n-decane+n-dodecane+ n-hexadecane	2.4	12.9	0.8	4.6
n-heptane+n-nonane+n-dodecane+ n-hexadecane	2.0	10.4	1.7	3.0
n-decane+n-dodecane+ n-tetradecane+n-hexadecane		5.3	4.8	4.6

Mixtures	Version 1	Version 2		
		$\beta_{ij} = 0$	β_{ij} est. 1	β_{ij} est. 2
n-pentane+n-decane	6.8	2.7	1.5	1.4
n-pentane+n-decane+carbon dioxide	29.4	13.2	8.6	9.6
n-butane+n-hexane+n-decane	11.3	5.2	3.1	3.4
n-butane+n-hexane+ n-decane+carbon dioxide	9.8	11.0	7.4	7.6
n-pentane+n-hexane+n-heptane+ n-decane	15.3	7.2	4.9	5.2
n-pentane+n-hexane+n-heptane+ n-decane+carbon dioxide	15.6	12.5	8.6	9.6
n-tridecane+ 2,2,4,4,6,8,8-heptamethylnonane	6.2	11.7	13.1	11.1
n-tridecane+1-methylnaphthalene	7.0	7.9	7.9	11.2
1-methylnaphthalene+ 2,2,4,4,6,8,8-heptamethylnonane	6.8	8.1	11.5	8.1
n-tridecane+1-methylnaphthalene+ 2,2,4,4,6,8,8-heptamethylnonane	9.7	6.9	10.2	6.7
Methylcyclohexane+ 2,2,4,4,6,8,8-heptamethylnonane	3.9	9.2	6.9	5.3
cis-decalin+methylcyclohexane	9.8	12.1	10.5	12.1
cis-decalin+ 2,2,4,4,6,8,8-heptamethylnonane	16.6	17.9	12.7	16.4
cis-decalin+ 2,2,4,4,6,8,8-heptamethylnonane+ methylcyclohexane	14.3	15.4	7.7	9.5
n-heptane+1-methylnaphthalene	7.5	7.9	8.2	6.8
1-methylnaphthalene+ methylcyclohexane	5.3	8.5	11.1	7.7
n-heptane+1-methylnaphthalene+ methylcyclohexane	15.1	8.9	11.2	6.3
cyclohexane+toluene	5.2	10.3	10.4	8.0
cyclohexane+decalin	2.4	4.8	7.1	4.8
cyclohexane+n-tetradecane		11.6	3.9	4.9
toluene+decalin	6.2	12.2	17.5	14.1
cyclohexane+n-hexane+n-heptane	11.9	4.3	3.8	6.8
toluene+n-hexane+n-heptane	*230.1*	1.5	1.2	5.1
n-tridecane+ 2,2,4,4,6,8,8-heptamethylnonane+ heptylcyclohexane+ heptylbenzene+1-methylnaphthalene	11.3	8.8	11.4	4.7
n-tridecane+heptylcyclohexane+ heptylbenzene	2.7	4.0	4.0	6.4

APPENDIX D: DETAILED RESULTS OF VISCOSITY MODELING OF PURE HYDROCARBONS IN CHAPTER SEVEN

Table D.1: Summary of the deviations of the predicted viscosity for n-paraffins with fluid-specific parameters of the EF correlation calculated by the developed estimation methods. Original regressed values of the parameters are also reported for reference.

Compound	PSU	MW (g/mol)	SG	*Regressed*		*Predicted with Estimation Methods*			
				c_2	ρ_s^o (kg/m³)	c_2	ρ_s^o (kg/m³)	MARD (%)	AARD (%)
methane		16.0	0.300	0.1000	540.0	0.1323	586.1	34	17
ethane		30.1	0.355	0.1560	724.0	0.1622	729.4	23	7
propane		44.1	0.506	0.1740	778.0	0.1806	783.1	29	10
n-butane		58.1	0.585	0.1900	813.0	0.1941	811.9	15	6
m-pentane		72.2	0.632	0.1980	837.0	0.2052	830.1	65	22
n-hexane		86.2	0.665	0.2050	849.1	0.2152	842.8	35	13
n-heptane		100.2	0.690	0.2130	857.8	0.2245	852.4	37	16
n-octane		114.2	0.707	0.2210	862.7	0.2335	859.9	26	15
n-nonane		128.3	0.722	0.2304	865.9	0.2423	866.0	28	15
n-decane		142.3	0.734	0.2360	868.1	0.2510	871.0	20	9
n-dodecane		170.3	0.752	0.2490	871.4	0.2680	879.1	15	5
n-tetradecane		198.4	0.767	0.2650	875.5	0.2848	885.2	12	3
n-hexadecane		226.5	0.773	0.2780	878.6	0.3011	890.2	9	4
n-heptadecane	535	240.5	0.782	0.2878	881.3	0.3095	892.4	6	3
n-octadecane	537	254.5	0.787	0.2974	885.1	0.3175	894.4	22	6
n-eicosane	540	282.6	0.792	0.3060	885.5	0.3329	897.8	9	4
n-docosane		310.6	0.798	0.3100	885.2	0.3483	900.8	5	4
n-tricosane	619	324.6	0.800	0.3310	891.4	0.3562	902.2	4	3
n-tetracosane	541	338.7	0.802	0.3350	893.2	0.3634	903.4	5	2
n-hexacosane	106	366.7	0.808	0.3727	903.9	0.3785	905.8	1	0
n-octacosane	176	394.8	0.810	0.3788	903.2	0.3929	907.9	2	1
n-dotriacontane	197	450.9	0.815	0.4082	908.6	0.4211	911.4	4	4
n-pentatriacontane	220	492.9	0.822	0.4493	919.9	0.4415	913.7	9	8
n-hexatriacontane	190	507.1	0.821	0.4397	914.9	0.4483	914.4	10	9
n-tetratetracontane	205	619.3	0.828	0.5071	926.9	0.4999	918.9	19	15

Table D.2: Summary of the deviations of the predicted viscosity for hydrocarbons in the development group with fluid-specific parameters of the EF correlation calculated by the developed estimation methods. Original regressed values of the parameters are also reported for reference. PSU is the unique identifier of the compounds in API project 42.

Compound	PSU	MW (g/mol)	SG	*Regressed*		*Predicted with Estimation Methods*			
				c_2	ρ_s^o (kg/m^3)	c_2	ρ_s^o (kg/m^3)	MARD (%)	AARD (%)
cyclopentane		70.1	0.750	0.2150	933.0	0.2540	936.0	29	26
benzene		78.1	0.883	0.2260	1066.4	0.2298	1056.2	25	13
cyclohexane		84.2	0.782	0.2370	922.1	0.2294	942.8	38	27
cycloheptane		98.2	0.814	0.2310	933.7	0.2205	956.5	42	36
cis-bicyclo[330]octane	543	110.2	0.880	0.2694	1010.3	0.2123	1006.7	36	33
cyclooctane		112.2	0.840	0.2541	950.7	0.2179	967.6	57	49
naphthalene		128.2	1.028	0.3054	1212.5	0.1937	1141.7	33	24
tetralin		132.2	0.973	0.2365	1099.9	0.2034	1080.8	11	6
trans-decahydronaphthalene	569	138.2	0.902	0.2743	1018.3	0.2170	1008.7	35	33
cis-decahydronaphthalene	570	138.2	0.876	0.2566	997.8	0.2215	984.8	11	8
spiro[54]decane	620	138.2	0.886	0.2792	1016.6	0.2198	993.8	17	10
1-methylnaphthalene		142.2	1.024	0.2180	1133.9	0.2000	1126.3	15	9
spiro[55]undecane	622	152.3	0.901	0.2651	1007.6	0.2239	1001.9	16	14
spiro[65]dodecane	623	166.3	0.910	0.2635	1010.7	0.2298	1005.1	18	17
penantherene		178.2	1.063	0.2375	1215.4	0.2135	1146.4	180	80
perhydrofluorene	561	178.3	0.962	0.2747	1055.1	0.2271	1048.9	18	12
1,2,3,4,5,6,7,8-octahydroanthracene	625	186.3	1.022	0.2180	1097.2	0.2226	1103.2	45	31
perhydrophenanthrene	626	192.3	0.957	0.2574	1040.5	0.2359	1040.1	9	4
perhydroanthracene	637	192.3	0.981	0.2574	1020.0	0.2318	1062.6	23	15
1,2,3,4-tetrahydrofluoranthene	576	206.3	1.105	0.2213	1164.4	0.2252	1178.6	47	43
perhydroindeno(2,1-a)indene	645	218.4	0.962	0.2596	1039.2	0.2500	1039.7	30	21
pehydropyrene	578	218.4	0.995	0.2621	1067.6	0.2445	1068.9	32	24
perhydrofluoranthene	577	218.4	0.988	0.2539	1062.5	0.2456	1062.7	8	6
perhydrochrysene	575	246.4	0.984	0.2273	1035.2	0.2623	1055.0	83	46

Table D.3: Summary of the deviations of the predicted viscosity for hydrocarbons in the test group with fluid-specific parameters of the EF correlation calculated by the developed estimation methods. Original regressed values of the parameters are also reported for reference. PSU is the unique identifier of the compounds in API project 42.

Compound	PSU	MW (g/mol)	SG	*Regressed*		*Predicted with Estimation Methods*			
				c_2	ρ_s^o (kg/m³)	c_2	ρ_s^o (kg/m³)	MARD (%)	AARD (%)
Branched Paraffins									
7-methyltridecane	512	198.4	0.767	0.2418	868.1	0.2857	883.8	14	9
2,2,3,3,5,6,6-heptamethylheptane	556	198.4	0.804	0.2751	899.3	0.2747	911.6	41	28
2-methylpentadecane	582	226.4	0.775	0.2737	873.8	0.3029	886.9	13	5
7-n-propyltridecane	545	226.4	0.780	0.2324	866.6	0.3012	890.8	24	14
4,9-dipropyldodecane	557	254.5	0.792	0.2339	871.1	0.3158	898.0	29	17
7-n-hexyltridecane	500	268.5	0.791	0.2619	874.5	0.3249	897.3	22	11
2,6,10,14-tetramethylpentadecane	642	268.5	0.786	0.2656	868.1	0.3268	893.2	33	14
2,6,11,15-tetramethylhexadecane	643	282.5	0.792	0.2813	875.1	0.3336	897.0	35	14
8-hexylpentadecane	554	296.6	0.796	0.2729	877.2	0.3407	900.1	24	12
9-hexylheptadecane	163	324.6	0.801	0.2890	881.8	0.3558	903.0	24	12
9-octylheptadecane	25	352.7	0.806	0.3055	887.2	0.3705	906.1	19	12
11-butyldocosane	1	366.7	0.808	0.3195	890.0	0.3777	907.5	23	11
6,11-dipentylhexadecane	22	366.7	0.811	0.3092	887.3	0.3766	909.9	41	19
9-ethyl-9-heptyloctadecane,	210	380.7	0.817	0.3211	891.5	0.3823	914.2	51	25
2,2,4,10,12,12-hexamethyl-7-(3,5,5-rimethylhexyl) tridecane	184	394.7	0.808	0.3010	868.8	0.3932	907.4	84	48
11-n-decyl-docosane	7	450.8	0.817	0.3575	900.4	0.4199	914.0	26	13
13-n-dodecylhexacosane	134	535	0.822	0.3856	905.0	0.4602	918.5	31	26
Non-Fused Aromatics									
diphenylmethane	524	168.2	1.011	0.2485	1132.6	0.2144	1099.0	49	31
1,1-diphenylethane	516	182.3	1.004	0.2359	1106.2	0.2229	1087.0	120	58

Compound	PSU	MW (g/mol)	SG	*Regressed*		*Predicted with Estimation Methods*			
				c_2	ρ_s^o (kg/m³)	c_2	ρ_s^o (kg/m³)	MARD (%)	AARD (%)
Non-Fused Aromatics-cont.									
1-phenyl-2-cyclohexylethane	521	188.3	0.930	0.2418	1027.8	0.2384	1017.5	53	28
1-phenyl-3-cyclopentylpropane	522	188.3	0.922	0.2564	1031.1	0.2401	1009.7	108	54
1-cyclohexyl-1-phenylethane	517	188.3	0.940	0.2300	1022.5	0.2367	1025.8	8	3
1,3-diphenylbenzene	631	230.2	1.103	0.2464	1155.6	0.2387	1169.2	36	32
1,2-diphenylbenzene	633	230.2	1.086	0.2219	1120.6	0.2400	1152.5	73	53
1,1-diphenylheptane	503	252.4	0.954	0.2389	1024.4	0.2713	1028.4	42	38
1,5-diphenyl-3-(2-phenylethyl) pentane	89	328.5	1.012	0.2569	1072.2	0.3037	1072.0	334	179
1-phenyl-3(2-phenylethyl) hendecane	18	336.5	0.925	0.2717	997.3	0.3257	998.9	182	120
9(2-phenylethyl)heptadecane	87	344.6	0.860	0.2978	942.1	0.3480	947.2	66	53
1,1-diphenyltetradecane	12	350.6	0.923	0.2957	994.6	0.3341	996.6	73	58
Fused Aromatics									
2-n-butylnaphthalene	606	184.3	0.969	0.2204	1060.2	0.2293	1053.5	73	44
1-tert-butylnaphthalene	646	184.3	0.996	0.2086	1061.8	0.2251	1079.0	65	37
2-tert-butylnaphthalene	652	184.3	0.972	0.2020	1047.7	0.2288	1056.5	14	11
2-(ar) butyltetralin	592	188.3	0.933	0.2357	1026.6	0.2378	1020.2	46	28
4,5-dimethylphenanthrene	616	206.3	1.104	0.2366	1154.1	0.2253	1177.2	55	49
4,5-dimethyl- 9,10-dihydrophenanthrene	617	208.3	1.072	0.2447	1121.3	0.2291	1144.4	72	55
1,2,3,4,5,6,7,8,13,14,15,16-dodecahydrochrysne	574	240.4	0.996	0.2392	1024.2	0.2568	1067.0	100	89
1,4-dimethyl-5-octylnaphthalene	638	268.4	0.954	0.2532	1020.6	0.2805	1027.1	18	10
2-butyl-3-hexylnaphthalene	613	268.4	0.937	0.2656	1008.5	0.2841	1012.4	16	10
7-butyl-1-hexylnaphthalene	610	268.4	0.933	0.2724	1007.4	0.2851	1008.5	22	15
7(ar)-n-butyl-1-n-hexyltetralin	611	272.5	0.908	0.2746	981.9	0.2933	987.7	11	6
1-alpha-naphthyl-hendecane	559	282.5	0.932	0.2728	1005.5	0.2935	1006.9	33	27
1-alpha-naphthyl-pentadecane	174	338.6	0.889	0.2824	953.4	0.3362	970.2	18	9
2-n-octylchrysene	224	340.5	1.058	0.2670	1094.5	0.3036	1111.9	21	13

Compound	PSU	MW (g/mol)	SG	*Regressed*		*Predicted with Estimation Methods*			
				c_2	ρ_s^o (kg/m³)	c_2	ρ_s^o (kg/m³)	MARD (%)	AARD (%)
2-octyltriphenylene	226	340.5	1.061	0.2757	1107.0	0.3033	1114.4	16	11
9-n-octyl(1,2,3,4-tetrahydro) naphthacene	179	344.5	1.028	0.3175	1070.0	0.3098	1085.2	94	76
2-decyl-4b,5,9b,10-tetrahydroindno(2,1-a) indene	230	346.5	0.985	0.3210	1047.2	0.3181	1048.7	15	10
1-n-decyl-3,4,5,8,9,10-hexahydropyrene	218	348.5	0.999	0.3022	1046.0	0.3168	1059.7	27	22
1,10-di-(alpha-naphthyl)decane	131	394.6	1.033	0.2931	1081.3	0.3355	1087.6	40	37
11-alpha-ar-tetralylheneicosane	173	426.7	0.892	0.3535	962.8	0.3831	970.9	26	14
Non-Fused Naphthenics									
bicyclopentyl	551	138.2	0.869	0.2640	1015.3	0.2227	978.8	55	27
bicyclohexyl	608	166.3	0.888	0.2527	990.8	0.2342	985.5	9	8
1,1-dicyclopentylethane	580	166.3	0.882	0.2611	1005.3	0.2352	980.9	64	33
1,1-dicyclohexylethane	518	194.4	0.897	0.2608	982.2	0.2488	987.4	41	29
1-cyclohexyl-3-cyclopentylpropane	523	194.4	0.871	0.2637	967.6	0.2546	965.8	8	6
1,3-dicyclopntyl-cyclopentane	548	206.4	0.913	0.2802	1026.5	0.2525	999.3	137	67
tricyclopentylmethane	564	220.4	0.940	0.2444	1020.6	0.2552	1020.5	25	19
1,2-dicyclohexyl-cyclohexane	634	248.4	0.944	0.2345	987.7	0.2709	1020.2	98	73
7-cyclopentylmethyltridecane	542	266.5	0.826	0.2608	906.8	0.3122	923.7	17	10
7-cyclohexyltridecane	504	266.5	0.835	0.2612	909.1	0.3095	930.6	45	20
1-cyclopentyl-4-(3-cyclopentylpropyl) dodecane	111	348.6	0.862	0.3196	939.4	0.3497	948.6	20	9
1-cyclohexyl-3-(2-cyclohexylethyl) undecane	19	348.6	0.870	0.3239	936.6	0.3473	954.7	75	48
9(3-cyclopentylpropyl)heptadecane	110	350.7	0.833	0.3142	913.4	0.3600	926.5	16	9
9-(2-cyclohexylethyl)heptadecane	88	350.6	0.837	0.3163	913.0	0.3588	929.3	41	20
1,7-dicyclopentyl-4-(3-	113	346.6	0.893	0.3272	966.1	0.3397	972.8	33	18
11-cyclohexylmethylhenicosane	91	392.7	0.838	0.3211	912.2	0.3815	930.2	36	17

Compound	PSU	MW (g/mol)	SG	*Regressed*		*Predicted with Estimation Methods*			
				c_2	ρ_s^o (kg/m³)	c_2	ρ_s^o (kg/m³)	MARD (%)	AARD (%)
Fused Naphthenics									
2-n-butyldecalin	607	194.3	0.880	0.2486	969.5	0.2525	973.0	11	6
2-butyl-1-hexylhexahydroindan	601	264.5	0.872	0.2535	937.6	0.2977	959.5	61	30
5-butyl-6-hexylhexahydroindan	605	264.5	0.873	0.2597	944.7	0.2974	960.3	38	17
1,4-dimethyl-5-octyldecalin	640	278.5	0.879	0.2703	951.2	0.3041	964.4	34	14
2-n-butyl-3-n-hexyldecalin	615	278.5	0.879	0.2676	944.1	0.3041	964.5	67	36
7-butyl-1-hexyldecalin	612	278.5	0.875	0.2772	945.1	0.3053	961.0	54	29
Perhydrodibenzo[a,i]fluorene	587	286.5	1.002	0.2345	1033.2	0.2821	1066.4	98	78
di(alpha-decalyl)methane	586	288.5	0.974	0.2481	1005.5	0.2880	1042.6	99	83
1-alpha-decalylhendecane	544	292.5	0.876	0.2948	953.0	0.3133	961.3	28	13
1,2-bis(decahydro-1-naphthyl)ethane	562	302.5	0.970	0.2742	1006.8	0.2968	1037.6	98	82
1,1-di(alpha-decalyl)ethane	563	302.5	0.980	0.2453	1003.2	0.2948	1046.6	99	86
1-n-hexadecylindan	16	342.6	0.889	0.3315	973.6	0.3384	970.1	29	23
6-n-octylperhydrobenz(de) anthracene	196	344.6	0.947	0.3004	1000.5	0.3251	1016.5	85	54
1-alpha-decalylpentadecane	175	348.6	0.872	0.3288	948.3	0.3468	956.2	20	11
9,10-dihydro-2-dodecylphenanthrene	142	348.5	0.963	0.3089	1027.4	0.3237	1029.5	12	12
1,2,3,4,5,6,7,8,9,10,17,18-dodecahydro-9(n-octyl) naphthacene	165	352.6	0.983	0.2999	1025.9	0.3218	1046.7	80	62
11-octyl-1,2,3,4,5,6,7,8,13,14,15,16-	232	352.6	0.987	0.3182	1027.8	0.3210	1050.1	91	77
1,1-di(5-perhydroacenaphthyl) ethane	200	354.6	1.031	0.2390	1037.0	0.3148	1087.5	96	92
2-octylperhydrotriphenylene	228	358.6	0.942	0.2943	992.0	0.3338	1012.3	75	42
2-decylperhydroindeno-(2,1-a) indene	231	358.6	0.920	0.3513	989.9	0.3392	994.1	53	37
9-octylperhydronaphthacene	166	358.6	0.943	0.3002	984.9	0.3335	1013.1	86	68
3-decylperhydropyrene	216	358.6	0.933	0.2916	991.6	0.3359	1004.7	15	9
2-octylperhydrochrysene	225	358.6	0.943	0.2969	989.6	0.3335	1013.3	87	63
4-decylperhydropyrene	219	358.6	0.936	0.3086	996.2	0.3353	1006.9	57	28
2-n-dodecylperhydrophenanthrene	143	360.6	0.905	0.3377	976.6	0.3440	982.4	28	19

Compound	PSU	MW (g/mol)	SG	*Regressed*		*Predicted with Estimation Methods*			
				c_2	ρ_s^o (kg/m³)	c_2	ρ_s^o (kg/m³)	MARD (%)	AARD (%)
Fused Naphthenics-cont.									
9-n-dodecylperhydrophenanthrene	141	360.6	0.910	0.3116	972.7	0.3427	986.3	43	25
7-hexadecylspiro[54]decane	229	362.7	0.863	0.3528	948.0	0.3572	949.4	2	1
cholestane	155	372.8	0.952	0.2784	982.5	0.3393	1019.7	70	63
1-(5-perhydroacenaphthyl) pentadecane	193	374.7	0.899	0.3425	973.9	0.3534	977.1	5	3
9(4-as-perhydroindacenyl) heptadecane	177	402.7	0.898	0.3449	991.6	0.3686	976.4	55	30
1,10-di(alpha-decalyl)decane	132	414.7	0.934	0.3423	990.8	0.3655	1004.9	67	45
1-cyclohexyl-4(alpha-decalyl) tetradecane	192	416.7	0.902	0.3489	959.9	0.3750	979.0	89	60
1,1-di(alpha-decalyl)hendecane	122	428.8	0.939	0.3264	978.3	0.3716	1008.6	90	72
11-alpha-decalylheneicosane	62	432.8	0.873	0.3498	942.3	0.3917	956.8	53	27
Alcylcyclopentanes									
methylcyclopentane		84.2	0.754	0.2464	944.5	0.2284	917.5	30	17
ethylcyclopentane		98.2	0.771	0.2630	966.8	0.2230	918.3	59	25
propylcyclopentane		112.2	0.781	0.2483	950.5	0.2249	916.8	56	26
n-butylcyclopentane		126.2	0.789	0.2440	939.0	0.2303	916.5	53	23
n-pentylcyclopentane		140.3	0.795	0.2550	937.2	0.2374	916.3	56	21
n-hexylcyclopentane		154.3	0.801	0.2700	937.7	0.2454	916.4	59	17
n-heptylcyclopentane		168.3	0.805	0.2858	938.9	0.2537	916.9	61	15
n-octylcyclopentane		182.4	0.809	0.3002	939.6	0.2622	917.4	62	13
n-nonylcyclopentane		196.4	0.812	0.3145	940.7	0.2708	918.0	66	12
n-decylcyclopentane		210.4	0.815	0.3309	942.8	0.2794	918.7	75	12
n-undecylcyclopentane		224.4	0.818	0.3293	937.5	0.2878	919.4	41	7
n-dodecylcyclopentane		238.5	0.820	0.3276	932.7	0.2963	920.1	21	5
n-tridecylcyclopentane		252.5	0.822	0.3314	930.4	0.3046	920.8	9	4
n-tetradecylcyclopentane		266.5	0.824	0.3424	931.4	0.3128	921.5	9	5
n-pentadecylcyclopentane		280.5	0.825	0.3443	929.0	0.3209	922.2	7	5

Compound	PSU	MW (g/mol)	SG	*Regressed*		*Predicted with Estimation Methods*			
				c_2	ρ_s^o (kg/m³)	c_2	ρ_s^o (kg/m³)	MARD (%)	AARD (%)
Alcylcyclopentanes-cont.									
n-hexadecylcyclopentane		294. 6	0.827	0.3461	926.7	0.3290	922.9	8	6
Alcylcyclohexanes									
methylcyclohexane		98.2	0.775	0.2505	937.9	0.2228	921.3	4	2
ethylcyclohexane		112.2	0.793	0.2495	950.1	0.2236	926.5	21	8
propylcyclohexane		126.2	0.798	0.2472	941.7	0.2289	923.8	25	12
n-butylcyclohexane		140.3	0.803	0.2447	933.7	0.2359	922.6	32	12
n-pentylcyclohexane		154.3	0.808	0.2345	920.6	0.2438	922.1	9	7
n-hexylcyclohexane		168.3	0.812	0.2464	920.7	0.2521	922.0	7	3
n-heptylcyclohexane		182.4	0.815	0.2574	920.8	0.2607	922.1	5	2
n-octylcyclohexane		196.4	0.818	0.2660	921.0	0.2693	922.4	3	1
n-nonylcyclohexane		210.4	0.820	0.2794	921.9	0.2778	922.8	10	4
n-decylcyclohexane		224.4	0.822	0.2783	917.8	0.2864	923.1	11	6
n-undecylcyclohexane		238.5	0.824	0.2852	917.0	0.2949	923.7	13	10
n-dodecylcyclohexane		252.5	0.826	0.2867	914.6	0.3032	924.1	15	8
n-tridecylcyclohexane		266.5	0.828	0.2916	913.6	0.3115	924.7	15	8
n-tetradecylcyclohexane		280.5	0.829	0.3005	914.6	0.3197	925.2	14	8
n-pentadecylcyclohexane		294.6	0.830	0.3095	915.4	0.3278	925.6	16	9
n-hexadecylcyclohexane		308.6	0.832	0.3060	911.7	0.3357	926.2	15	9
Alcylbenzenes									
methybenzene (toluene)		92.1	0.874	0.2155	1049.6	0.2170	1021.1	76	40
ethylbenzene		106.2	0.874	0.2222	1042.4	0.2131	1004.3	108	47
propylbenzene		120.2	0.868	0.2214	1017.8	0.2157	988.2	113	42
n-butylbenzene		134.2	0.866	0.2247	1005.8	0.2213	978.3	134	48
n-pentylbenzene		148.3	0.862	0.2026	976.5	0.2289	969.4	96	59

Compound	PSU	MW (g/mol)	SG	*Regressed*		*Predicted with Estimation Methods*			
				c_2	ρ_s^o (kg/m³)	c_2	ρ_s^o (kg/m³)	MARD (%)	AARD (%)
Alcylbenzenes-cont.									
n-hexylbenzene		162.3	0.862	0.2159	975.2	0.2369	964.9	131	66
n-heptylbenzene		176.3	0.862	0.2270	968.7	0.2454	961.2	98	66
n-octylbenzene		190.3	0.860	0.2437	967.7	0.2545	957.3	106	53
n-nonylbenzene		204.4	0.860	0.2505	963.6	0.2635	954.8	115	71
n-decylbenzene		218.4	0.859	0.2661	963.4	0.2725	952.6	81	43
n-undecylbenzene		232.4	0.859	0.2857	965.0	0.2813	951.0	86	56
n-dodecylbenzene		246.4	0.860	0.2973	963.8	0.2898	950.6	61	44
n-tridecylbenzene		260.5	0.858	0.3068	962.0	0.2987	948.8	65	46
n-tetradecylbenzene		274.5	0.859	0.3164	960.7	0.3072	948.3	49	38
n-pentadecylbenzene		288.5	0.859	0.3258	959.5	0.3156	947.7	38	32
n-hexadecylbenzene		302.5	0.859	0.3361	958.8	0.3239	947.2	36	31

APPENDIX E: MEASURED VISCOSITY AND DENSITY DATA OF BITUMEN AND HEAVY OIL AND THEIR DILUTED MIXTURES

Table E.1: Measured viscosity and density of WC-B-B1 bitumen.

Pressure (MPa)	Temp. (°C)	Viscosity (mPa.s)	Density (kg/m^3)	Pressure (MPa)	Temp. °C	Viscosity (mPa.s)	Density (kg/m^3)
0.1	20.6	66000	1013.1	2.5	80	297	976.9
2.5	20.7	73200	1014.8	5	80	318	978.5
5	20.9	81200	1016.3	7.5	80	339	980.1
7.5	20.9	89300	1018.0	10	80	367	981.0
10	21.0	97500	1019.7	0.1	100	97.6	962.5
0.1	25	40700	1012.1	2.5	100	109	964.7
2.5	25	42300	1013.0	5	100	117	966.5
5	25	44400	1014.1	7.5	100	122	967.7
7.5	25	46600	1015.7	10	100	129	969.6
10	25	49000	1017.3	0.1	120	47.5	947.3
0.1	40	7280	1001.0	2.5	120	50.1	947.8
2.5	40	7680	1002.6	5	120	54.6	950.6
5	40	8500	1004.1	7.5	120	59.4	952.2
7.5	40	9520	1005.8	10	120	63.6	954.5
10	40	10400	1006.8	0.1	125	36.8	945.1
0.1	50	2710	994.9	2.5	125	39.9	946.7
2.5	50	3020	996.2	5	125	43.7	948.9
5	50	3320	997.7	7.5	125	45.1	950.2
7.5	50	3550	999.2	10	125	47.4	952.2
10	50	3800	1000.5	2.5	150	19.9	929.6
0.1	55	1800	991.8	5	150	21.3	932.6
2.5	55	1910	992.9	7.5	150	22.2	933.7
5	55	2090	994.4	10	150	23.2	936.0
7.5	55	2290	995.8	2.5	175	11.5	914.2
10	55	2530	997.3	5	175	12	916.2
0.1	75	425	978.9	7.5	175	12.4	918.2
2.5	75	457	980.9	10	175	12.9	920.3
5	75	495	982.2	2.5	195	7.8	901.2
7.5	75	527	983.3	5	195	8.2	903.8
10	75	568	985.1	7.5	195	8.5	906.5
0.1	80	269	975.0	10	195	8.8	908.4

Table E.2: Measured viscosity and density of WC-B-B2 bitumen.

Pressure (MPa)	Temp. (°C)	Viscosity (mPa.s)	Density (kg/m^3)	Pressure (MPa)	Temp. °C	Viscosity (mPa.s)	Density (kg/m^3)
0.1	19.4	89200	1014.9	0.1	100	121	962.9
2.5	19.4	104000	1015.9	2.5	100	129	964.5
5	19.4	120000	1017.0	5	100	137	966.2
7.5	19.4	138000	1018.5	7.5	100	146	967.9
10	19.4	160000	1020.0	10	100	155	969.5
0.1	35	13200	1004.3	0.1	125	45.9	945.7
2.5	35	14900	1005.2	2.5	125	48.4	947.6
5	35	16500	1006.4	5	125	50.9	949.5
7.5	35	18300	1007.9	7.5	125	53.8	951.1
10	35	20200	1009.4	10	125	56.7	953.1
0.1	50	2930	994.2	0.1	150	21.9	929.2
2.5	50	3180	995.3	2.5	150	22.8	931.3
5	50	3490	996.7	5	150	24	933.4
7.5	50	3820	998.2	7.5	150	25.2	935.4
10	50	4200	999.5	10	150	26.2	937.3
0.1	75	460	978.3	2.5	175	13	915.5
2.5	75	500	979.7	5	175	13.5	917.8
5	75	536	981.3	7.5	175	14.1	920.2
7.5	75	577	982.7	10	175	14.6	922.2
10	75	609	984.3				

Table E.3: Measured viscosity and density of WC-B-B3 bitumen.

Pressure (MPa)	Temp. (°C)	Viscosity (mPa.s)	Density (kg/m^3)	Pressure (MPa)	Temp. °C	Viscosity (mPa.s)	Density (kg/m^3)
0.1	19.9	118000	1016.3	5	100	159	967.5
2.5	19.6	141000	1017.6	7.5	100	169	969.1
5	19.6	158000	1018.9	10	100	180	970.6
7.5	19.7	177000	1020.1	0.1	125	51.6	947.6
10	19.8	196000	1021.6	2.5	125	54.7	949.6
0.1	50	3620	995.9	5	125	57.4	951.4
2.5	50	4010	997.3	7.5	125	60.7	953.0
5	50	4370	998.6	10	125	64	954.9
7.5	50	4750	999.9	0.1	150	24	931.3
10	50	5220	1001.3	2.5	150	25.4	933.7
0.1	75	538	979.9	5	150	26.5	935.8
2.5	75	589	981.5	7.5	150	27.9	937.6
5	75	631	983.0	10	150	29.1	939.5
7.5	75	672	984.3	2.5	175	13.7	917.6
10	75	725	985.9	5	175	14.2	919.9

Pressure (MPa)	Temp. (°C)	Viscosity (mPa.s)	Density (kg/m^3)	Pressure (MPa)	Temp. °C	Viscosity (mPa.s)	Density (kg/m^3)
0.1	100	142	964.0	7.5	175	14.8	922.0
2.5	100	150	965.8	10	175	15.4	923.9

Table E.4: Measured viscosity and density of WC-HO-S1 heavy oil.

Pressure (MPa)	Temp. (°C)	Viscosity (mPa.s)	Density (kg/m^3)	Pressure (MPa)	Temp. °C	Viscosity (mPa.s)	Density (kg/m^3)
0.1	25	5000	990.3	7.5	100	70.4	946.0
2.5	25	5640	991.5	10	100	73.9	947.9
5	25	6320	992.8	0.1	125	25.5	923.9
7.5	25	6990	994.3	2.5	125	27.3	926.1
10	25	7690	995.9	5	125	29.2	928.2
0.1	50	803	973.5	7.5	125	31	930.2
2.5	50	871	974.6	10	125	32.6	932.4
5	50	924	976.2	0.1	150	14.4	907.4
7.5	50	1020	977.9	2.5	150	15.1	910.0
10	50	1090	979.3	5	150	15.8	912.3
0.1	75	187	957.0	7.5	150	16.4	914.4
2.5	75	197	958.6	10	150	17.2	916.5
5	75	204	960.1	0.1	175	8.6	891.2
7.5	75	218	961.8	2.5	175	8.9	894.1
10	75	232	963.3	5	175	9.4	896.6
0.1	100	61.1	940.7	7.5	175	9.8	899.1
2.5	100	64.2	942.6	10	175	10.2	901.4
5	100	67.3	944.4				

Table E.5: Measured viscosity and density of WC-B-B3-DA de-asphalted bitumen (contaminated with 0.41 and 3.83 wt% n-pentane and toluene).

Pressure (MPa)	Temp. (°C)	Viscosity (mPa.s)	Density (kg/m^3)	Pressure (MPa)	Temp. °C	Viscosity (mPa.s)	Density (kg/m^3)
0.1	20.15	1280	982.3	5	100	18.3	931.9
2.5	20.16	1390	983.5	7.5	100	19.2	933.6
5	20.16	1540	984.6	10	100	20.1	935.4
7.5	20.1	1650	985.9	0.1	125	8.8	911.5
10	20.12	1810	987.6	2.5	125	9.1	913.9
0.1	50	145	961.4	5	125	9.4	915.8
2.5	50	157	962.9	7.5	125	9.8	917.6
5	50	167	964.4	10	125	10.2	919.6
7.5	50	176	966.0	2.5	150	5.4	897.2
10	50	186	967.3	5	150	5.6	899.5
0.1	75	41.8	945.1	7.5	150	5.8	901.5

Pressure (MPa)	Temp. (°C)	Viscosity (mPa.s)	Density (kg/m^3)	Pressure (MPa)	Temp. °C	Viscosity (mPa.s)	Density (kg/m^3)
2.5	75	44.5	946.9	10	150	6.0	903.5
5	75	47.2	948.5	2.5	175	3.6	880.3
7.5	75	49.8	950.0	5	175	3.7	882.8
10	75	52.6	951.6	7.5	175	3.8	885.3
0.1	100	16.9	928.2	10	175	3.9	887.5
2.5	100	17.5	930.2				

Table E.6: Measured viscosity and density of WC-B-B1 condensate.

Pressure (MPa)	Temp. (°C)	Viscosity (mPa.s)	Density (kg/m^3)	Pressure (MPa)	Temp. °C	Viscosity (mPa.s)	Density (kg/m^3)
0.1	25	0.35	693.5	7.5	100	0.19	636.3
2.5	25	0.35	696.1	10	100	0.20	640.9
5	25	0.36	698.3	2.5	125	0.15	601.5
7.5	25	0.37	700.2	5	125	0.16	607.2
10	25	0.39	704.2	7.5	125	0.16	612.7
2.5	50	0.28	673.0	10	125	0.17	617.8
5	50	0.29	676.1	2.5	150	0.12	572.2
7.5	50	0.30	678.9	5	150	0.13	580.4
10	50	0.30	682.1	7.5	150	0.14	587.5
2.5	75	0.22	649.3	10	150	0.14	593.8
5	75	0.23	653.3	2.5	175	0.10	539.7
7.5	75	0.24	656.6	5	175	0.11	551.1
10	75	0.24	660.3	7.5	175	0.12	560.4
2.5	100	0.18	627.8	10	175	0.12	568.6
5	100	0.19	632.1				

Table E.7: Measured viscosity and density of dead WC-B-B3+ 5.2 wt% ethane.

Pressure (MPa)	Temp. (°C)	Viscosity (mPa.s)	Density (kg/m^3)	Pressure (MPa)	Temp. °C	Viscosity (mPa.s)	Density (kg/m^3)
2.5	20.3	681	957.1	5	75	37.8	919.2
5	20.1	723	958.6	7.5	75	39.6	921.0
7.5	20.2	762	960.3	10	75	41.3	922.9
10	20.2	810	962.0	5	100	16.8	901.0
3	50	108	935.6	7.5	100	17.5	903.2
5	50	113	937.0	10	100	18.1	905.4
7.5	50	119	938.8	7.5	125	9.4	884.7
10	50	125	940.5	10	125	9.7	887.2
4	75	37.2	918.4	10	150	6.0	869.6

Table E.8: Measured viscosity and density of dead WC-B-B3+ 7.6 wt% propane.

Pressure (MPa)	Temp. (°C)	Viscosity (mPa.s)	Density (kg/m^3)	Pressure (MPa)	Temp. °C	Viscosity (mPa.s)	Density (kg/m^3)
2.5	19.2	1030	958.0	10	75	48.7	922.5
5	19.2	1100	959.3	5	100	19.1	901.8
7.5	19.3	1180	960.9	7.5	100	19.8	903.9
10	19.3	1260	962.8	10	100	20.7	906.1
2.5	50	133	934.8	5	125	10.1	883.5
5	50	140	936.6	7.5	125	10.5	885.7
7.5	50	149	938.3	10	125	10.8	888.2
10	50	158	940.0	7.5	150	6.3	868.4
2.5	75	41.5	916.8	10	150	6.5	870.9
5	75	43.6	918.8	10	175	4.3	853.7
7.5	75	46.2	920.6				

Table E.9: Measured viscosity and density of dead WC-B-B3+ 16 wt% propane.

Pressure (MPa)	Temp. (°C)	Viscosity (mPa.s)	Density (kg/m^3)	Pressure (MPa)	Temp. °C	Viscosity (mPa.s)	Density (kg/m^3)
2.5	19.8	76.3	898.3	7.5	75	9.6	858.4
5	19.8	79.5	899.9	10	75	10	860.6
7.5	19.8	83.2	901.8	5	100	5.0	836.4
10	19.8	86.9	904.0	7.5	100	5.2	839.2
2.5	50	19.3	873.3	10	100	5.4	842.0
5	50	20.2	875.4	7.5	125	3.3	819.3
7.5	50	21	877.5	10	125	3.4	822.7
10	50	22.1	879.7	7.5	150	2.2	799.0
2.5	75	9.0	853.6	10	150	2.3	802.8
5	75	9.3	856.0				

Table E.10: Measured viscosity and density of dead WC-B-B2+ 15.1 wt% propane.

Pressure (MPa)	Temp. (°C)	Viscosity (mPa.s)	Density (kg/m^3)	Pressure (MPa)	Temp. °C	Viscosity (mPa.s)	Density (kg/m^3)
1.6	17.9	108	905.3	5	75	10.5	862.5
2.5	18.0	110	905.8	7.5	75	11	864.8
5	18.0	114	907.4	10	75	11.4	867.1
7.5	17.9	120	909.2	5	100	5.7	842.7
10	17.9	126	911.6	7.5	100	5.9	845.3
2.1	50	22.7	879.2	10	100	6.2	848.1
2.5	50	22.9	879.4	5	125	3.5	821.9
5	50	23.8	881.5	7.5	125	3.6	825.2
7.5	50	24.8	883.8	10	125	3.8	828.4
10	50	25.8	885.8	8	150	2.5	806.5
2.5	75	10	859.9	10	150	2.5	809.3

Table E.11: Measured viscosity and density of dead WC-B-B2+ 11.3 wt% propane.

Pressure (MPa)	Temp. (°C)	Viscosity (mPa.s)	Density (kg/m^3)	Pressure (MPa)	Temp. °C	Viscosity (mPa.s)	Density (kg/m^3)
0.8	15.2	287	932.5	2.5	75	17.1	887.6
1.6	15.2	295	933.0	5	75	17.9	889.7
2.5	15.2	299	933.3	7.5	75	18.7	891.7
5	15.2	315	934.5	10	75	19.4	893.8
7.5	15.2	337	936.3	3	100	8.85	869.3
10	15.2	356	938.5	5	100	9.08	870.7
1.6	50	42.3	905.2	7.5	100	9.39	873.2
2.1	50	42.7	905.4	10	100	9.77	875.6
2.5	50	43.3	905.8	5	125	5.31	852.3
5	50	45.4	907.8	7.5	125	5.49	855.0
7.5	50	47.6	909.7	10	125	5.69	857.8
10	50	50.2	911.7	8	150	3.61	837.8
1.6	75	16.8	886.8	10	150	3.74	840.1

Table E.12: Measured viscosity and density of dead WC-B-B3+ 7.3 wt% n-butane.

Pressure (MPa)	Temp. (°C)	Viscosity (mPa.s)	Density (kg/m^3)	Pressure (MPa)	Temp. °C	Viscosity (mPa.s)	Density (kg/m^3)
1.2	20.81	992	967.5	5	100	21.1	914.7
2.5	20.76	1040	968.3	7.5	100	22.1	916.6
5	20.77	1100	969.5	10	100	23	918.6
7.5	20.78	1180	971.1	1.2	125	10.5	893.9
10	20.79	1260	972.8	2.5	125	10.8	895.2
1.2	50	145	946.7	5	125	11.2	897.4
2.5	50	150	947.5	7.5	125	11.6	899.6
5	50	159	949.1	10	125	12.1	901.8
7.5	50	168	950.8	1.2	150	6.4	876.1
10	50	178	952.4	2.5	150	6.5	877.6
1.2	75	45.9	929.0	5	150	6.7	880.3
2.5	75	47.1	929.9	7.5	150	7.0	882.6
5	75	49.5	931.6	10	150	7.2	884.9
7.5	75	51.6	933.4	2.5	175	4.3	860.1
10	75	53.9	935.0	5	175	4.4	862.9
1.2	100	20	911.7	7.5	175	4.6	865.8
2.5	100	20.3	912.8	10	175	4.7	868.2

Table E.13: Measured viscosity and density of dead WC-B-B3+ 14.5 wt% n-butane.

Pressure (MPa)	Temp. (°C)	Viscosity (mPa.s)	Density (kg/m^3)	Pressure (MPa)	Temp. °C	Viscosity (mPa.s)	Density (kg/m^3)
2.5	20.1	145	926.8	7.5	100	8.0	871.7
5	20.1	151	928.3	10	100	8.3	874.1
7.5	20.1	157	929.6	2.5	125	4.5	848.4
10	20.1	167	932.0	5	125	4.7	851.0
2.5	50	33.6	904.0	7.5	125	4.9	853.6
5	50	35.1	905.7	10	125	5.0	856.2
7.5	50	36.3	907.6	2.5	150	3.0	829.3
10	50	37.9	909.6	5	150	3.1	832.6
2.5	75	14.3	885.4	7.5	150	3.2	835.6
5	75	14.8	887.6	10	150	3.3	838.3
7.5	75	15.5	889.8	2.5	175	2.1	810.5
10	75	16	891.8	5	175	2.2	814.1
2.5	100	7.5	867.2	7.5	175	2.3	817.6
5	100	7.7	869.4	10	175	2.4	820.7

Table E.14: Measured viscosity and density of dead WC-B-B3+ 15 wt% n-pentane.

Pressure (MPa)	Temp. (°C)	Viscosity (mPa.s)	Density (kg/m^3)	Pressure (MPa)	Temp. °C	Viscosity (mPa.s)	Density (kg/m^3)
0.1	20.5	216	937.0	7.5	100	10.4	885.4
2.5	20.3	224	938.5	10	100	10.8	887.6
5	20.4	238	939.9	2.5	125	5.7	863.3
7.5	20.4	247	941.4	5	125	5.9	865.7
10	20.5	263	943.4	7.5	125	6.1	868.2
2.5	50	48.6	917.2	10	125	6.3	870.5
5	50	51.8	918.8	2.5	150	3.7	844.9
7.5	50	54.9	920.5	5	150	3.8	847.6
10	50	59.1	922.3	7.5	150	4.0	850.3
2.5	75	20	899.4	10	150	4.1	852.9
5	75	20.8	901.3	2.5	175	2.6	826.2
7.5	75	21.8	903.1	5	175	2.7	829.5
10	75	22.6	905.0	7.5	175	2.8	832.6
2.5	100	9.6	881.3	10	175	2.9	835.6
5	100	9.9	883.3				

Table E.15: Measured viscosity and density of dead WC-B-B3+ 30 wt% n-pentane.

Pressure (MPa)	Temp. (°C)	Viscosity (mPa.s)	Density (kg/m^3)	Pressure (MPa)	Temp. °C	Viscosity (mPa.s)	Density (kg/m^3)
0.1	20.1	20.6	869.1	2.5	100	2.7	808.0
2.5	20	21.9	871.1	5	100	2.7	810.6
5	20	22.5	872.8	7.5	100	2.8	813.1
7.5	19.9	23.4	874.4	10	100	2.9	816.1
10	19.9	24.2	876.8	2.5	125	1.8	788.0
2.5	50	7.9	847.5	5	125	1.9	791.3
5	50	8.2	849.6	7.5	125	1.9	794.2
7.5	50	8.5	851.6	10	125	2	797.5
10	50	8.8	853.8	2.5	150	1.3	767.2
2.5	75	4.3	827.8	5	150	1.4	771.2
5	75	4.4	830.2	7.5	150	1.4	774.7
7.5	75	4.6	832.4	10	150	1.5	778.3
10	75	4.7	834.7				

Table E.16: Measured viscosity and density of dead WC-B-B2+ 15 wt% n-heptane.

Pressure (MPa)	Temp. (°C)	Viscosity (mPa.s)	Density (kg/m^3)	Pressure (MPa)	Temp. °C	Viscosity (mPa.s)	Density (kg/m^3)
0.1	20.01	587	953.2	2.5	100	15.2	898.4
2.5	20	634	954.4	5	100	15.8	900.4
5	19.97	683	955.7	7.5	100	16.5	902.4
7.5	19.97	737	957.2	10	100	17.2	904.3
10	19.97	794	958.9	0.1	125	7.99	878.3
0.1	50	90.7	930.4	2.5	125	8.28	880.6
2.5	50	96.2	931.8	5	125	8.63	882.9
5	50	102	933.5	7.5	125	8.95	885.0
7.5	50	107	935.2	10	125	9.32	887.3
10	50	113	936.9	2.5	150	5.15	863.5
0.1	75	31.6	913.8	5	150	5.34	866.1
2.5	75	32.9	915.5	7.5	150	5.55	868.6
5	75	34.5	917.4	10	150	5.74	871.0
7.5	75	36.3	919.1	5	175	3.61	848.9
10	75	37.9	920.9	7.5	175	3.73	851.9
0.1	100	14.5	896.5	10	175	3.84	854.4

Table E.17: Measured viscosity and density of dead WC-B-B2+ 30 wt% n-heptane.

Pressure (MPa)	Temp. (°C)	Viscosity (mPa.s)	Density (kg/m^3)	Pressure (MPa)	Temp. °C	Viscosity (mPa.s)	Density (kg/m^3)
0.1	18.9	41.1	894.9	7.5	75	6.9	858.9
2.5	18.9	42.7	896.4	10	75	7.17	861.0
5	18.9	44.5	897.8	2.5	100	3.82	837.3
7.5	18.9	46.8	899.4	5	100	3.95	839.5
10	18.9	48.6	901.6	7.5	100	4.07	841.8
2.5	50	12.7	872.8	10	100	4.21	844.3
5	50	13.1	874.7	2.5	125	2.52	818.9
7.5	50	13.7	876.6	5	125	2.6	821.5
10	50	14.3	878.6	7.5	125	2.69	824.2
2.5	75	6.43	854.8	10	125	2.77	826.8
5	75	6.65	857.0				

Table E.18: Measured viscosity and density of dead WC-B-B3+ 5.1 wt% carbon dioxide.

Pressure (MPa)	Temp. (°C)	Viscosity (mPa.s)	Density (kg/m^3)	Pressure (MPa)	Temp. °C	Viscosity (mPa.s)	Density (kg/m^3)
3.5	19.8	1900	1012.0	7.5	75	75.7	974.7
5	19.8	1980	1012.9	10	75	79.4	976.4
7.5	19.8	2120	1014.4	7.5	100	30.6	956.8
10	19.8	2270	1016.2	10	100	31.7	958.9
5	50	250	990.8	8.5	125	15.7	940.1
7.5	50	264	992.5	10	125	16	941.5
10	50	276	994.1	10	150	9.7	924.4
6	75	73.7	973.7				

Table E.19: Measured viscosity and density of live WC-HO-S1.

Pressure (MPa)	Temp. (°C)	Viscosity (mPa.s)	Density (kg/m^3)	Pressure (MPa)	Temp. °C	Viscosity (mPa.s)	Density (kg/m^3)
2.5	20.3	5180	987.5	7.5	100	50.3	936.9
5	20.3	5550	988.8	10	100	52.8	938.8
7.5	20.3	6270	990.3	3	125	21.8	916.7
10	20.3	6790	991.9	5	125	22.7	918.3
2.5	50	498	966.5	7.5	125	23.7	920.4
5	50	532	968.1	10	125	24.7	922.6
7.5	50	568	969.5	3.5	150	12.2	901.1
10	50	607	971.0	5	150	12.5	902.5
2.5	75	123	950.0	7.5	150	13	904.6
5	75	132	951.6	10	150	13.6	906.7
7.5	75	140	953.2	3.5	175	7.6	884.1

Pressure (MPa)	Temp. (°C)	Viscosity (mPa.s)	Density (kg/m^3)	Pressure (MPa)	Temp. °C	Viscosity (mPa.s)	Density (kg/m^3)
10	75	148	955.0	5	175	7.8	885.7
3	100	46.1	933.6	7.5	175	8.1	888.3
5	100	47.9	935.1	10	175	8.4	890.8

Table E.20: Measured viscosity and density of live WC-B-B1.

Pressure (MPa)	Temp. (°C)	Viscosity (mPa.s)	Density (kg/m^3)	Pressure (MPa)	Temp. °C	Viscosity (mPa.s)	Density (kg/m^3)
2.5	18.7	16000	1011.5	5	100	64.4	958.4
5	18.7	17300	1012.7	7.5	100	68.5	960.1
7.5	18.6	18500	1014.2	10	100	71.9	962.0
10	18.6	20000	1015.9	5	125	28.9	941.3
2.5	50	823	989.4	7.5	125	30.2	943.3
5	50	935	991.1	10	125	31.5	945.3
7.5	50	1020	992.5	5	150	15.1	924.6
10	50	1080	993.8	7.5	150	15.7	926.7
3	75	191	973.0	10	150	16.4	928.9
5	75	200	974.3	5	175	9	908.0
7.5	75	214	975.9	7.5	175	9.4	910.5
10	75	226	977.5	10	175	9.8	912.6
3	100	62.5	957.0				

Table E.21: Measured viscosity and density of dead WC-HO-S1+ 3 wt% WC-C-B1.

Pressure (MPa)	Temp. (°C)	Viscosity (mPa.s)	Density (kg/m^3)	Pressure (MPa)	Temp. °C	Viscosity (mPa.s)	Density (kg/m^3)
0.1	25	2150	977.8	5	100	45.4	931.7
2.5	25	2460	979.1	7.5	100	47.4	933.4
5	25	2700	980.4	10	100	49.4	934.9
7.5	25	2980	981.9	0.1	125	19.8	911.7
10	25	3300	983.2	2.5	125	20.4	913.9
0.1	50	407	961.7	5	125	21	915.8
2.5	50	434	963.1	7.5	125	21.6	917.2
5	50	463	964.9	10	125	22.7	919.5
7.5	50	483	966.2	0.1	150	10.8	894.1
10	50	496	967.5	2.5	150	11.1	896.7
0.1	75	105	944.1	5	150	11.6	898.9
2.5	75	111	945.9	7.5	150	12.1	901.0
5	75	119	947.7	10	150	12.4	903.5
7.5	75	126	949.3	2.5	175	7.0	879.9
10	75	132	950.9	5	175	7.2	882.7

Pressure (MPa)	Temp. (°C)	Viscosity (mPa.s)	Density (kg/m^3)	Pressure (MPa)	Temp. °C	Viscosity (mPa.s)	Density (kg/m^3)
0.1	100	41.2	927.8	7.5	175	7.5	885.4
2.5	100	43.1	929.9	10	175	7.9	887.6

Table E.22: Measured viscosity and density of dead WC-HO-S1+ 6 wt% WC-C-B1.

Pressure (MPa)	Temp. (°C)	Viscosity (mPa.s)	Density (kg/m^3)	Pressure (MPa)	Temp. °C	Viscosity (mPa.s)	Density (kg/m^3)
0.1	25	1090	967.6	5	100	32	921.5
2.5	25	1140	969.0	7.5	100	33.1	923.2
5	25	1250	970.2	10	100	34.2	925.3
7.5	25	1400	971.9	0.1	125	14.7	900.8
10	25	1570	973.6	2.5	125	15.1	903.1
0.1	50	230	951.5	5	125	15.7	905.2
2.5	50	251	952.8	7.5	125	16.3	907.3
5	50	272	954.9	10	125	17	909.6
7.5	50	294	956.4	2.5	150	8.8	885.9
10	50	314	958.0	5	150	9.1	888.9
0.1	75	71.5	934.4	7.5	150	9.4	891.3
2.5	75	74.9	936.0	10	150	9.8	894.1
5	75	78.3	937.8	2.5	175	6.0	868.9
7.5	75	81.8	939.5	5	175	6.1	871.5
10	75	85.4	941.1	7.5	175	6.2	874.1
0.1	100	28.9	917.6	10	175	6.3	876.6
2.5	100	30.7	919.7				

Table E.23: Measured viscosity and density of dead WC-B-B1+ 3 wt% WC-C-B1.

Pressure (MPa)	Temp. (°C)	Viscosity (mPa.s)	Density (kg/m^3)	Pressure (MPa)	Temp. °C	Viscosity (mPa.s)	Density (kg/m^3)
0.1	25	11100	1000.0	5	100	77.6	954.1
2.5	25	11900	1000.6	7.5	100	82.4	956.0
5	25	12700	1001.7	10	100	86.8	957.9
7.5	25	13900	1003.2	0.1	125	30.2	933.8
10	25	15400	1004.9	2.5	125	31	935.8
0.1	50	1110	982.5	5	125	32.4	937.7
2.5	50	1210	983.8	7.5	125	33.7	939.4
5	50	1330	985.2	10	125	35.4	941.5
7.5	50	1460	986.9	2.5	150	15.9	920.3
10	50	1590	988.1	5	150	16.6	922.3
0.1	75	224	966.9	7.5	150	17.3	924.4
2.5	75	236	968.4	10	150	17.8	926.5

Pressure (MPa)	Temp. (°C)	Viscosity (mPa.s)	Density (kg/m^3)	Pressure (MPa)	Temp. °C	Viscosity (mPa.s)	Density (kg/m^3)
5	75	253	970.1	2.5	175	9.3	903.9
7.5	75	272	971.6	5	175	9.7	906.4
10	75	293	973.1	7.5	175	10.1	909.0
0.1	100	69.7	951.9	10	175	10.5	911.3
2.5	100	73.7	952.2				

Table E.24: Measured viscosity and density of dead WC-B-B1+ 6 wt% WC-C-B1.

Pressure (MPa)	Temp. (°C)	Viscosity (mPa.s)	Density (kg/m^3)	Pressure (MPa)	Temp. °C	Viscosity (mPa.s)	Density (kg/m^3)
0.1	25	4140	989.6	2.5	100	46.9	941.0
2.5	25	4620	990.5	5	100	48.2	942.8
5	25	5000	991.7	7.5	100	51.1	944.7
7.5	25	5480	993.4	10	100	56	946.5
10	25	5960	995.0	2.5	125	21.4	925.0
0.1	50	488	972.2	5	125	22.2	926.8
2.5	50	553	973.5	7.5	125	23.5	928.6
5	50	613	975.0	10	125	24.5	930.6
7.5	50	665	976.6	2.5	150	11.9	907.9
10	50	744	978.5	5	150	12.4	910.3
0.1	75	137	957.2	7.5	150	12.8	912.4
2.5	75	142	958.7	10	150	13.4	914.5
5	75	148	960.5	2.5	175	7.1	892.3
7.5	75	158	962.3	5	175	7.4	894.9
10	75	174	963.9	7.5	175	7.6	897.5
0.1	100	45.1	939.2	10	175	7.8	899.7

Table E.25: Measured viscosity and density of dead WC-B-B2+ 30 wt% WC-C-B1.

Pressure (MPa)	Temp. (°C)	Viscosity (mPa.s)	Density (kg/m^3)	Pressure (MPa)	Temp. °C	Viscosity (mPa.s)	Density (kg/m^3)
0.1	20.5	39.4	899.7	2.5	100	3.93	841.8
2.5	20.5	41.4	901.2	5	100	4.07	844.2
5	20.5	43.3	902.7	7.5	100	4.2	846.6
7.5	20.5	45.2	904.5	10	100	4.34	849.2
10	20.5	47.4	906.6	2.5	125	2.58	823.0
2.5	50	13.1	878.6	5	125	2.68	825.7
5	50	13.7	880.4	7.5	125	2.76	828.3
7.5	50	14.2	882.3	10	125	2.86	831.1
10	50	14.8	884.4	2.5	175	1.36	784.0
2.5	75	6.66	860.3	5	175	1.41	787.9

Pressure (MPa)	Temp. (°C)	Viscosity (mPa.s)	Density (kg/m^3)	Pressure (MPa)	Temp. °C	Viscosity (mPa.s)	Density (kg/m^3)
5	75	6.88	862.6	7.5	175	1.46	791.5
7.5	75	7.12	864.6	10	175	1.51	794.8
10	75	7.41	866.5				

Table E.26: Measured viscosity and density of live WC-HO-S1+ 3 wt% WC-C-B1.

Pressure (MPa)	Temp. (°C)	Viscosity (mPa.s)	Density (kg/m^3)	Pressure (MPa)	Temp. °C	Viscosity (mPa.s)	Density (kg/m^3)
2.5	20.3	2360	976.8	7.5	100	37.2	927.9
5	20.4	2550	978.1	10	100	39	929.8
7.5	20.4	2770	979.6	3	125	16.7	907.4
10	20.5	3000	981.3	5	125	17.2	908.7
2.5	50	306	957.6	7.5	125	17.9	910.7
5	50	324	959.3	10	125	18.6	912.8
7.5	50	345	960.9	3.5	150	9.7	890.8
10	50	365	962.4	5	150	9.9	892.3
2.5	75	85.4	940.8	7.5	150	10.3	894.4
5	75	90.2	942.6	10	150	10.6	896.7
7.5	75	95.3	944.2	3.5	175	6.2	873.9
10	75	101	945.8	5	175	6.33	875.6
3	100	34.1	924.6	7.5	175	6.57	878.2
5	100	35.5	926.0	10	175	6.79	880.6

Table E.27: Measured viscosity and density of live WC-HO-S1+ 6 wt% WC-C-B1.

Pressure (MPa)	Temp. (°C)	Viscosity (mPa.s)	Density (kg/m^3)	Pressure (MPa)	Temp. °C	Viscosity (mPa.s)	Density (kg/m^3)
2.5	20.7	1250	967.1	7.5	100	26.2	916.5
5	20.7	1350	968.4	10	100	27.4	918.5
7.5	20.7	1440	969.8	3	125	12.8	896.4
10	20.7	1560	971.7	5	125	13.2	898.3
2.5	50	179	945.9	7.5	125	13.6	900.2
5	50	187	947.5	10	125	14.1	902.5
7.5	50	200	949.1	3.5	150	7.6	878.4
10	50	214	950.7	5	150	7.8	880.0
2.5	75	56.6	929.2	7.5	150	8.1	882.3
5	75	59.3	931.0	10	150	8.4	884.8
7.5	75	62.3	932.7	3.5	175	5.0	861.2
10	75	65.2	934.5	5	175	5.1	862.9
3	100	24.4	913.1	7.5	175	5.3	865.6
5	100	25.2	914.7	10	175	5.5	868.1

Table E.28: Measured viscosity and density of live WC-B-B1+ 3 wt% WC-C-B1.

Pressure (MPa)	Temp. (°C)	Viscosity (mPa.s)	Density (kg/m^3)	Pressure (MPa)	Temp. °C	Viscosity (mPa.s)	Density (kg/m^3)
2.5	19.2	4110		5	100	39.1	946.7
5	19.2	4450		7.5	100	41.1	948.6
7.5	19.2	4890		10	100	43	950.4
10	19.2	5340		5	125	18.6	929.4
2.5	50	374	978.8	7.5	125	19.4	931.4
5	50	407	980.3	10	125	20.2	933.4
7.5	50	433	981.9	5	150	10.6	912.1
10	50	457	983.4	7.5	150	11	914.5
3	75	101	962.1	10	150	11.5	916.7
5	75	106	963.5	5	175	6.7	895.3
7.5	75	112	965.1	7.5	175	6.9	897.9
10	75	118	966.6	10	175	7.2	900.3
3	100	37.7	945.1				

Table E.29: Measured viscosity and density of live WC-B-B2+ 5.9 wt% WC-C-B1.

Pressure (MPa)	Temp. (°C)	Viscosity (mPa.s)	Density (kg/m^3)	Pressure (MPa)	Temp. °C	Viscosity (mPa.s)	Density (kg/m^3)
2.5	20.74	1660		5	100	27	
5	20.74	1730		7.5	100	28.2	
7.5	20.74	1880		10	100	29.2	
10	20.74	2040		5	125	13.9	
2.5	50	208		7.5	125	14.5	
5	50	219		10	125	15.1	
7.5	50	233		5	150	8.11	
10	50	245		7.5	150	8.41	
3	75	64		10	150	8.72	
5	75	66.6		5	175	5.26	
7.5	75	70.1		7.5	175	5.43	
10	75	73.9		10	175	5.61	

APPENDIX F: GC ASSAY DATA OF CRUDE OILS IN CHAPTER SEVEN

Note: the minute non-hydrocarbon contents were all lumped into CO_2 contents of the crudes.

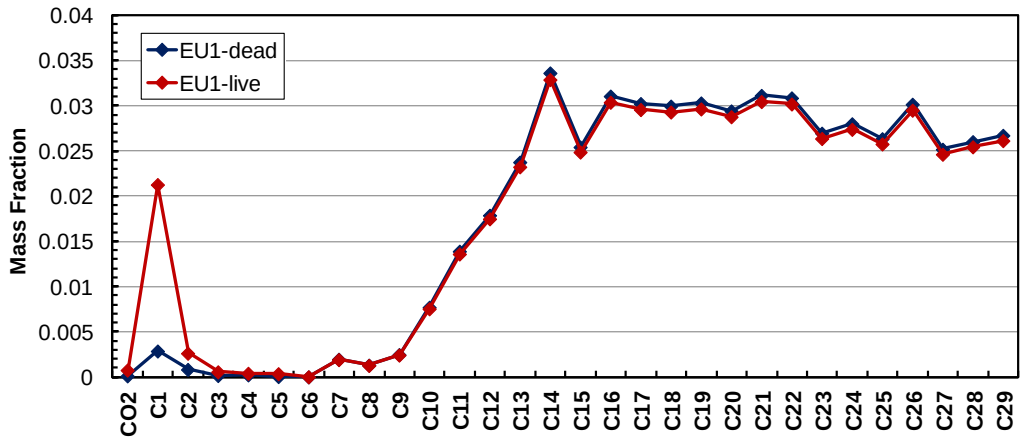

Figure F.1: GC assay of the crudes EU1 dead and live.

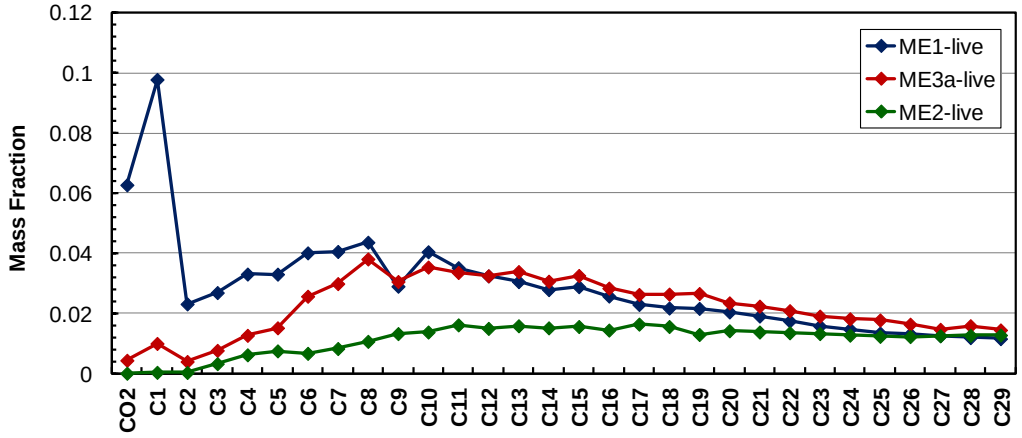

Figure F.2: GC assay of the crudes ME1, ME3a and ME2.

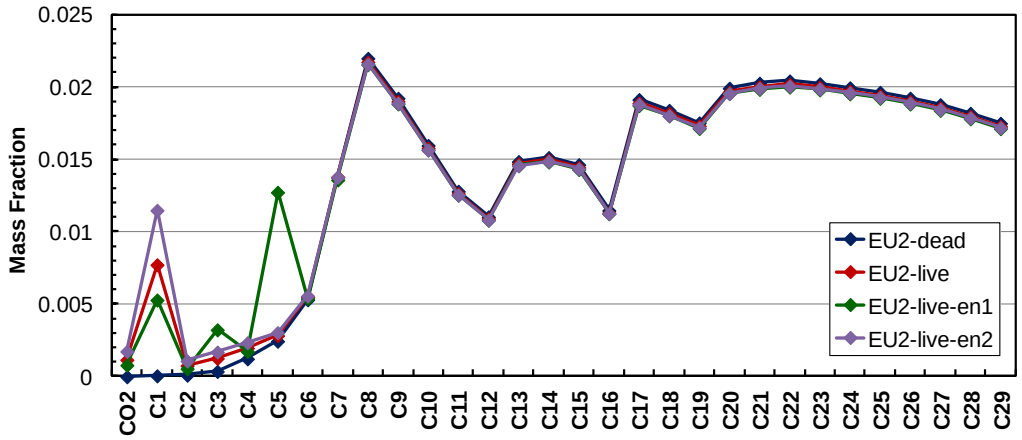

Figure F.3: GC assay of the crudes EU2 dead, live and enriched with light n-alkanes.

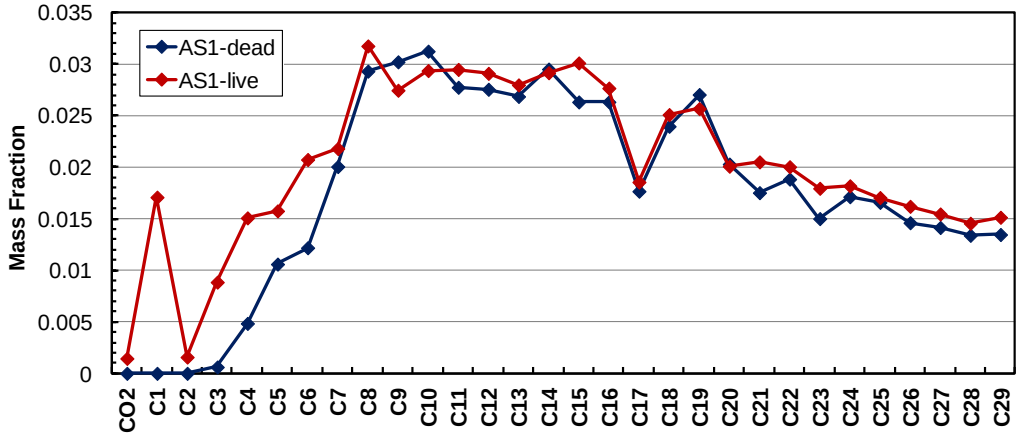

Figure F.4: GC assay of the crudes AS1 dead and live.

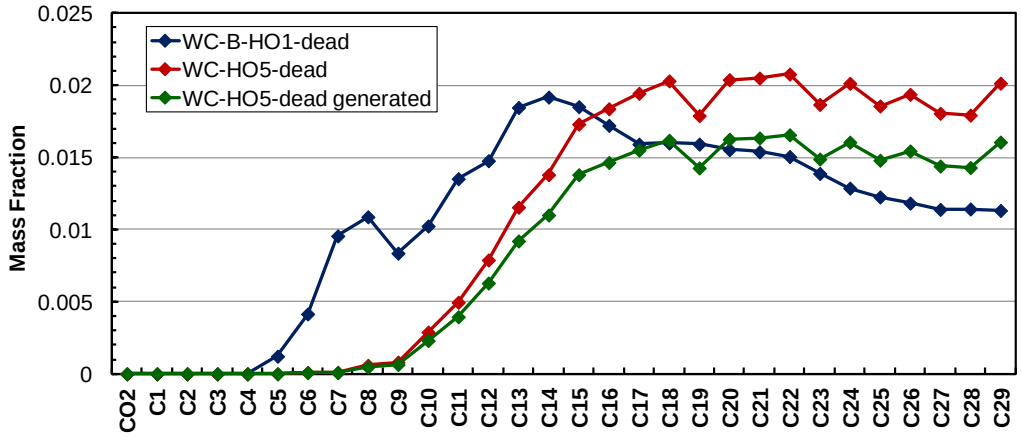

Figure F.5: GC assay of the WC-B-HO1 and WC-HO5 (original and scaled assay).

APPENDIX G: EXAMPLE CALCULATIONS

A. Estimate viscosity of n-heptylcyclohexane at P=20 MPa and T=293 K.
input data: MW=182.35 g/mol, SG=0.8148 from API (1997) handbook, measured density=822.8 kg/m^3 from (Baylaucq et al., 2002).

a. calculation of the fluid-specific parameters of EF correlation for the reference n-paraffin with MW=182.35:

$SG_{(ref)}$=0.7622, $c_{2(ref)}$=0.2755, $\rho_s^{o}{}_{(ref)}$=881.98 kg/m^3 from Equations 7.20, 7.22 and 7.23, respectively.

b. calculation of the departures:

ΔSG=0.0526 from Equation 7.18.

then: Δc_2=-0.0146 and $\Delta\rho_s^{o}$=40.11 kg/m^3 from Equation 7.24 with constants from Table 7.4.

c. calculation of the fluid-specific parameters for n-heptylcyclohexane:

c_2=0.2609 and ρ_s^{o}=922.09 kg/m^3 from Equation 30.

$c_3=2.34\times10^{-7}$ kPa^{-1} from Equation 7.16.

d. calculation of the viscosity at P=20 MPa and T=293 K:

$\mu_o=4.58\times10^{-3}$mPa.s from Equation 2.13 with constants from Yaws (2008) handbook.

ρ_s^{*}=926.42 kg/m^3 from Equation 4.5.

ρ=822.8 kg/m^3 → β=11.9831 from Equation 4.2 → μ=3.60 mPa.s from Equation 4.1

Experimental viscosity of n-heptylcyclohexane is 3.53 mPa.s from (Baylaucq et al., 2002).

B. Estimate viscosity of WC-B-B2 at P=5 MPa and T=293 K.

data: the crude is characterized by 13 pseudo-components (Table 7.8) based on GC assay data.

measured density=1017 kg/m^3 (see Appendix E).

a. sample calculation of the fluid-specific parameters for Pseudo-component #1 with MW=189 g/mol, SG=0.885:

MW=189 g/mol → $SG_{(ref)}$=0.7653, $c_{2(ref)}$=0.2794 and $\rho_s^{o}{}_{(ref)}$=883.42 kg/m^3.

and SG=0.885 → ΔSG=0.1197 → Δc_2=-0.0313 and $\Delta\rho_s^{o}$=94.72 kg/m^3.

then: c_2=0.2481, ρ_s^{o}=978.14 kg/m^3 and $c_3=2.38\times10^{-7}$ kPa^{-1}.

b. sample calculation of dilute gas viscosity of Pseudo-component #1 (MW=189 g/mol, SG=0.885) at T=293 K:

MW=189 g/mol, SG=0.885 → v_c=713.8 cm^3/mol and NBP=949.7 K from the Hall and Yarbrough (1971) and Soreide (1989) correlations, respectively.

NBP=949.7 K, SG=0.885 → Tc=725.5 K, ω=0.558 from the Lee-Kesler (Lee and Kesler, 1975; Kesler and Lee, 1976) correlations.

then: μ_o= 0.0045 mPa.s from Equations 2.5 to 2.10.

c. calculation of fluid-specific parameters for WC-B-B2:

ρ_s^{o}, c_2 and c_3 of the pseudo-components determined as demonstrated in "a" and reported in Table 7.8.

$\rho_s^{o}{}_{mix}$=1074.7 kg/m^3, $c_{2,mix}$=0.5149 and $c_{3,mix}=2.73\times10^{-7}$ kPa^{-1} from Equations 5.16, 5.17 and 5.18 with β_{ij}=0.

d. calculation of the viscosity at P=5 MPa and T=293 K:

dilute gas viscosities of the pseudo-components determined at 293 K as demonstrated in "b".

then: $\mu_{o,mix}$=0.0028 mPa.s from Equations 2.14 and 2.16.

ρ_s^{*}=1076.2 kg/m^3 from Equation 4.5.

ρ=1017 kg/m^3 → β=26.1975 from Equation 4.2

→ μ=119000 mPa.s from Equation 4.1

Experimental viscosity of WC-B-B2 is 120000 mPa.s (see Appendix E).

APPENDIX G: REGRESSION AND STATISTICAL DEFINITIONS

G.1 Regression

Several times throughout this thesis, the EF model were regressed to the experimental viscosity data to determine: 1) the fluid-specific parameters for pure compounds; 2) the coefficients of the developed estimations methods; and 3) the viscosity binary interaction parameters (βij). These regressions was done by minimizing the following objective function:

$$OF = \sum_{i=1}^{N} \left[\ln \left(\frac{\mu_{calc\,(i)}}{\mu_{\exp\,(i)}} \right) \right]^2$$

where N is the number of data points, and μ_{exp} and μ_{calc} are the measured and calculated viscosities by the model, respectively. The objective function was minimized by the Generalized Reduced Gradient (GRG2) nonlinear optimization code (Fylstra et al., 1998) as it is implemented in SOLVER add-in of Microsoft Excel. In general, this form of the objective function is equivalent to the least square fit of the natural logarithm of the viscosities by model.

G.2 Statistical Definitions

The quantitative measures of the deviations of the predicted/fitted model from the experimental values throughout this thesis were assessed as below:

Average Absolute Deviation (AAD):

$$AAD = \frac{1}{N} \sum_{i=1}^{N} \left| \mu_{calc\,(i)} - \mu_{\exp\,(i)} \right|$$

Average Absolute Relative Deviation (AARD) in percent:

$$AARD = \frac{100}{N} \sum_{i=1}^{N} \frac{\left| \mu_{calc\,(i)} - \mu_{\exp\,(i)} \right|}{\mu_{\exp\,(i)}}$$

Maximum Absolute Deviation (MAD):

$$MAD = Maximum\ of \quad \left|\mu_{calc\,(i)} - \mu_{\exp\,(i)}\right| \quad for\ i = 1...N$$

Maximum Absolute Relative Deviation (MARD) in percent:

$$MARD = Maximum\ of \quad \frac{100\left|\mu_{calc\,(i)} - \mu_{\exp\,(i)}\right|}{\mu_{\exp\,(i)}} \quad for\ i = 1...N$$

Bias in percent:

$$Bias = \frac{100}{N}\sum_{i=1}^{N}\left(\frac{\mu_{calc\,(i)} - \mu_{\exp\,(i)}}{\mu_{\exp\,(i)}}\right)$$